INVESTIGATIONS INTO THE KINETICS OF NITRIFICATION

BY

ANDREW P.G. NEWTON

THESIS SUBMITTED FOR THE DEGREE OF DOCTOR OF PHILOSOPHY

IN THE FACULTY OF ENGINEERING,

HERIOT-WATT UNIVERSITY

DEPARTMENT OF CHEMICAL AND PROCESS ENGINEERING

SEPTEMBER 1990

TABLE OF CONTENTS

CHAPTER PAGE

APPENDICES

(The numbers refer to the relevant chapters)

LIST OF TABLES AND ILLUSTRATIONS

TABLE PAGE

FIGURE

ACKNOWLEDGEMENTS

I would like to acknowledge my gratitude to the many friends who have helped me in completing this thesis. I would like to thank my supervisor, Dr. L. R. Weatherley, for suggesting improvements to the text and for his assistance in general. I would also like to thank those in the biology department who leant technical assistance or enthusiasm. However, above all I am most indebted to Angelika for her support and faith.

If you would be a real seeker after truth, it is necessary that at least once in your life you doubt, as far as possible, all things.

René Descartes

ABSTRACT

This thesis proposes mechanisms for the nitrification reactions compatible with previous literature data and with the unsteady-state kinetic data collected. The mechanisms provide a comprehensive explanation of the reactions and represent a significant departure from previously assumed mechanisms. The thesis strongly questions the common assumption that hydroxylamine is an intermediate in the oxidation of ammonia. It proposes that the nitrification reactions are brought about by the creation of two esters: a carboxy phosphate ester and a carboxy nitrite ester. The formation of the esters is assumed to require ATP. The reaction kinetics shows sigmoidal behaviour and is compatible with protons and ATP influencing the reaction rate. A rate equation to describe these reactions and other enzyme reactions is proposed. The bacteria's control system appears to be responsible for the difficulties in analyzing nitrification data from biological filters. Nitrification reaction rates can be increased by utilizing short residence times and low substrate concentrations.

The work proposes mechanisms for denitrification and nitrate reduction based on those for nitrification. It also suggests mechanisms for the oxidation of methane.

Fluid mixing is investigated and a mixing model is proposed which describes vessels with mean residence times greater than their space times.

ABBREVIATIONS

ADP	Adenosine diphosphate
ATP	Adenosine triphosphate
B.O.D.	Biological Oxygen demand
L.H.S.	Left Hand Side
NAD^+, NADH	Nicotinamide adenine dinucleotide
R.H.S.	Right Hand Side
U.S.E.P.A.	United States Environmental Protection Agency

NOMENCLATURE

a	Constant used by equation 55 to determine equilibrium constants (degrees Kelvin).
$B_{n\,j}$	as defined by equation 34.
b	Constant used by equation 55 to determine equilibrium constants.
C_A	Concentration of reactant A. (mg/l -N or mmol/l)
C_{AF}	Final concentration of reactant A. (mg/l -N or mmol/l)
C_{AI}	Initial concentration of reactant A. (mg/l -N or mmol/l)
C_{AP}	Concentration of reactant A for plug flow. (mg/l -N or mmol/l)
$C_{n\,j}$	as determined in equation 34.
C_1 , C_2	Concentration of tracer in tanks 1 and 2. (kg/m^3 or mol/m^3)
c	Constant used by equation 55 to determine equilibrium constants (degrees $Kelvin^{-1}$).
D	Apparent diffusion coefficient.
E	Exit age distribution in mixing studies. (min^{-1})
E	Dimensionless exit age distribution in mixing studies.
E	Enzyme concentration (kg/m^3).
f	Flow velocity through soil column (ms^{-1}).
ΔG	Gibbs free energy (kJ/mol).
h	Hill coefficient.
i	Inhibitor concentration (kg/m^3).

K1, K2	as defined by on page 38.
K_m, K_m^{app}	Michaelis-Menten constant and apparent constant. (kg/m^3)
k_s	Monod coefficient (kg/M^3).
$K_{subscript}$	Equilibrium constant for subscripted component.
k_d	Cell decay rate (s^{-1}).
k_h	Equilibrium constant for the Hill equation (units dependent on the Hill coefficient).
$k_{subscript}$	Rate constants as defined in the rate equation (units dependent on the reaction order).
L	Percentage of maximum stem travel.
m	Molecularity of binding.
M_I	Mass of bacteria at influent (mg).
n	Number of tanks or cells in series.
n	Order or pseudo order of reaction.
n	Valve-flow coefficient.
N	Number of particles in a given distribution interval.
N	Parameter influenced by enzyme and other substrate concentrations (kg/min).
P	Product concentration (kg/m^3).
p	Flowrate into the dead volume (l/min).
Q	Percentage of maximum flow.
q	Flowrate through the vessel (l/min).
R	Recycle ratio in recycled crossflow model.
r_A	Rate of reaction for reactant A (kg/m^3).
r'_A	Rate of reaction for reactant A compensated for growth along the filter length (kg/m^3).

r_1 , r_2	as defined by equation 32.
S, s	Concentration of substrate (mg/l-N of kg/m^3).
S_0 K_0	Yield coefficent for a continuous process.
s_0	Inlet substrate concentration (mg/l-N, mmol/l or kg/m^3).
T	Actual reaction time (min).
T	Temperature (Kelvin).
T_{MM}	Time predicted by Michaelis-Menten kinetics (min).
T_P	Time predicted for a specified rate equation assuming plug flow (min).
t	Time (min).
t	Mean residence time (min).
V	Volume of vessel (litres).
V_1 , V_2	Volume of each split tank in figure 4 (litres).
V', V^{APP}	Maximum rate velocity for Michaelis-Menten kinetics (s^{-1}).
v, v_1 , v_2	Flowrates into the split tanks of figure 4 (l/min).
X	Cell concentration (kg/m^3).
Xm	Mean size of particle in a distribution interval (mm).
X, x	Intermediate concentration (kg/m^3).
x	Distance through column (m).
Y	Fractional saturation of binding sites.
$Y_{x/s}$	Cell yield.
$Y_{p/s}$	Product yield.
α	Fraction of vessel considered as deadspace.
α	As defined on page 171.

$\beta, \alpha, \gamma, \lambda$	As defined on page 35.
λ	Fraction of enzyme not in singly protonated form.
θ	Dimensionless residence time.
μ	Specific-growth-rate-coefficient (s^{-1}).
μ_o	Maximum specific growth rate (s^{-1}).
μ	Central moments.
$\tilde{\tau}$	Space time (min^{-1}).
v, v_o	Rate of reaction and initial rate of reaction (page 143).

INTRODUCTION

This thesis deals with nitrification and other biological reactions associated with inorganic nitrogen. It is based on the requirement to remove low-level ammonia concentrations in recycle aquaculture systems. The scope of the work also extends to many other areas, such as fluid mixing, biological control systems and waste water treatment.

Nitrification in Recycle Aquaculture Systems

Clean, unpolluted water is more essential to the aquaculture industry than any other resource. The maintenance of water quality is of primordial importance to the long-term success of the industry. At present, large-scale aquaculture developments in Scotland concern high-value species, such as salmon and trout. Marine species, such as turbot, cod and halibut, are farmed on an experimental basis.

The use of recycled aquaculture systems has several potential advantages: lower utilization of water resources, independence from weather and seasonal variations, and the control of the environment in order to create optimal conditions for the species being cultured. A limited supply of suitable water (locations) for aquaculture, and legislation to limit effluent discharges can only encourage the greater use of recycle systems. If the water from a once-through system has to be reconditioned, then clearly the aquaculturist has an incentive to reuse it.

The recycling of water in aquaculture systems does create problems as the system becomes more dynamic. The

feeding of the fish and the subsequent metabolites are unsteady-state disturbances to the system. Recycling can therefore create high transient concentrations of toxic chemicals. Thus, maintenance of water quality is a key issue in the advancement of recycle systems.

Recycle systems, with varying degrees of water reuse, are found most frequently in hatcheries. At present, recirculation is involved where energy must be conserved[1], rather than pollution minimized. For example, the water temperature is altered artificially to enhance growth or to determine its timing. In hatching marine species, it is often more cost-effective to recycle the water than to pump filtered seawater to a shore location. However, recycle systems always require some additional water to replace evaporation losses or to purge metal ions from the system. An example of a recycle system is given in figure 1 (see next page).

Recycle systems are currently used to rear the fish to a size where they can be transferred to a loch, pond, or to the sea. The principal reason is one of cost-efficiency. The circulation of water incurs pumping costs and more capital is required for tanks and pipework. However, the return of untreated water to its source incurs no extra cost. This economic situation, in which fish are held in recycle systems until they have reached a certain size, would change if companies were forced to treat metabolic waste. Intensive agriculture and the waste water industry are coming under increased pressure to meet higher water standards. There is no reason to suppose that aquaculture will be able to evade this pressure.

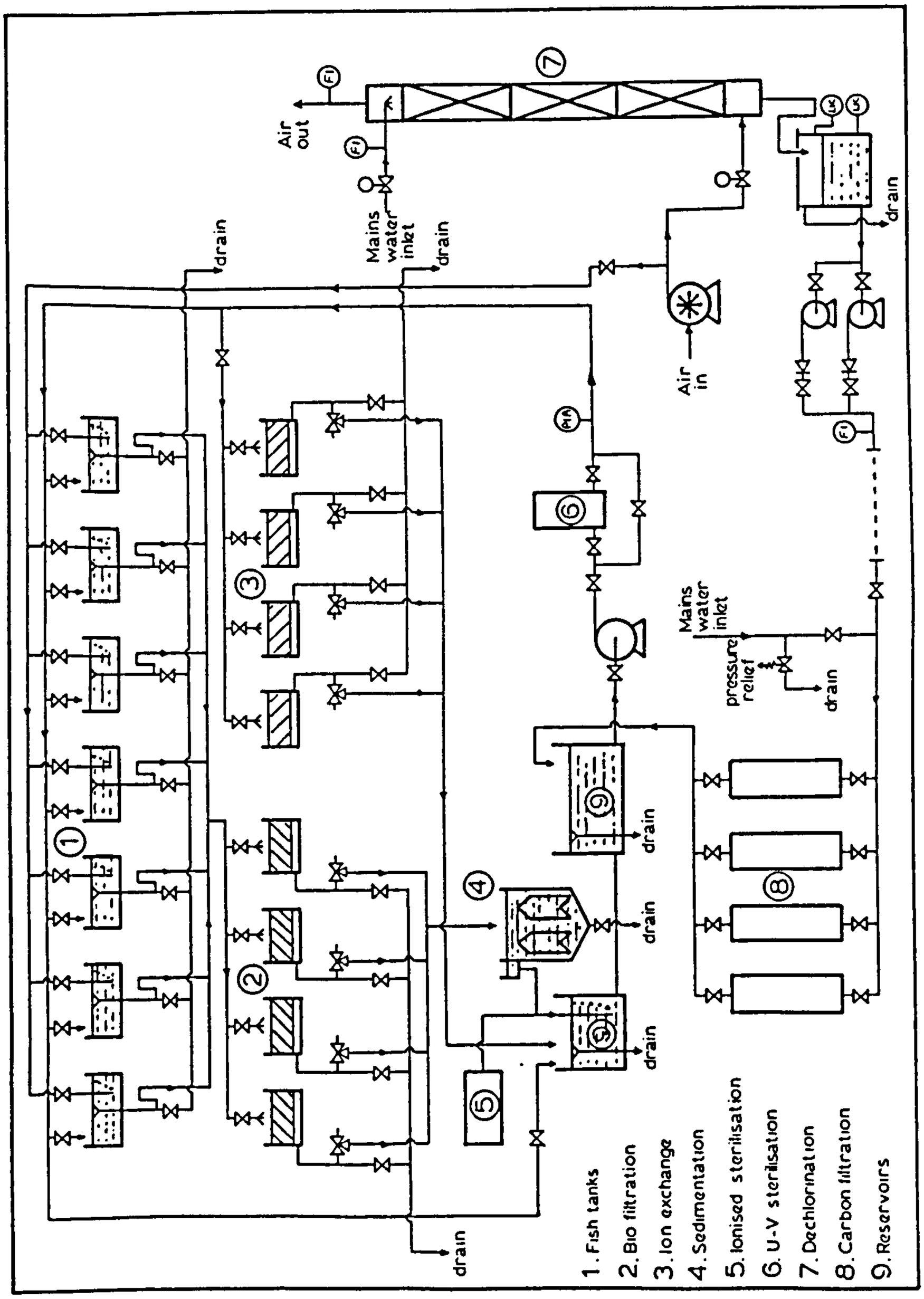

Figure 1. An example of a recycle system.

The minerals, micronutrients and gases found in a natural water source depend on the local geology and geography[2] (Poxton et al.[3] have outlined the minerals in natural sea water). However, most naturally-occurring toxic chemicals are associated with the fish themselves. Urea, uric acid and organic nitrogen compounds are produced as a result of the metabolism of the fish.

The principal method of treating waters containing metabolic waste of animal and human origin is biological filtration[4-14]. This term is used to describe the series of biological reactions that break down complex organic molecules to simple inorganic ones. The reactions are performed by naturally-occurring bacteria, and no filtration in the physical sense occurs.

Aquaculture waste water has a very low biological oxygen demand, compared to most waste water processes. Also, a far greater fraction of the oxygen is required to oxidize inorganic nitrogen compounds. In fish farming, organic sources are excess food and fish excreta. These organics undergo mineralization by two processes, ammonification and deamination. Excess food, in the form of proteins, undergoes ammonification to form organic nitrogen molecules. These molecules and the metabolic products undergo biological breakdown to ammonia by heterotrophic bacteria. This process is named deamination. The main product from these biological processes is ammonia, and an example is the conversion of urea to ammonia and carbon dioxide.

In recycle aquaculture units it is important to keep pathogenic organisms to a minimum and the water as clear as possible. To these ends, solids are removed by sedimentation

tanks or, more recently, by Delta Stack units (K.R. Murray, private communication[15]). Mineralizing bacteria colonize the surfaces of the separating equipment. These bacteria excrete chemicals that bind the insoluble organics before breaking them down to ammonia. The water from the separating equipment therefore contains quantities of ammonia.

Ammonia gas is extremely toxic to life, even in very low concentrations. It is also very soluble in water, forming ammonium ion and ammonia gas. Thus, the toxicity is related to the pH, temperature and ionic strength, all of which determine the amount of ammonia gas (see 5.6.1).

In a recycle aquaculture system, if ammonia is not removed, it will, at higher concentrations, kill the fish. The level of ammonia tolerated depends on the duration of exposure, species of fish, stage of development and their health. Salmonids' growth has been reported[10,16,17] to be impaired at concentrations above 0.01 mg/l NH_3-N. Toxicity data for other species are available[3].

In natural water courses, ammonia is oxidized to nitrite and then nitrate by nitrifying bacteria. These bacteria will colonize most surfaces providing the level of ultraviolet light is low. The nitrates produced are then absorbed by algae and plants to be rebuilt into organic nitrogen molecules, this requiring energy from photosynthesis. In anaerobic conditions, nitrate can be reduced to atmospheric nitrogen by other bacteria. This process requires an energy-rich carbon substrate. The oxygen concentration required by nitrifying bacteria is too high for denitrification and thus both processes are not efficient in the same location.

In recycle aquaculture units, an opaque vessel is filled with a packing which acts in the same way as the stones, pebbles, and sand in a water course. As is common with waste water treatment, this vessel is normally referred to as a biological filter. It is, however, suggested that biological filters containing water from which the solids have previously been removed, are better described as nitrification filters. Diagrams of horizontal submerged nitrification filters, as used in the recycle aquaculture system studied, are given in appendix 3.a. Nitrifying bacteria can also colonize mechanical filters, activated charcoal filters, ion exchange resins, and tank/pipe surfaces. For this reason, it is advisable to have the ammonia removed before units sensitive to blockage are reached.

The process of nitrification yields nitrite and nitrate ions which are both toxic[10,16]. Nitrite concentrations of 0.012 mg/l NO_2-N have been reported[16] to stress salmonids. However, nitrate is much less toxic, and concentrations of 50 mg/l NO_3-N and higher are common in recycle aquaculture systems. It is difficult to attribute changes in fish health to nitrate toxicity. Nitrates are potentially toxic in that they can be reduced biologically to nitrites. Also, nitrate may be toxic only over a long time, complicating any analysis.

Nitrite concentrations are not normally problematic if a steady state is maintained, because the oxidation of nitrite by bacteria is slightly faster than the oxidation of ammonia. However, feeding fish and adding new stock represent unsteady-state situations. These disturbances can

be acute in dynamic recycle systems. In particular, the addition of new stock can cause problems with nitrites. Nitrite-oxidizing bacteria grow at a slower rate than ammonia oxidizers, even though the kinetics of the reaction are slightly faster. (As shown in appendix 5.a, at a pH of 9.0 550 mg/l - N was oxidized by Nitrosomonas in about 17 minutes, but it took Nitrobacter, which prefers low pHs, 15 minutes). The slow growth of Nitrobacter is due to the lower amount of energy involved in nitrite oxidation. Problems of nitrite toxicity may then arise if the aquaculturist does not precondition a filter to handle a given nitrifying load. If any step increase in the nitrifying load, such as unit startup or the addition of new stock, is planned, ammonia must be added to build up the bacterial numbers prior to the introduction of the fish.

Nitrates build up in recycle aquaculture systems and can be removed by algae, plants, denitrification or partial recycle. The solids collected from sedimentation could be used with non-recycled water in a denitrification process. This is, however, problematic, as settled fish farm waste is low in carbon-containing substrates.

The chemical alternative to nitrification is the use of ion exchange to remove the ammonia. Dryden[17] investigated the natural zeolite clinoptilolite. He characterized its capacity and selectivity under conditions representative of those in aquaculture. Ion exchange does, however, have a number of disadvantages. Firstly, ion exchange is not an option in marine or brackish water, and its performance is reduced in hard freshwater. Furthermore, zeolite is smaller than nitrification packing and thus has higher pressure head

losses and clogs more easily. Although the zeolite can be regenerated, it loses performance with time and has to be replaced. The use of zeolite is expensive in comparison to self-regenerating nitrifying bacteria obtainable from a soil sample. In ion exchange systems, both regeneration and performance have to be monitored. Ion exchange removes almost all the ammonia and other ions, but it does so in an uncontrolled manner. It has been advanced that ion exchange copes better with fluctuating loads than nitrification does. Nonetheless, the ability of nitrifying bacteria to adjust to load fluctuations may have been underestimated. The bacteria's control system is discussed in chapter 7.

There are situations in which ion exchange is very useful. An ion exchange column is not affected by antibiotics or drugs used to treat fish. For the transport of live freshwater fish that require ammonia removal, it is also more practical to use ion exchange than to grow nitrifying bacteria in a filter for the journey.

After almost exponential growth in the last decade, salmon farming (and aquaculture) is no longer in its infancy. Hatcheries employing recycle or partial recycle are a recent development, but they are becoming common. However, the growth in the use of recycle systems has yet to produce a unified body of design data. Many of the unit operations such as sedimentation, ion exchange or sterilization are used in the process industry. As a consequence, a lot of design data are available for these unit operations. However, not a great amount of hard engineering data is available for biological filtration, which is a crucial operation in maintaining water quality. Waste water

treatment design data are of limited use because of the very different nature of the waste and the much higher water quality demands. Recycle system design has yet to be integrated, as is commonplace in the continuous process industries. This is largely due to the unquantified nature of biological unit operations, such as nitrification.

Research Objective

The overall research objective was to develop accurate mathematical equations to facilitate the design and simulation of nitrification filters. This objective was tackled in several stages:

1. The literature was reviewed to obtain information on nitrification relevant to conditions found in aquaculture. This encompassed the stoichiometry and the kinetics of the reactions. The various (design) rate equations were critically evaluated (chapter 1). A further review was also conducted into the mechanisms of nitrification, after it was deduced that the reaction mechanisms were responsible for the design problems.

2. Tracer response experiments were conducted to determine the nature of fluid mixing in packed bed biofilters. This work was prompted by the possibility raised (G. Goldsworthy,[18] private communication) that the presence of biomass on the packing could affect mixing. The extent to which the mixing deviated from plug flow was

evaluated (chapter 2) and a new mixing model suitable for describing deadspace was developed.

3. Ten rate equations, resulting from over thirty mechanisms for the oxidation of ammonia, were tested with data collected from submerged packed bed filters (chapter 3). These included all the previously proposed rate and design equations found in the literature.

4. Unsteady-state experiments into the oxidation of ammonia (chapter 5) and nitrite (chapter 6) were conducted. These experiments indicated that bacterial growth (lag phase, logarithmic growth, stationary phase, death phase) was not the principal problem. The unsteady-state experiments also indicated that bicarbonate ions were, in all probability, involved in the reactions. On the basis of the experiments and known organic and inorganic chemistry reactions, new detailed mechanisms for nitrification and other inorganic nitrogen reactions were developed.

5. The unsteady-state experiments also indicated that the enzymes responsible for nitrification are sigmoidal, that is, they react with decreasing sensitivity as substrate concentrations rise. An equation suitable to describe nitrification (and sigmoidal behaviour) was developed, analogous to the equation used for control valves. The method by which nitrification data can be analyzed to obtain the constants in the equation is given (chapter 7).

Experiments and research paths which future investigators might wish to follow are outlined (chapter 8).

CHAPTER 1

PREVIOUS WORK

1.1 Main Sources of Information

It should be said that there is a considerable amount of literature on nitrification and denitrification. The book "Nitrification"[19] and two review papers, "Nitrification and Nitrogen Removal"[20] and "A Review of Literature on Inorganic Nitrogen Metabolism in Microorganisms"[21], provide a good insight into the subject. Much work has been undertaken into the electron transport mechanism and proton pumping in nitrifying bacteria. However, these subjects are outside the scope of this work, because they must rely on an understanding of the nitrification reactions themselves.

Previous work of relevance to nitrification in aquaculture and reported in the literature can broadly be split into three categories:

1.1.1 Data Taken from a Running Aquaculture System

This type of data normally consists of nitrification rates expressed as a percentage of the ammonia or nitrite oxidized. The data normally also contain the dimensions of the biological filter used. No fluid mixing experiments will have been carried out to determine the hydraulics through the filter. The dimensions of the filter are based on the materials available and the design on personal preference. On the whole, these data have been collected by practising aquaculturists or marine biologists.

Whilst this type of data should be of great use in developing rate equations, because it comes from an operational system, in practice this was not found to be the case. In many experiments problems arise from the large number of variables. The more variables, the harder the analysis becomes, and in turn the more information is required. Frequently, many of the key variables have not been recorded in the literature, or the experimental details have not been fully described. As a result, the data are often of limited use.

1.1.2 Nitrification Growth Studies

In general, nitrification growth studies have determined the various species of bacteria that occur and have identified the minerals required for growth[19,20,21,22]. They have also explored the sources of the oxygens in the oxidation through purifying and labelling experiments and the effect of alternative substrates on the growth of nitrifying bacteria. Studies into nitrification rates of reaction have been confined to growing the bacteria and estimating Michaelis-Menten constants. These studies have been carried out on a small-batch scale and cover several temperatures and a few pH-values. Most of these experiments have been carried out by biochemists or microbiologists.

It was not intended at the outset to investigate the reaction mechanisms, but rather to develop rate equations that reflected what occurred in nitrifying filters. However, in attempting to fit the kinetic data, clues to the mechanisms have been revealed. Data from labelling

experiments have helped to indicate the source of the oxygens in the reactions[23,24,25].

1.1.3 Studies to Develop Design Equations

These studies have either come from a pilot rig or from a full-size system. To reduce the number of process variables, assumptions (often unvalidated) have been made to facilitate the analysis of the data. The data normally come from waste water treatment. Thus, this work involves water with high ammonia concentrations and a high biological oxygen demand (B.O.D.). Very few studies have been directed at water with levels of ammonia and B.O.D. found in aquaculture. The data from this type of experiment have usually been fitted to a chosen rate equation, and little attempt has been made to compare these data with any other rate data. These experiments have been conducted by civil engineers or aquaculturists interested in designing aquaculture systems.

1.2 The Nitrification Reactions

There are three areas of investigation into reactions, stoichiometry, kinetics and mechanism. Discoveries in one can lead to insights that require changes in another.

1.2.1 Stoichiometry

The stoichiometry of the oxidation of ammonia to nitrite is given by the United States Environmental Protection Agency[26] as:

$$NH_4^+ + 1.5\ O_2 \longrightarrow 2H^+ + H_2O + NO_2^- \quad (1)$$

The estimated energy released is between 244 and 353 kJ/mol. The hydrogen ions produced are buffered by the bicarbonate system to yield:

$$NH_4^+ + 1.5\ O_2 + 2HCO_3^- \longrightarrow 2H_2CO_3 + H_2O + NO_2^- \quad (2)$$

The stoichiometry given[26] for the oxidation of nitrite to nitrate is:

$$NO_2^- + \tfrac{1}{2}O_2 \longrightarrow NO_3^- \quad (3)$$

The energy released is given as between 64.7 and 87.8 kJ/mol.

1.2.2 Kinetics and Rate Equations

In biological systems there are, or may appear to be, many more variables than in an equivalent chemical process. There are, for example, often many types of bacteria, multiple substrates and a sensitivity to different (local) conditions. The large number of variables perceived as important has meant that assumptions have been made

explicitly or implicity by all investigators. The principal question must then be whether the assumptions are valid.

The types of approach to the problem of nitrification can be split into three categories:

a) Diffusion and Dispersion

The process is treated as being controlled by diffusion/ dispersion[27] and as following a simple reaction order. This approach is similar to that taken in investigating the reaction rate in a catalyzed chemical reaction. It implies that a steady state is assumed to prevail and that the numbers of bacteria and their activity do not change.

A typical example of this approach is the set of partial differential equations given by Cho[28].

$$\frac{\partial NH_4^+}{\partial t} = D\frac{\partial^2 NH_4^+}{\partial x^2} - f\frac{\partial NH_4^+}{\partial x} - k_1\ NH_4^+ \qquad (4)$$

$$\frac{\partial NO_2^-}{\partial t} = D\frac{\partial^2 NO_2^-}{\partial x^2} - f\frac{\partial NO_2^-}{\partial x} - k_2\ NO_2^- - k_1\ NH_4^+ \qquad (5)$$

$$\frac{\partial NO_3^-}{\partial t} = D\frac{\partial^2 NO_3^-}{\partial x^2} - f\frac{\partial NO_3^-}{\partial x} - k_3\ NO_3^- + k_2\ NO_2^- \qquad (6)$$

In the above example, the reaction is assumed to be given by first order kinetics. Jennings et al.[4] developed a theoretical model for a diffusion-limiting biofilm and Monod kinetics. However, they concluded that first order kinetics was a good approximation of their model over a wide range of parameters.

Fluid mixing and dispersion is examined in detail in chapter 2. It will be shown that the inclusion of dispersion becomes an unnecessary complication as it does not control the reaction.

Newton[29] used correlations for fluid film diffusion[30] and found that they gave reaction rates faster than those observed. This implied that nitrification in the concentrations prevailing in aquaculture is not limited by diffusion and that fluid film diffusion, in particular, is not rate-controlling.

b) Michaelis-Menten Kinetics and Bacterial Growth

In the second approach, which has been confined to growth studies conducted on a batch laboratory scale, a specific-growth-rate coefficient is assumed to apply (e.g. Monod). This is then corrected for bacterial growth using assumed yield constants and the kinetic constants estimated. This implies that diffusion and dispersion effects can be ignored. It also assumes that the activity is at a steady state and that, to a certain extent, the bacteria grow steadily.

Monod kinetics with corrections for growth is very frequently used to describe the behaviour of organisms. The Monod equation results from the theory of a rate-limiting nutrient, but the equation has the same form as the Michaelis-Menten equation. In the nitrification literature, authors have often referred to growing bacteria as following Michaelis-Menten kinetics. The equations also often appear with different notation. Equation 7 gives the cell growth,

equation 8 the substrate removal rate and 9 the rate at which the product is formed. The Monod equation 10 relates the specific-growth-rate coefficient to the substrate concentration. These equations are discussed by Atkinson[31] and Sharma et al.[20].

$$\frac{dX}{dt} = (\mu - k_d)\,X \qquad (7)$$

$$-\frac{ds}{dt} = \frac{1}{Y_{x/s}}\,\mu X \qquad (8)$$

$$\frac{dp}{dt} = \frac{Y_{p/s}}{Y_{x/s}}\,\mu\,X \qquad (9)$$

$$\mu = \frac{\mu_0 s}{k_s + s} \qquad (10)$$

By assuming certain cell and product yields, data from growth studies have been used to obtain the rate constants. Knowles et al.[32] and Poduska et al.[3] both used a computer to fit the experimental data and assumed yield co-efficients. Knowles's experiments were conducted at concentrations less than 1 mg/l nitrogen and are thus relevant to aquaculture.

Ammonia gas concentrations of greater than 0.1 mg/l-nitrogen have been reported to inhibit nitrite oxidation[33], but these concentrations are fatal to fish.

c) Fixed Bacterial Populations at Steady State

Other studies have used data from continuous (full or pilot scale) nitrification filters. The data have been used to develop rate or design equations on the basis that the bacterial concentration remained constant. Dispersion and diffusion have been assumed not to influence the reaction, and it has been assumed that the activity was at a steady state. Several authors have suggested a wide range of reaction orders for ammonia oxidation.

Weatherley[8] calculated first order rate constants covering the pH ranges, temperatures and dissolved oxygen concentrations found in aquaculture. However, the data were not very extensive and came from a small experimental rig.

Newton[29] used the integrated plot for Michaelis-Menten (saturation) kinetics on data from two submerged aquaculture filters believed to have a fixed bacterial population. It was shown that the reaction followed Michaelis-Menten (saturation) kinetics at a given residence time. However, it was pointed out that strong deviations occurred with different residence times. For now, the rate equations for saturation kinetics and Michaelis-Menten kinetics will be taken as equivalent. In chapter 7 (7.1.5) the subtle differences will be discussed.

Huang[34], Metcalf and Eddy[35] suggested zero order, their experiments being conducted at concentrations of greater than 2.5 mg/l nitrogen. Anthonisen[33] found that ammonia oxidation was inhibited at free (gas) ammonia-N concentrations of above 10 mg/l ammonia gas.

Srna and Baggley[14] conducted experiments on a large

trickling filter with a slow recycle. They treated the system as a batch reactor, and no attempt was made to investigate the fluid flow, check the validity of the implicit assumptions or correct for any possible air stripping. Zero and first order kinetics were the only reaction orders they tested.

Forster[9] noticed higher ammonia oxidation rates at higher fluid flowrates, as did Brune and Gunther[7]. Brune and Gunther, who did not present the data in a standard format, suggested that a particular packing was responsible for the increased performance. Similar increases in performance are seen in the data collected from the recycle aquaculture system (see figures 27 and 28), although the packing used was limestone chips. As is explained in detail in chapter 7, the observed increase in performance is proposed to be due to the bacteria's control system.

Haug and McCarty[6] attempted to fit nitrification data from a pilot water treatment plant. They gave an empirical reaction order of between 0.94 and 1.48 for ammonia oxidation. However, the method used to estimate the rate of reaction by Haug et al.[6] and also by Brune et al.[7] is a poor one, as is explained below.

The rate of change or derivative of a function, $y = f(x)$, is defined by:

$$f'(x) = \lim_{\Delta x \to 0} \frac{\Delta y}{\Delta x} \qquad (11)$$

By definition, the influent minus effluent concentration all divided by the residence time only gives the reaction rate, as the residence time tends to zero.

Since the residence time in the experiments was measured in minutes, it cannot be assumed to tend to zero. The error in the estimation increases with longer residence times.

It is also worth examining the relationship discovered by Brune and Gunther. To test a rate equation, the most accurate method is to integrate it. If the nitrification filter is assumed to approximate plug flow, then the space time (volume/flowrate) is given by:

$$\tau = - \int_{C_{AI}}^{C_{AF}} \frac{d\ C_A}{-\ r_A} \qquad (12)$$

$$-\ r_A = \frac{k_1\ C_A}{1 + k_2\ C_A} \qquad (13)$$

Separating variables and Integrating equation (13) which describes saturation (Michaelis-Menten) kinetics, one obtains the plot for saturation kinetics:

$$\frac{\ln\ (C_{AI}\ /\ C_{AF})}{(\ C_{AI} - C_{AF}\ )} = \frac{k_1 \tau}{(\ C_{AI} - C_{AF}\ )} - k_2 \qquad (14)$$

If equation 14 is inverted, the L.H.S. gives a log mean concentration. The R.H.S. then contains the term that Brune and Gunther plotted, plus a constant. Thus the "discovered" plot is a similar but incorrect form of the one for Michaelis-Menten kinetics.

Hirayama[13] developed a design equation for aquaculture

based on oxygen consumption during filtration. The rate of oxygen consumption was assumed to be second order. The implicit assumption was that oxygen is the rate-limiting step. This was shown to be untrue[6], unless it fell below stoichiometric requirements. Using the integrated second order rate equation, it is not possible to obtain the equation that Hirayama used as the basis of the design equation. It is therefore assumed that a mistake has been made in the method of calculating the reaction rate.

Liao and Mayo[10] developed a steady-state equation to "predict metabolic by-product concentration in a rearing unit at any degree of water reuse and treatment". However, the equation as presented is not very useful, because the removal efficiency depends on the metabolic by-product concentration as well as on many other factors (e.g the residence time in the filter) not considered.

1.2.3 Mechanisms

The oxidation of ammonia to nitrite requires the removal of three protons and the addition of two oxygen molecules. The oxidation of nitrite to nitrate requires the addition of a further oxygen. The free-energy diagram for nitrogen indicates that ammonia has an oxidation state of -3, nitrite +3 and nitrate +5. Thus it has always been realized that the oxidation of ammonia to nitrite must occur via several steps.

It has been theorized that ammonia is first oxidized to hydroxylamine (oxidation state -1) and then to another intermediate[36,37]. This second intermediate has been

postulated to be hyponitrite, dihydroxyammonia, nitroxyl, and nitrohydroxylamine[21]. However, biochemical investigations since the early 1950s have totally failed to observe any of the postulated secondary intermediates. This second step is currently represented by a question mark in reaction mechanisms, in recognition of the fact that the intermediate is unknown. It has been postulated that the oxidation of ammonia takes place by at least three steps, each consisting of two electron changes[38]:

$$\underset{[-3]}{NH_4^+} + \tfrac{1}{2}O \longrightarrow \underset{[-1]}{NH_2OH} + H^+ \longrightarrow \underset{[+1]}{?} \longrightarrow \underset{[+3]}{NO_2^-} \qquad (15)$$

The first postulated intermediate, *hydroxylamine, has never been observed during the normal oxidation of ammonia either*. Authors have not represented, however, the first intermediate by a question mark. Before discussing hydroxylamine as an intermediate further, two well-known properties of hydroxylamine require emphasis.

The first important fact is that the oxidation of ammonium ions to hydroxylamine requires 17 kJ/mol of energy[39]. Thus its formation is thermodynamically unfavourable and energy must be supplied if the reaction is to overcome this barrier.

The second fact is that hydroxylamine is mutagenic and highly toxic to living cells. In addition, its toxicity, unlike that of ammonia, is insensitive to pH. Hydroxylamine is not converted to its ionic form until the pH (see figure 22) falls below pH 4.

The addition of hydroxylamine to Nitrosomonas cells in

concentrations as low as a few micrograms per litre inhibits the oxidation of ammonia. However, Lees (1952) discovered that if the concentration of added hydroxylamine was below 1.5 micro g/ml N the hydroxylamine was oxidized. Secondly, he observed that the hydroxylamine was oxidized "a good deal more rapidly than ammonia". On this basis, he said, "it seems probable that hydroxylamine is an intermediate compound in the nitrification of ammonia". A second set of experiments was then conducted by Hofman and Lees[37], using hydrazine. Hydrazine is an inhibitor of ammonia oxidation although its *mode of action has not been demonstrated.* Hofman and Lees's experiment consisted of incubating Nitrosomonas cells with ammonia and hydrazine for 30 minutes. They observed that trace amounts of hydroxylamine accumulated. Consequently, they postulated that hydroxylamine, resulting from ammonia oxidation, accumulated because of hydrazine inhibiting the oxidation of the second intermediate. This experiment was later repeated by Yoshida and Alexander[41], using another assay for hydroxylamine. The repeated experiment indicated that 2.63 p.p.m.- N hydroxylamine and 6.3 p.p.m. - N nitrite accumulated over 60 minutes. However, in all their experiments no hydroxylamine was ever observed without the addition of hydrazine. Yoshida and Alexander stated that the hydroxylamine could be "in equilibrium with an enzymatically or organically bound form of hydroxylamine"[41]. This statement still remains valid. No new experimental evidence has been presented to indicate that hydroxylamine is the intermediate, as opposed to an organic form of hydroxylamine.

Unfortunately, recent authors have interpreted the data

as indicating that hydroxylamine itself is the intermediate. The possibility that a hydroxylamine compound or organically bound form of hydroxylamine could be the intermediate has been overlooked. This is possibly due to the title of Lees's paper, "hydroxylamine as an intermediate in nitrification"[40], as well as Hofman and Lees's [37] experiments with hydrazine. However, their analysis relies solely upon an unstated assumption. The assumption made by Hofman and Lees, as well as by more recent authors, is that (the trace amounts of) hydroxylamine results from the direct oxidation of ammonia. The possibility that it could arise from the breakdown of the intermediate has not been considered.

The question of hydroxylamine's thermodynamic barrier and its toxicity has not been addressed either. In addition, the chemistry of ammonia oxidation has not been closely examined. Biochemistry follows all the rules of organic chemistry, although the reactants may come from unusual sources. Attention should be paid to the probable chemical reactions involved.

Hydroxylamine has not been established as an intermediate, even though it has frequently and confidently been repeated as such. It would require the specific and unequivocal observation of hydroxylamine during the normal oxidation of ammonia to identify it as an intermediate. Despite increasingly powerful analytical techniques over almost forty years, hydroxylamine has yet to be observed during the normal oxidation of ammonia. The fact that it has not been discovered is even more surprising since the intermediate must travel between the two enzymes known to be

involved. Hydroxylamine must be oxidized to a second intermediate closely related to it. Despite testing many chemicals, the second intermediate's identity has not been established.

In summary, the experimental findings are:

1. No hydroxylamine has ever been discovered during the normal oxidation of ammonia.
2. The second intermediate in the oxidation of ammonia remains undetected.
3. Trace amounts of hydroxylamine accumulate during the oxidation of ammonia with hydrazine.
4. Trace amounts of hydroxylamine are oxidized to nitrite, larger amounts are inhibitory.
5. Trace amounts of hydroxylamine are oxidized faster than ammonia.

No detailed mechanism has been proposed in the literature for the oxidation of ammonia. However, hydroxylamine as an intermediate implies a certain reaction mechanism. This mechanism, as presented in the literature[39], is now given.

The enzyme ammonia (ammonium) mono-oxygenase is said to oxidize ammonia to hydroxylamine. It has been debated whether the true substrate of the mono-oxygenase is ammonia gas or ammonium ion. The oxygen in hydroxylamine, obtained by the addition of hydrazine, is known to come from

atmospheric oxygen[23,24]. The implied mechanism for the case of ammonia gas is:

$$NH_3 + O_2 + 2[H] \longrightarrow NH_2OH + H_2O \quad (16)$$

The direct oxidation of ammonium ions is given by:

$$NH_4^+ + \tfrac{1}{2}O_2 \longrightarrow NH_2OH + H^+ \quad (17)$$

The oxidation of hydroxylamine to nitrite is then said to be brought about by an enzyme, thus named hydroxylamine oxidoreductase, and water is the source of the additional oxygen[24]. The stoichiometry thus becomes:

$$NH_2OH + H_2O \longrightarrow NO_2^- \; 5H^+ + 4e^- \quad (18)$$

The implied mechanism for the step between hydroxylamine and nitrite is[39]:

$$E + H_2NOH \longrightarrow E\text{-}NO^+ + 3H^+ + 4e^- \quad (19)$$

$$E\text{-}NO^+ + H_2O \longrightarrow E + NO_2^- + 2H^+ \quad (20)$$

The chemical method by which the protons and electrons are removed has not been given. The removed electrons are said to be transported by various cytochromes, and several electron transport systems have been proposed for both bacteria. Examples are contained in "Nitrification"[19]. It has been suggested that proton pumping occurs[29], driving the synthesis of ATP, which is required for growth. Proton

pumping relies on an organism being able to generate and maintain a significant proton gradient across a membrane. This proton gradient is then used to generate ATP from ADP (+ Pi).

Nitrite oxidation is said to occur "without detectable intermediates"[42] by the enzyme nitrite oxidoreductase, and from isotope studies it has been shown that the oxygen required comes from water[43]. This gives a stoichiometry of:

$$NO_2^- + H_2O \longrightarrow NO_3^- + 2H^+ + 2e^- \qquad (21)$$

No mechanisms compatible with this stoichiometry have been proposed in the literature. Lees and Simpson[44] proposed a mechanism that involved the oxygen required coming from atmospheric oxygen. This mechanism has now been discounted as a result of the isotope labelling experiments. The actual form the substrate takes (ionic or not) has not been established. The method by which the electrons and protons might be obtained has not been given, as in the implied mechanism for ammonia oxidation. Proton pumping has also been suggested for the production of ATP for growth.

No detailed mechanisms for denitrification have been proposed in the literature although nitrite has been established as the starting point for the reaction[25]. It has also been established that hyponitrite, nitroxyl, nitramide and dihydroxyammonia are not intermediates[21].

CHAPTER 2

FLUID FLOW AS A VARIABLE IN NITRIFICATION KINETICS

This chapter of the thesis evaluates the effect that fluid mixing and deadspace had on the collected nitrification data[29]. Experimental tracer response data obtained by the author[29] from a packed bed biofilter are re-analyzed. The E-curves from the tracer data had long tails, indicating deadspace. Deadspace does not contribute to conversion and is thus undesirable. To evaluate the size of the deadspace, several well-known models were evaluated, but they did not accurately represent the deadspace. A mixing model which does appear to represent deadspace is developed. Deadspace is believed to be a result of sudden contractions and expansions in the fluid flow stream. Thus, they can be eliminated by careful design. The effect that deviations from plug flow have on the nitrification reaction is evaluated using the equation of Pasquon and Dente[41].

2.1 Multi-Parameter Mixing Models for Quantifying Deadspace

The author's initial analysis of the mixing data has already been published[45] (a copy of the paper is presented in appendix 2.a). Several of the most commonly suggested mixing models in the literature, including the Deans[46]-Levich[47] model, were tested. The use of moments to fit the parameters of the models was found to be unsatisfactory. It was recommended that curve-fitting should be used to fit the parameters of the models. The method of weighting the curves was also found to be subjective and not very satisfactory.

The two multi-parameter models tested were termed the "tanks in series with deadspace" and the "tanks in series with crossflow model". The "tanks in series with crossflow model" was developed to quantify mixing through a porous medium with stagnant zones. The model was found to give a reasonable approximation if the peak height was used to obtain the fractional deadspace. However, at low fluid velocities there was a significant decrease in the quality of the fit. The models were tested using the computer program described in the next section.

2.2 Fitting the Deans-Levich Model

A computer program was written to fit the Deans-Levich model. The language used was PASCAL, which meant that the program would be easily portable between micro computers and the university mainframe. The program was written in "MCC Pascal" on a Commodore Amiga, using "ISO Pascal" where practical. Extensions used are common to "Turbo Pascal" and "VAX Pascal". The actual dimensionless E-curve was tested against the calculated dimensionless E-curve by the sum of least squares method.

Many methods for minimizing functions exist, but most of them rely on having the derivative of the function. Suitable "canned" minimization programs (for example NAG routines on the mainframe) were available. These were not used, because it would have been hard to determine the cause of any convergence difficulties without the program code. For this reason, a minimization method based on that described in BASIC Optimisation Methods[48] was used.

The minimizing routine used was a modification by Box[49] of the simplex method of Nelder and Mead[50]. The simplex method is given and described later in the thesis (see 3.2). Box's method is used when the variables must be restrained. The routine was converted from BASIC to PASCAL.

The program is given in appendix 2.b and obtains the parameters for multiple recycled crossflow cells (see 2.4). This model is a more general solution than the Deans-Levich model, which is a special case for which the recycle ratio is zero. It is easy to alter the program to test the Deans-Levich model. The explicit constraints are that the crossflow and the recycle ratios are limited to values between zero and unity. In addition, the explicit constraint that the dead fraction should be within the possible limits was imposed. The model is fitted for a number of cells in series supplied by the user. Care must be shown in ensuring that the initial conditions are within the explicit and implicit constraints. Any 16-bit number can be used as the seed for the random number generator. Testing the model when more than 17 cells are in series requires that the factorials and powers are calculated as 32-bit numbers (double precision). 17 cells, for example, require the calculation of 34 factorial, which is (approx. $2.95*10^{38}$) at the limit of single precision.

Using this program, the behaviour of large numbers of cells in series can be studied. It was found that with high numbers of cells in series the solution is insensitive to changes in the variables. The overriding variable that determines the quality of the fit is the bulk fluid tank residence time ($v(1-\alpha)/q$). The bulk fluid tank residence

time dictates how much of a tail is possible. This illustrates the inadequacy of the Deans-Levich model.

2.3 The Mixing Model Puzzle

The Deans-Levich model is a complex mixing model developed to quantify mixing through a porous medium with stagnant zones. However, it failed to fit the data collected[29] (unbound material on magnetic media) any better than the "tanks in series with deadspace" model. The raw data contained on the magnetic media is presented in appendix 2.c.

The assumed reasons for the poor fits are enlisted under reference 45 and, in summary, the tested mixing models do not give the long tails observed in the tracer data for large numbers of tanks or cells.

The explanation of the causes of deadspace given by Levenspiel[31] is that fluid is held up in stagnant pockets at the contact points or by absorption on the solid surface. A sketch of a typical E-curve is given (see figure 2), as shown in the paper by Levich et al.[47], and a sketch of the tanks in series with crossflow model is shown. However, the problem with the Deans-Levich model is that it does not behave as suggested in the diagram. The mixing model can give long tails for a couple of tanks in series, but not for a large number, as has been suggested. Flow in packed beds normally yields values for numbers of tanks greater than twenty[31]. Thus, the Deans-Levich model should not be expected to yield long tails in packed beds.

The failure in fitting the Deans-Levich model suggested

that another mechanism was responsible for the long tails. The mean residence time or first moment was observed to be different from the volumetric hold-up divided by the flowrate (the ideal mean residence time). In all of the models given earlier (see appendix 2.a), the mean residence time is equal to the ideal value.

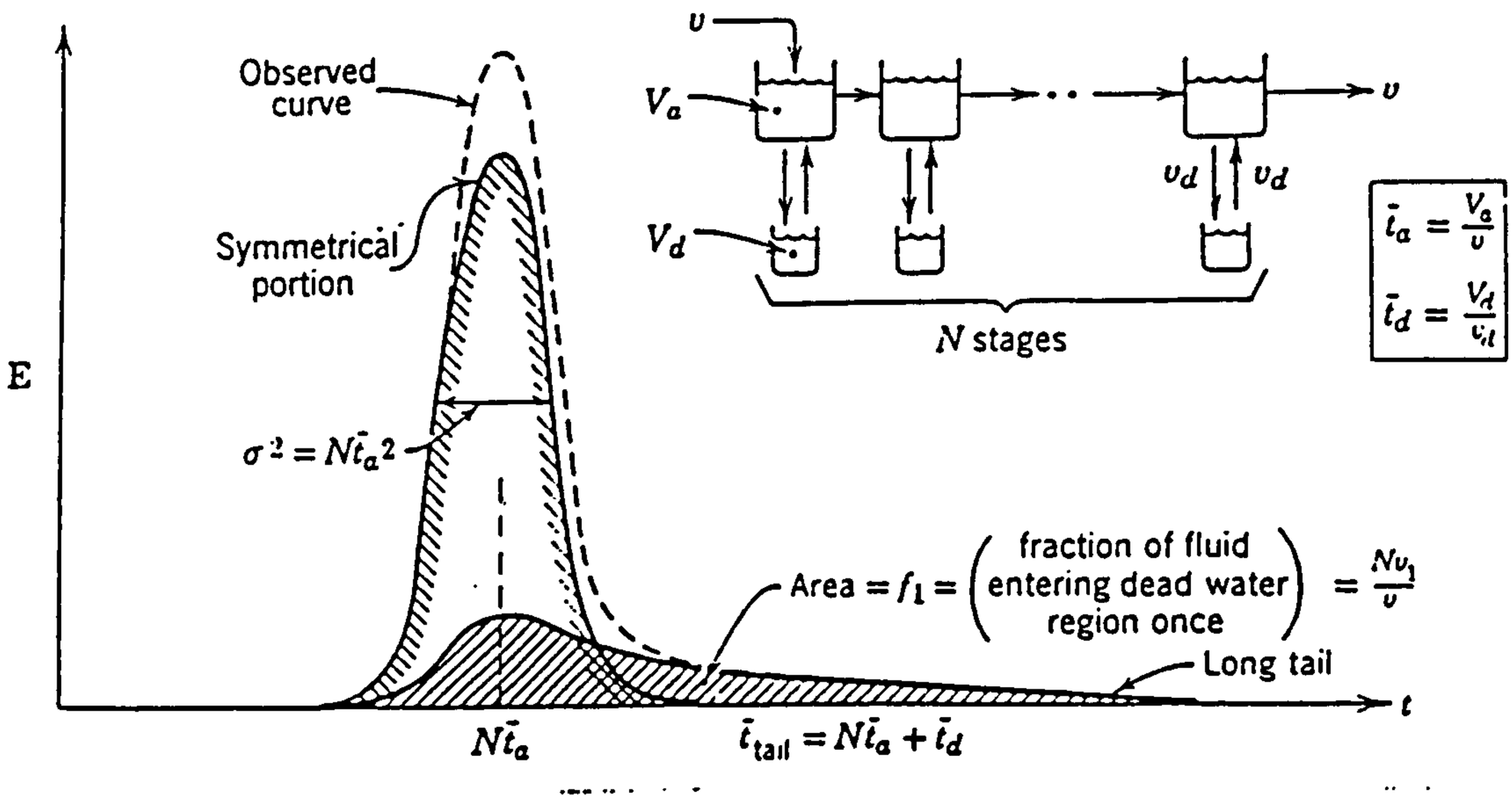

Figure 2. The Deans-Levich Model as sketched by Levenspiel.

A fluid mixing model was developed using the idea that the mean residence time could be greater than the fluid volume divided by the flowrate. In developing the mixing model, it was felt that an analytical solution was desirable in order to curve-fit the data. This suggested that dispersion models would not be suitable because they require boundary conditions, which often do not give analytical solutions. The model was named the "Recycled Crossflow Model" and is now described.

2.4 The Recycled Crossflow Model

The basis for the model is two tanks, one representing the "bulk fluid" volume and the other the "dead" volume. The fluid in the dead volume must have the ability to increase the mean residence time. The model is an adaptation of an existing one used to model real stirred tanks[51]. The Laplace transform for a single tank (cell) is developed first. Integration gives the exit age distribution (E-curve) of the fluid to an idealized pulse of tracer entering the vessel.

The first step is to derive the differential equation for each fluid volume. A diagram of the model is given below:

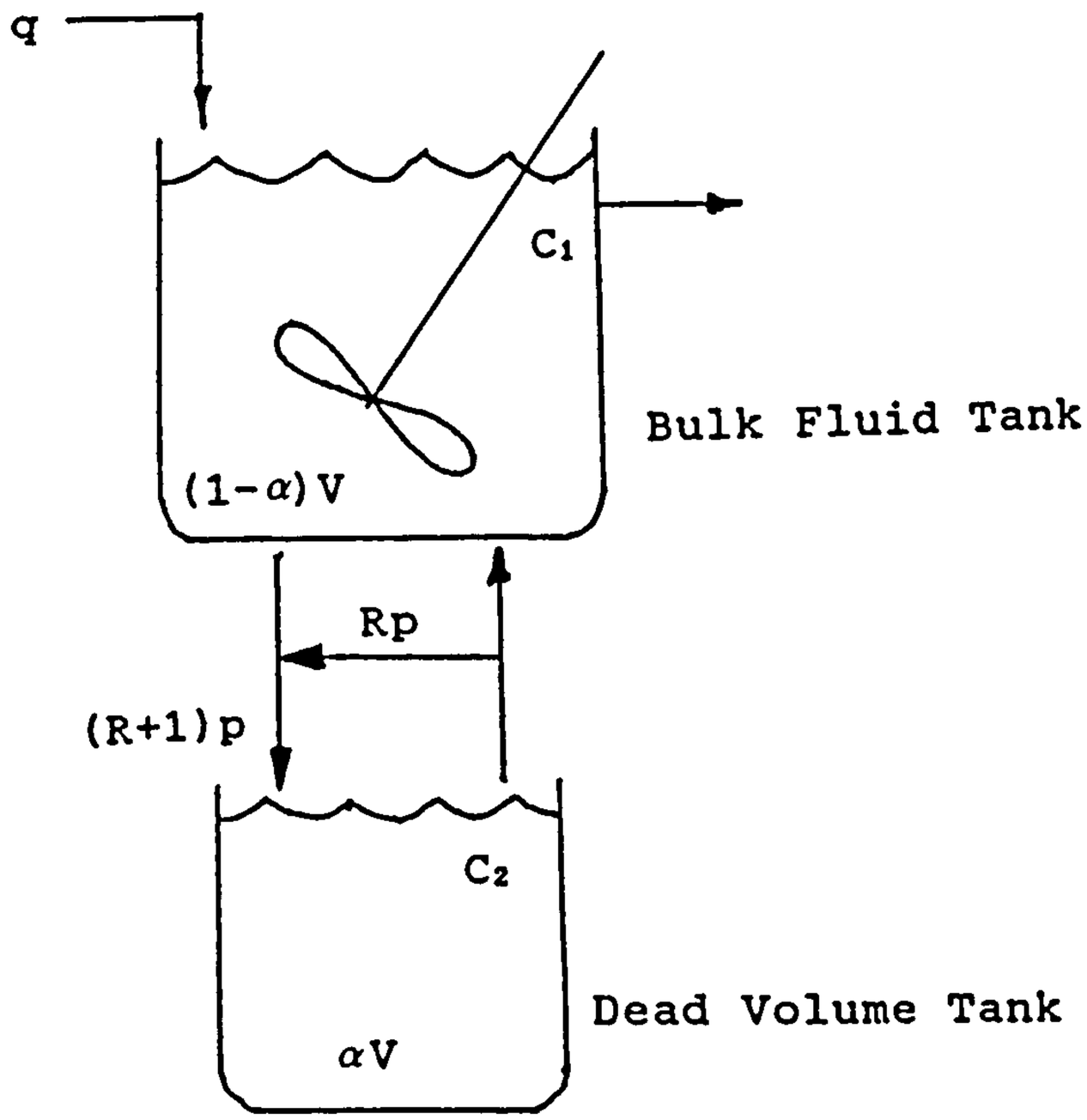

Figure 3. The proposed recycled crossflow cell.

Performing a mass balance on the bulk fluid tank yields:

$$(1-\alpha)V\frac{dC_1}{dt} = -(q+p)C_1 + pC_2 \quad (22)$$

The mass balance for the dead volume tank yields:

$$\alpha V\frac{dC_2}{dt} = p(C_1 + RC_2) - pC_2 \quad (23)$$

and gathering terms leads to:

$$\frac{\alpha V}{p}\frac{dC_2}{dt} = C_1 + (R-1)C_2 \quad (24)$$

Using the same parameters as Levich[47] and Buffham[52], the equations can be written:

If $\gamma = \frac{p}{\alpha V}$; $\upsilon = \frac{p}{(1-\alpha)V}$; $\lambda = \frac{q}{(1-\alpha)V}$

$$\frac{dC_1}{dt} = \upsilon C_2 - C_1(\lambda + \upsilon) \quad (25)$$

$$\frac{dC_2}{dt} = \gamma C_1 + (R-1)\gamma C_2 \quad (26)$$

The initial conditions are :

$$C_1(0) = \frac{1}{(1-\alpha)V} \quad ; \quad C_2(0) = 0 \ ;$$

Thus taking Laplace transforms:

for equation 25.

$$r\tilde{C}_1(r) - C_1(0) = \gamma\tilde{C}_2(r) - \tilde{C}_1(r)(\lambda + \upsilon)$$

$$(r + \lambda + \upsilon)\tilde{C}_1(r) - \upsilon\tilde{C}_2(r) = C_1(0) = 1/((1-\alpha)V) \qquad (27)$$

for equation 26.

$$r\tilde{C}_2(r) - C_2(0) = \gamma\tilde{C}_1(r) + (R-1)\gamma\tilde{C}_2(r)$$

$$(r + (1-R)\gamma)\tilde{C}_2(r) - \gamma\tilde{C}_1(r) = C_2(0) = 0$$

$$C_2(r) = \frac{\gamma\tilde{C}_1(r)}{(r + (1-R)\gamma)} \qquad (28)$$

substituting $C_2(r)$ into equation 25.

$$(r + \lambda + \upsilon)\tilde{C}_1(r) - \frac{\upsilon\gamma\tilde{C}_1(r)}{(r + (1-R)\gamma)} = \frac{1}{(1-\alpha)V} \qquad (29)$$

Multiplying by q as $F(t) = q\,C_1(t)$ we have:

$$f(r) = \frac{\lambda(r + (1-R))}{(r + \lambda + \upsilon)(r + (1-R)\gamma) - \upsilon\gamma} \qquad (30)$$

If we now create another parameter that contains the recycle ratio we obtain:

Let $\beta = (1-R)\gamma$

$$f(r) = \frac{\lambda(r + \beta)}{r^2 + r(\lambda+v+ \beta) + (\beta(\lambda+v) - v\gamma)} \qquad (31)$$

This equation could be integrated to yield the exit age distribution for a single tank. However, it is not too difficult to give the general solution for several cells (tanks) in series. Buffham and Gibilaro[32] have already given the solution to the Deans-Levich model and it is possible to use the same solution method.

For a series of cells, the poles of the Laurent series then become:

$$r_1, r_2 = \frac{(\lambda + v + \beta) \mp \sqrt{((\lambda +v+ \beta)^2 - 4(\beta(\lambda + v) - v\gamma)}}{2} \qquad (32)$$

The solution to the model for n number of the cells in series then becomes:

$$f_n(t) = K1\left(\sum_{j=0}^{n-1} B_{nj}\, t^j\right) Exp(-r_1 t) + K2\left(\sum_{j=0}^{n-1} C_{nj}\, t^j\right) Exp(-r_2 t) \qquad (33)$$

where:

$$B_{nj} = \frac{n}{j!} \sum_{k=0}^{n-1-j} \frac{(-1)^{n-1-j-k} (2n-2-j-k)!}{k!(n-k)!(n-1-j-k)!(\beta-r_1)^{k} (r_2-r_1)^{n-1-j-k}} \qquad (34)$$

C_{nj} is obtained by interchanging r_1 and r_2.

and $K1 = \lambda(\beta - r_1)/(r_2 - r_1)$; $K2 = \lambda(\beta - r_2)/(r_1 - r_2)$;

note:- $f_n(t)$ is the exit age distribution or E-curve.

The procedure for obtaining the moments of the recycled crossflow model is now described.

2.5 Moments of the Recycled Crossflow Model

The moments of the model can be obtained by differentiation of the Laplace transform for a single cell (equation 31). The k-th moment is then given by:

$$\mu_k = (-1)^k \lim_{r \to 0} \frac{d^k f(r)}{dr^k} \qquad (35)$$

The cumulants of the distribution are given by the central moments. A property of cumulants is that they are additive for independent systems in series. Thus the solution for multiple mixing cells is obtained by multiplying the cumulants by the number of cells. The first three cumulants are equal to their central moments. For more details see "Kendall's Advanced Theory of Statistics"[53].

The first four central moments for the recycled

crossflow model were found using a mathematical package "MACSYMA". The moments are long expressions and only the first is given here.

The first moment or mean residence time is given by:

$$\bar{t} = \frac{nV}{q}\left[\frac{(R-1)^2 + \alpha R(2-R)}{(R-1)^2 + (p/q)R(R(p/q)+2R-2)}\right] \qquad (36)$$

This differs from the model without recycle (i.e. the Deans-Levich model). The recycle ratio, the crossflow ratio and the deadspace fraction all contribute to the mean residence time. Deadspace then exists when:

$$\frac{(R-1)^2 + \alpha R(2-R)}{(R-1)^2 + (p/q)R(R(p/q)+2R-2)} > 1 \qquad (37)$$

2.6 Similarities with Other Mixing Models

The general solution for multiple recycled crossflow cells is given in section 2.4. However, the solution for a single recycled crossflow cell is of particular interest. Substituting for a single cell (n = 1) into equation 33, one obtains:

$$f_1(t) = E = K1\ \mathrm{Exp}(-r_1 t) + K2\ \mathrm{Exp}(-r_2 t) \qquad (38)$$

This has the same form as a well-known model in which fluid is split into two mixing tanks with the exits recombined (see figure 4). The E curve of this model is given by the equation:

$$E = (v_1 / v)/\bar{t}_1 \ \mathrm{Exp}(-t/\bar{t}_1) + (v_2 / v)/\bar{t}_2 \ \mathrm{Exp}(-t/\bar{t}_2) \qquad (39)$$

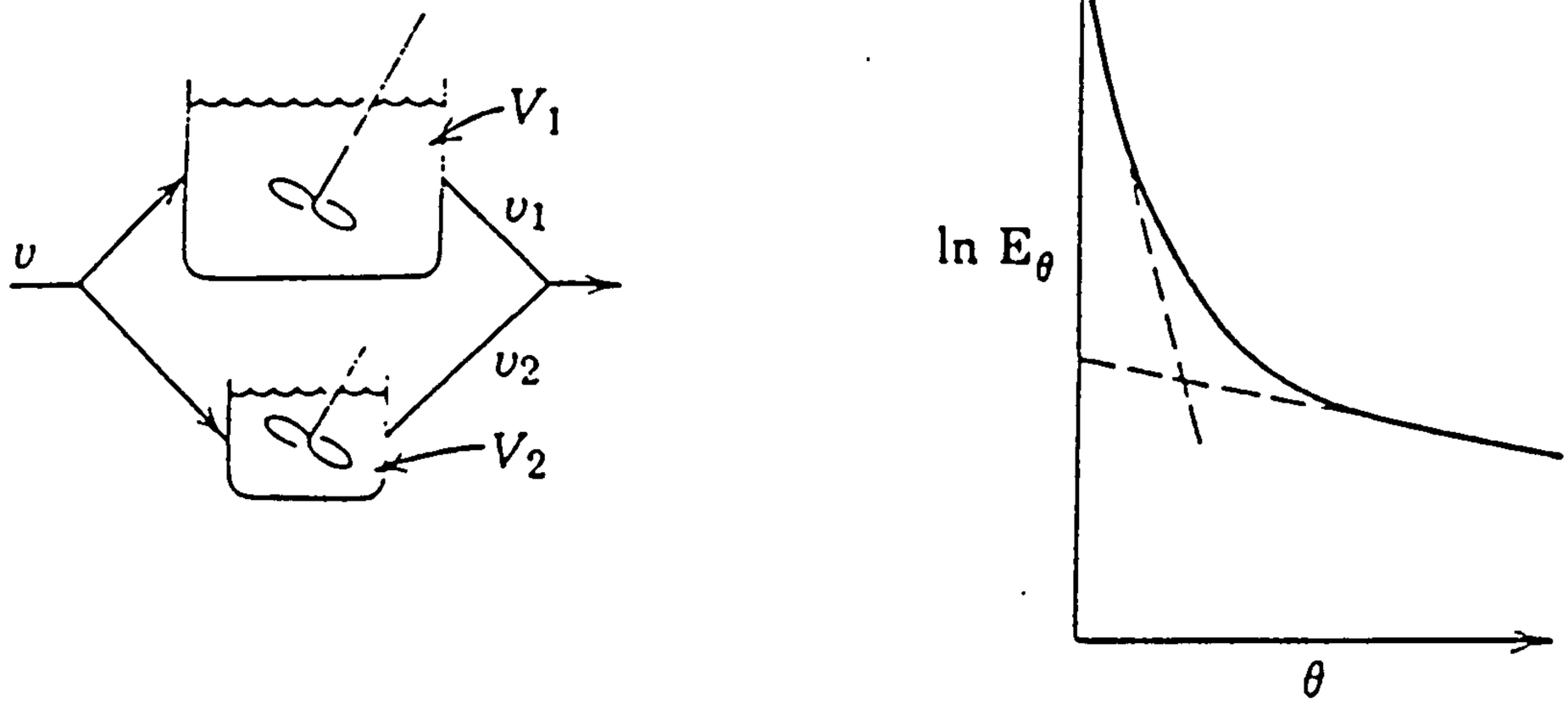

Figure 4. Fluid split into two tanks of different sizes.

This poses the question of which of the two models to use. The recycled crossflow model is the more general solution, whereas the other model is a particular solution (in which R = 0). In the recycled crossflow model, the residence time in the deadspace is able to assume greater values than those obtained from the fluid volume and flowrate alone. There is no reason why the other model should not be used, but if the mean residence time differs from the ideal value, then it is a simplified representation.

The dimensionless E-curves can be obtained by multiplying equations 38 and 39 by the mean residence time. Plotting ln E_θ versus θ allows the determination of the model parameters through the slopes and intercepts of the two asymptotes. This is illustrated by Levenspiel[31] and is shown in figure 4.

To describe the fluid flow in a single mixing tank, the recycled crossflow model could be altered without too much difficulty to include by-pass or plug flow. Thus, the Cholette and Cloutier[54] model, for example, could be enhanced.

2.7 Modelling Flow in Packed Beds with End Effects

As in the Deans-Levich model, the recycled crossflow cell does not give the long tails observed in the E-curve data for many cells in series. This suggests that the long tails are caused by an effect that occurred only once or twice, rather than continuously along the whole filter length. The filter contained larger packing at the ends. However, mixing experiments without packing in the ends also gave long tails. It is therefore proposed that the tails are the result of fluid expansion and contraction at the filter entrance and exit.

To develop a model incorporating such "end effects", the mean residence time must be able to increase from the ideal value. Thus, the number of recycled crossflow cells required in series with the mixing tanks is thought to be only one or two. From a mathematical point of view it is of no importance whether the cells are located before or after the tanks. Since it is proposed that the long tail is due to end effects, it is probably better to place the cells after the tanks in series. The overall model is illustrated in figure 5.

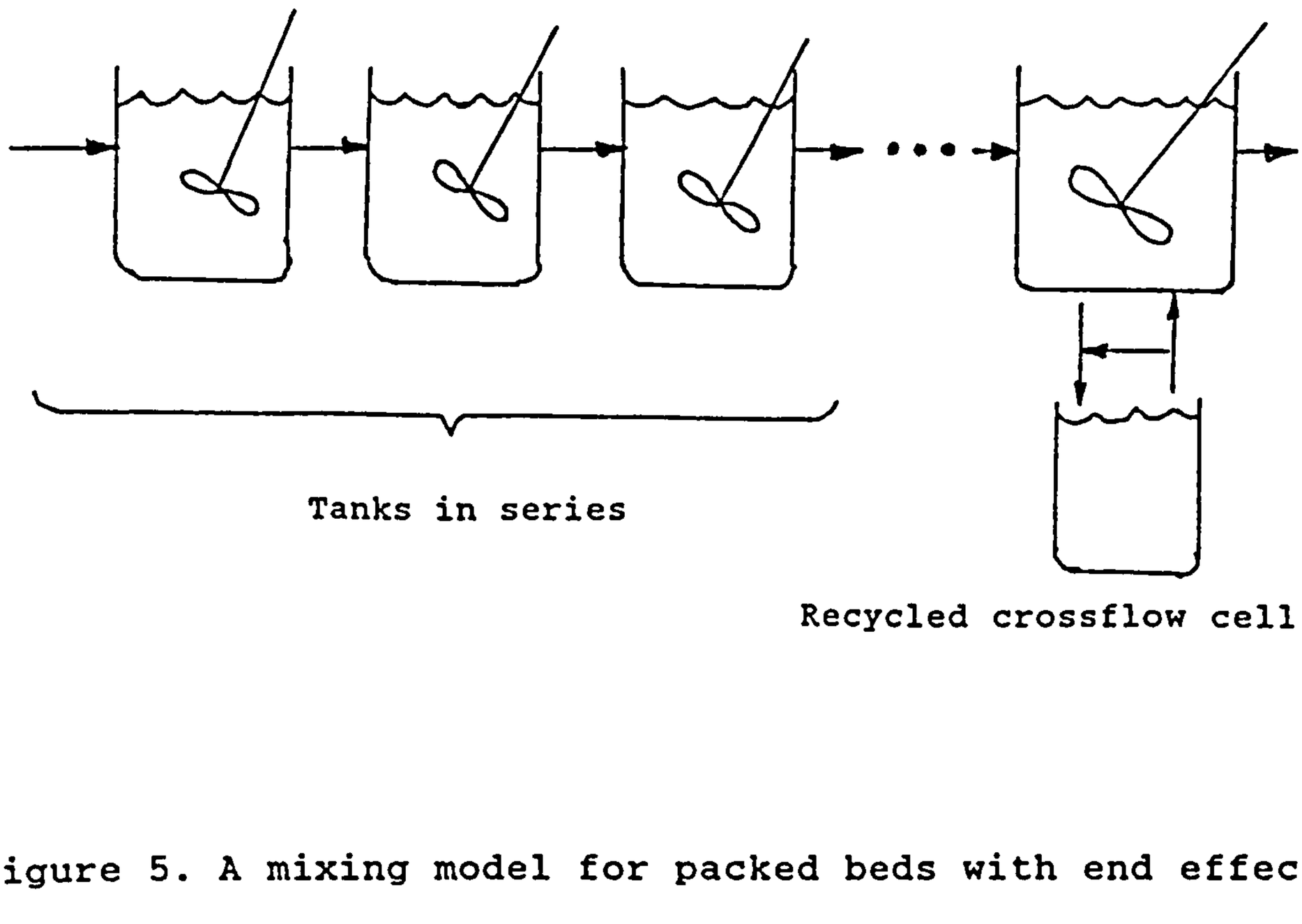

Figure 5. A mixing model for packed beds with end effects.

The moments for this model are easy to calculate because the cumulants for the two models are additive. Unfortunately, the analytical solution is more difficult. If this is not attainable, a combination of moments and the use of the tail characteristics may help to estimate some of the parameters. The "dead tank" residence time (r_2) and K2 could be estimated as in the single cell case. However, the model may require simulation using a digital computer. The method is outlined in "Mixing in Continuous Flow Systems"[53].

To test quickly that the model was of use, the curves were adjusted to remove the effect of the number of tanks in series given by the peak. This involves deconvolution; the method is illustrated in Levenspiel[51]. The conductivity

curve was represented by a cubic spline whose slope was continuous and whose second derivative was zero. From the spline procedure the curve was split into intervals of equal width, allowing numerical differentiation. When deconvolution is used, some problems occur which are not mentioned by Levenspiel. The process involves differentiation, which "roughens" the curve. Repeated differentiation causes the breakdown of the process. In order to avoid this, the new conductivity curve must be smoothed after each differentiation, which adds error to the process. However, the biggest problem is that it is not possible to obtain all of the curve. The computer program is given in appendix 2.d.

A sample of a deconvoluted tracer curve is given in figure 6. The mean residence time used in the plot is that for the whole filter. A glance at the x-axis indicates that a very small fraction of tracer stays inside the filter for over thirteen times longer than the mean residence time. The "ends" of the asymptotes show small curves, probably as a result of the numerical differentiation involved. However, the overall shape of the curve is as illustrated in figure 4. Thus it appears that the model does fit the data and that one recycled crossflow cell can represent the end effects.

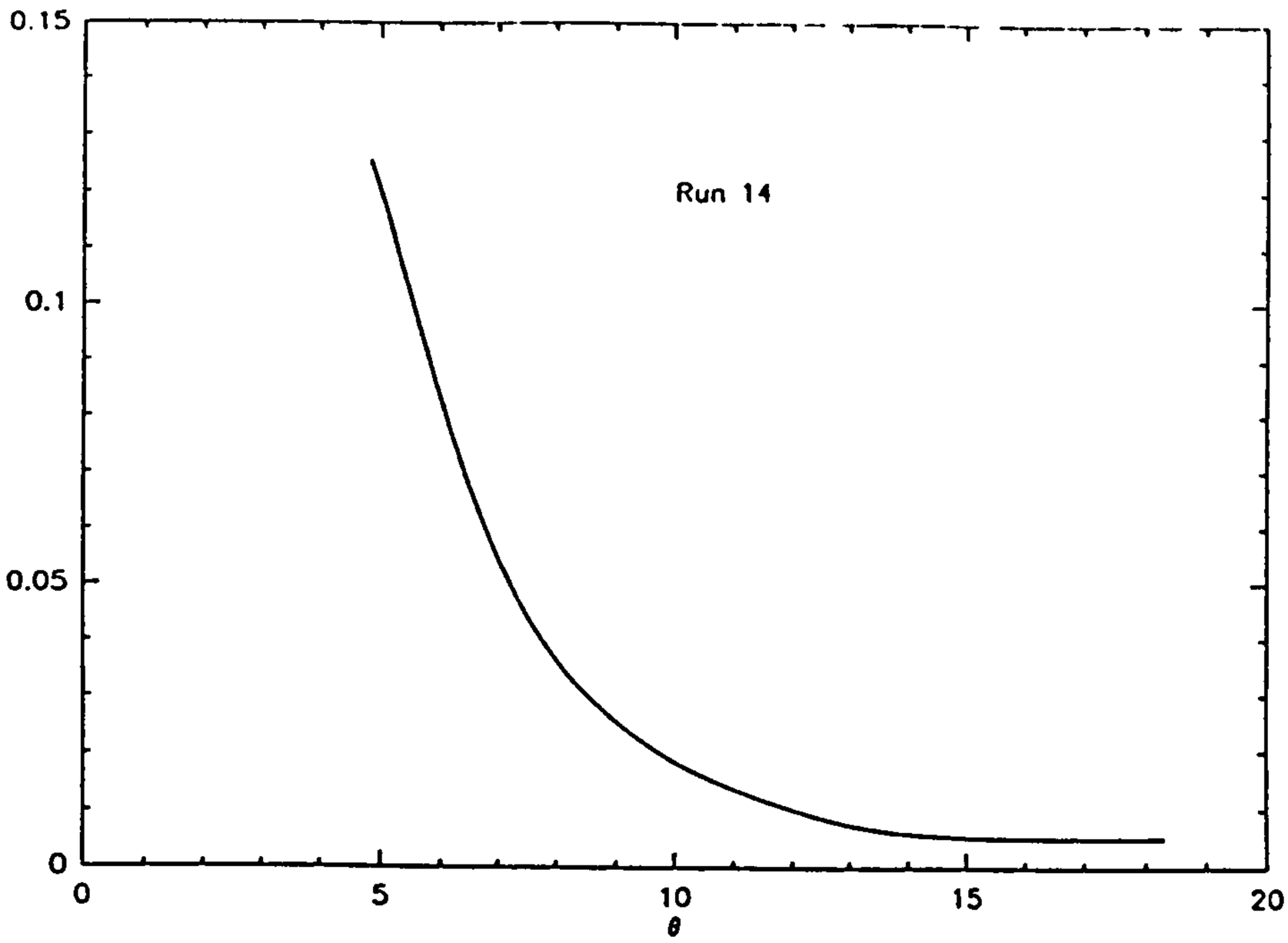

Figure 6. A deconvoluted tracer curve.

2.8 Deadspace and Increased Mean Residence Times

In the previous section, a mixing model has been given which appears to describe accurately exit age distributions (E-curves) with long tails. This then poses the difficult question of how the model relates to the physical system studied. In addition, it requires a clarification of the definition of deadspace and the way it is formed.

Deadspace is sometimes referred to as fluid that is "stagnant". However, stagnant regions, as modelled by the Deans-Levich model, do not alter the mean residence time. How then does a region increase the mean residence time?

The assumed answer to this question seems to be found by looking at a fluid undergoing a sudden enlargement in a vessel. As the higher velocity fluid entering the vessel is

injected into the slower moving fluid, turbulence occurs. This turbulence causes energy to be lost and is reflected in the parameter called the discharge coefficient. It is assumed that the turbulence is responsible for fluid interchanging with fluid outside the main expanding flow stream. The way the fluids interchange is believed to cause the long tails observed in the tracer data. Fluid from the dead volume is proposed to be incorporated into the main flow stream when the relative fluid velocities are greatest. When the relative velocities are lower, fluid from the main flow stream enters the dead volume. The assumed result is that fluid circulates between the two fluid streams. The dead volume residence times may be very long indeed. A diagrammatic sketch is given below:

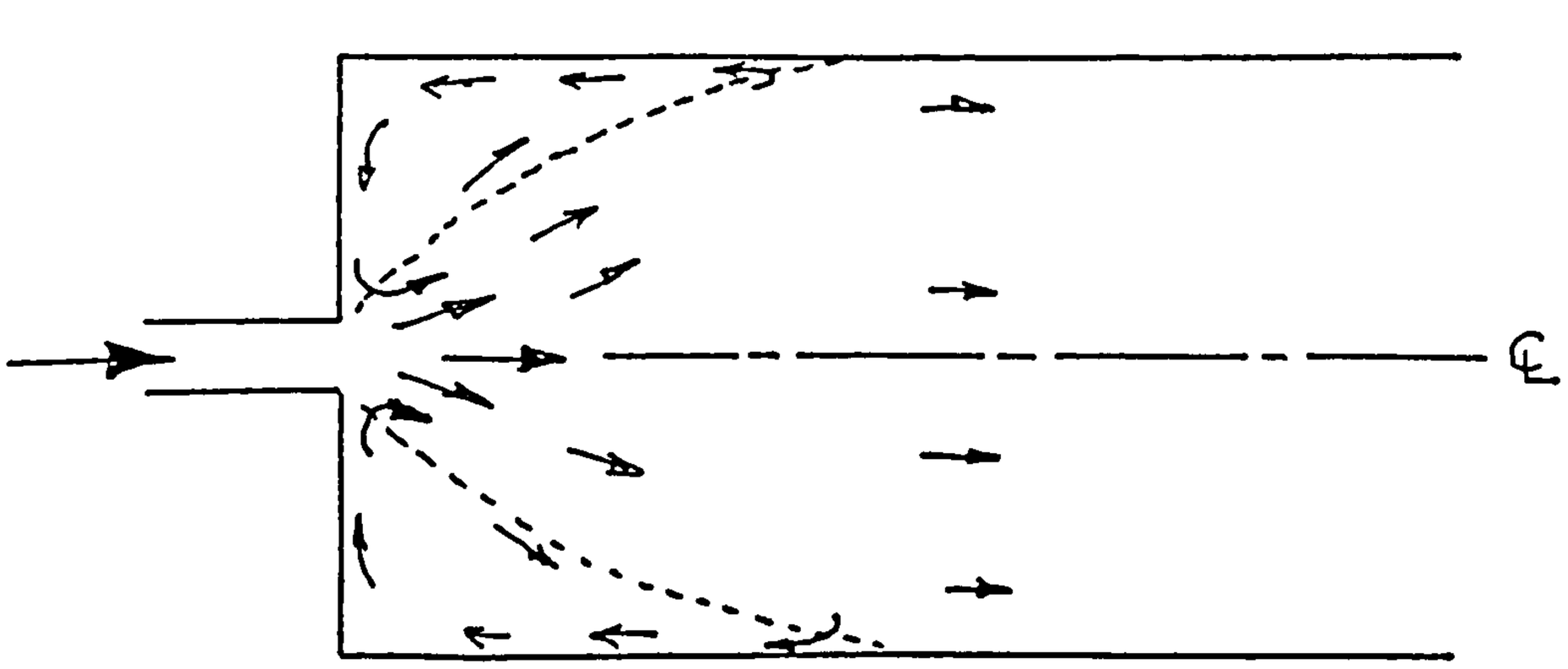

Figure 7. Fluid expansion at a filter entrance.

A simple definition of deadspace would be a fluid region that has the effect of increasing the mean residence time from the space time (i.e. the ideal residence time). The believed cause is rapid expansion or contraction in the fluid flow stream creating recirculation of a small fraction of the fluid.

2.9 Interaction of Mixing and Kinetics

Fluid flow in the submerged filters studied[29] has been shown to have two effects; firstly, the flow deviates from plug flow to a small degree and, secondly, the mean residence time is increased as a result of end effects. The effect that deviations from plug flow (dispersion) had on nitrification is examined first.

The significance of dispersion with respect to conversion (or volume of reactor required) depends greatly on the reaction order. For a zero order reaction dispersion has no effect. In a first order reaction the exit concentration ratio for identical filter size is given[31] by:

$$\frac{C_A}{C_{AP}} = 1 + \frac{(k\tau)^2}{2n} \qquad \text{for } n > 10 \qquad (40)$$

This is valid for small deviations from plug flow (large number of tanks in series), as found in the filters. The space time has a potentially significant effect on the ratio of actual to plug flow exit concentrations. The dispersion effects are greater at long residence times. However, in practice the effect of dispersion is very small. This is so because the rate of reaction is not first order (as indicated in 3.3).

The reaction, as was shown previously[29], can be approximated to saturation (or Michaelis-Menten) kinetics for a given residence time. Thus the reaction order shifts from first order to zero order at higher concentrations. The equation relating exit concentration ratios for small deviations from plug flow and saturation kinetics was

derived using the Pasquon and Dente[56] formula. Thus for an identical filter size the exit concentration ratio is:

$$\frac{C_A}{C_{AP}} = 1 + \frac{k_1 \tau}{2n\ (1 + k_2\ C_{AP})} \ln \left(\frac{C_{AI}\ (1 + k_2\ C_{AP})}{C_{AP}\ (1 + k_2\ C_{AI})} \right) \qquad (41)$$

The number of mixing tanks for a given residence time was obtained from the tracer data[29]. The kinetic constants were determined from kinetic data with the same residence time[29] using the integrated saturation kinetic plot and assuming plug flow. To obtain the plug flow exit concentration, the above equation was iterated using the actual exit concentration as the starting value. At the longest residence time (17 minutes) the plug flow exit concentration for 21 tanks in series was 7% less. However, at shorter residence times with 34 tanks in series, the exit concentration was only 2% less.

The saturation plots (see 7.2) are not affected by this magnitude of error. Although at the longest residence times a small mixing effect is noticed, it is not significant. Thus, the previously-observed increased rates of reaction with decreasing residence time[29] could not be attributed to mixing. The emphasis of the research was thus shifted towards an examination of the reaction kinetics and, in particular, deviations from saturation (Michaelis-Menten) kinetics.

The second mixing effect noticed in the filters was attributed to "end effects". Dead volumes caused by rapid fluid expansion or contraction have a large effect on the

tracer curves, even though only a small fraction of the tracer is involved. However, as only a small fraction of reactant enters the dead volumes, the effect on the fractional conversion is very small.

The deadspace values calculated using the "tanks in series with deadspace" model (see appendix 2.a) are an approximation to the "tanks in series with a recycled crossflow cell". The values given when using the "tanks in series with deadspace" model overestimate the deadspace. This is due to the fact that the long tracer tails observed at low fluid velocities increase the mean residence time.

Calculations using the "tanks in series with crossflow" model, as suggested in the literature, overestimated the magnitude of the active filter volume (residence time). The problem of increased mean residence times was resolved only by the development of the recycled crossflow cell. The recycle crossflow mixing model had been developed, but not tested at the time of the earlier publication[45]. The dead fractions reported in this paper, with the "tanks in series with deadspace" model, are thought to be too high, particularly at low flowrates. This is in agreement with the poorer fits obtained when the low flowrate curves are fitted. At different fluid velocities the amount of circulation will be altered, but the dead volume should remain almost the same.

It has been suggested[51] that the number of tanks in series can be obtained from the length of the vessel divided by the packing characteristic length. In the experiments carried out[29], this was seen to be a poor indicator (see appendix 2.a). This method should be used with caution in

estimating the number of tanks in series in submerged biofilters with end effects.

CHAPTER 3

PRELIMINARY REVIEW AND ANALYSIS OF NITRIFICATION DATA

The context of the experimental research on biological filtration was set within a multi-disciplinary aquacultural engineering research group at Heriot-Watt. A major part of the activities within the group comprised the operation of recycle aquaculture systems, and a substantial amount of nitrification data arising from system operation was available.

A preliminary analysis of some of these data was conducted prior to a more detailed controlled experimental study. The kinetic data were collected from two nitrification filters while monitoring the water quality in an experimental recycle smolt hatchery system. However, the substrate concentrations are important to the nitrifying bacteria, but their source is immaterial.

Murray[13] designed several identical aquaculture recycle systems. Each system was known by a colour. The research data come from the red system. A single one-metre-square rearing tank with a central overflow take-off held the smolts. The waste water entered a series of three settling tanks for the removal of solids immediately ahead of the filters. This meant that the filters ran with a very low organic load and were essentially nitrification filters. The treated water was then pumped to a header tank, topped up as necessary, and gravity-fed to the rearing tank.

When designing the recycle aquaculture system, Murray specified two filters. The filters were named R1 (Red system filter 1) and R2. Filter R2 differed from R1 in that it had

a gradual expansion and contraction at its ends. Since both filters were in parallel, the influent conditions were identical. The dimensions of the filters, as contained in the author's undergraduate research project, are given in appendix 3.a.

During the time the kinetic data were collected, the smolts were fed the same quantity of food daily and their size did not alter significantly. From this it seems fair to assume that the amount of nitrogen supplied daily to the filters remained constant. This suggests that the total bacterial population was constant. However, their numbers are assumed to have varied along the filters' length according to substrate concentration.

According to Pooley[37], water samples were taken at a fixed time each morning, prior to feeding the fish. The volumetric flowrate through the filters was then altered and left for 24 hours. The water samples were then immediately analyzed, using methods described in chapter 4. The temperature and pH were controlled to 15°C ±1 and 7.2 ±0.1 respectively.

The data consisted of percentage substrate removed and ammonia and nitrite influent concentrations for the two biofilters in the system. The data covered flowrates from 1.3 l/min to 19 l/min with some repetitions. No data concerning filter loading were given. The data were manipulated to obtain the inlet and outlet concentrations of total ammonia and total nitrite.

3.1 Different Rate Equations Tested

The kinetic data from the system summarized above were used to evaluate a number of well-known rate equations. In addition they were used to test the implied mechanisms of section 1.2.3 in which ammonia is oxidized to hydroxylamine. The mechanisms were evaluated by hypothesis testing[58]. The null hypothesis for the experimental data was that the ammonia was not oxidized to hydroxylamine. Over thirty possible mechanisms for the oxidation of ammonia formed the alternative hypothesis. An alternative hypothesis can be accepted if the data agree with it to a certain significance level. The significance level chosen was 0.05 (experimental error). Thus, an alternative hypothesis would be accepted if the hypothesis agreed with the data to within experimental error.

Through assumptions compatible with known information concerning the reaction, the corresponding rate equations were reduced to nine. The reduction in the number of equations is due to different mechanisms giving the same rate equation. The principle assumptions were that the oxidizing agent and the product concentrations remained constant. An additional assumption was that the rate-limiting step was irreversible.

The inlet dissolved oxygen concentration was believed to be constant, but was not continuously measured. The concentration of dissolved oxygen was known always to exceed the stoichiometric requirement. Therefore, the dissolved oxygen concentration was assumed not to lower or raise the rate of reaction[6]. This implies that the concentration of

the second reactant, the peroxide, is constant.

The main product suggested by equations 16 and 17 is hydroxylamine. As has been mentioned earlier (see 1.2.3), nobody has ever measured any hydroxylamine during the normal oxidation of ammonia. Thus, its free concentration, assuming it to be an intermediate, must be unmeasurably low. Wood[39] suggested this could be due to it being a potential mutagen and its concentration being strictly controlled. The assumption that the hydroxylamine concentration was constant is consistent with this view.

It was also necessary to assume that the rate-limiting step was irreversible. The addition of the oxygen in hydroxylamine, however, has previously been indicated[39] to be irreversible. This is compatible with the thermodynamics of the reaction and the irreversibility of reactions involving molecular oxygen.

These assumptions indicate that the rate of ammonia oxidation according to equation 16 or 17 should depend on the ammonia concentration alone.

The rate equations tested were derived from table 4-8 in "Perry's Chemical Engineers' Handbook"[58] for solid catalyzed reactions. Using the assumptions given above, the rate equations were simplified to yield nine rate equations. The empirical n-th order rate equation was also tested and forms the tenth equation.

Table 1. The tested rate equations.

Equation	Simplified Rate Equation	Rate Order
A	$r_A = kC_A$	First Order
B	$r_A = \frac{kC_A}{1 + K_A C_A}$	Saturation
C	$r_A = kC_A^2$	Second Order
D	$r_A = \frac{kC_A^2}{(1 + K_A C_A)^2}$	
E	$r_A = \frac{kC_A}{(1 + K_A C_A + K_A' C_A)^2}$	
F	$r_A = \frac{kC_A}{(1 + (K_A C_A) + K_A' C_A)^{1/2}}$	
G	$r_A = \frac{k}{(1 + (K_A C_A) + K_A'/C_A)}$	
H	$r_A = \frac{k}{(1 + (K_A C_A)^{1/2} + K_A'/C_A)}$	
I	$r_A = \frac{kC_A}{(1 + (K_A C_A)^{1/2})^3}$	
J	$r_A = kC_A^n$	n-th Order

k = constant;

r_A = rate of reaction of reactant A;

K_A , K_A' = equilibrium constants;

3.2 Fitting the Rate Equations using Least Squares

The method of least squares was used to evaluate each of the above rate equations (see Table 1) with respect to the available kinetic data.

The flow was assumed to be plug flow, which the mixing studies had confirmed to be a very good approximation. The ten rate equations given in the previous section were tested by integrating numerically the rate equations to obtain the calculated residence time. The rate constants were adjusted repeatedly to obtain the least squares fit between the calculated and the actual residence time.

A computer program was written in order to minimize the least squares fit. To avoid recompilation of the main program, the rate equations were written as modules. To test a rate equation, the relevant module needs to be linked to the main program. The program listing is given in appendix 3.b.

The method used in the program is a search method developed by Nelder and Mead[30]. It works by reflecting, expanding and contracting the vertices of a simplex in n-dimensional space. The method is "a very robust direct search method which is extremely powerful provided that the number of variables does not exceed five or six"[48]. The flowsheet was taken from Basic Optimisation methods[48] and the routine converted to PASCAL from BASIC. The starting values for the rate constants were taken to be 1.0 and the step length 0.49, not 0.5, because the latter can lead to problems with the early evaluations of the simplex. The reflection, contraction and expansion coefficients were

taken as 1.0, 0.5 and 2.0, respectively, as recommended by Nelder and Mead.

The numerical integration is performed by Romberg integration, using a routine taken from Scientific Pascal[59]. This method has the advantage that the integration is performed to a fixed accuracy. The number of intervals evaluated is not fixed, but is adjusted depending on the function.

3.3 Ammonia Oxidation Kinetic Results

The measured pH during the experiments was 7.2, which meant that the ammonia existed almost entirely (99.7%) as ammonium ions. Since neither the ionic strength nor the conductivity was measured, it was not possible to calculate exactly the ammonia equilibrium for ionic strength. A review of ionic strength data measured during the operation of the system showed that the ammonium ion/ammonia gas ratio was 10% higher compared to that at zero ionic strength. This correction was used in the calculations, but the trends in the results would not be affected even if the ammonia existed solely as ammonium ions.

Ammonia gas and ammonium ions were both tested as possible substrates, and very little difference was observed between the fits. This indicates that the enzyme reaction site was at a different pH from that of the fluid. Alteration of the starting values in the minimizing program suggests that the determined rate constants are accurate to two significant figures.

The graphs of the relative differences in the residuals

are presented in appendix 3.c. Examination of the residuals indicates graphically that the null hypothesis is correct and that the alternative hypothesis must be rejected. The actual relative differences vastly exceed the expected errors. The probable error in measuring the ammonia concentration is only 5% (see 4.5.2). The horizontal dashed lines indicate the limits given by experimental error. As the data fall outside this band for all the rate equations, a statistical statement can be made: *On the basis of the kinetic data tested, the null hypothesis is accepted, i.e. that ammonia is not oxidized to hydroxylamine*. In addition, it implies that *the tested rate equations are not compatible with the kinetic data*.

Thus, on the basis of the data tested, the reaction pathway is not as straightforward as given in section 1.2.3.

The large differences between the predicted and actual residence times are a good illustration of the problems involved in sizing a biological filter. The kinetic rate equations given by previous authors (see 1.2.2), such as first order, Michaelis-Menten or n-th order, are unable to cover the wide range of conditions (e.g. residence times) to be expected in operational aquacultural nitrification filters.

The correlation coefficients for the ten rate equations tested are tabulated below. The correlation coefficients indicate the association between the measured residence time and the predicted value for a given rate equation. Correlation coefficients do not form the basis for accepting or rejecting a hypothesis and as such do not indicate any proof for a hypothesis. They are given here to allow

comparisons of each rate equation to be made.

Table 2. Correlation coefficients for the tested rate equations

Rate Equation	Filter	Number of Variables	Correlation Coefficient Total	Gas	Ion
A	R1	1	0.876	0.876	0.876
	R2		0.948	0.948	0.948
B	R1	2	0.912	0.876	0.912
	R2		0.948	0.948	0.948
C	R1	1	0	0	0
	R2		0.883	0.883	0.883
D	R1	2	0.519	0	0.520
	R2		0.889	0.883	0.889
E	R1	3	0.912	0.876	0.912
	R2		0.949	0.948	0.949
F	R1	3	0.905	0.905	0.905
	R2		0.938	0.937	0.938
G	R1	3	0.890	0.890	0.875
	R2		0.912	0.912	0.912
H	R1	3	0.908	0.876	0.908
	R2		0.949	0.945	0.949
I	R1	2	0.918	0.918	0.918
	R2		0.949	0.948	0.948
J	R1	2	0.925	0.925	0.925
	R2		0.949	0.949	0.949

The best-fitting rate equation (n-th order kinetics) shows a correlation coefficient of 0.949 between the

calculated residence time and the measured residence time. However, the fit for saturation (Michaelis-Menten) kinetics is not found to be much worse.

As was mentioned in the introduction to the chapter, the bacterial numbers were believed to be constant because of the fixed amount of nitrogen supplied daily. However, the bacterial numbers were assumed to vary along the length of the filter. More bacteria are present at the inlet than at the filter exit due to the substrate concentration being higher at the inlet. It was thought prudent to check that this was not responsible for any large systematic effect upon the kinetic data.

Bacteria use a certain amount of substrate for their own metabolism. *Nitrosomonas* uses some ammonia for nitrogen metabolism. This fraction (the yield coefficient) is assumed to be constant and its value has been reported in the literature[20] as between 0.03 and 0.13. Poduska et al.[5] suggested it was constant; he assumed a value of 0.05, that is 5% of the ammonia removed was assumed to be assimilated. The yield coefficient can be used to compensate for the small change in the concentration of bacteria (growth) along the filter. This was done according to the equation below[31,32].

$$r'_A = (M_I + S_o K_o * (C_{AI} - C_A)) * r_A \qquad (42)$$

Neither the yield coefficient ($S_o K_o$) nor the mass of bacteria at the inlet (M_I) were assumed. Thus, the program had the maximum freedom to obtain a best fit. This brought two additional variables into the analysis. The program

became slower with the greater number of variables, but least squares fits were obtained. Although the residuals to the fits were marginally improved, the kinetic data again rejected the alternative hypothesis.

3.4 The Thermodynamics of Ammonia Oxidation.

The statistics above indicate that, on the basis of the kinetic data tested, ammonia is not oxidized to hydroxylamine, as implied by the mechanism of section 1.2.3. The very credible reason for this appears to be that the thermodynamic barrier involved in this biological oxidation cannot be overcome. As was pointed out earlier (see 1.2.3), the Gibbs energy change is positive and about 17 kJ/mol. The lack of any "unique *reversible* oxygenase" plus this barrier led Wood [39] to conclude that "the direct oxidation (of ammonia) is not a biological possibility".

The salient point, perhaps not appreciated before, is that this statement is incompatible with the rate equations and implied mechanisms previously attributed to ammonia oxidation. The tested kinetic data reject both the rate equations previously suggested and the theory that ammonia is oxidized to hydroxylamine. This leaves the question of what path the reaction takes.

The author was aware of the role played by ammonia in removing carbon dioxide from process gases before the advent of methyl, dimethyl, and trimethylamine. The limited nature of the reactions of amines[60] at biologically-feasible pHs, suggested these equilibrium reactions might form an alternative pathway. As thermodynamic considerations appear

to dominate ammonia oxidation, the thermodynamics of these reactions requires close scrutiny.

3.5 Carbon Dioxide and Aqueous Ammonia Solutions

In aqueous solutions of ammonia and carbon dioxide the following equilibria are established as given in the "Chemical Engineers' Handbook (4th ed)"[61].

$$NH_3 + CO_2 + H_2O \rightleftharpoons NH_4^+ + HCO_3^- \quad (43)$$

$$NH_3 + HCO_3^- \rightleftharpoons NH_2COO^- + H_2O \quad (44)$$

$$NH_3 + HCO_3^- \rightleftharpoons NH_4^+ + CO_3^= \quad (45)$$

The second equilibrium shows the formation of carbamate (of ammonia) NH_2COO^-, also called carbamic acid. The equilibrium data for the formation of carbamate, given by Van Krevelen[62], were curve-fitted, as is explained in section 4.6. The equilibrium constant and the Gibbs energy for this reaction is given by the equations:

$$\log K_2 = 1101/T + 0.0024T - 3.9358 \quad (46)$$

$$\Delta G = -2.303*R*T*\log K_2 \quad (47)$$

The Gibbs energy change at 20 C, as calculated from the above, is negative 3 kJ/mol. The magnitude is well within the range ± 12 kJ/mol (reference 63), indicating that the equilibrium has no overwhelming tendency to shift to the left or right.

If carbamate were, even briefly, to be involved in an

alternative path, a method of forcing its formation would be required. This suggested the involvement of an activator which supplied energy. The involvement of an activator was also compatible with figures 27 and 28. The plots are presented and discussed in greater detail in section 7.2. The ammonia oxidation thermodynamic barrier and the possible formation of carbamate suggests that various activators need to be considered.

3.6 Adenosine Triphosphate (ATP) as an Activator

The two most common sources of energy in biological reactions are ATP and NADH (Nicotinamide Adenine Dinucleotide).

$$ATP \longrightarrow ADP + P_i \qquad 30\ kJ/mol \tag{48}$$

$$NADH + \tfrac{1}{2}\ O_2 \longrightarrow NAD^+ + H_2O \qquad 220\ kJ/mol \tag{49}$$

The amount of energy transferred by ATP upon reaction is about 30 kJ/mol and for NADH about 220 kJ/mol (reference 64). The most likely source of chemical energy to overcome the thermodynamic barrier (17 kJ/mol) for the oxidation of ammonia is, thus, ATP. ATP phosphorylates, i.e. it adds a phosphate group ($PO_3^=$) to an alcohol group. The substrate receives energy contained in the phosphate bonds of ATP (reference 65). The phosphate group is often represented by P_i, as the number of attached protons depends on pH. To form carbamate of ammonia as an intermediate, the energy from the ATP must be used. Thus, the overall reaction is as follows: Ammonia gas, a bicarbonate ion and an ATP molecule combine

to give carbamic acid (carbamate) and ADP (+ P_i). To check if such a reaction had already been found elsewhere, a biological pathway chart was consulted[66].

3.7 The Urea Cycle and Carbamyl Phosphate

The formation of carbamate of ammonia by enzymes is not only possible, but is already known to occur. On the urea cycle, an enzyme-catalyzed reaction involving ammonia gas, bicarbonate ion and ATP is observed. The reaction forms carbamate phosphate, a key intermediate in the formation of pyrimidines, arginine, and urea[67].

A well-understood enzyme that performs this reaction is carbamyl phosphate synthetase obtained from *Escherichia coli*. The substrate to this reaction is either ammonia gas or glutamine. Meister and collaborators[68], through extensive experiments, suggest five steps in the reaction.

$$E + ATP + HCO_3^- \rightleftharpoons E\text{-}(CO_3PO_3^{3-}) + ADP \quad (50)$$

$$E\text{-}(CO_3PO_3^{3-}) \rightleftharpoons E\text{-}(CO_2) + P_i \quad (51)$$

$$E\text{-}(CO_2) + \text{L-glutamine} \rightleftharpoons E\text{-}(CO_2)\text{-}(\text{L-glutamine}) \quad (52)$$

$$E\text{-}(CO_2)\text{-}(\text{L-glutamine}) \rightarrow E\text{-}(NH_2CO_2^-) + \text{l-glutamate} \quad (53)$$

$$E\text{-}(NH_2CO_2^-) + ATP \rightleftharpoons E + NH_2COPO_3^{3-} + ADP \quad (54)$$

In the fourth step, carbamate is formed irreversibly. The first two steps involve bicarbonate ions and ATP, forming what is described as "active CO_2". The "active CO_2" then reacts with the ammonia or glutamine to form carbamate. The final step is the phosphorylation of carbamate to carbamyl (also named carbamoyl) phosphate.

Another bacterial enzyme called carbamate kinase also forms carbamate phosphate, but this is reversible and favours ATP synthesis.

The possible formation of carbamate from ammonia as a reaction mechanism still left unresolved the rest of the ammonia oxidation mechanism. However, the most important unresolved problem was that the reaction kinetics of, and mechanism for, nitrite oxidation remained unknown.

3.8 Nitrite Oxidation

To calculate the nitrite oxidation rate, allowance has to be made for the ammonia in the influent oxidized to nitrite. The amount of ammonia oxidized to nitrite was significant in the submerged filter experiments. Thus, rate constants determined from the analysis of ammonia oxidation are needed to be able to evaluate the nitrite kinetic data. Since such poor fits were obtained for the ammonia reaction, no analysis of the nitrite data was performed. There is a danger of overfitting data when many variables are being evaluated. In addition, it was felt that more information would be obtained from more specific experiments using the designed nitrification rig.

CHAPTER 4

EXPERIMENTAL PROCEDURE AND SAMPLE ANALYSIS

In the experiments described in the previous chapter, the bacteria were not disturbed for twenty-four hours after each alteration of the flowrate to the filters. Thus the data result from a series of experiments each conducted at a steady state. It is assumed that the bacteria's control system re-established new internal conditions for optimum efficiency during the period of time they were undisturbed.

In section 3.5 it was also indicated that there was good reason to believe that an activator/inhibitor was involved in the reaction. However, the investigation of the reaction mechanisms, using the specific enzymes and activators, would be a major investigation in itself. In addition, the resources to conduct such a study were not available.

On the other hand, the investigation of the unsteady-state behaviour of the bacteria was possible and a suitable experimental rig had already been designed and built. The objective of the experiments detailed in the next chapters was to obtain insights into the bacteria's control mechanism. An understanding of the unsteady-state behaviour of the bacteria was seen as important in developing a rate equation that might describe the nitrification reactions.

4.1 The Experimental Rig

The experimental rig was designed and built as part of the author's MSc (reference 69). The design methodology is

discussed in that thesis. Flow sensors used to determine the flowrate accurately during the mixing experiments were not required for the batch kinetic experiments and were removed.

The referenced flowsheet for the kinetic experiments is shown in figure 8. The substrate, nutrients and buffer were mixed in the mixing tank [A]. The fluid from the mixing tank was then pumped from the tank using a ¾" centrifugal pump (Beresford PV 22) [B] on a recycle. The flowrate was controlled by a diaphragm valve and measured using a rotameter [C]. To ensure reasonable accuracy in determining the flowrate, a high flowrate of 20.4 l/min was used. The water samples were taken from the sampling point [D] after the rotameter. To check that the conversion per pass was small, some water samples were also taken after the filter. The filter by-pass valve [E] was kept closed, so that all the flow measured by the rotameter passed through a single filter. Incorporated into the experimental rig were couplings used to facilitate the easy removal of key pieces of equipment. The nitrifying filter [F] was equipped with couplings for easy removal for weighing. The fluid exiting the filter was then recycled back to the mixing tank. An open T-junction was used to entrain air into the water, allowing continual oxygenation of the fluid in the mixing tank. A metering pump [G] supplied the nutrients and buffer so that the bacterial population was maintained when no experiments were taking place.

The impulse kinetic experiments performed required a fast acting system to control the temperature and pH. The temperature was regulated using a heater/cooler. The pH was adjusted by the addition of buffer to the mixing tank.

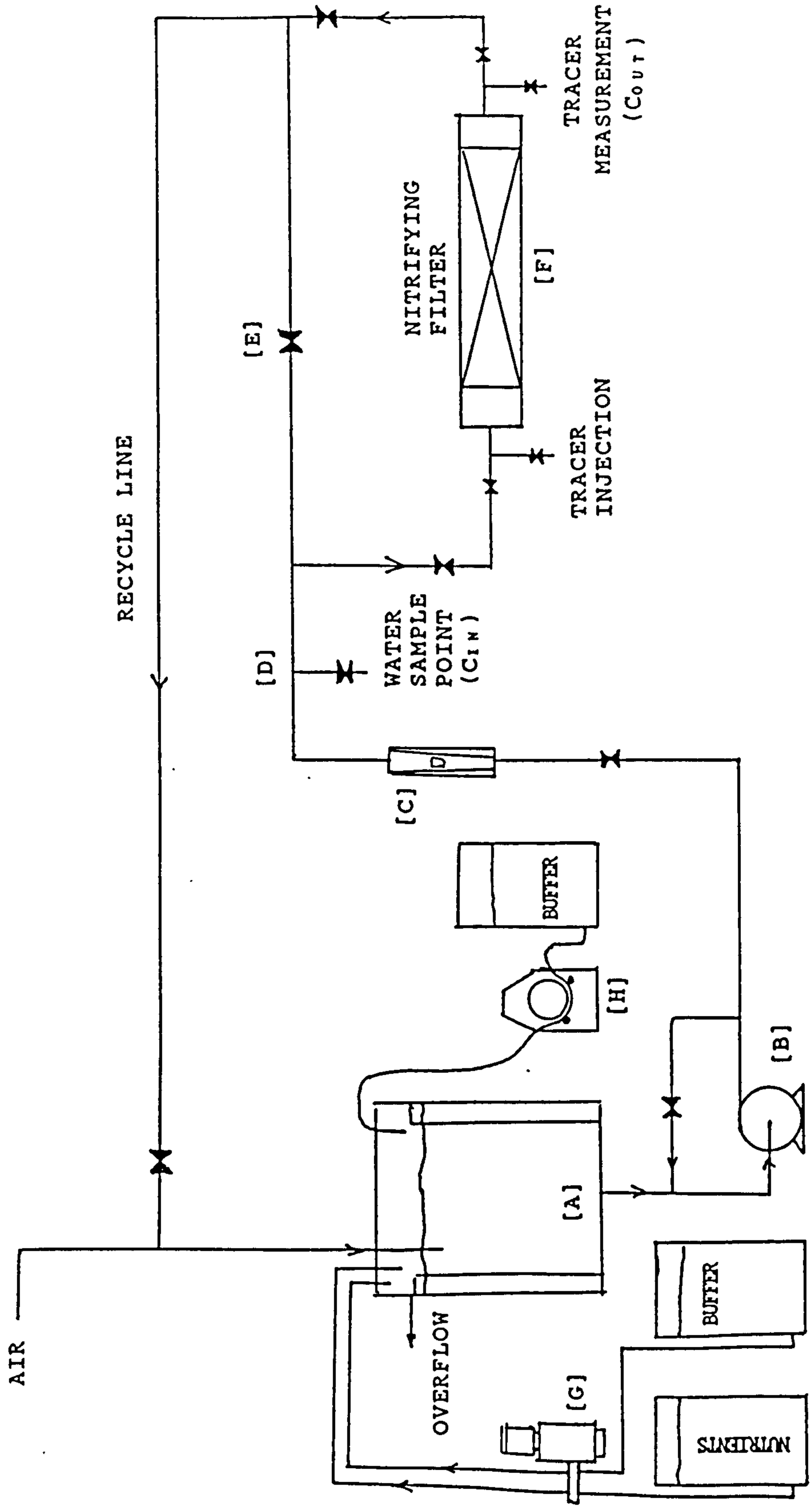

Figure 8. Experimental rig flowsheet.

A "Perspex" mixing tank lid was made to reduce evaporation losses and to mount the pH electrode and temperature compensator. The pH was measured with a "Russell" CE7L/LCW electrode for use in freshwater in conjunction with a stainless steel PCT 103 automatic temperature compensating electrode. During the experiments, a "Jenway 3090 HL" pH controller switched a "Watson-Marlow MHRE 100" flow inducer [H]on and off, which was adding the buffer. The tank lid was equipped with two ¼" diameter pipes for connection to a heater/cooler. The dimensions and location of the tank lid fixtures are given in appendix 4.a. The first time the cooler was used, it failed to operate and had to be stripped. The cause appears to have been the presence of solids and rust particles, which prevented the free rotation of the pump impeller. It is therefore advisable to follow the manufacturer's instructions during long periods of storage and when using fluids containing solids. In order to avoid possible toxic effects of the copper cooling- coil, the cooler was only connected during the kinetic experiments. The cooler lowered the temperature by 25°C over a period of 12 hours. The length of the piping was kept as short as possible so that fluid residence time through the cooler was minimized to ensure the uniformity of the fluid composition.

As detailed previously[69], mixing studies were carried out on the experimental rig prior to the kinetic experiments. It has been demonstrated that the mixing tank and the centrifugal pump together can be considered as an ideal stirred tank with small dead volumes. It was therefore assumed that the substrate was fully mixed when added to the

rig. The flow through the nitrifying filter was shown to approximate plug flow well. However, it was found that the distributor plate used caused two flow paths. As recommended, the distributor plates inside the filters were removed and were replaced by ½" plastic packing in the ends of the filters. The larger plastic packing corrected the flow path and proved very satisfactory.

The filter used in the kinetic experiments was a horizontal submerged filter made from grey PVC piping of an internal diameter of 155 mm and a length of 102 cm. The full filter dimensions are given in appendix 4.b. The two ends were made from flanges, the end plate with the pipe coupling being attached with stainless steel bolts. A rubber gasket provided a seal between the flange and the end plate. A stainless steel bolt was threaded into the top of the filter to release trapped air during startup. The fluid volume inside the filter was measured by weighing the dry filter and the wet filter. Using this method, the fluid volume was calculated as 11.7 litres, giving a voidage of 0.606.

The filter medium was crushed rock (granite-based), which was sieved to remove fines. A representative sample was taken and the size distribution measured by enlarging the particles' image, using an overhead projector. The projected Feret's diameter of the particle was measured with a rule. The actual particle Feret's diameter was calculated from the projected image. The particle distribution and the estimated specific area is given in appendix 4.c.

During the kinetic experiments, conditions were varied between pH 4 and 10 at a temperature of 22°C and from 5°C to 30°C at pH 8.0. However, at no time was the biomass

30°C at pH 8.0. However, at no time was the biomass killed, avoiding the necessity of a restart.

4.2 Development of the Experimental Method

During the investigations into nitrification, it was always felt that the observed reaction kinetics were due to the nitrification reactions, rather than being associated with the growth of the bacteria. Many of the experiments conducted to investigate the nitrification reactions involved growing the bacteria on a small batch scale. The experiments were designed to be carried out on a fixed bacterial population, so that growth associated reactions could be eliminated from the analysis.

From the previous work it was apparent that a sudden addition of substrate to an otherwise constant supply would prove to be the most informative. An equivalent would be pulse testing in control system analysis. Henceforth, the experimental method will be described as an impulse reaction study. This name is suggested because it describes how the substrate is added and implies that the response has to be investigated. This method has the advantage that no significant change in the numbers of bacteria can be expected if the experiment is conducted fast enough. It also has the advantage that the rate of reaction with time can be more easily studied than with influent and effluent data.

By altering the amount of substrate added, the shape of the curve of the substrate concentration versus time can be studied. To obtain the most information from such a curve, it is important to choose the part of the curve where the

rate changes most, as is illustrated below in figure 9. At the same time, however, the concentrations studied should be close to those found in the process.

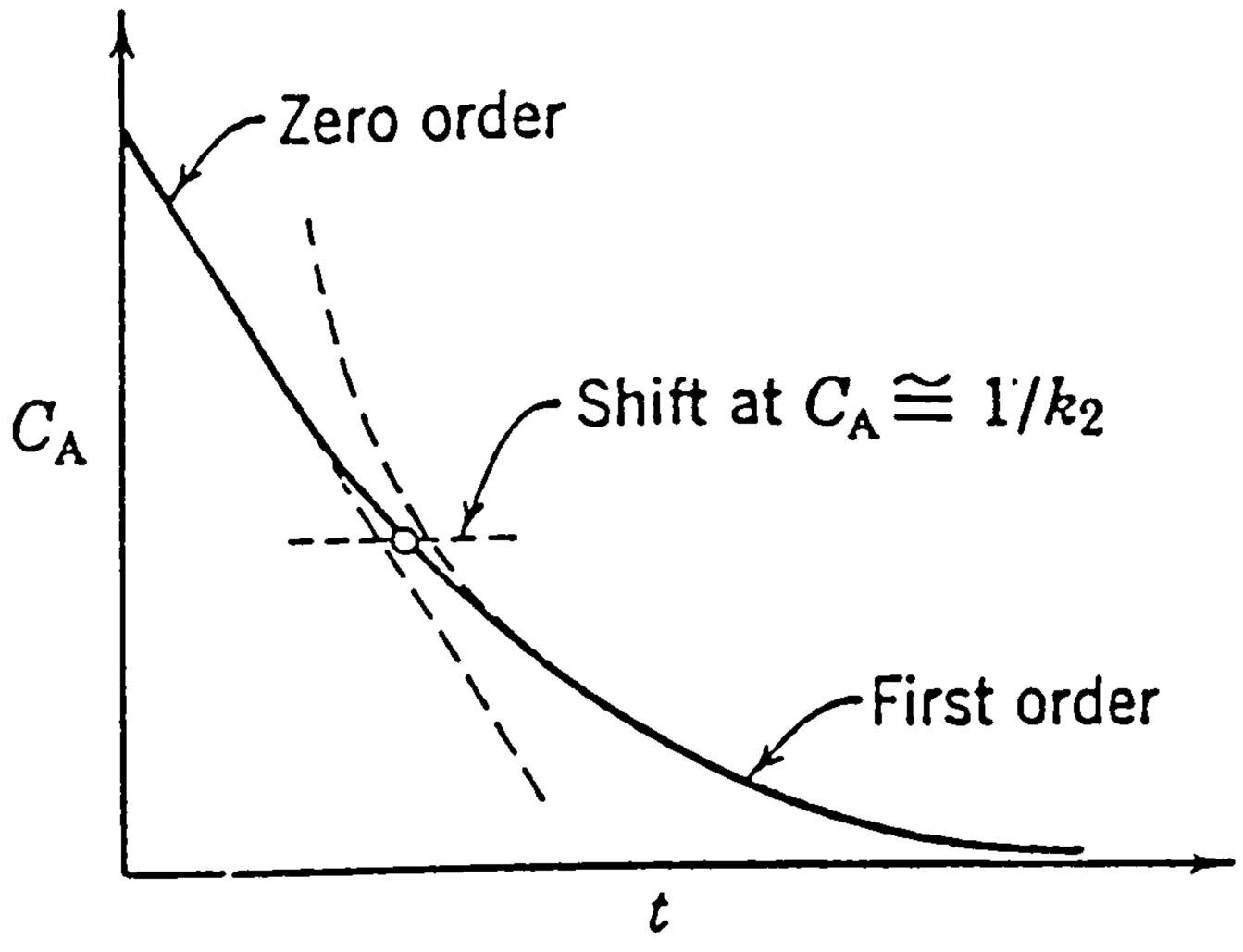

Figure 9. Reactions of shifting order.

It required a trial-and-error-approach to determine the amount of substrate that had to be added and the best time to take the readings.

If a recycle reactor with no through-flow is to be considered as a batch reactor, the conversion per pass should be small and the concentration almost uniform. To check that this was indeed the case, the influent and effluent concentrations were measured.

Experiments were also performed to test whether the experimental data could be reproduced.

4.3 Rig Startup Procedure

To seed the nitrifying filters, pure cultures of *Nitrosomonas europea* and *Nitrobacter europea* were grown from cultures supplied by Dr J.I. Prosser[70]. They were grown in Skinner and Walker's[71] medium (see appendix 4.d), as suggested by Dr J.I. Prosser.

To slow their growth, the supplied cultures were placed in a refrigerator at 5°C. Both cultures appeared almost transparent but slightly pink, which indicated that they had not outgrown the medium. One per cent of culture to medium was recommended for inoculation. Since not enough culture was supplied to inoculate the rig with a good chance of success, more culture was grown.

Half-litre aliquots of Nitrosomonas and Nitrobacter medium were made up. The micro ingredients for the medium were made up into a stock solution. The media were placed into 2-litre-flasks for good aeration. The flasks were topped with foam bungs. They were then autoclaved along with pipette tips and 5% (w/v) Sodium Carbonate solution. After cooling, both flasks were inoculated with 1% of their respective bacteria. The media were then buffered with the sterile Sodium Carbonate until the colour changed, indicating a pH of 8. The flasks were then placed in a covered water bath kept at 32°C. After 5 days, the colour of the Nitrosomonas medium had changed, indicating bacterial growth. Sodium Carbonate was added to restore the pH. The flasks were kept in the water bath for a further 5 days, adding Sodium Carbonate daily to the Nitosomonas. At no time was there a colour change in the Nitrobacter flask, but the

flask did become marginally opaque.

The size of rig required for mixing studies meant that sterilized operation would have been prohibitively expensive. In addition to this it was felt that the experiments should be carried out in conditions similar to those that could be obtained in an aquacultural recycle system.

During the week preceding inoculation, distilled water had been circulated and the temperature kept at 20°C without any problems occurring. The two flasks containing the bacteria were then emptied into the mixing tank. Nutrients were added to give the same strength in the rig water as in the medium. As the medium lacks a carbon source, it was assumed that this kept non-nitrifiers to a very low level. It was also assumed that the population of nitrifiers were predominantly of the species added. No analysis of the nitrifying species was attempted, as separating the nitrifying contribution of different species was not felt to be feasible, in view of the large number of variables already being evaluated.

A MPL metering pump was used to supply the substrate/nutrients and buffer continuously from 25 l plastic stock tanks, calibrated in litre intervals. The metering pump's two heads, SS 5C's, were found to give 540 ml/hr each at 100% flow. The metering pump flowrate was set at 50% of full flow and the concentration of the buffer required to keep a constant pH constant of 8.0 was determined. Once the bacteria were successfully started, the amount of buffer required was approximately 1 g/l of sodium carbonate, 113 mg/l Na_2CO_3-C. This compares favourably with

the buffering requirement given by the United States Environmental Protection Agency[26] equation. The tanks used provided enough medium for three days' continuous operation at 50% of the full metering pump flowrate before replacement.

The non-substrate nutrients supplied were the same as in Skinner and Walker's medium, except that phenol red and the EDTA were omitted. The concentration of the ammonium sulphate in the stock tanks was 0.235 g/l and is equivalent to 50 mg/l NH4-N. Ammonium Sulphate was used as the substrate in providing the ammonia for the Nitrosomonas, as in the medium used in the startup. The use of ammonium chloride would have produced sodium chloride, which could affect the freshwater Nitrifiers. Sodium Carbonate was used as the buffer and, when required for the experiments, Sodium Nitrite as the substrate for the Nitrobacter.

For the first two weeks no bacterial growth was observed, as no buffer was required. This is thought to be due to the bacteria being in flocculant form and being subjected to light in the mixing tank. For the next week the "Perspex" mixing tank lid was covered in aluminium foil. This led to noticeable bacterial growth on the sides of the mixing tank and a need to buffer the rig. It seemed that the bacteria had developed into a biofilm. To test that the light in the mixing tank was indeed responsible for the inhibition, the biofilm on the mixing tank was removed along with the aluminium foil. Thereafter, no growth of a biofilm was noticed in the mixing tank. This corresponds to light disrupting nitrification[72,73,74,75] and possibly biofilm adhesion.

The likely causes of a difficult startup seem to be the presence of light or organic carbon. In some cases added "nutrients" may supply an organic carbon source. Resulting heterotrophs compete for the nitrogen very effectively and nitrification is severely reduced or even stopped. The culture tanks in the system are open. Thus, light encourages the growth of heterotrophs, and disrupts nitrification if the bacteria are in a flocculant form.

4.4 Experimental Procedure

4.4.1 Impulse Reaction Experiments

This type of experiment was used to obtain all the data from the experimental rig. The experimental rig is a recycle reactor with no-through flow and can be considered as a batch reactor. This type of reactor is explained in standard chemical reaction engineering texts[51]. The main requirement in this design is that the composition of the fluid throughout the system must be uniform. This means that the conversion per pass must be small. In this type of reactor, the changing concentrations of reactants against time are followed, as is done in a homogeneous batch reactor. This greatly simplifies the mathematics involved in the kinetic models. The major reason for using this type of experiment, rather than influent and effluent data from an aquaculture recycle system, was that it was possible to control the substrate concentrations and input times.

To build and maintain the bacterial population at a constant level, the metering pumps supplied nutrients and

buffer at a constant rate for over 8 weeks. The excess fluid exited the system via an overflow. The mode of operation is identical to a recycle reactor with a small through flow. Any significant change in the rate of nitrification would have altered the pH. The bacterial population was assumed to be constant because the pH remained constant.

Prior to an experiment, sufficient sample bottles were prepared, as is described in 4.4.2, and all the electrodes were calibrated with buffers. The temperature was measured using a mercury-in-glass-thermometer accurate to +/- 0.5°C in the mixing tank. The amount of substrate to be used was weighed, and the volumetric flowrate was read from the rotameter. It was also necessary to adjust the low-level alarm sensitivity, because the water level dropped as samples were taken. The metering pump was then switched off and the pH controller switched on. The peristaltic pump delivered dilute sodium carbonate during ammonia oxidation and dilute sulphuric acid during nitrite oxidation experiments. The concentration was adjusted to avoid feedback to the controller. A quantity of water was then taken from the sampling point after the rotameter, and the substrate was dissolved in it. The water was then returned to the rig and left for a fixed time to ensure that the substrate had been mixed and that the concentration was uniform throughout the system. At their allotted time, the water samples were taken from the sample point after the rotameter. Prior to taking each sample, water was taken from the sample point and returned to the tank to ensure a fresh sample. The required fluid volume for analysis was measured and placed in its labelled polyethylene container for

freezing. Instrument readings were then taken as described in section 4.4.4.

A new experiment was not conducted until the substrate concentrations and the conductivity had returned to their previous level.

4.4.2 Analyses Carried Out

Many possible mineral ions can affect the growth[20,22] and possibly the rate of a biochemical reaction. To measure all the mineral ions would have been a massive undertaking. Equipment and human resources being limited, only a few of the mineral ions were tested for. In most cases, the ions should be in concentrations in line with those of the supplied medium.

The mineral ions tested for were:

- Ammonia and nitrite as the substrates;
- Nitrate concentration as the end product;
- Alkalinity, as a possible additional substrate and because it buffers the reaction.

In this type of experiment it was not practical to determine the changes of $MgATP^{2-}$ concentration inside the bacteria. $MgATP^{2-}$ is often the true substrate in reactions described as ATP dependent[76]. The ions Mg^{2+} and ATP^{4-} may even act as inhibitors, as has been reported in rat-liver glucokinase.

The concentration of inorganic phosphates in aquaculture units tends to rise as organic molecules are

broken down. The concentration levels out as insoluble magnesium and calcium salts are formed.

4.4.3 Sample Preparation

The methods for water analysis were the same as those practised by the marine biological department at Heriot-Watt University, with a few additional modifications. All the glasswear, sampling bottles and pipette tips were soaked in "Decon 90" overnight, acid-washed and rinsed with de-ionized water.

All the measurements, except the colourimetric tests, were carried out immediately, and the remaining sample was then frozen at -20°C.

4.4.4 Immediate Measurements

Temperature

Temperature was measured using a mercury-in-glass thermometer, accurate to ± 0.25°C, and placed in the mixing tank so that half its length was in contact with the water.

Hydrogen Ion Activity (pH)

Hydrogen ion activity was measured using a Russell CE7L/LCW electrode compensated for temperature sensitivity.

Dissolved Oxygen

The dissolved oxygen concentration was measured using a "Y.S.I. model 57 oxygen meter" calibrated for temperature and used as recommended in the operating instructions.

Conductivity

This was measured using a Corning 220 conductivity meter with a platinum electrode. The meter was calibrated and used in accordance with the manufacturer's manual. The ionic strength (mmol l^{-1}) was estimated by dividing the conductivity (micro Scm^{-1}) by one hundred[77].

Alkalinity

The methods used to measure alkalinity were taken from "Methods for Physical and Chemical Analysis of Fresh Waters"[77]. Phenolphtalein alkalinity, total alkalinity, carbonate alkalinity and total CO_2 were measured. This was done by titration with acid to endpoints determined by indicators.

Total alkalinity can be affected by $Si(OH)_3^-$, $H_2BO_3^-$, NH_4^+, HS^-, organic anions, and colloidal or suspended $CaCO_3$. In the experiments, the concentration of NH_4^+ ions was potentially high enough to affect the result. Thus, the sample for the total alkalinity was normally taken at the end of the experiment, when the ammonium ion concentration was at its lowest level.

A gas chromatographic method could have been used, but a suitable column was not available.

Ammonia Gas Electrode

During the experiments to establish the shape of the curve of ammonia versus time, a Philips IS 570-NH_3 ammonia gas electrode was used to obtain quick estimates of the ammonia concentration. This method was employed in order to

estimate the dilutions for the longer colourimetric method. The method involves adding alkali so that all the ammonia was in gaseous form. A calibration chart must be made for the temperature in question prior to the use of the electrodes. This method has several drawbacks. Only relatively high concentrations of ammonia can be measured accurately, the electrode is sensitive to changes in temperature and adding the alkali causes the temperature to rise. The electrode can only detect ammonia gas, and the sample takes over 10 minutes to equilibrate at the concentrations in the mg/l range. During this time ammonia gas is liberated.

An ammonium ion electrode would have been much more useful, but none was available. This method has the advantage of not destroying the sample and could be used in control systems. Ammonium ion electrodes are also sensitive to temperature changes, but by using a constant temperature cell this may be reduced. It is possible that the lower limit of repeatable detection may be reduced with a constant temperature cell.

4.5 Colourimetric Determinations

4.5.1 Developing a Good Analytical Technique

Colourimetric tests were used to determine ammonia, nitrite and nitrate concentrations during the reactions. The total volume of water in the system was about 50 litres. To ensure that the sampling did not remove significant amounts of substrates from the system, the water used for analysis was

minimized. The sample volumes, frequency and substrate required were determined by trial and error. As the rate of reaction was found to vary more at the beginning of the reaction, more samples were taken during the first fifteen minutes. The overall time for the reaction was reduced to about half an hour by choosing the right amount of substrate to be added. This was done in a way which ensured that as little change as possible in the numbers of bacteria was encouraged. The timing and volume of the samples taken for each experiment can be determined from the results in appendix 5.a.

The water samples were defrosted at room temperature, a few at a time. They took over two hours to defrost. To ensure that the samples were at the right temperature prior to their analysis, they were then placed in water at room temperature.

In reading the extinctions, 4-cm-long cells were used where 10 cm ones are recommended, as these are the largest that would fit the Pye Unicam SP1700 spectrophotometer. This means that the standard F factors were different from those suggested in " A Practical Handbook of Seawater Analysis"[78]. All the colourimetric methods used have ranges in which Beer's law is followed. In order to determine concentrations outside the linear range of the test, the samples were diluted with the appropriate quantity and type of water. This was common practice in analyzing the water quality in the aquaculture units. The samples were prepared each with different dilutions. To obtain the actual sample concentration, the dilution factor had then to be applied.

The lowest dilution within this linear range was used

for analyzing the reaction rate. In the rare case of the dilution in question being significantly different from the other dilutions and outside experimental error, the next lowest dilution was used. The most likely reason for such occurrences is that an incorrect dilution is performed or an incorrect amount of reagent added.

An automatic pipette was used for adding the reagents and for adding the smaller sample quantities required for large dilutions. The automatic pipette was calibrated prior to use. An automatic pipette is essential for fast analysis, particularly for ammonia.

4.5.2 Total Ammonia

This was measured using a colourimetric method taken from "A Practical Handbook of Seawater Analysis"[78], which can be used in both sea and freshwater. The required glasswear was acid-washed in 0.5 M HCl, not dicromate acid, and rinsed with de-ionized water. Fresh de-ionized water was used in diluting the samples.

Thus the required factor to obtain the actual total ammonia concentration expressed in mg/l Nitrogen is:

E*F*14.01/1000*Dilution Factor.

E and F are defined in the method.

The dilutions used for ammonia range from no dilution to 25 times dilution. The table below gives the quantities.

Table 3. Dilutions for ammonia and nitrite.

Dilution	Sample volume	Ammonia Free volume	Total
None	50	0	50
*2	25	25	50
*5	10	40	50
*10	5	45	50
*25	2	48	50

The value of F for the 4 cm cell was between 21 and 33, depending on the amount of ammonia in the blank. The standard extinction was about 0.245.

The accuracy of the method as used was about ± 5% for a particular dilution of a known standard concentration. This compares with ± 2% for the stated method[78]. This discrepancy is attributed to four factors:

1. Inaccuracies in making the dilutions;
2. Ammonia gas escaping during dilutions or ammonia contamination of the ammonia free water;
3. The use of a 4 cm spectrophotometer cell;
4. An optimistic evaluation of the likely errors in the stated method.

To minimize the error, fresh de-ionized water was always used, dilutions were performed quickly and the condition of the de-ionization column was checked regularly.

The effect of light was assumed to be significant, and during colour development flasks were kept away from light.

4.5.3 Total Nitrite

The method for the determination of total nitrite was taken from "A Practical Handbook of Seawater Analysis"[78]. The nitrite samples were diluted, where necessary, in the same way as the total ammonia samples. The concentrations of total nitrite were in the micro g/l-N range, and therefore the concentrations are expressed in micro g/l Nitrogen. The total nitrite is thus calculated using:

Corrected Extinction * F * 14.01 * Dilution factor

For the 4-cm-cells the value of F is about 4.6 to 5.6

The accuracy of the nitrite and nitrate determination was ± 5 % for a given dilution. This is again more than the stated method and the discrepancy is attributed to factors one, three and four given for ammonia.

4.5.4 Nitrate

The concentration of Nitrates in the rig water was between 30 and 40 mg/l NO_3-N and corresponds to that measured in the aquaculture recycle units. The method for the determination of total nitrate was taken from "A Practical Handbook of

Seawater Analysis"[78]. The samples required to be diluted 50- and/or 100-fold.

Dilution	Sample volume	Nitrate	Free volume	Total
*50	2	98		100
*100	1	99		100

Nitrates are reduced to nitrites using a cadmium-copper column in alkaline solution. The analysis then follows the same procedure as for nitrite determination.

The design of the reduction column given in the stated method was modified and had a burette tap on the end. This provided better control of the flow through the column than tilting. When not in use, the column was covered in parafilm to avoid evaporation and the column drying out. As the concentration of nitrate was always a magnitude higher than the nitrite, no nitrite correction was required. The total mg/l- N nitrate is thus calculated using:

corrected Extinction*14.01/1000*F*Dilution Factor.

4.6 Substrates and Ionic Equilibria

The largest effect on the fractions of each ion in equilibrium is exerted by pH, followed by temperature and, to a smaller extent, ionic strength.

Many of the possible substrates in nitrification form ionic equilibria. In order to determine the required form of the substrate, the degree of ionization must be known at the pH, temperature and ionic strength in question. To allow

computer calculation of the fraction of each possible substrate in the rate equations, equilibrium constants were incorporated into formulae. The formula used to correct the equilibrium constant for temperature was:

$$pK = -\log K = (a/T) + cT - b. \qquad (55)$$

This was curve-fitted using the least squares method. In calculating an equilibrium constant over a pH-range, the readings were converted to concentrations and averaged. The log of the average was then taken to yield pK. When calculating the average pH, this method must be used[79].

The ionic strength estimated from the conductivity was high because of the large amounts of sodium nitrate. The corrections for a conductivity of 550 (micro S cm^{-1}) were used[77] for the various alkalinities. The corrections for pHs between 7.2 and 9.0 were small, and so was the likely error.

4.6.1 Ammonia Equilibrium

$$pK \qquad NH_3(g) + H_2O \rightleftharpoons NH_4^+ + OH^- \qquad (56)$$

Ammonia gas exists in equilibrium with ammonium ions in water, the quantities of each depending on temperature, pH and salinity. The "ammonia" concentrations calculated by using the modified colourimetric method refer to total ammonia-nitrogen. This is the concentration of the gas and ion combined, expressed in mg/l of Nitrogen. To obtain the fraction of ion or gas present requires knowledge of the pH, the temperature and the salinity. Since the experiments were

confined to freshwater, no salinity correction was necessary. Emerson et al.[80] have produced tables giving the percentage ammonia gas for 0-30°C and a pH of 6-10. This was curve-fitted and the correlation ratio was 1.0 to 5 decimal places. The values of the constants were found to be:

$$a = 2.804 * 10^{3} \quad b = 0.4227 \quad c = 0.88 * 10^{-3}$$

and these are valid for the temperature and pH limits above. The fraction of the ammonia gas to the total ammonia is given by :

$$\frac{\text{ammonia gas}}{\text{total ammonia}} = \frac{1}{1 + \dfrac{\text{ammonia ion}}{\text{ammonia gas}}} \qquad (57)$$

A correction for ionic strength obtained from reference 79 was applied to the ammonia ion/ammonia gas fraction. This correction was of the order of 1.1, which is equivalent to a 10% increase in the ammonium ion/gas fraction (note that the correction should <u>not</u> be used as suggested on the ammonia gas/total ammonia fraction as suggested in reference 79):

$$\frac{\text{ammonia ion}}{\text{ammonia gas}} = 10^{(pK + \text{Correction} - pH)} \qquad (58)$$

$$\text{Correction} = \frac{A' I^{\frac{1}{2}}}{1 + I^{\frac{1}{2}}} \qquad (59)$$

Where I is the ionic strength (less than 0.1 M) and A' is a coefficient given by:

$$A' = 1.82483 \times 10^{6} \times [\ E \times (T_c + 273.16)]^{-1.5}$$

E is the dielectric constant:

$$E = 87.74 - 0.4008 \times T_c + 9.398 \times T_c^{2} - 1.41 \times 10^{-6} \times T_c^{3}$$

where T_c is the temperature in Celsius.

4.6.2 Nitrite Equilibrium

$$pK \quad HNO_2 \rightleftharpoons H^+ + NO_2^- \qquad (60)$$

Total nitrite forms nitrite ions and nitrous acid in solution. The equilibrium is dependent on ionic strength, as well as temperature and pH. Sodium nitrate builds up in aquatic environments. This increases the ionic strength of the water. Tummavuori and Lumme[81] investigated the equilibrium constant for nitrite and expressed the relationship to temperature as above. Their values for the constants are:

$$a = 5.8554*10^{3} \quad b = 34.558 \quad c = 60.571*10^{-3}$$

The fraction of the nitrous acid is given by:

$$\frac{\text{nitrous acid}}{\text{total nitrite}} = \frac{1}{1 + 10^{(pH-pK)}} \qquad (61)$$

A correction for ionic strength is also given. Very little nitrous acid is found above pH 6 and thus in aquaculture total nitrite tends to exist as nitrite ion. The colourimetric method measures total nitrite and is expressed as total nitrite-nitrogen. Since the pH in the nitrification

experiments was above pH 6 for all the experiments, the nitrite ion was considered to be equal to the total nitrite concentration.

4.6.3 The Carbonate, Bicarbonate, Carbonic Acid System

The stoichiometry of nitrification, given in 1.2.1, indicates that hydrogen ions are produced. These are buffered, the most important buffer system in natural waters being the carbonate, bicarbonate, carbonic acid system. This system is also important in understanding the proton concentrations required for the proposed formation of a carboxy phosphate ester. A pH of less than 4 at the formation site would provide no bicarbonate ions.

Carbon dioxide gas dissolves in water and forms an ionic equilibrium with bicarbonate ions and carbonate.

$$pK_1 \qquad H^+ + HCO_3^- \rightleftharpoons H_2CO_3 \rightleftharpoons H_2O + CO_2(g) \qquad (62)$$

$$pK_2 \qquad HCO_3^- \rightleftharpoons H^+ + CO_3^= \qquad (63)$$

This equilibrium is established in a very short time. The amount of each component depends on the pH, temperature and ionic strength. If the equilibrium shifts because of a change in concentration of a component, the dissolved carbon dioxide is no longer in equilibrium. The result is that the carbon dioxide in solution forms a new equilibrium with that in the air. The series of equilibria acts as a buffer. This system is predominant in freshwater lakes. The dominant cation in most freshwater is Ca^{2+}, followed by Na^+. However, in the recycle reactor Na^+ was dominant, because of the

addition of Sodium Carbonate. The series of equilibria formed with Na+ along with ionization constants is given in "Chemical Analysis of Fresh Waters"[77]. These ionization constants were curve-fitted with a correlation ratio of 0.9995. The temperature correction constants for the two resultant equilibria are:

pK_1 a = 3821.6, b = 17.7106, c = 0.0377

pK_2 a = 2988.6, b = 7.0530, c = 0.0247

Strictly speaking, these constants are valid at temperatures between 0 and 25°C for water of zero ionic strength. When calculating the various alkalinities, corrections for ionic strength based on conductivity were used[77].

The fraction of bicarbonate ion goes through a maximum at a pH given by $(pK_1 + pK_2)/2$, approximately pH 8.3. Below pH 7.5 no carbonate ion exists, and above pH 9.5 no carbon dioxide exists. Between these pHs carbon dioxide, bicarbonate and carbonate ion all exist and to obtain the bicarbonate fraction the other two fractions must be calculated.

The CO_2 fraction is given by:

$$\frac{\text{carbon dioxide}}{\text{total carbon}} = \frac{1}{1 + 10^{(pH-pK_1)}} \quad (64)$$

The $CO_3^=$ fraction is given by:

$$\frac{\text{carbonic acid}}{\text{total carbon}} = \frac{1}{1 + 10^{(pK_2 - pH)}} \qquad (65)$$

The bicarbonate fraction is given by:

$$HCO_3^- \text{ fraction} = 1 - CO_2 \text{ fraction} - CO_3^= \text{ fraction} \qquad (66)$$

To illustrate all the above equilibria and their relationship to pH, figure 10 has been calculated using the curve-fitted equilibrium constants for 24°C.

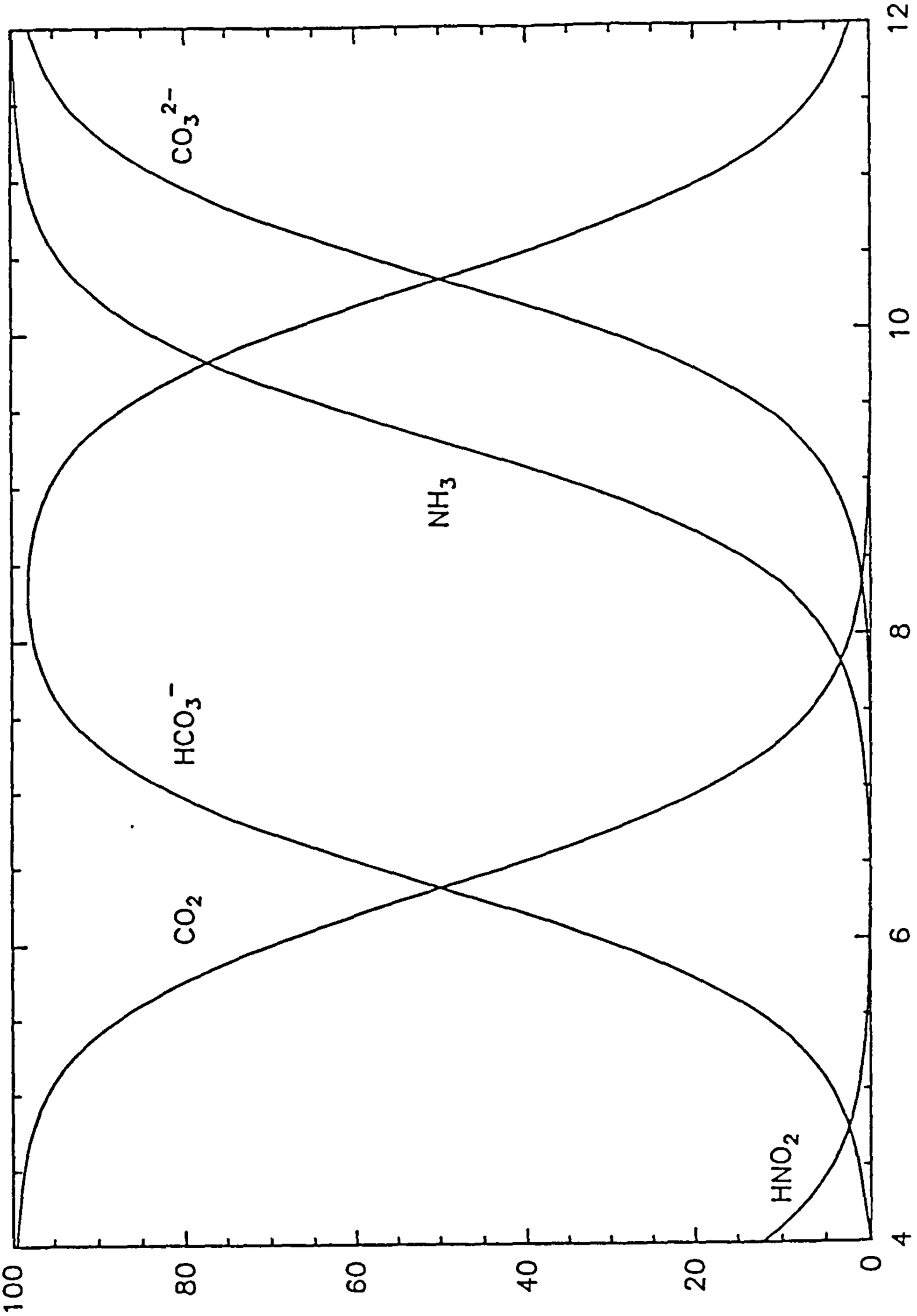

Figure 10. Nitrification Substrates and their Equilibria.

CHAPTER 5

THE OXIDATION OF AMMONIA AND THE IMPULSE REACTION RESULTS

The unsteady-state experiments revealed findings to which no comprehensive explanation could be offered without the involvement of bicarbonate ions in the reactions. The kinetic experiments and their associated observations are described in sections 5.1, 5.2, 5.3 and 5.6. Mechanisms are proposed that include bicarbonate ions in the reactions.

5.1 Initial Impulse Reaction Studies

The first experiment was conducted to investigate the nature of the curve of the ammonia concentration versus time (see figure 11). This served to find where the rate of reaction changed most and to check whether the conversion per pass was small, justifying the batch reactor assumption. The experiment was conducted at a pH of 8.0, and influent and effluent samples were taken from the filter. An impulse addition of ammonia (7.15 mg/l-Nitrogen) - large by aquaculture standards - was made, and samples were taken over a time of more than 13 hours. Ammonia, nitrite, nitrate, conductivity, alkalinity, (see figures 11 to 15) dissolved oxygen, pH and temperature were all measured, as is described in the chapter 4. All the kinetic results are presented in appendix 5.a.

The ammonia gas electrode gave concentrations of total ammonia significantly below those found by the colourimetric method. This is attributed to loss of ammonia gas after the addition of alkali.

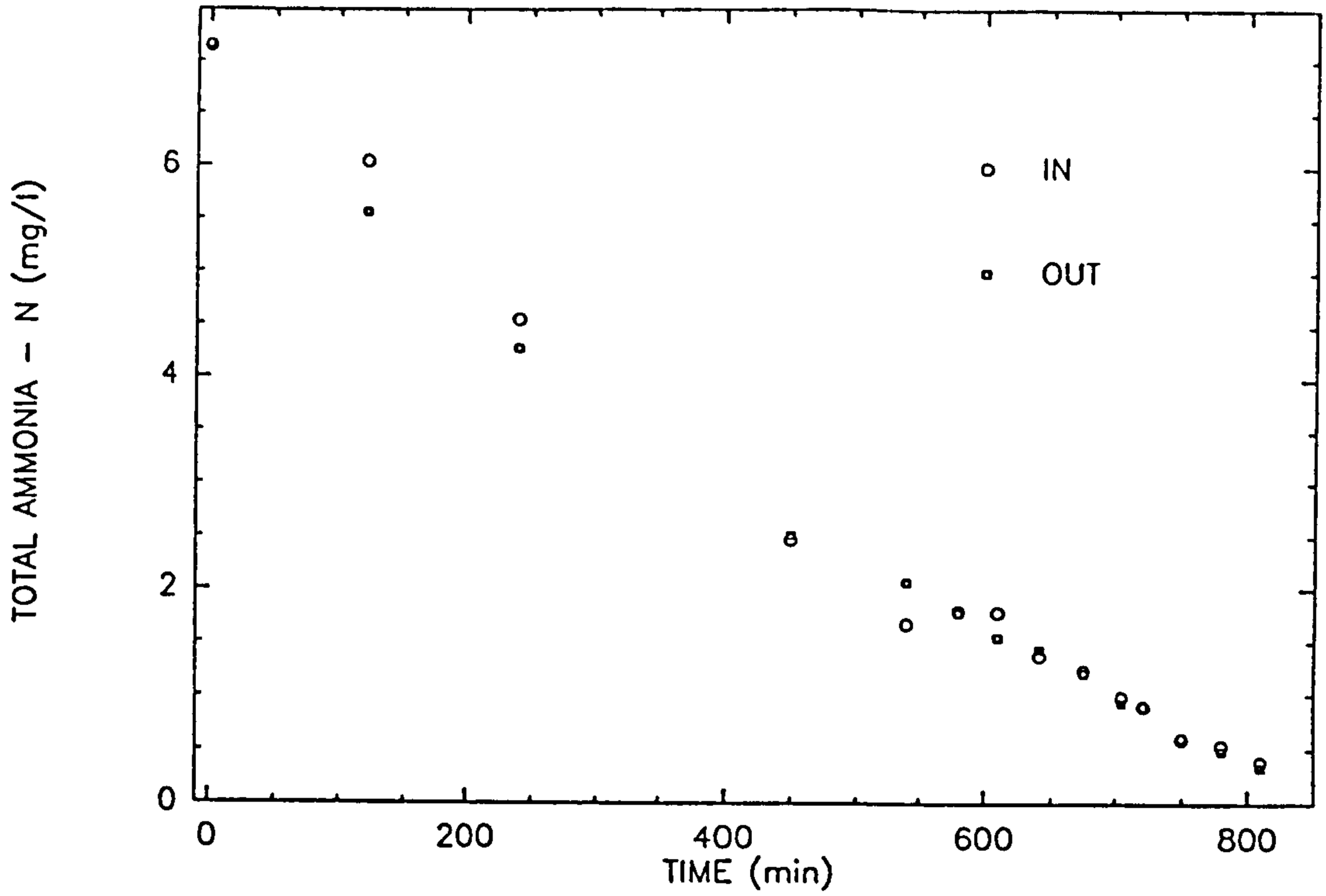

Figure 11. Ammonia concentration versus time curve.

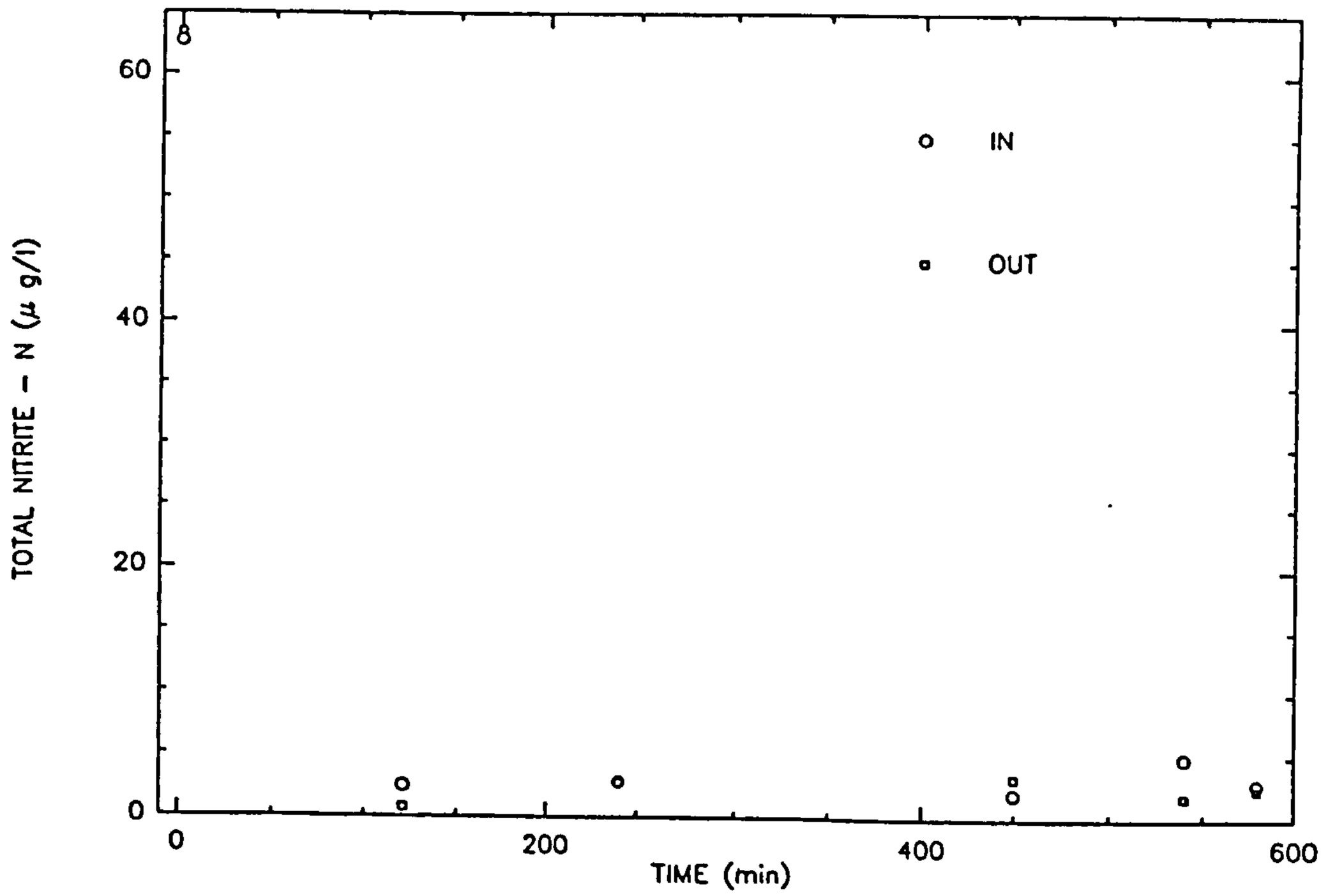

Figure 12. Nitrite concentration versus time curve.

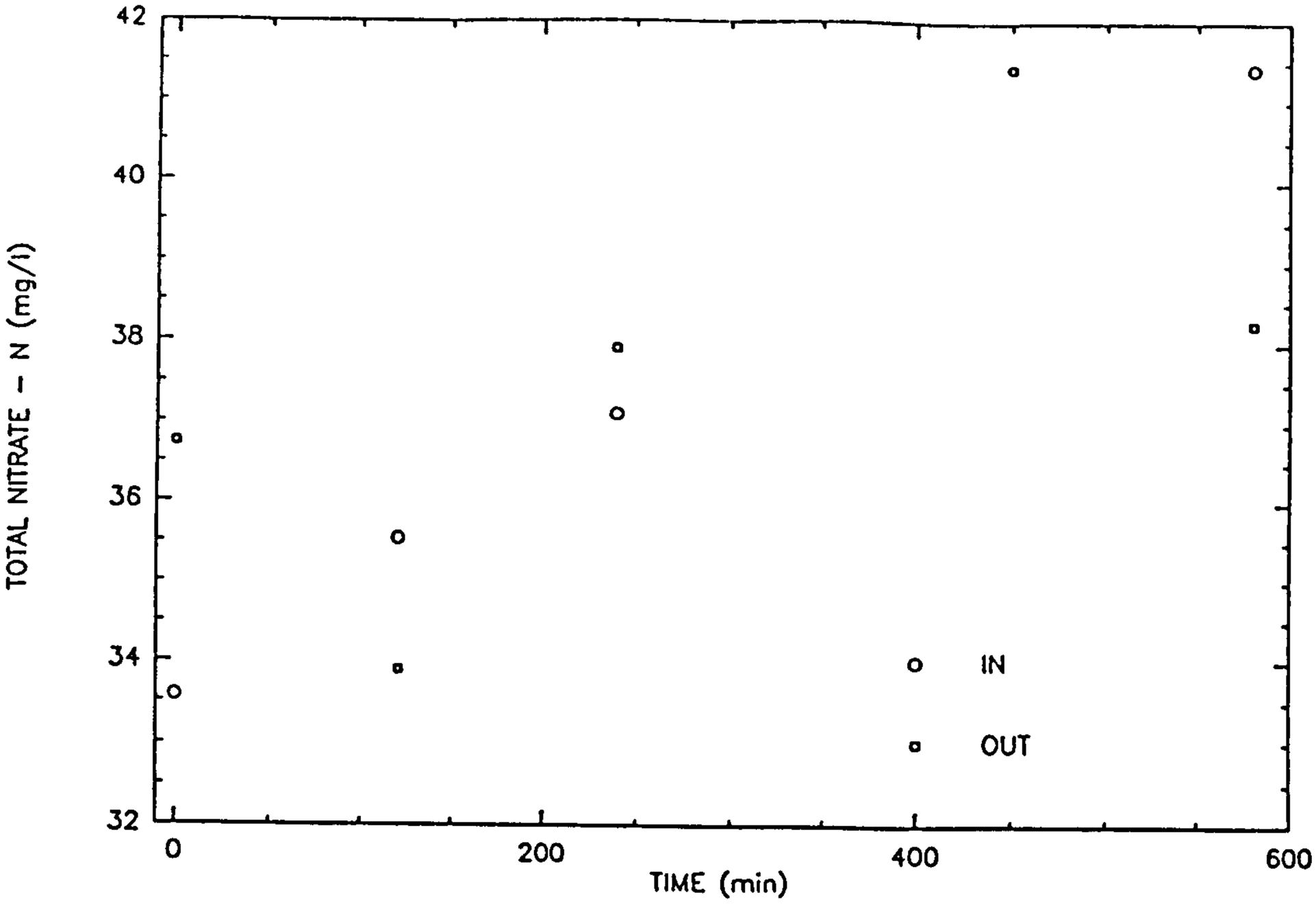

Figure 13. Nitrate concentration versus time curve.

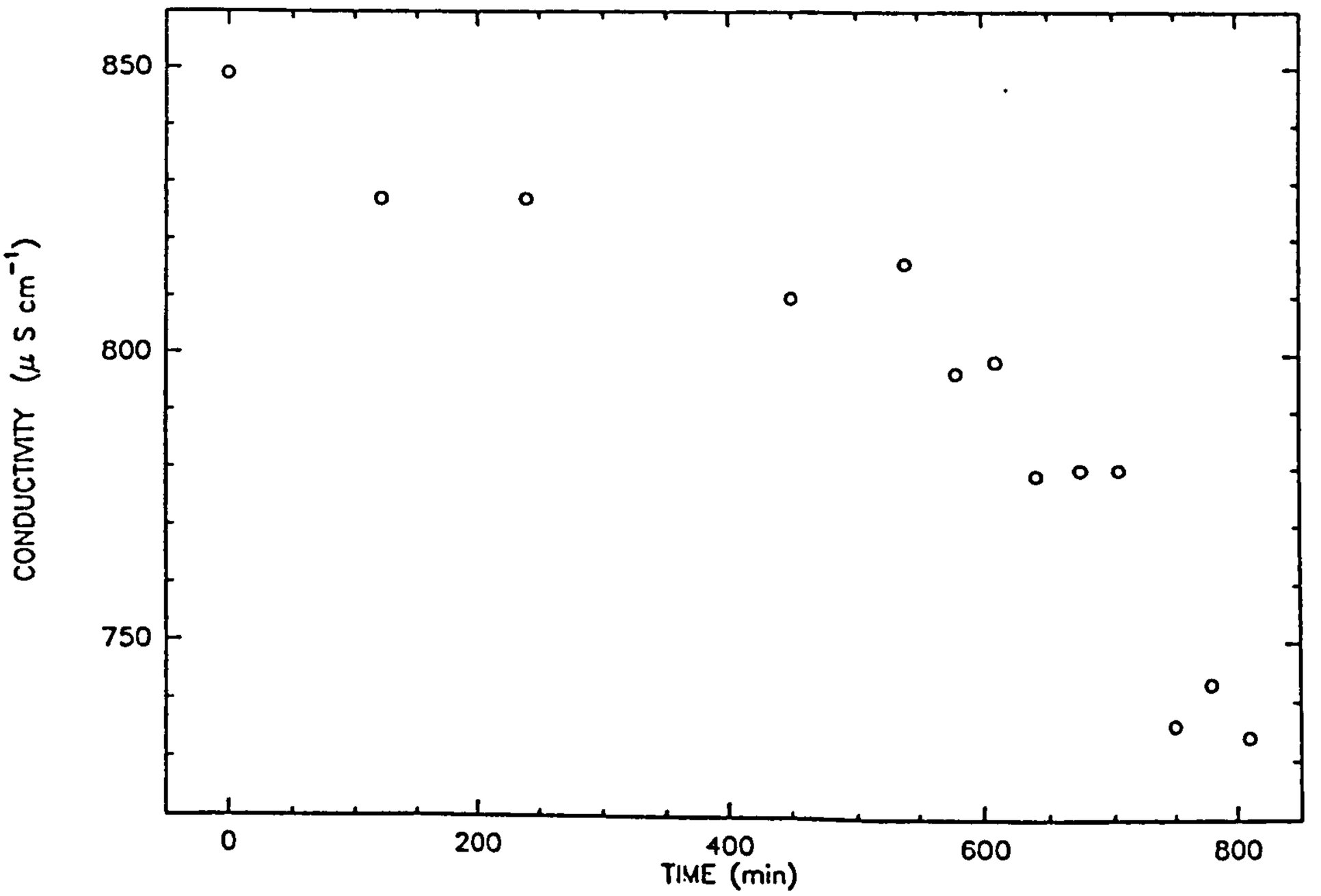

Figure 14. Conductivity versus time curve.

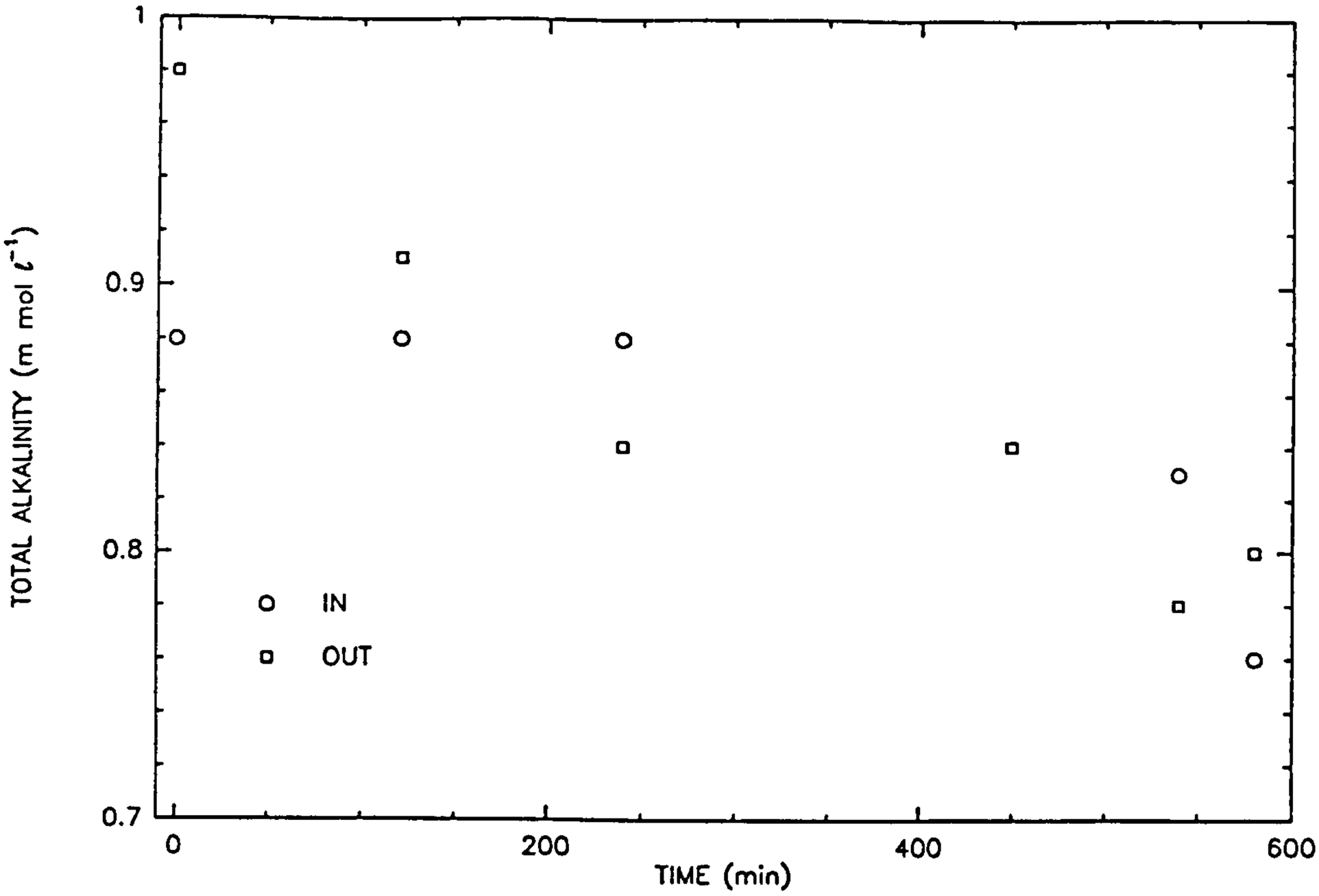

Figure 15. Total alkalinity versus time curve.

The rate of ammonia oxidation is observed (figure 11) not to have changed dramatically during the experiment. The difference between the ammonia concentration at the filter inlet and that at the outlet is at most 10%, 5% being the accuracy of the colourimetric test used. From this, it can be deduced that the conversion per pass is indeed small. Therefore, the recycle system can be equated to a batch reactor. As there was little change in the rate of reaction, it was decided that total ammonia concentrations of less than 1 mg/l Nitrogen would be studied, because these correspond to the concentrations found in recycle aquaculture systems.

It is of interest to note that, at the start of the reaction, the nitrite concentration was only 64 micro g/l NO_2-N, falling below 5 micro g/l nitrogen after two hours.

This indicates that the nitrite reaction is faster than the ammonia reaction (note the change in scale between figures 11 and 12). Its low concentration in this experiment is linked to the fact that it is an intermediate in the series of reactions forming nitrification.

As expected, the nitrate concentration rose during the experiment (see figure 13). The concentration of dissolved oxygen never fell below 7.5 mg/l, and thus it is assumed that no significant denitrification occurred.

The conductivity (see figure 14) and the total alkalinity (out of the filter, see figure 15) were observed to decrease. The drop in conductivity and the alkalinity is explained by the removal of bicarbonate ions from solution. At a pH of 8, the vast majority of the measured total alkalinity is a result of bicarbonate ions (see figure 10). Thus, figure 15 represents the bicarbonate ion concentration during the experiment.

The experimental error in the stated method[77] is 2% for measured total alkalinities of 1 mmol/l, rising to 10% for 0.1 mmol/l. (However, the data have not been corrected for any ammonium ion included in the total alkalinity estimate). As the measured alkalinity is just below 1 mmol/l, the error is probably between 2 and 5%. The drop in total alkalinity during the experiment, as shown in figure 15, is between 10 and 13 %.

The removal of bicarbonate ions is also reflected in the drop in conductivity. The total alkalinity was only measured for 540 minutes but the conductivity was measured for longer.

The measurement of total alkalinity is not without

problems. How does one distinguish between carbon dioxide removed for growth and bicarbonate ions that might be removed to make "active CO_2"?

Sodium carbonate was added to the system during the experiment to maintain a constant pH. The balanced equation from the known reaction stoichiometry (see 1.2.1) is:

$$(NH_4)_2SO_4 + 4O_2 + 2Na_2CO_3 \longrightarrow Na_2SO_4 + 2NaNO_3 + 2H_2CO_3 + 2H_2O \quad (67)$$

The addition of buffer would be expected to maintain the ionic equilibrium, and from this equation the number of ions in solution would be expected to remain the same or increase (for H_2CO_3 breaking down to ions).

The unexpected observation is the magnitude of the fall in alkalinity and conductivity. This indicates two possible causes for the observed behaviour, i.e. bacterial growth and the formation of "active CO_2". In examining the amounts of bicarbonate ions removed, it should be remembered that Nitrosomonas grow very slowly by bacterial standards. Furthermore, all bacteria take a certain time before growth occurs, after a step input of substrate, called the lag phase. The conductivity graph suggests that significant carbon (growth) was taken up after 600 minutes. This begs the question of how much carbon was taken up before significant growth started.

The total amount of carbon, i.e. the carbon (CO_2 / HCO_3^-) removed from the water plus the carbon added as sodium carbonate, was 6.25 mg/l - C during the first 580 minutes. The United States Environmental Protection Agency[26]

indicates that five carbons are used for every nitrogen (i.e. bacteria have the stoichiometry $C_5H_7NO_2$) by growing bacteria. If all the carbon removed formed cells, this would give a yield coefficient (see 3.3) of 0.23 . It is most unlikely, if not impossible, for the bacteria to manage this solely on thermodynamic grounds. Thus, in all probability, a significant amount of the bicarbonate ions removed have not been used to form new cells.

5.2 Impulse Reaction Rates and Bacteria History

The next experiment was conducted to check that the impulse reaction studies could be reproduced. Two impulse experiments were performed under the same experimental conditions at an interval of 24 hours. After allowing a few minutes for the substrate to mix thoroughly with the rig water, samples were taken over the next 80 minutes. The graph of total ammonia concentration versus time for both experiments is shown below in figure 16.

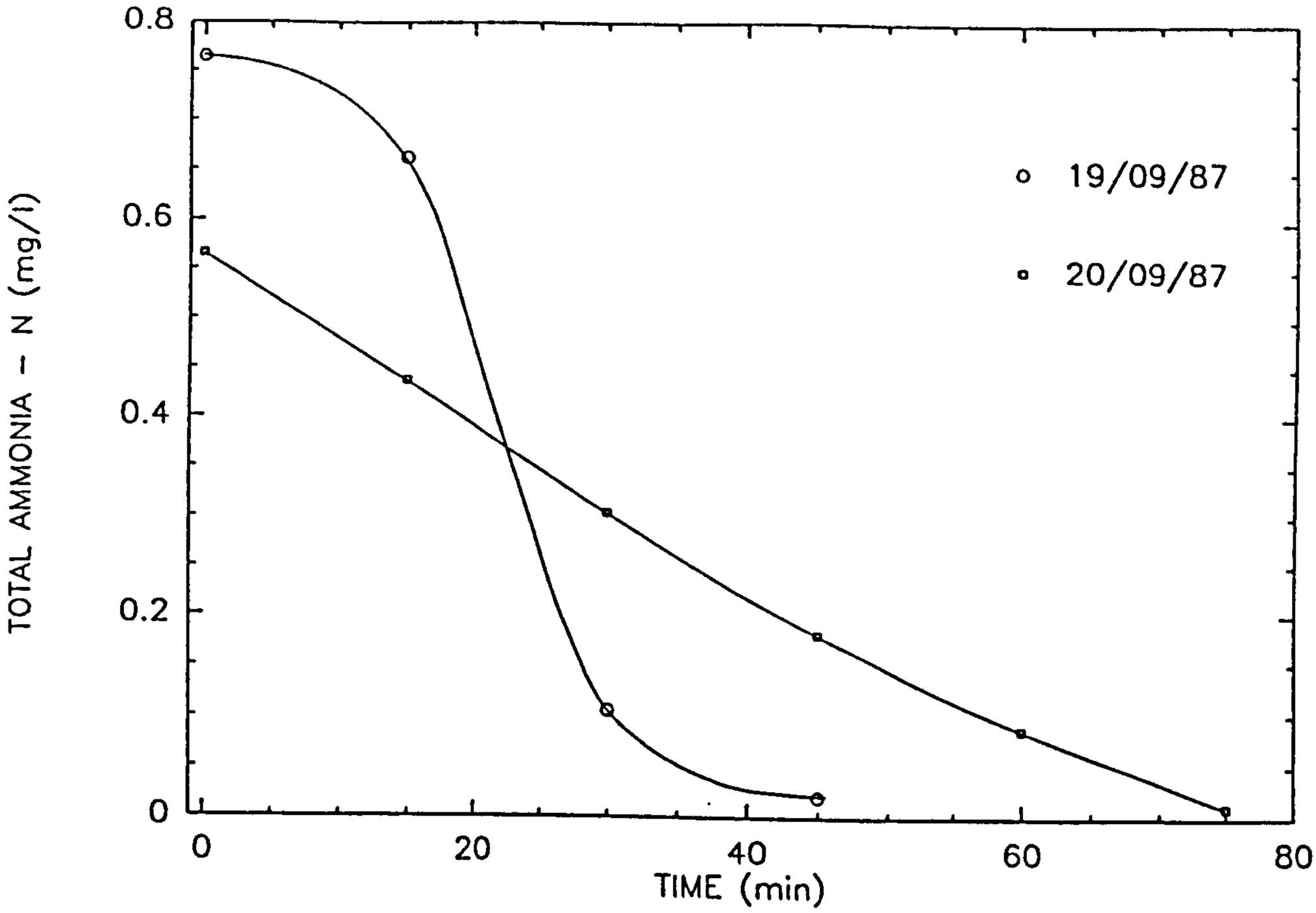

Figure 16. Bacteria history and the observed reaction rate.

The differences between the two curves were so great that the reaction kinetics was thought to be different in each experiment. Subsequent experiments confirmed the experiments to be reproducible, but never exactly. The particular result above appears to be connected with the experiment conducted prior to it. The first of the reproducibility experiments was conducted two days after the investigation of the curve of ammonia versus time. This experiment lasted for over 13 hours and added significantly more ammonia (426 mg N) than the metering pump would have done over the same time interval (189 mg N).

It might be thought that the number of bacteria was

higher on the 19th than on the 20th. However, a change in the number of bacteria would be expected to alter the slope of the reaction curve, but not its shape. The shape of the curve observed on the 19th suggests sigmoidal behaviour (see 7.5). Sigmoidal behaviour in enzymes is associated with control mechanisms. This will be examined more closely in chapter 7.

The results indicate that some chemical accumulated as a result of the earlier experiment, which <u>increased</u> the reaction rate on the 19th, but was present in lesser amounts on the 20th. A further restriction is that it should control the reaction in a sigmoidal manner.

In previous literature (see 1.2.3), hydroxylamine has been put forward as an intermediate and as such it could accumulate. However, hydroxylamine is an inhibitor and would decrease the rate, contrary to the behaviour observed.

The following explanation for the observations is offered. It is assumed that, between the experiments, the bacteria adapted (as observed by Haug et al.[6] with changes to pH) to the different ammonia concentrations. It is suggested that the chemical increasing the reaction rate is ATP, which has been shown to exhibit sigmoidal behaviour with carbamate synthetase (this is expanded on in 7.5). The reaction rate is assumed to have depended on the number of binding sites activated by ATP and bicarbonate ions. This is supported by the observations described in the previous section, which suggested that bicarbonate ions were removed during the experiment to make "active CO_2". The bacteria appear able to alter the reaction rate to maintain optimum efficiency. The result is that the nitrification reactions

depend to a certain extent on the bacteria's recent history. The realization that bacteria control the reaction rate is crucial to understanding nitrification data. The method by which bacteria are assumed to control the reactions is examined in detail in chapter 7.

5.3 The Lower pH-Limit at which Ammonia Oxidation Stops

During preliminary experiments, conducted to determine the required substrate additions and sampling procedure, a further experiment was conducted. Ammonium sulphate was added with the metering pump and the flow inducer was switched off. Thus, the system was not buffered other than by carbon dioxide in the air. The pH fell from pH 8.0, as would be expected, to 4.01 ± 0.01, but it did not fall any lower.

This corresponds exactly to the lower pH-limit at which bicarbonate ions exist in solution (see figure 10), strongly suggesting bicarbonate ions are involved in the reaction. It should be stressed that this experiment does not indicate that growth is possible at this pH, but rather that ammonia oxidation stops.

The cessation of ammonia oxidation at a pH of 4.01 has the improbable alternative explanation that this value is a coincidence and that some unknown mechanism also shares this lower pH limit. The implied mechanisms of section 1.2.3 give no explanations for this observed lower pH limit.

The conclusion drawn from this experiment and the others detailed in sections 5.1, 5.2 and 5.6 is that bicarbonate ions are very probably involved in the oxidation

of ammonia. In order to elucidate on how the bacteria's control mechanism might operate with bicarbonate ions and ATP, the oxidation of ammonia via carbamate was investigated.

5.4 Ammonia Oxidation and its Proposed Mechanisms

There are two steps in the oxidation of ammonia, each carried out by a different enzyme (see 1.2.3). The first involves the oxidation of ammonia to an intermediate by ammonia mono-oxygenase. The second step, as seen by previous authors, is the oxidation of the intermediate hydroxylamine (see 1.2.3) to nitrite, by the enzyme hydroxylamine oxidoreductase.

While the oxidation of ammonia occurs in two stages, the rate-determining step has been considered by all authors[19.20.21] to be the step involving ammonia mono-oxygenase.

5.4.1 The Proposed Mechanism for Ammonia Mono-oxygenase

The mechanisms of carbamyl phosphate synthetase have already been discussed (see 3.7) in relation to the role of intermediates. However, the weakness of hydroxylamine as a proposed intermediate in the oxidation of ammonia requires reiteration.

Hydroxylamine is a potential mutagen, [19,20,21] and it stops the oxidation of ammonia at low concentrations[40,41]. It has been indicated that it inhibits the oxidation of ammonia because of its toxicity [19,20,21]. As a proposed

intermediate, it must move between the two enzymes involved. It has been suggested [39] that it may be transferred by a special carrier molecule. The structure of such a carrier, other than the formation of a C-N (organic) bond, is not obvious.

The experimental observations dictate a series of requirements. Hydroxylamine is required to move between the enzymes involved at low concentrations, because of its toxicity. However, the oxidation of ammonia must be controlled by the bacteria if they are to use the substrate efficiently. Feedback control by hydroxylamine would require concentrations that inhibit (not stimulate) the reaction[41, 40, 37], but these concentrations are detectable. However, *no hydroxylamine has ever been detected [39] during the normal oxidation of ammonia.*

In summary,

1. Hydroxylamine as an intermediate fails to account for the observed reaction kinetics.
2. It has never been detected during the normal oxidation of ammonia despite the requirement for it to move between the two enzymes involved in detectable concentrations.
3. Hydroxylamine as an intermediate leaves unanswered many questions regarding toxicity, thermodynamic barriers, the second intermediate, alternative substrates and inhibitors.

The kinetic data and the many unanswered questions

reveal a need for an alternative mechanism. The following proposed mechanisms can explain the kinetic data and answer many questions.

The statistical analysis of kinetic data (chapter 3) rejects the hypothesis that hydroxylamine is formed by the direct oxidation of ammonia. However, the possibility that hydroxylamine could be formed from carbamate was investigated as a possible alternative path still involving hydroxylamine. After examining chemical mechanisms[60,65] relevant to the formation of hydroxylamine from carbamate, it seemed that this was improbable. The oxidation of carbamate to hydroxamic acid seems to be a more promising route. Both carbamate and hydroxamic acid are unstable and break down readily. Hydroxamic acid forms complexes which increase its stability. It is proposed that hydroxamic acid, and not hydroxylamine, is the true intermediate. If this is the case, the enzyme hydroxylamine oxidoreductase is incorrectly named.

The manner in which the oxidation of ammonia is proposed to proceed is now given. In the first steps, carbamate is formed in a similar way to that given by Meister et al. [68]. The carbamate is then oxidized by a peroxide to the proposed intermediate hydroxamic acid.

The formation of carbamate is thought to be similar to the acylation of amines by esters[60]. The ester is the phosphate ester formed by reaction of bicarbonate with ATP. The mechanism suggested corresponds to the one given in "Advanced Organic Chemistry"[60].

Formation of the Carboxy Phosphate Ester

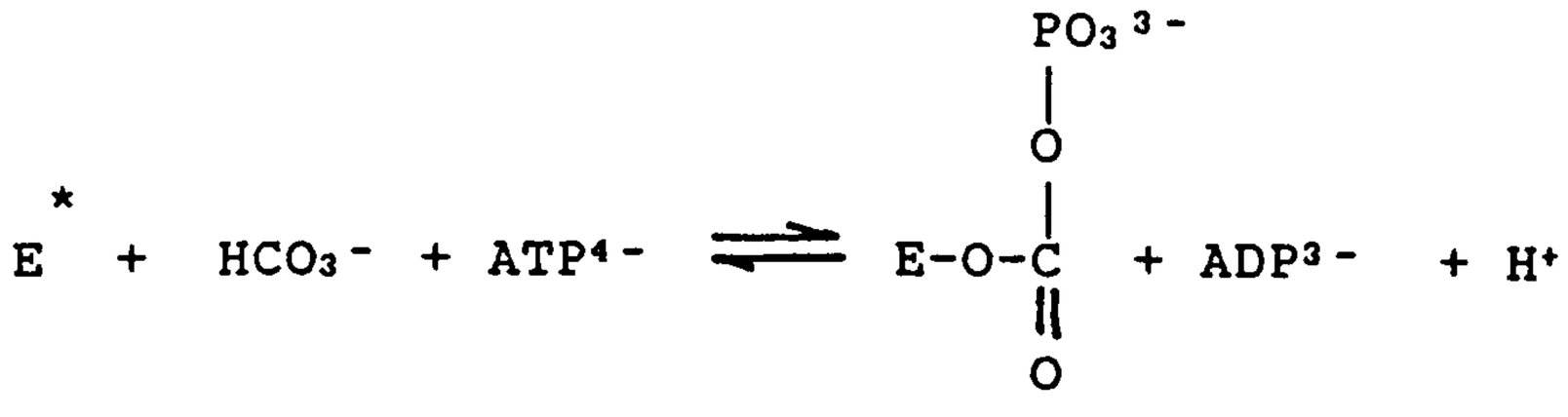

* Enzyme or Haem location.

The Acylation of Ammonia in Basic Conditions

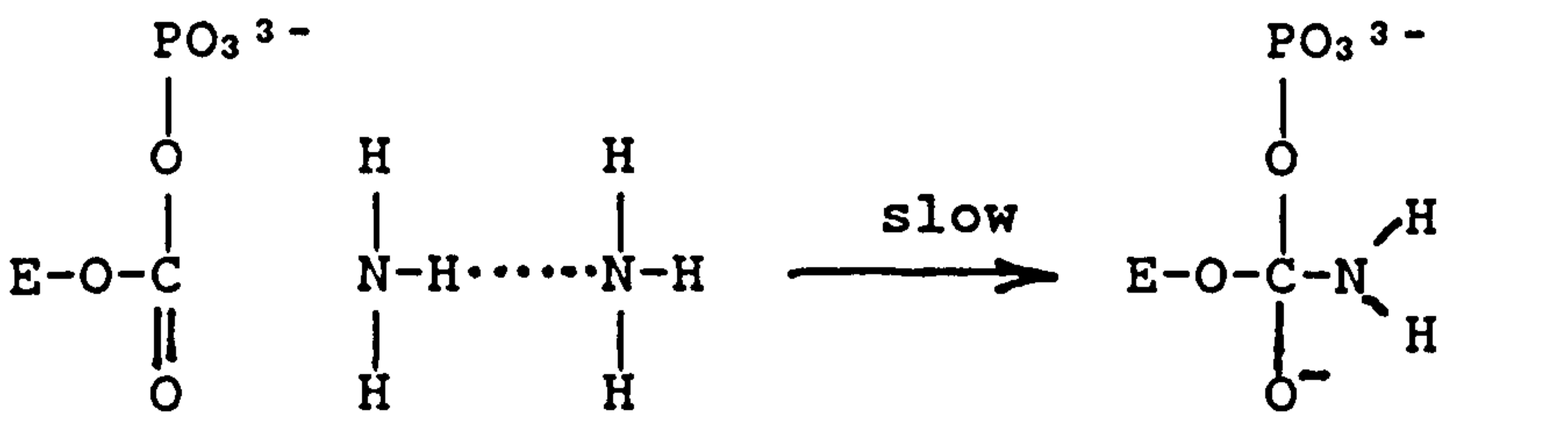

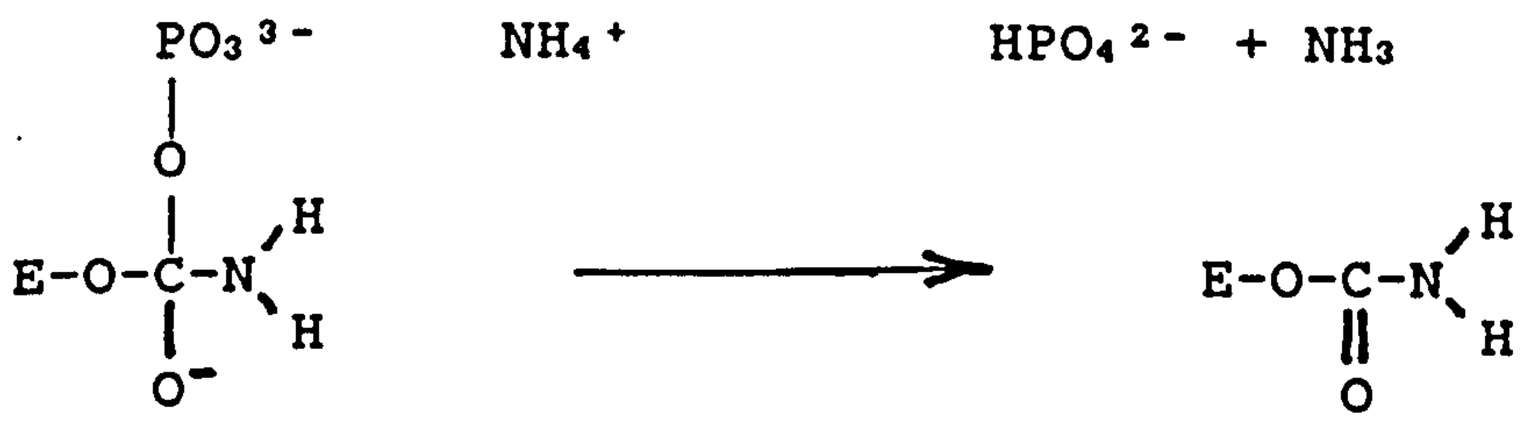

The Acylation of Ammonia in Acid Conditions

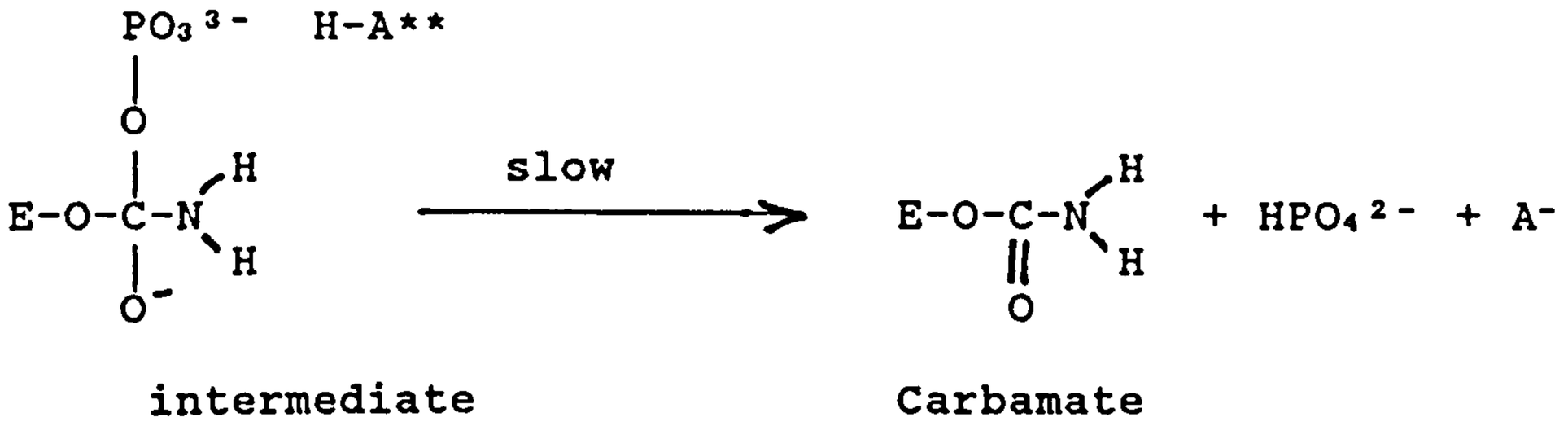

** Can be ammonium ion or another acid.

Ammonia gas is seen to be the reactant for the given reaction. The mechanism given above requires an ammonia gas molecule, or another proton accepting molecule, before the enzyme becomes active. An important difference from the mechanism suggested by Anderson et al.[67] and Meister et al.[68] for carbamate phosphate synthetase consists in the speculation that two molecules are required to transfer a proton. In the case of two ammonia gas molecules, they transfer a proton, yielding an ammonium ion and carbamate. In the case of the phosphate group transferring the proton, it yields carbamate and the phosphate group gains a proton. Meister et al. suggested the formation of "activated CO_2", which means that the phosphate group always removes the proton. "Active CO_2" is thought to be the transitional state after a proton has been removed from the ammonia.

The need for protons would explain why the Nitrosomonas have an optimum pH of about 8.3. At high local pHs, ammonia gas may become plentiful, but protons for the breakdown of the intermediate become scarce.

The reaction is assumed to involve ATP, because of energy considerations. However, another activator which

stores energy in breakable phosphate bonds could be involved.

The Oxidation of Carbamate of Ammonia

From the stoichiometry (see 1.2.1), 1.5 moles of oxygen are required to oxidize one mole of ammonia. One oxygen in nitrite is known to come from atmospheric oxygen. From the amount of energy involved in the reaction, it is thought that a further oxygen goes into oxidizing two protons to water. This implies that a further oxygen is used, and it is believed that this forms water as a result of a peroxide reaction. A peroxide is the only oxidizing group to react with an amine($R-NH_2$)/ imine to give R-NOH. Aldehydes give toxic oximes which do not undergo further reactions easily.

In enzyme reactions, a biological equivalent of a peroxide is used. Oxygen is bound to a metal, which has several oxidizable states, in such a way that it behaves as a peroxide. The process of binding and forming the peroxide is cyclical and requires electrons. The sensitivity of ammonia mono-oxygenase to inhibitors with an affinity for copper and methane mono-oxygenase's requirement for cuprous copper indicates that "ammonia mono-oxygenase is in all probability a copper enzyme" [82]. Copper has two oxidizable states Cu^{+} and Cu^{2+}.

Shears and Wood[82,39] suggest that two copper atoms are involved in forming a copper complex. The copper complex is based on tyrosinase, which has similarities[82,39] to ammonia mono-oxygenase, and is given by the catalytic cycle below:

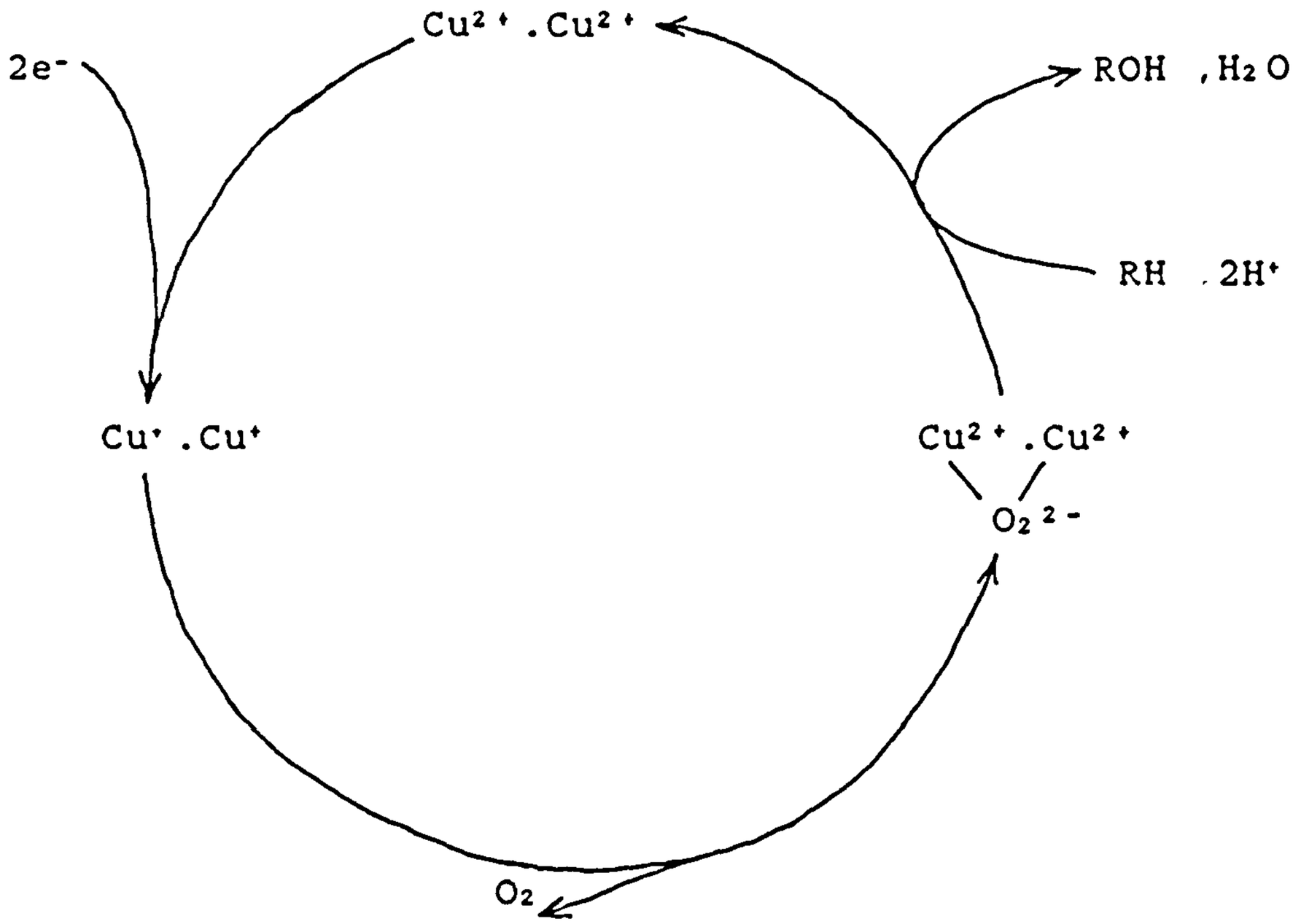

As is shown in this cycle, two electrons are required to form the complex. Thus, the cycle requires electrons from hydroxamic acid oxidation via cytochromes.

The reaction of Cu^{2+} ions with ammonia (amines) might have a bearing on the oxidation of ammonia and requires a mention. Copper (II) can form ammoniated ions [6] 3 $[Cu(NH_3)_n^{2+}$ where n = 1 to 4] in ammonia solutions. This property could be used to hold ammonia gas molecules prior to their reaction. The ammonia gas molecules would be released upon the supply of electrons, changing the oxidation state of the copper. It is also possible that the amine group of carbamate could also be held and released.

The oxidation of carbamate, like that of ammonia, is thermodynamically unfavourable. The Gibbs free energy change will be close in magnitude (17 kJ/mol) to that for the oxidation of ammonia. The instability of hydroxamic acid poses difficulties in determining exact values. The thermodynamic barrier must be overcome to oxidize ammonia to

hydroxamic acid. This is proposed to take place using the energy obtained from ATP and carbamate. ATP yields 30 kJ/mol of energy upon reaction, and the formation of carbamate from ammonia and bicarbonate ion (see 3.5) yields 3 kJ/mol. Thus, 33 kJ/mol is used to overcome the 17 kJ/mol barrier. The difference (16 kJ/mol) is assumed to be lost as heat.

The energy supplied by ATP in making the phosphate ester would be stored for a very brief time. The "active CO^2" described by Meister et al. [68] was estimated to exist for less than 2 seconds. Carbamate must be oxidized immediately after its formation so as to utilize this high energy state. As "active CO_2" has not been isolated or detected, it is improbable that carbamate will be detectable during the normal oxidation of ammonia.

Ammonia mono-oxygenase is proposed to oxidize the carbamate following the chemical mechanism for peroxides:

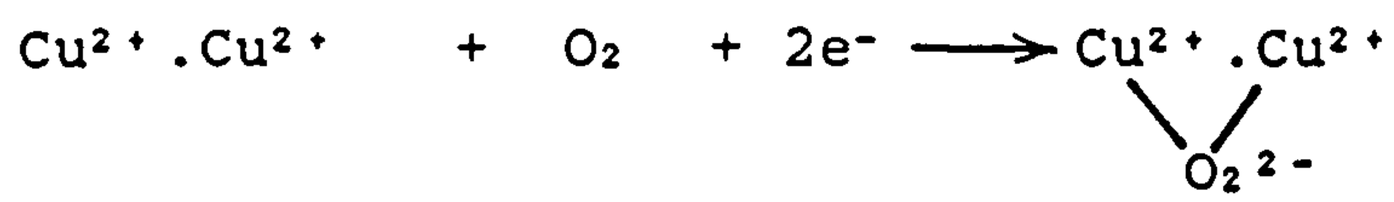

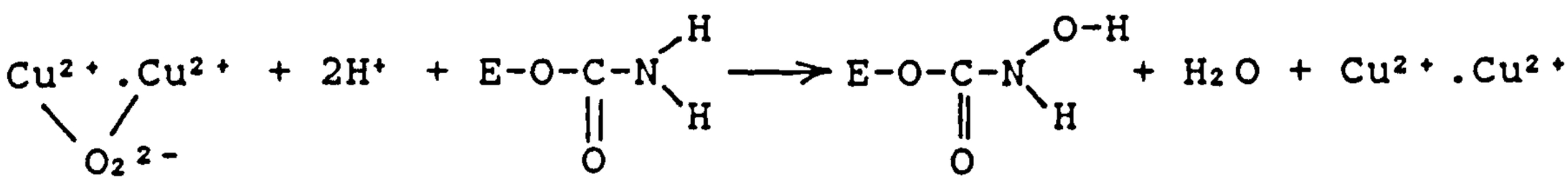

Peroxide Carbamate Hydroxamic acid

The oxygens from the reaction of the peroxide go to hydroxamic acid and water, respectively. The reaction has been illustrated with two copper atoms, as above. However, "there is no precedent for a single copper at the active site of a mono-oxygenase" [82]. The principal reaction, regardless of the number of copper atoms involved, is that

between the peroxide and carbamate (amine). The two protons required are assumed to be obtained from ammonium ions (to form more ammonia gas) or from the protonated phosphate resulting from carbamate formation.

Having formed hydroxamic acid, the next step is to stop it from breaking down due to its unstable nature. Hydroxamic acid forms coloured complexes in the presence of ferric ions, as in the test for esters in organic chemistry. These coloured complexes are stable.

Reconstituted systems of membranes containing ammonia mono-oxygenase with purified hydroxylamine oxidoreductase have only converted ammonia to nitrite in the presence of cytochrome c-554 [83,84]. This indicates that cytochrome c-554 is essential in the oxidation of ammonia. Andersson et al. [85] carried out a very extensive investigation into this ferric cytochrome. Their studies were "consistent with either an electron transport role or an enzymatic function" for cytochrome c-554. However, "the role of cytochrome c-554 in ammonia metabolism by *Nitrosomonas* remains unknown"[85]. Ammonia and hydroxylamine had no effect on the optical or EPR spectrum of ferric cytochrome c-554. In addition, "no oxygen uptake was observed with ammonia or hydroxylamine in the presence or absence of reducing agents". These observations indicate that cytochrome c-554 does not interact with ammonia or hydroxylamine. Andersson et al. showed that cytochrome c-554 has four ferric haems and that unique magnetic interactions exist. These complex magnetic interactions were indicated to be pH dependent.

The author suggests that the role of cytochrome-554 is two-fold and reflects both an enzymatic and an electron

transport function. The suggested enzymatic function is to form ferric complexes with hydroxamic acid. The binding of hydroxamic acid may be controlled by pH. The electron transport role is thought to be two-fold. The first role consists in supplying electrons to form the peroxide, as suggested by Tsang and Suzuki [84]. The second electron transport role is assumed to consist in transferring electrons from the hydrolysis of hydroxamic acid to cytochrome c-552. This role was postulated by Yamanaka and Shinra [86]. For the peroxide to be formed, these electrons must be supplied from the oxidation of the intermediate, hydroxamic acid, and this is considered in the next section.

5.4.2 The Proposed Mechanism for the Oxidation of Hydroxamic Acid

This oxidation is fully reversible and is catalyzed by the enzyme named "hydroxylamine" oxidoreductase. The proposed mechanism for this reaction is given below:

The Hydrolysis of Hydroxamic Acid

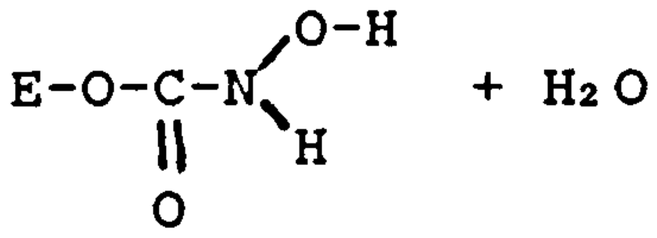

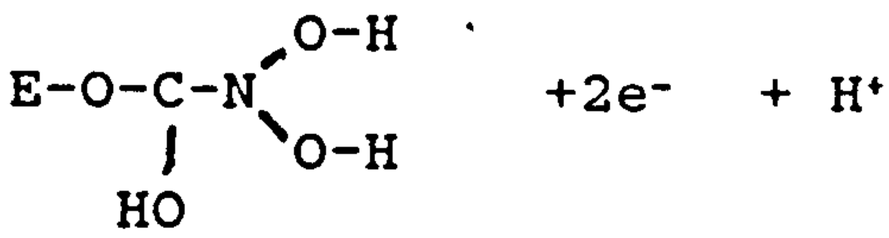

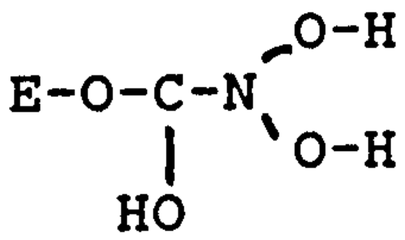

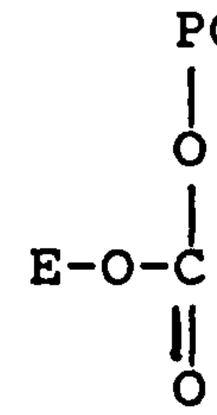

Nitrite

Carboxy phosphate ester

It is proposed that the oxidation of hydroxamic acid occurs by a hydrolysis step, leading to nitrite and to the carboxy phosphate ester. The nitro group($R-NO_2$) is seen to form nitrite(R-ONO). This type of reaction is known to be photo-sensitive[87].

A similar reaction in organic chemistry is thought to be the hydrolysis of aliphatic nitro compounds, in particular the mechanism given for the last stages of the reaction. For primary nitro compounds, hydroxamic acid is an intermediate, but "the mechanism is not known with certainty"[60].

The electrons are assumed to be transferred between cytochrome c-554 and cytochrome c-552. The electrons then pass along the cytochrome chain to form ATP or NADH. The NADH could undergo oxidative phosphorylation, yielding 3 ATP molecules. The ATP made could be used to make more carboxy phosphate ester, and/or for growth.

5.5 Inhibitors and Ammonia Oxidation

The oxidation of ammonia has a number of inhibitors and alternative substrates that require examination. In particular, the reactions of hydrazine and hydroxylamine demand detailed discussion. These reactions led previous authors to suppose that hydroxylamine was an intermediate in the oxidation of ammonia (see 1.2.3).

Hydrazine is a competitive inhibitor [19,20,21]. The proposed mechanism gives an explanation as to its mode of action. Hydrazine binds to the ester used by ammonia gas. Organic chemistry indicates that both hydrazine and hydroxylamine react faster with esters than ammonia[60]. Thus hydrazine acts as a competitive inhibitor to ammonia. Hydrazine's chemical structure is very similar to two ammonia gas molecules. As the proposed mechanism suggests, two molecules are required for the transfer of a proton. It would appear that hydrazine cannot be distinguished from two ammonia molecules. This mode of action is compatible with another enzyme. The aforementioned enzyme carbamate synthetase (see 3.7) reacts with hydrazine, to form what appeared to be N-aminocarbamyl phosphate[68]. It was found that hydrazine replaced the ammonia gas.

The carboxy phosphate ester has been indicated to be involved in the hydrolysis of hydroxamic acid. The blocking of the ester and the presence of hydrazine are assumed to destabilize hydroxamic acid, causing its breakdown to hydroxylamine. This is the explanation offered for the trace amounts of hydroxylamine reported when ammonia is oxidized with hydrazine. This explanation is in line with Yoshida's

and Alexander's cautionary statement that hydroxylamine might not be on the "direct pathway of nitrogen oxidation by bacterium"[41]. They indicated that the intermediate could be an "organically bound form of hydroxylamine". Hydroxamic acid fits this description.

The proposed reason why trace amounts of hydroxylamine "stimulate resting cells"[39] is that, unlike carbamate synthetase, it is assumed to react with the carboxy phosphate ester. Hydroxylamine has a very similar structure to hydroxamic acid and it can hardly be deterred from binding with the ester. Hydroxylamine can then be converted to hydroxamic acid. Thus, any hydroxamic acid that breaks down to hydroxylamine is reconstituted.

Hydroxylamine has only been shown to stimulate resting cells at the very low concentrations of less than 1.5 micro g/ml - N. This would suggest that, above this concentration, the phosphate ester cannot convert enough of the hydroxylamine. Hydroxylamine then acts as a competitive inhibitor to the carboxy phosphate ester. It was mentioned earlier in this section that both hydrazine and hydroxylamine react faster with esters than ammonia does. The addition of hydrazine and/or significant amounts of hydroxylamine would be expected to inhibit the reaction almost totally. This is in agreement with the observations [41].

Many other substrates have been listed as being oxidized by ammonia mono-oxygenase, as cited by Wood[39]. A number of these chemicals are different in structure from two ammonia molecules. Mechanisms by which these chemicals might be oxidized have not been given in previous

literature. However, the proposed mechanism for ammonia oxidation indicates the possible reaction mechanisms for these chemicals.

Carbon monoxide is oxidized to carbon dioxide. Carbon monoxide may react with ammonia in the presence of the peroxide to give carbamate, as in the known organic chemistry reaction [60]. This would be oxidized again, to hydroxamic acid, and in this way the carbon would eventually be released into the atmosphere as carbon dioxide or assimilated by the bacteria.

Nitrite and ammonia have both been indicated to cause inhibition at very high concentrations by aquacultural standards (see 1.2.2). Ammonia is thought to inhibit the bacteria because it reaches toxic levels. The reason why nitrite is thought to be inhibitory, before it becomes toxic, is that it causes the formation of the nitrite ester rather than the phosphate ester. This is thought to be responsible for a number of reactions not specifically encouraged by ammonia mono-oxygenase.

The assumed method by which methane and other C_1 compounds are oxidized is discussed in section 6.6. These compounds are thought to be oxidized by the mono-oxygenase through the accidental formation of the nitrite ester rather than the phosphate ester. The methods by which some C_3 and C_6 compounds are oxidized is not clear, but they may involve the nitrite ester.

Acetylene acts as an irreversible inhibitor[88] and this may also be caused by the accidental formation of the nitrite ester. The enzyme may attempt to oxidize the acetylene, causing damage to the enzyme. Near-ultraviolet

light is a well-known inhibitor; this is discussed further in section 6.7. Other inhibitors, such as thioureas, cyanide, diethyldithiocarbamate and $\alpha\alpha'$dipyridyl[73], have a high affinity for the copper in the ammonia mono-oxygenase, causing inhibition. It may be possible that some of these chemicals also block the proposed carboxy phosphate ester.

5.6 The Proposed Mechanisms and the Kinetic Results

The proposed mechanism accounts for the observed reaction kinetics in the experiment to check experimental reproducibility (see figure 16). The number of enzyme sites which are active at a given time depends on the ATP "pool", among other factors. The carboxy phosphate ester formed is in equilibrium with bicarbonate ions and ATP, and the higher the ATP concentration the greater the chance that the sites are active. The difference between the two experiments conducted 24 hours apart can be attributed to different amounts of ATP in the bacteria, caused by their recent history.

When ammonia is added to resting cells, a time lag is observed before the respiration rate "gains speed and settles down"[39]. This is entirely compatible with the proposed mechanism. The rate of ammonia oxidation depends upon the concentration of ATP which takes time to increase through hydroxamic acid oxidation. A maximum oxidation rate is reached when all the reaction sites become activated. The use of ATP, rather than sugars, has major advantages. ATP is made continuously and can thus be diverted from being an energy source required in growth synthesis to an activator.

The implied mechanisms of section 1.2.3 do not give an explanation for this observed behaviour. This has forced authors to assume another cause, that is, the behaviour "must" be due to "endogenous substrates, acting via NADH"[39]. However, this has not been demonstrated and the explanation is unconvincing. Endogenous substrates are chemicals stored for stress conditions. Marathon runners use endogenous substrates (fats) when all their other resources have been exhausted.

Endogenous bacterial substrates, such as sugars, fats or proteins, contain significant amounts of energy. To make these chemicals takes more energy than they contain, as their synthesis is not 100% efficient. In addition, these chemicals lose 60% and more[64] of their energy upon conversion to ATP or NADH. *Nitrobacter* and *Nitrosomonas* live on the poorest of energy sources. A single glucose molecule represents the energy obtained from tens of ammonia oxidations. In the case of *Nitrobacter*, it represents the energy of near a hundred oxidations. Two crucial questions have not been answered: why should the unstressed bacteria use these reserve substrates (stored for possible stress conditions) and how would they benefit from their use?

Sections 5.1, 5.2 and 5.3 described experiments conducted to check the batch reactor assumption, the reproducibility of the data and the lower pH-limit of nitrification. (The latter experiment was conducted out of experimental curiosity rather than as a deliberate attempt to demonstrate the involvement of bicarbonate ions). Having validated the assumptions and checked that the data were reproducible, the main ammonia experiments were performed at

various pHs. The amount of substrate to be added and the best time at which to take the samples were determined by trial and error. The main ammonia oxidation experiments were then performed. These experiments were monitored for 30 minutes after taking the first water sample. When no experiment was performed, the pH of the system was kept at a pH of 8.3, corresponding to the maximum fraction of bicarbonate ions.

The impulse ammonia reaction data for different pHs is best illustrated by a plot of fractional conversion versus time, as shown below in figures 17 and 18.

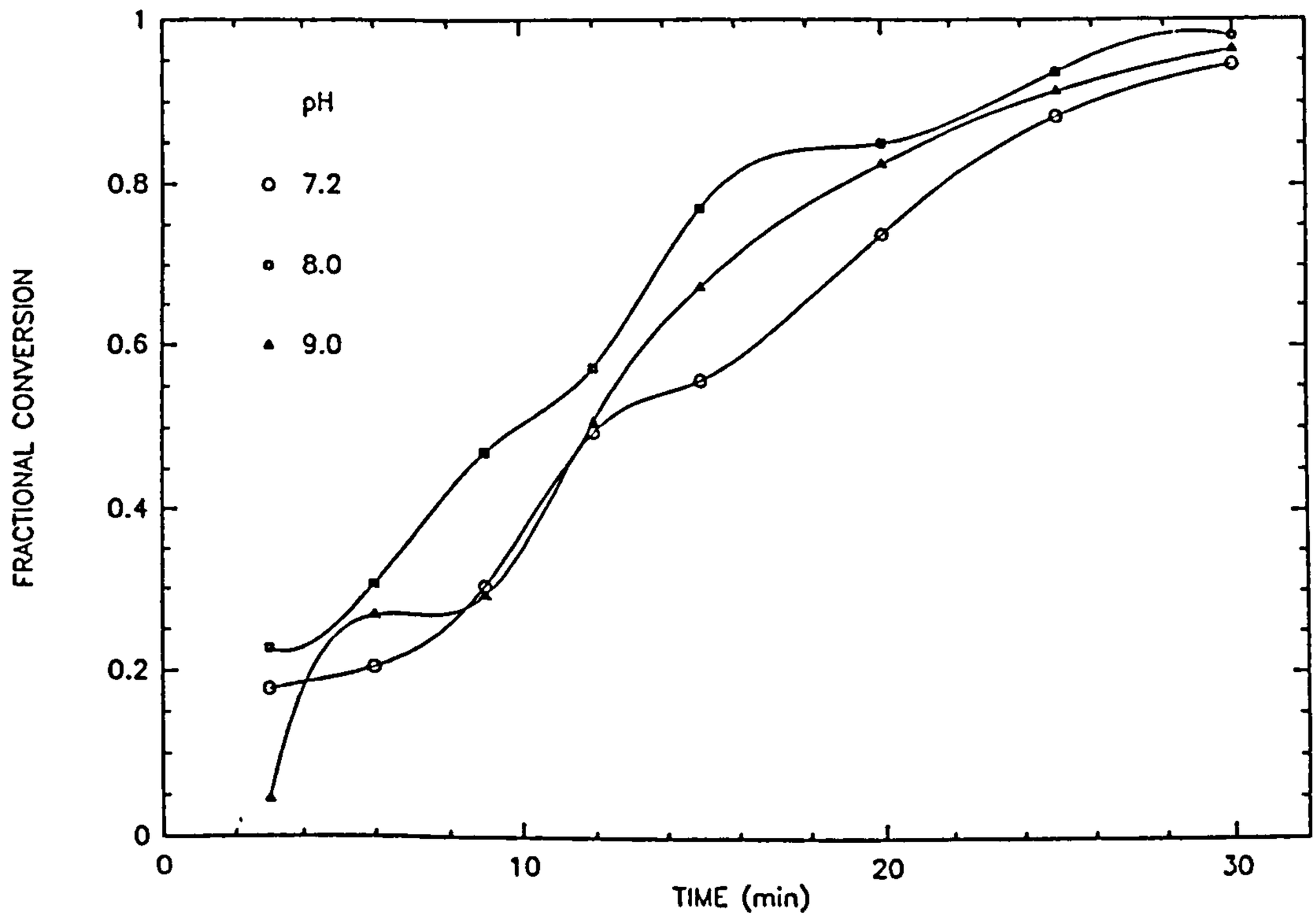

Figure 17. Ammonia oxidation at various pHs.

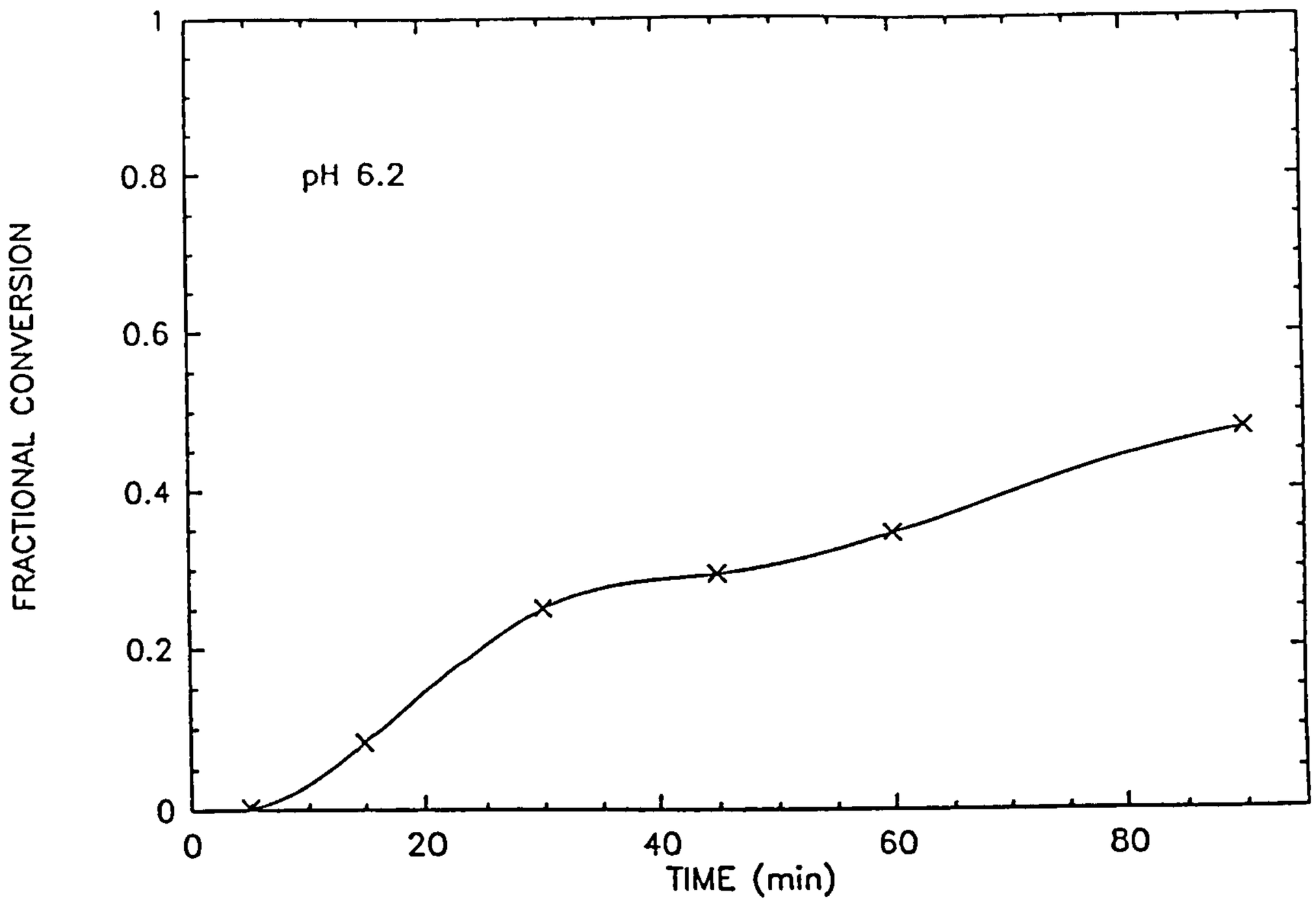

Figure 18. Ammonia oxidation at pH 6.2.

The reaction rate and, in particular, the initial rate are observed to fluctuate widely. The minimum doubling time of Nitrosomonas under the most favourable conditions is given by Sharma and Ahlert[20] as 10 hours 55 minutes. Thus, it is clear that significant growth cannot be the reason for the fluctuations in the reaction rate.

From the fractional conversion, it can be seen that the oxidation rate was fastest at a pH of 8.0. The rate is slightly lower at pHs of 7.5 and 9.0, but at a pH of 6.2 the rate is much reduced. This pH-dependence of ammonia oxidation is compatible with the proposed mechanism.

The mechanism of section 1.2.3 indicates that the reaction rate should increase with the concentration of ammonia gas. Thus, the higher the pH the faster the rate.

However, the data indicate that at the relatively low pH of 9.0 the rate decreases.

The most noticeable feature of the curves is that they fluctuate, indicating that the reaction rate is changing. This is unequivocal evidence for the existence of a control system. The relative differences from fitting Michaelis-Menten kinetics illustrate this better and these are given below in figures 19 and 20. These curves illustrate when the reaction rate is faster or slower than predicted by the Michaelis-Menten equation. The experimental error in the calculated relative differences is ±0.05 (see 4.5.2). Error bars have not been drawn for reasons of clarity. For the reaction to have followed Michaelis-Menten kinetics, the kinetic data would have had to lie within the dashed line ±0.05 as in appendix 3.c.

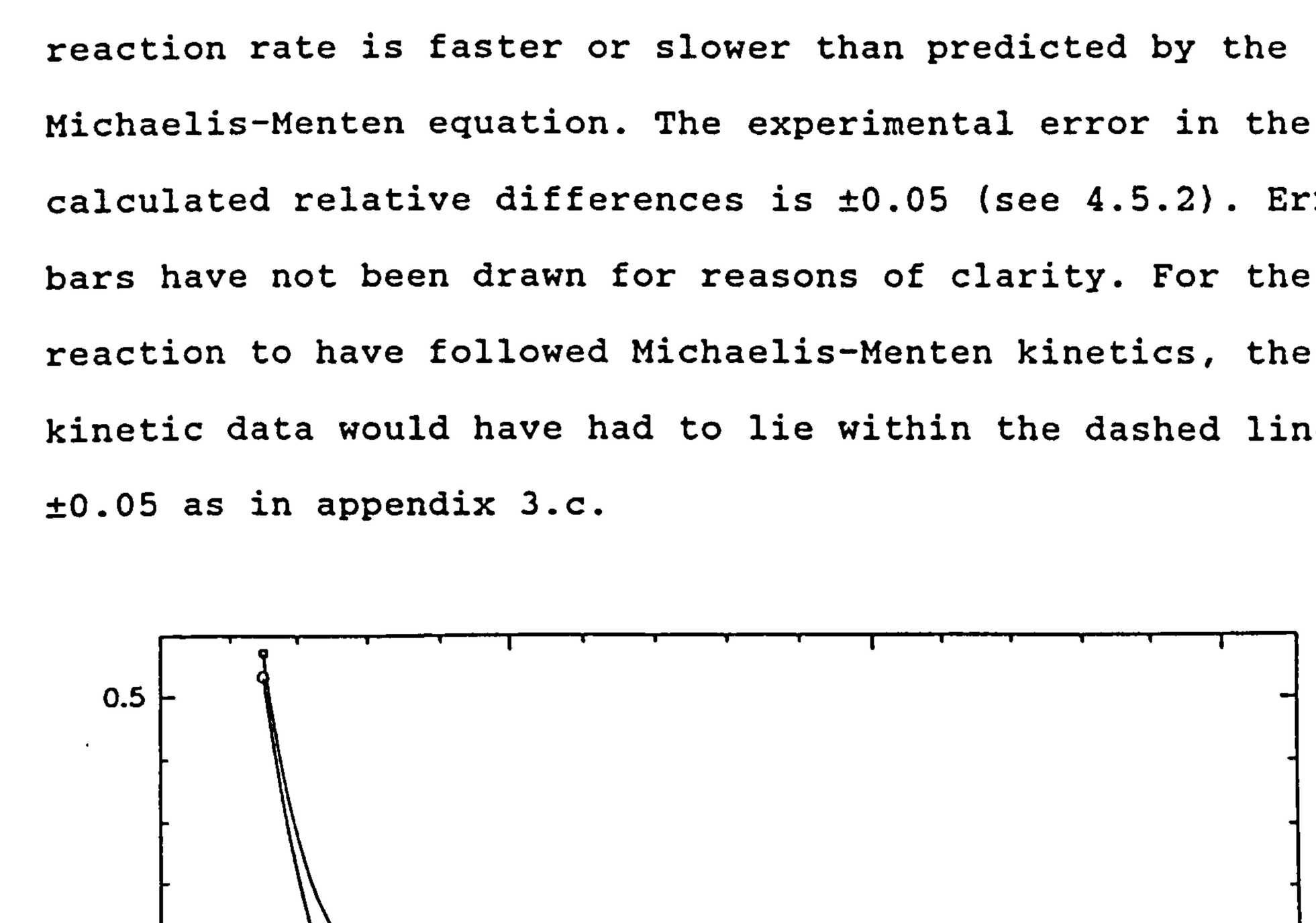

Figure 19. Relative differences for Michaelis-Menten kinetics at various pHs.

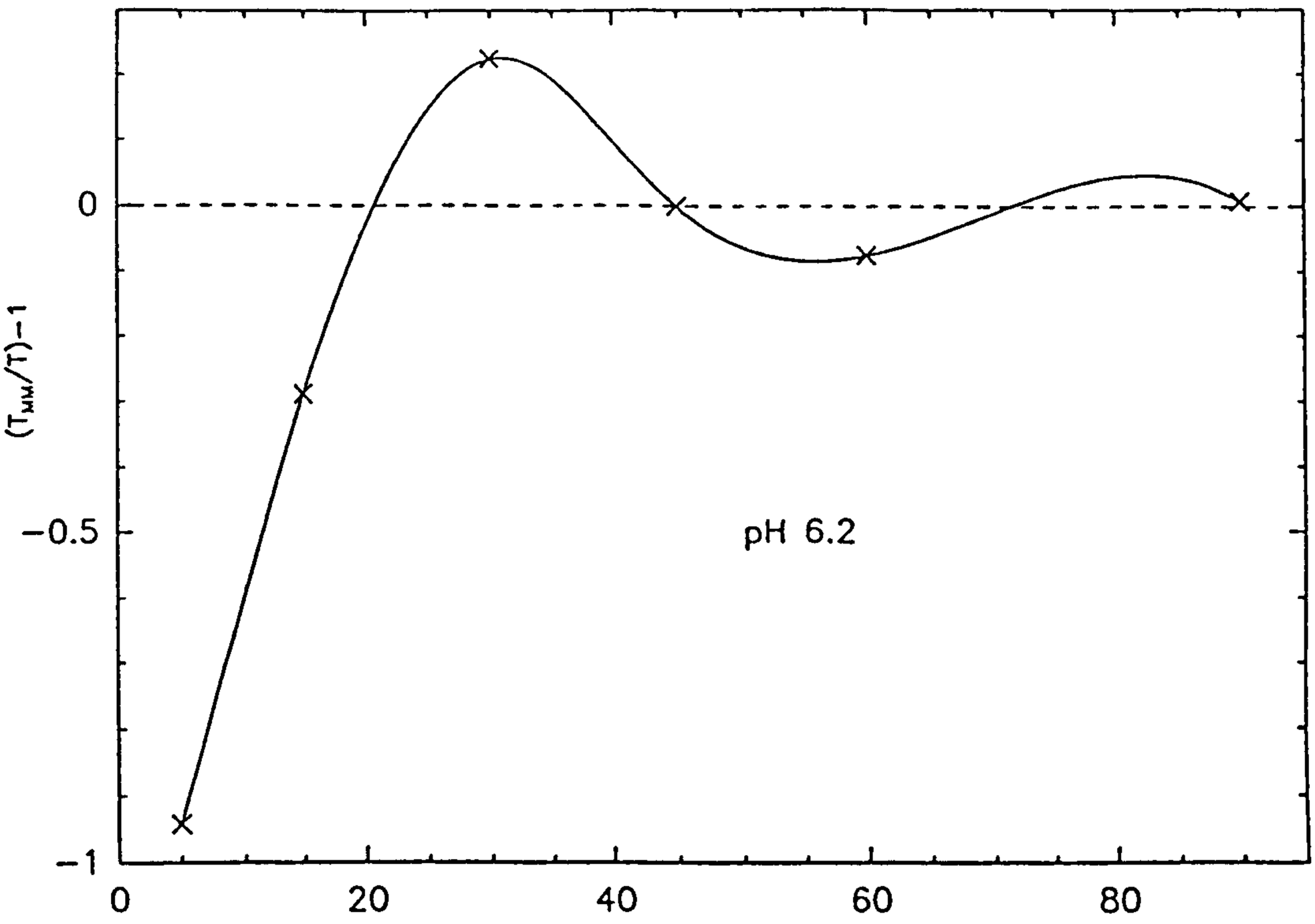

Figure 20. Relative differences for Michaelis-Menten kinetics at pH 6.2.

This begs the question of which product might be causing this behaviour. It has been indicated[39] that hydroxylamine might cause feedback control. It should be reiterated that this does not explain the observed initial acceleration of the reaction rate. Slowing of the reaction through the accumulation of hydroxylamine, however, would be expected. In this case one would have to ask again why it has never been detected without the addition of hydrazine.

Protons are indicated to be products of the ammonia oxidation as indicated in the reaction stoichiometry (equation 1). The oxidation of ammonia has been indicated[14,19,20,21] to depend on pH and, thus, the reaction is known to be influenced by pH. The manner in which protons, which are also reaction products, influence the

reaction is now examined.

5.7 The Control of Ammonia Oxidation by Protons

The control of reactions by pH in biological systems is exceedingly common and is the reason why biological experiments are traditionally conducted at a fixed pH. The pH during the experiments was kept constant by the addition of a buffer. Thus, the free concentration of protons was not affecting the reaction rate. However, the pH within the bacteria might be expected to be different, if only because of protons being reaction products. The alteration of the internal pH would not only alter the reaction rate of ammonia oxidation but also the rate of other enzymatic reactions carried out by the bacteria. This would lead to disruption of all the bacteria's other functions, a highly undesirable situation. Therefore, in all probability, the control of the reaction rate by protons must be localized.

The implied mechanisms of section 1.2.3 do not propose a localized mechanism but only the general observation that ammonia gas is not formed at lower pHs. The observation that the reaction rate is lowered at a pH of only 9.0 contradicts this.

The requirement for protons to only influence the reaction near the enzyme is wholly compatible with the proposed mechanism. The mechanism indicates that the reaction is controlled at the enzyme binding site. The concentration of ATP will determine the number and activity of the sites but the pH controls their reaction rate.

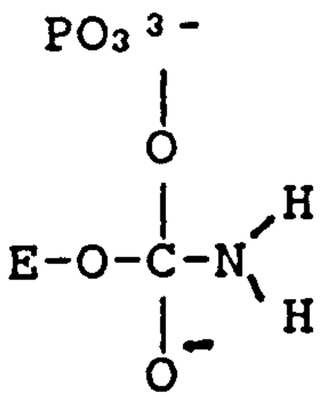

intermediate

Referring to the analysis given by March[60], the formation or breakdown of the above molecule is the rate-determining step. The reaction proceeds in acid or basic conditions and requires a proton donor. Thus, changes in the local proton concentration determine the rate of reaction.

The concentration of ammonium and phosphate ions will contribute to the rate of the formation or breakdown of the intermediate. It is speculated that protons are transferred in a direct way. It is possible that protons are brought to the enzyme site attached to phosphates, which then influence the reaction. For diagrammatical purposes, the phosphate ion was shown with a single proton. However, phosphate is found with different numbers of protons, depending on the pH, as is illustrated[2] in figure 21.

The effect that non-inhibitory concentrations of hydroxylamine have on the proposed reaction mechanism requires consideration. Hydroxylamine has been reported to "stimulate"[39] resting cells, but this would appear to be a poor description. As mentioned previously (see 5.5), hydroxylamine reacts faster with esters than ammonia and, thus, the reaction rate should increase. However, the true substrate ammonia gas will exist only when the pH is greater than seven. The protons from nitrification provide feedback control to slow down the formation of ammonia gas and the reaction. The addition of small quantities of hydroxylamine

creates hydroxamic acid, which, on hydrolysis, yields electrons and protons as reaction products. However, the protons providing feedback control are not effective on hydroxylamine. The local pH has to fall to below four to have a comparable effect (see figure 22 calculated from equilibrium data[63]) to that on ammonia gas. Adding small amounts of hydroxylamine results in the reaction going out of control. The reaction will proceed at its maximum rate until a local pH of four (or damage to the enzyme) occurs.

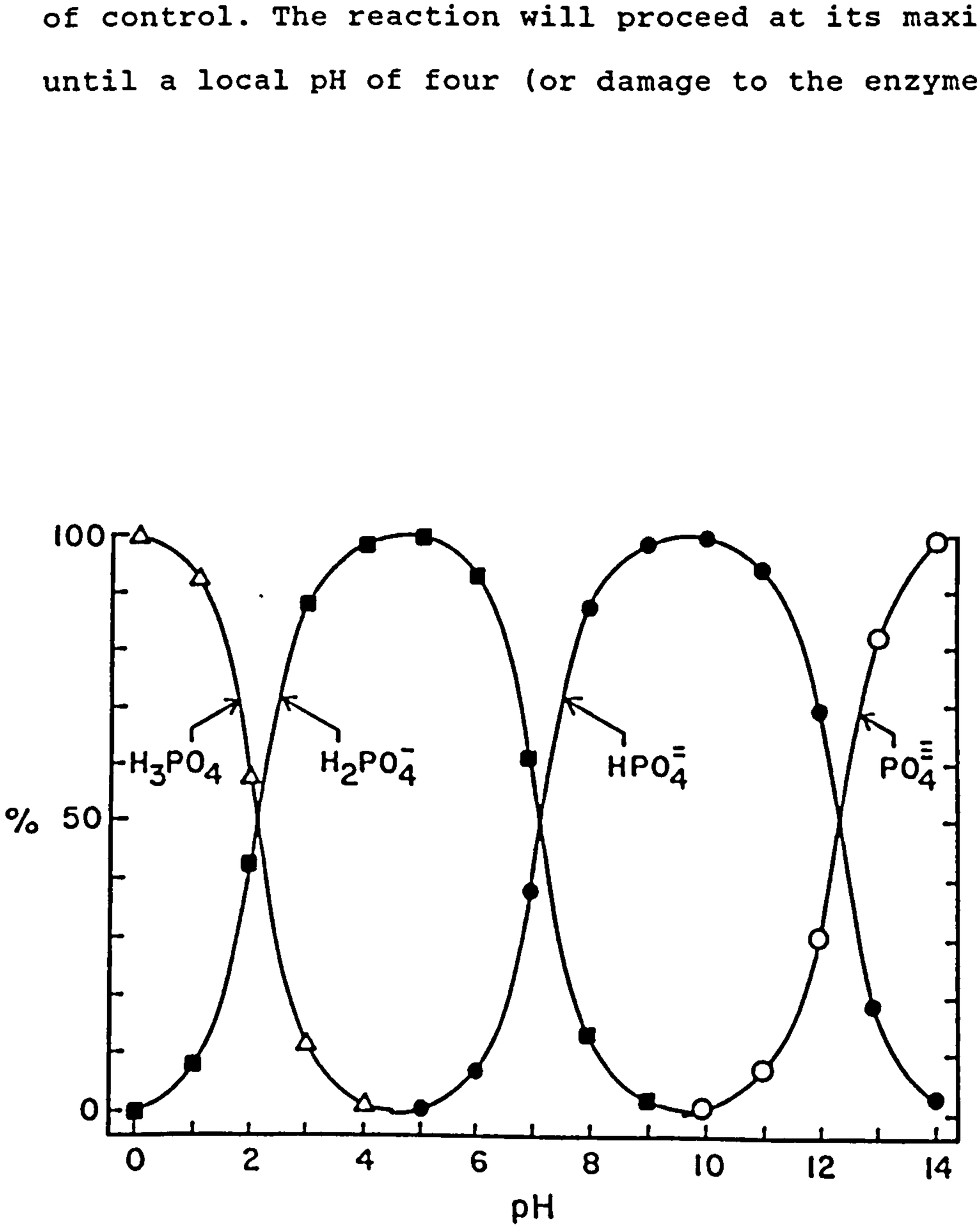

Figure 21. Phosphates species in equilibrium.

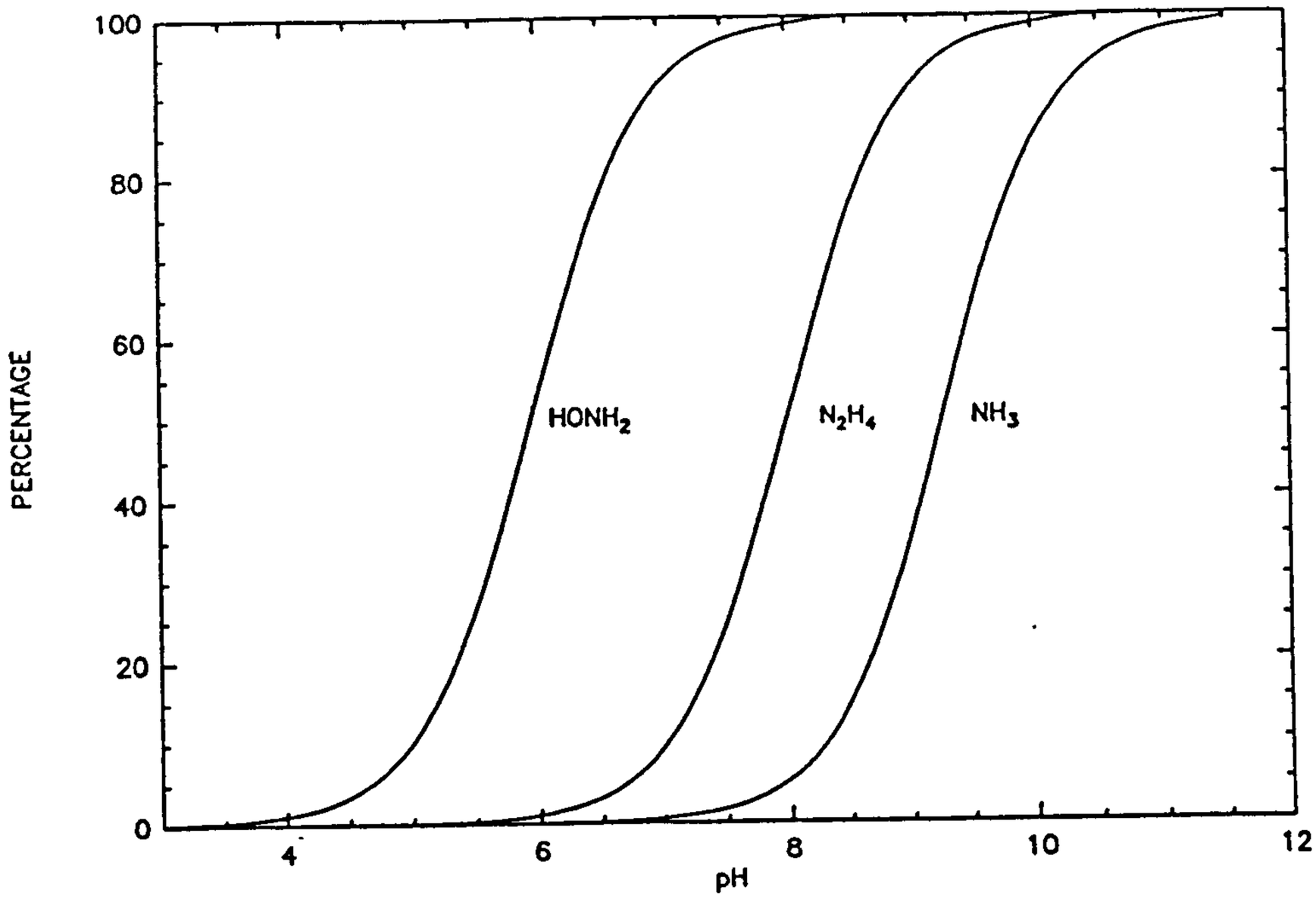

Figure 22. Equilibrium data for ammonia, hydrazine and hydroxylamine at 25 °C.

The oxidation of ammonia causes the pH to decrease. The process of oxidation of ammonia must, thus, be closely associated with the control of pH in the bacteria. It seems likely that the bacteria can become acclimatized to different pH-levels. This is probably done by altering the ATP pool. Acclimatization has been demonstrated by Huag et al. [6]. It would also explain the wide variations in reaction rate observed at various pHs, as illustrated below in figure 23 (from reference 22):

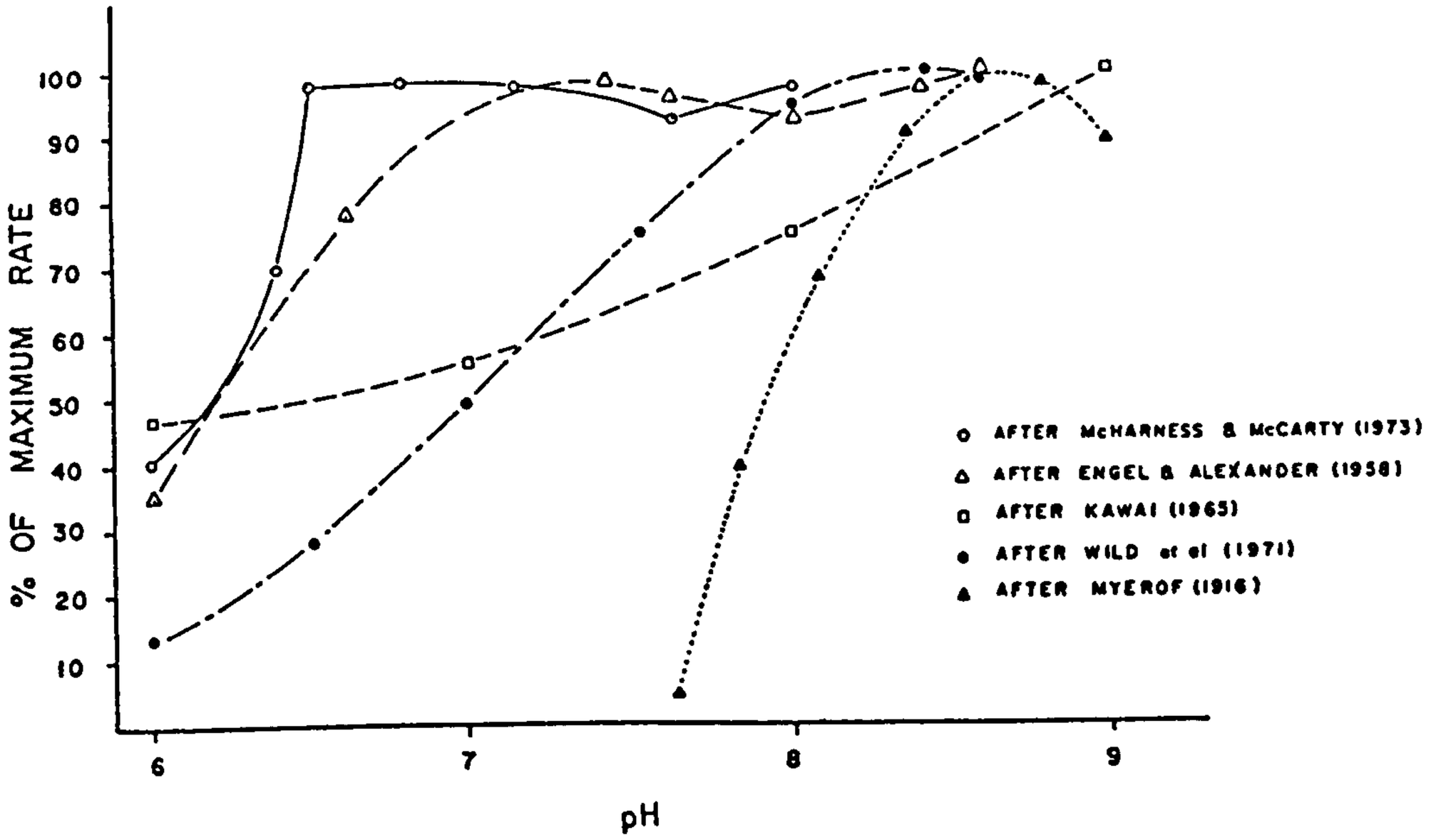

Figure 23. Percent of maximum rate versus pH.

It is possible that the mechanism described for carbamate formation could be used by other enzymes. For other enzymes to use this control mechanism, the only requirement is that the enzyme, co-enzyme or substrate has an amine group.

So far, proton pumping has deliberately not been discussed. Instead, the emphasis was put on the chemical reactions involved in nitrification. The reaction stoichiometry indicates that hydrogen ions (protons) are produced. Some ATP could possibly be made by a protonmotive force, but, as yet, there is no unequivocal evidence for it. Other protons (NADH) combine with atmospheric oxygen and electrons from the transport system to form water. In the case of ammonia oxidation, enough energy may exist for the oxidation of NADH. Because of the very limited energy in

nitrite oxidation, NADH must be made indirectly involving protons, electrons and oxygen, all combining to form water.

5.8 A Control Diagram for Ammonia Oxidation

The curves drawn through the relative differences data (figures 19 and 20) show an oscillating but diminishing property. Similar behaviour is observed in plots for damped control systems returning to a set point[89]. This was thought not to be very surprising. The control demands of enzymes are close to those required for chemical processes. A process control system should operate so as to meet the process objectives in an efficient manner. Biological organisms require the internal concentration of a large number of chemicals to be maintained between very strict limits. These limits must be adhered to despite wide fluctuations in the organisms external environment. In addition, returning the chemical concentrations to their desired levels must be carried out efficiently. Enzymes are not only responsible for the chemical reactions in organisms but also for the control of these reactions. It is suggested that both enzymes and process designers have developed similar solutions to these control problems.

To illustrate this, the believed control strategy of ammonia mono-oxygenase will initially be described as if it were a chemical process. This analogy, it is hoped, will help in illustrating the proposed enzyme control mechanism.

Let us consider a solid catalyzed gas phase reactor, familiar to chemical engineers. In the chemical equivalent, the reaction is controlled firstly by adjusting the

temperature of the reactor by means of a heat exchanger or steam jacket. The second form of control is performed by adjusting the stem travel of a control valve adjusting the flow of reactant (NH_3) to the reactor. The controller setting for temperature regulation is related to the concentration of a product (H^+). The control valve controller setting depends on the temperature controller setting.

The control system used is thought to be equivalent to cascade (multiloop) control, consisting of two feedback loops. Process control[8,9] provides an example of such a control system in a chemical plant. Only the main features of the control system and control block diagram can at present be sketched, as is illustrated below in figure 24.

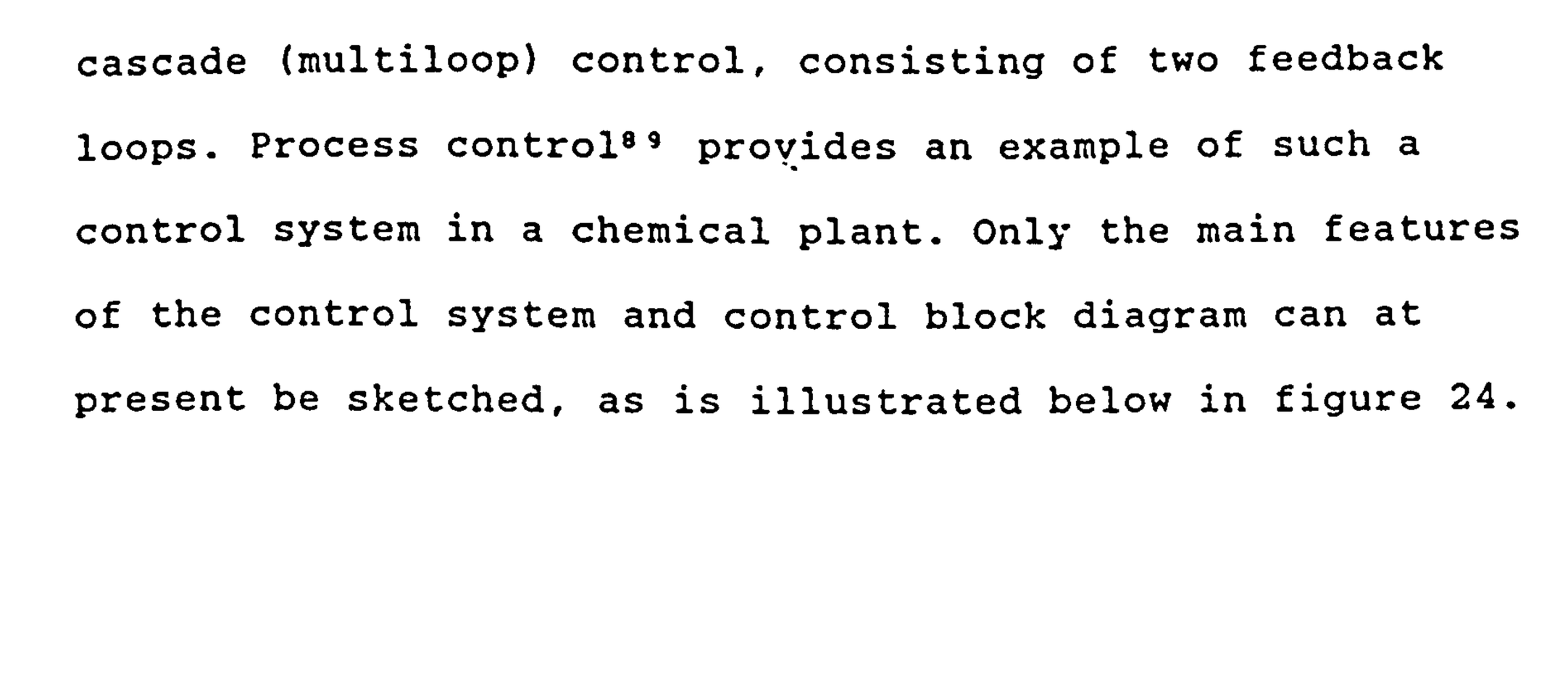

Figure 24. Sketch of feedback control mechanism for *Nitrosomonas*.

The formation of ATP by electrons/protons obtained from the hydrolysis of the reaction products is shown as the slower primary loop. In the catalytic reactor equivalent, this equates to raising or lowering the temperature of the steam jacket. The raising or lowering of the reaction temperature is a slow process but its alteration causes large changes in the reaction rate.

The production of protons by the hydrolysis of hydroxamic acid gives feedback control. This faster second feedback loop is analogous to the control valve stem which alters the flow of ammonia gas in the catalytic reactor equivalent.

The advantage of this control system lies in that it minimizes the disturbances to the process of ammonia oxidation. "Cascade control is especially effective where the main disturbances enter the inner loop and the reaction of the latter is much faster than that of the outer loop"[89]. The main disturbances to ammonia oxidation are changes in the ammonia concentration and/or pH. These are indicated in figure 24 to enter the inner loop.

The control block diagram shown above may not be the entire diagram. As in a chemical process, there may be back-up mechanisms. In particular, the situation where the amount of oxygen available is below stoichiometric requirements has not been examined. It would require a substantial amount of structural information on the chemical nature of ammonia mono-oxygenase to determine the exact nature of how this control system works. The chemical structures of only a few haems and enzymes have been determined from the vast numbers of enzymes. As ammonia mono-oxygenase has yet to be

purified[39], such information may not be available for a long time. The use of impulse experiments as conducted here may provide information into the nature of control systems which is difficult to obtain by other methods. A continuous measurement of the reactants' concentration is desirable to enable accurate determination of the process characteristics.

There may also be implications with respect to enzyme recovery processes. The act of "purifying" and separating enzymes from a biological process may have serious effects on the control system.

The oxidation of ammonia has been described above using a chemical process analogy. This analogy requires further discussion. In the chemical process equivalent, temperature is used to control the reaction rate. However, enzymes have narrow temperature ranges by catalyst standards. The ability of organisms to raise or lower their internal temperature is limited. An additional problem is that the alteration of internal temperature would influence many other enzymatic reaction. Indeed, stable temperatures are often demanded. In man a body temperature of 37°C is maintained.

It is believed that the analogy between enzymes and control valves is fairly close. As such, enzymes might be equated to a control valve controlling the addition of a reactant to the reactor. This may not be self-evident at first, but the analogy is explained in detail in sections 7.6 and 7.7. Enzymes are required to bring about large variations in the reaction rate, as temperature does in a catalytic reactor. The exact chemical process analogy is proposed to be that the valve characteristics are changed.

Control valves are normally specified to be either *linear* or *equal percentage*. It is proposed that an enzyme alters the equivalent property to control sensitively a wide range of substrate concentrations. In this way, the enzyme controls the reaction in a manner which would be difficult to achieve in the chemical equivalent using control valves.

CHAPTER 6

NITRITE OXIDATION AND THE REACTIONS OF A CARBOXY NITRITE ESTER

The unsteady-state nitrite experiments implicate bicarbonate ions to be involved in the reaction mechanism. These experiments are explained below. To obtain further clues as to how nitrite might be oxidized, known organic reactions yielding nitrates were investigated. These investigations resulted in a single known organic chemistry reaction of this type. A mechanism that is very similar to the known organic chemistry reaction which also involves bicarbonate ions is proposed.

6.1 Nitrite Unsteady-State Experiments

The amount of sodium nitrite to add and the best time to take the samples were determined in the same way as was done for ammonia oxidation. The nitrite experiments were also monitored for 30 minutes after taking the first water sample.

The first unexpected observation when using an impulse reaction technique was that the experiment had to be buffered with acid, particularly at pH-levels above 8.0. Without the addition of acid, the pH of the system would rise for more than 20 minutes before levelling out. It was puzzling that the system required buffering, because no buffering of the system was required while growing the Nitrobacter. According to the reaction stoichiometry (see 1.2.1), no acid should be required. Sulphuric acid was used

to maintain the pH during the experiments, because sulphate ions have not been reported to have an effect on nitrification[22].

The quantities of acid required indicated that significant amounts of ions were removed. However, the amount of acid required rose with increasing pH. Bicarbonate ions form a significant constituent of freshwater and this strongly suggested that the carboxy phosphate ester was again involved. At pHs above 8.0, CO_2 (gas) in solution is found in only small amounts, and thus buffering is achieved by bicarbonate ions or carbonate ions (see figure 10). The uncompensated removal of bicarbonate ions at high pHs would cause a rise in pH, as observed in the unsteady-state experiments.

A further puzzle was presented by the fact that in organic chemistry there are several reactions for nitrous acid, but that none could be found for its oxidation[60,65] to nitric acid. In inorganic chemistry, nitrogen dioxide can be oxidized with steam to produce nitric acid. This reaction is used in the chemical industry, although the mechanism is not fully understood. The reaction only occurs at elevated temperatures (100-425 C) with a catalyst[58].

The only reaction in organic chemistry that could be found to form nitrates from nitro groups was dinitro-addition, nitro-nitrosooxy-addition [60]. In the reaction, a nitrite ester intermediate that is "quite reactive"[60] (by organic chemistry standards) is formed. On oxidation with oxygen, the β-nitro alkyl nitrite compound formed in the reaction is oxidized to the nitrate or the ketone. However,

in the complete absence of oxygen -nitroso nitrate is formed:

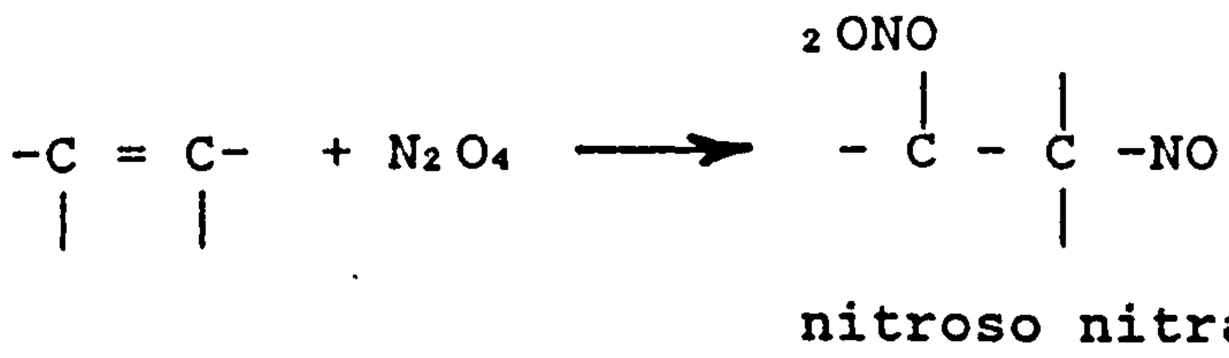

nitroso nitrate

Nitrogen tetroxide decomposes to nitrogen dioxide according to the equation below[63]:

colourless brown

The above equilibrium has no great tendency to go to the left or right. This indicated that NO_2 (a gas like NH_3) would be the probable reactant in any biological equivalent reaction.

6.2 The Proposed Mechanism for Nitrite Oxidoreductase

The following mechanism for the oxidation / reduction of nitrite / nitrate ions is proposed. The first step in the oxidation of nitrite is proposed to be the formation of the carboxy phosphate ester. The energy contained in the bonds of ATP is again assumed to be used to overcome a thermodynamic barrier (making NO_2).

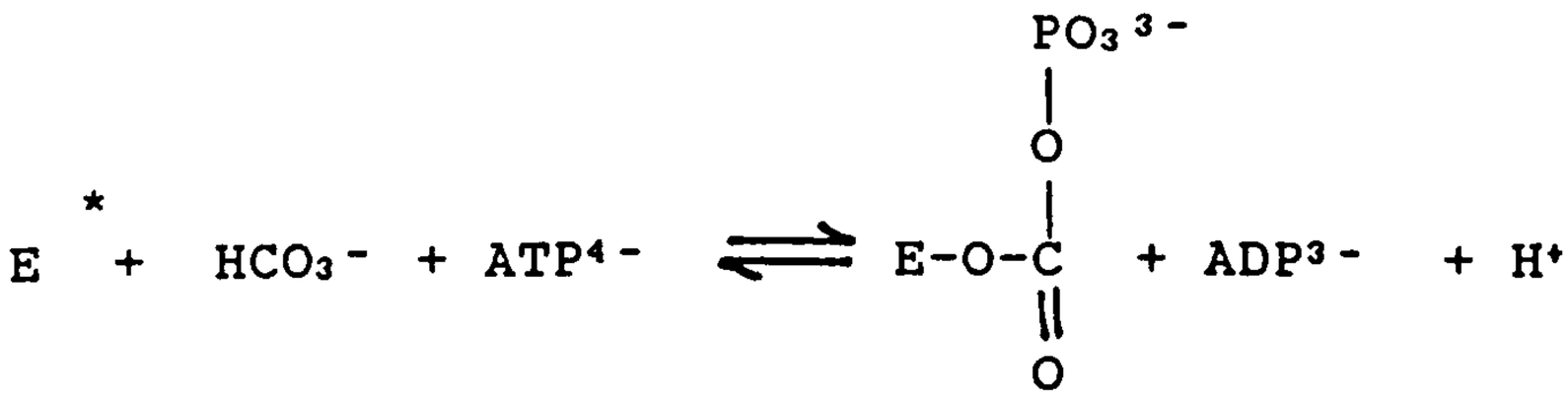

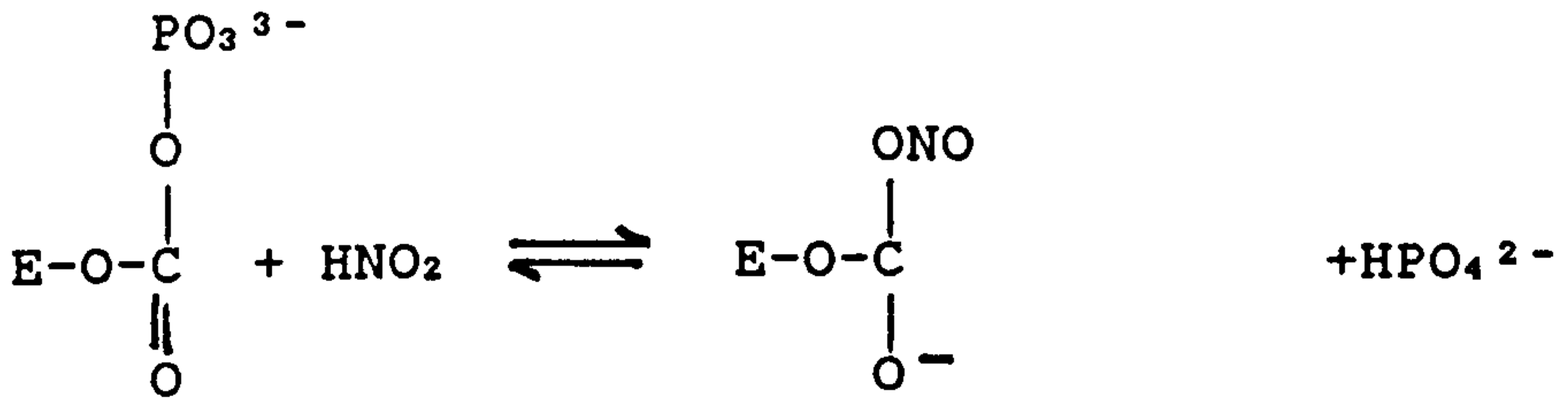

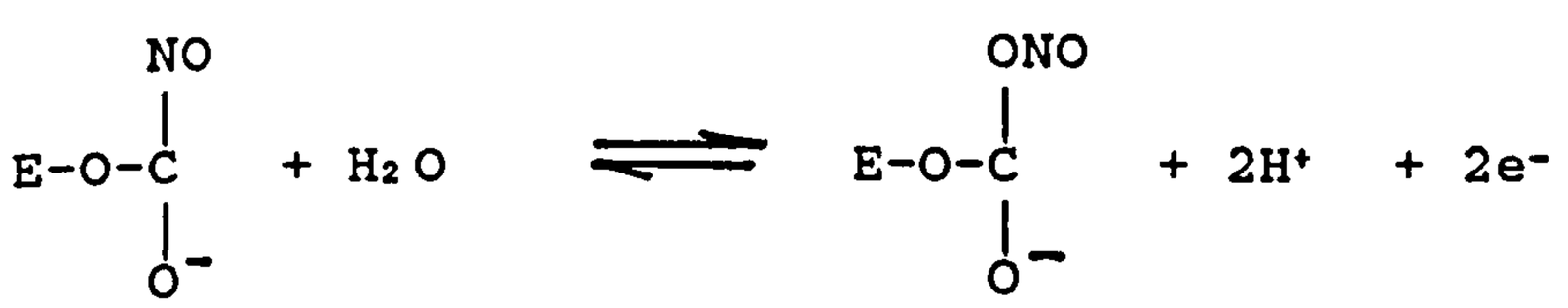

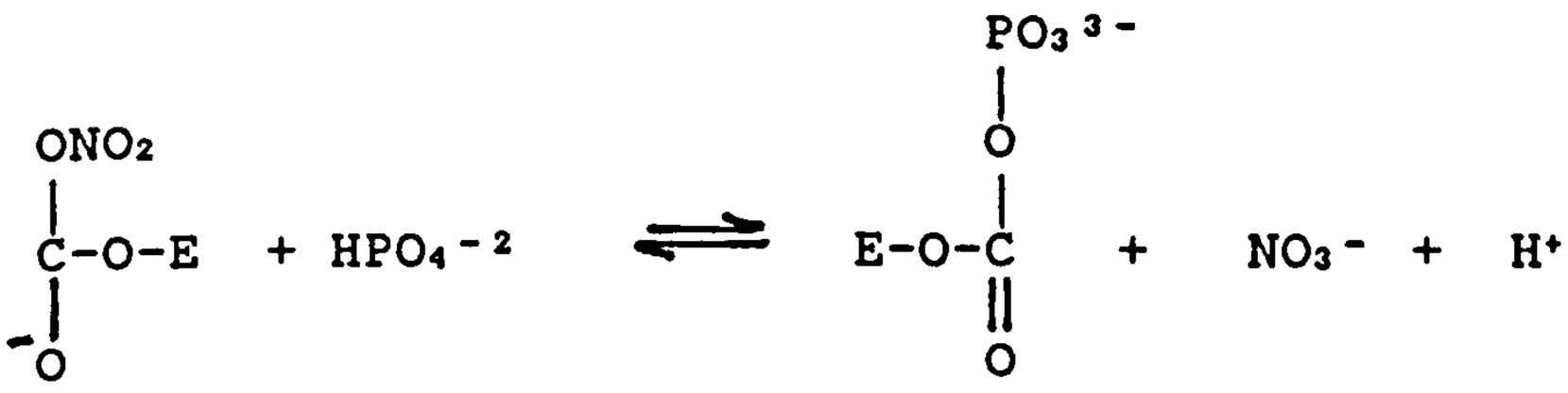

The proposed enzyme mechanism is relatively simple but the energy produced to enable growth is very low. As has already been mentioned in section 4.5.3, nitrous acid is not found naturally above pH 6.0. For an enzyme to catalyze the formation of nitrous acid in significant quantities, it is felt that an acid group is required. The presence of

sulphur[42] in nitrite oxidoreductase may be connected with promoting the formation of nitrous acid. The phosphate is indicated to remove a proton from nitrous acid to form the reactant species NO_2. "Nitrite oxidizing membranes possess a brownish colour which is typical for all nitrite oxidizers"[42]. This brownish colour could be the result of NO_2 formation. The nitrite ester formed by NO_2 is more reactive than the phosphate or nitrate ester and is very reactive by biological standards.

The reaction of nitrous acid with the carboxy phosphate ester is assumed to be the reverse of the reaction involved in the breakdown of the hydrolyzed product to form nitrite in hydroxamic acid oxidoreductase. The phosphate ester is assumed to form "active CO_2" (i.e. the phosphate removes a proton), enabling either nitric or nitrous esters to be formed.

The oxygen in the nitrate is shown to come via water, indicating that the reaction is reversible. It is believed that one nitro molecule donates one of its oxygens to its neighbour. The nitroso thus formed then undergoes hydrolysis, to form the nitro compound. A hydrolysis reaction is in agreement with section 1.2.3.

The reaction is believed only to be possible in the absence of oxygen. The presence of oxygen near the enzyme is assumed to inhibit the reaction through the formation of a nitro-nitrate. As the nitroso is not formed in the presence of oxygen, the protons and electrons are not obtained to provide energy. The bacteria are assumed to require that oxygen binding and nitrous acid binding occur at different locations.

Nitrite oxidoreductase also oxidizes formate[42,39]. The proposed mechanism can explain this observation. Formate has a very similar chemical structure to nitrite and presumably fits into the enzyme site. It is proposed that an oxygen from the nitro group oxidizes formate (to bicarbonate) rather than nitrate ions. The resulting nitroso is hydrolyzed to obtain electrons as for nitrite oxidation.

Nitrite oxidation also has a well-known inhibitor, ultraviolet light, which is discussed in section 6.7.

6.3 The Proposed Mechanism and the Kinetic Results

The nitrite reaction data shows the same behaviour with regard to pH as the ammonia data. However, the rate is seen not to fluctuate as wildly. This is best illustrated by a plot of fractional conversion versus time, as is illustrated below in figure 25.

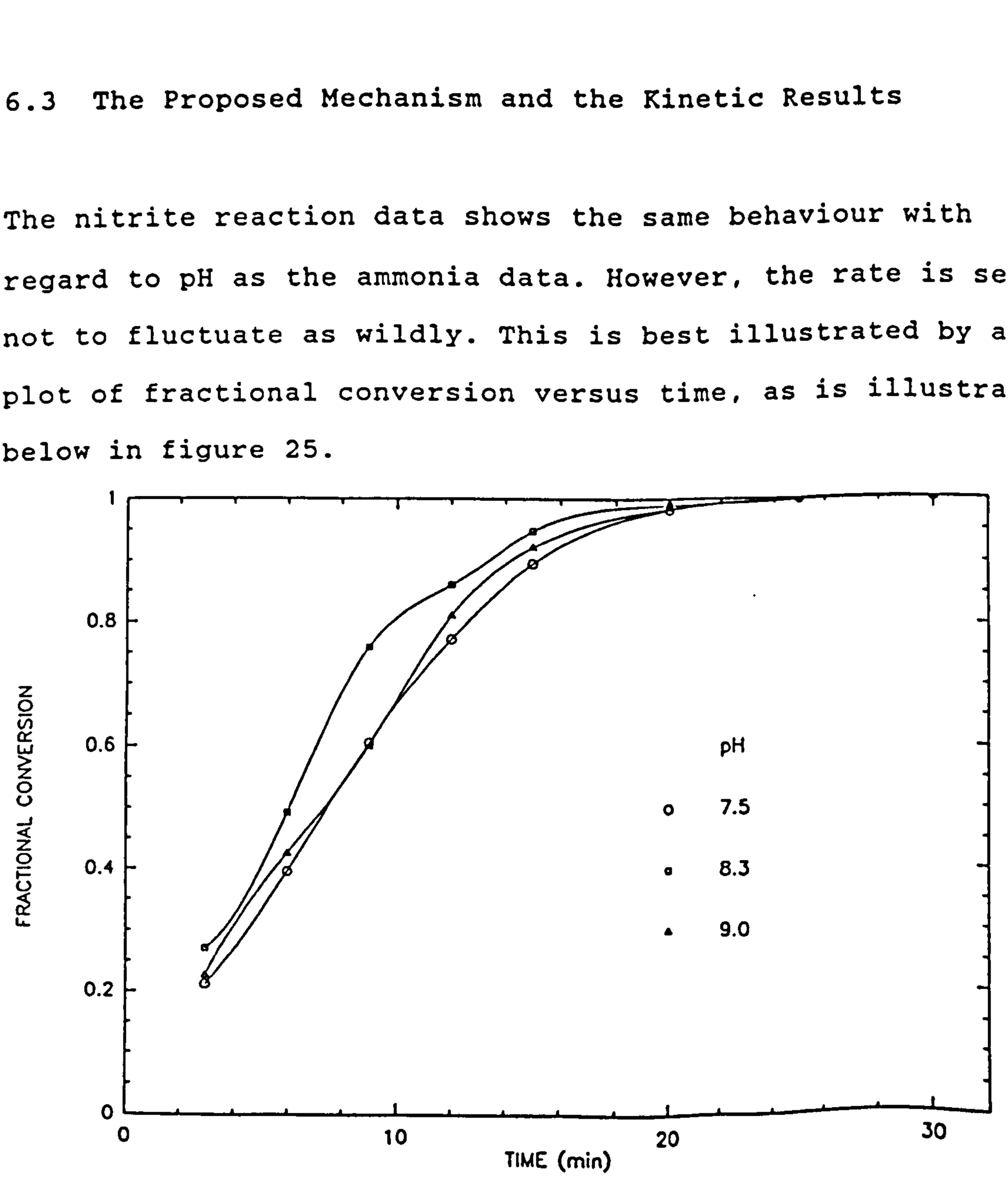

Figure 25. Nitrite oxidation at various pHs.

The relative differences in the residuals (see figure 26) for fitting Michaelis-Menten kinetics appear to be different from the ammonia oxidation residuals. *Nitrobacter* grow even slower than *Nitrosomonas*; thus, these curves cannot be explained by changes in the numbers of bacteria. The data once again lie outside the parallel lines of ±0.05 (experimental error), indicating that the reaction does not correspond to Michaelis-Menten kinetics.

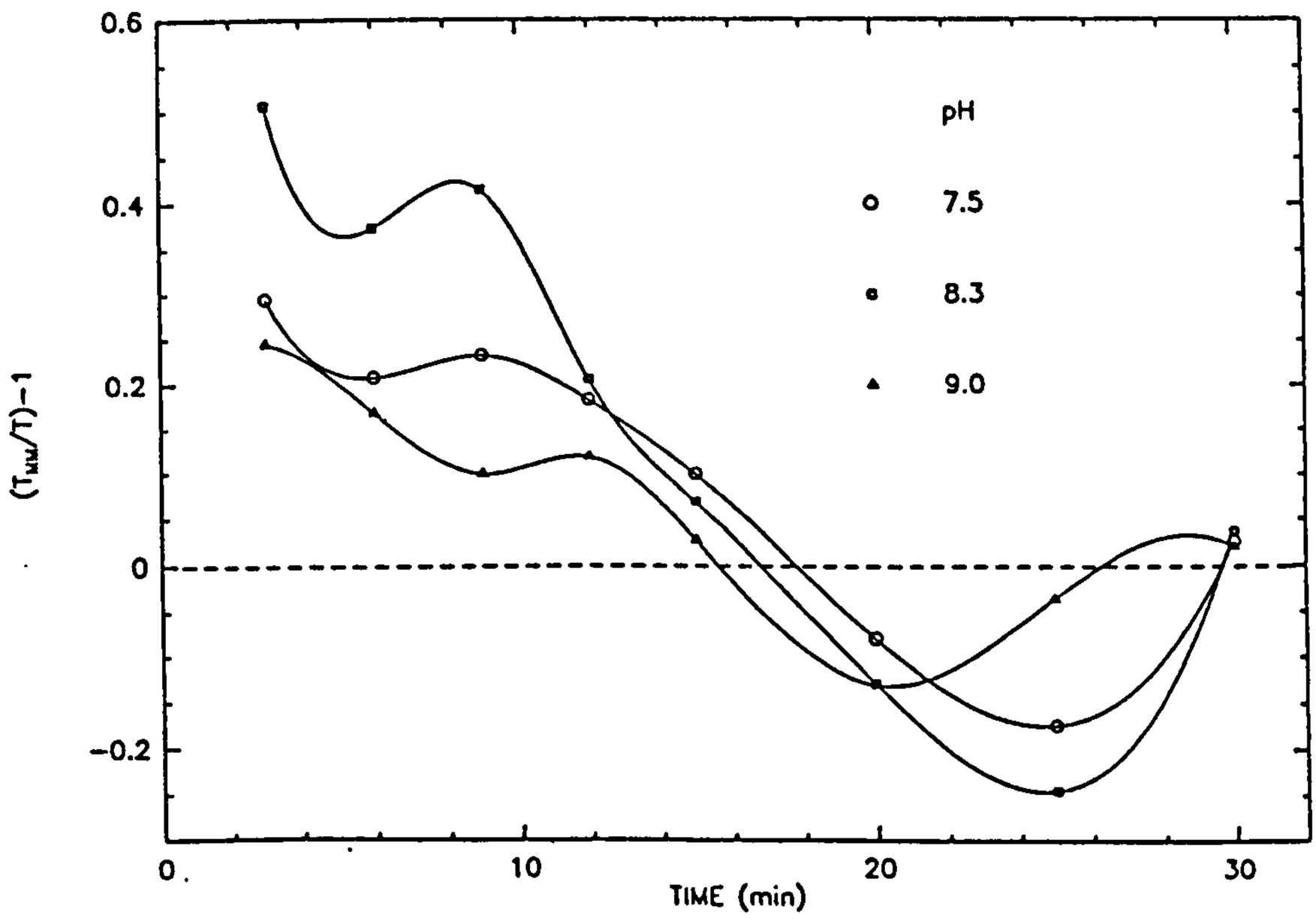

Figure 26. Relative differences for Michaelis-Menten kinetics at various pHs.

An examination of the graph for the relative differences reveals that it has a wave-like shape. A wave shape indicates sigmoidal behaviour and an equation of the Hill type is appropriate. The systematic nature of the curves

indicates that the reaction is again being controlled. No feedback control mechanism for *Nitrobacter* has been suggested in the published literature (see 1.2.3). The existence of a control mechanism and the requirement to add acid cannot be explained by the reaction stoichiometry (see 1.2.1). This clearly demands a mechanism that can account for both these observed features of nitrite oxidation.

The proposed mechanism suggests possible control via ATP and the mechanism also has a requirement for bicarbonate ions. Thus, the proposed mechanism can account for both observations. The sigmoidal behaviour is discussed further in section 7.7.

The experiments conducted were of an unsteady-state nature. As is explained in detail in section 7.7, the constants of Hill-type equations are thought to be constant only when a steady state exists. In the experiments performed here, the relative difference data fluctuate between 10 and 20 minutes after the impulse addition of the substrate. This is thought to be due to increases in the ATP concentration and the alteration of the proton concentration at the enzyme site.

This is in agreement with the need to add acid to buffer the reaction. Bicarbonate ions are required to activate more reaction sites as more ATP is produced. There is no need to add buffer during conditions in which the bacteria are close to a steady state (e.g. growth), as the amount required is easily met by the natural buffering capacity of the water.

The promotion of nitrous acid formation, like that of ammonia gas formation, depends on the proton concentration.

However, as the overall oxidation of nitrite does not alter the pH, it is not susceptible to immediate feedback control. Thus, the relative differences do not fluctuate in the same manner as for ammonia oxidation. In the equivalent chemical process, the primary control method consists of a single feedback loop, feedback by alteration of the ATP concentration. The reaction is influenced by the local pH, but this does not appear to be directly involved in the control system. The oxidation of ammonia, if not buffered, lowers the pH, thus also altering the nitrite oxidation rate.

6.4 The Stoichiometry of the Proposed Nitrification Reactions

Nitrosomonas

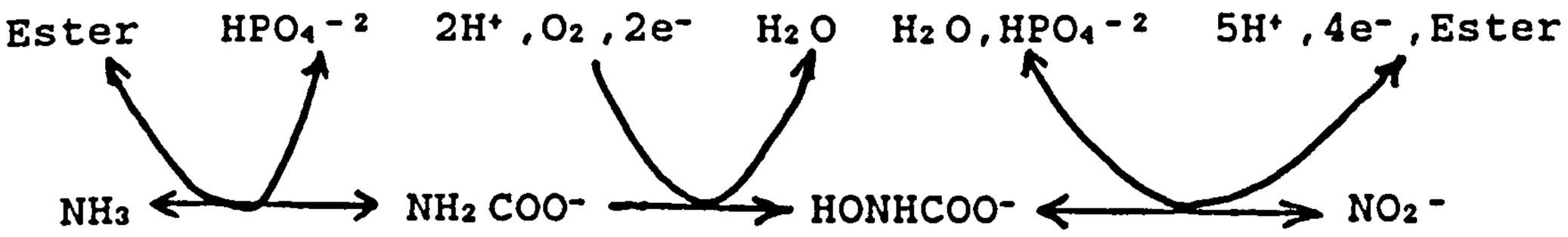

Ammonia | Carbamate | Hydroxamic Acid | Nitrite

via the cytochrome chain and respiration:

$$NAD^+ + 2H^+ + 2e^- \rightleftharpoons NADH$$

$$NADH + \tfrac{1}{2}O_2 \longrightarrow H_2O + NAD^+ + Energy$$

The overall reaction is:

$$NH_3 + 1\tfrac{1}{2}O_2 \longrightarrow NO_2^- + H_2O + H^+ + Energy$$

and is equivalent to that given by the U.S. E.P.A. [26].

Nitrobacter

via the cytochrome chain and respiration:

$$2H^+ + 2e^- + \tfrac{1}{2}O_2 \longrightarrow H_2O + \text{Energy}$$

The overall reaction is:

$$HNO_2 + \tfrac{1}{2}O_2 \longrightarrow HNO_3 + \text{Energy}$$

and is equivalent to that given by the U.S. E.P.A. [26].

6.5 Nitrate Removal

In future, the removal of nitrates can be expected to assume ever growing importance to aquaculture. Nitrate concentrations rise during nitrification, adding to nitrates from other sources. Waste water from recycle aquaculture systems is often high in nitrates, by drinking water standards. The maximum amount of nitrates currently allowed in drinking water under European Community law is 25 mg/l NO_3-N (50 mg/l NO_3-N being the absolute limit)[90]. While aquaculture waste water is not used as drinking water, its untreated return does break the spirit of the European Water Charter (appendix 6.a).

Dilution with water low in nitrates is a possibility, but this increases the total amount of water required. If the amount of organic and inorganic nitrogen entering the water cannot be reduced, then the other possibilities are to grow algae or plants (nitrogen metabolism), or to use denitrification. Both methods require energy either in the

form of light or as additional substrates containing carbon.

The proposed mechanisms for nitrification suggests the path that denitrification and nitrogen metabolism (the reverse reaction to nitrification) take. Paths in which nitrates are reduced will be considered in the next sections. The anaerobic process of denitrification is considered in the following section. Nitrogen metabolism, the conversion of nitrates to amino-acids, is considered in section 6.5.2.

6.5.1 Denitrification and its Possible Mechanism

Denitrification is an adaption of nitrification induced under low oxygen tension (anaerobic conditions). The enzymes responsible are nitrite reductase and nitrate reductase. Nitrite reductase has been found in *Nitrosomonas europea* [91,92] and is assumed to be responsible for the observed production of nitrous oxide. This is in agreement with Poth and Focht's [25] ^{15}N isotope studies, which indicated that *Nitrosomonas europea* can only convert nitrite to nitrous oxide. Other bacteria which contain nitrate reductase can convert nitrates to atmospheric nitrogen.

No detailed mechanisms have been proposed in the literature for denitrification (see 1.2.3). However, the proposed mechanisms for ammonia and nitrite oxidation suggest the method by which denitrification occurs. These mechanisms are now considered.

The first step is the formation of the nitrite ester.

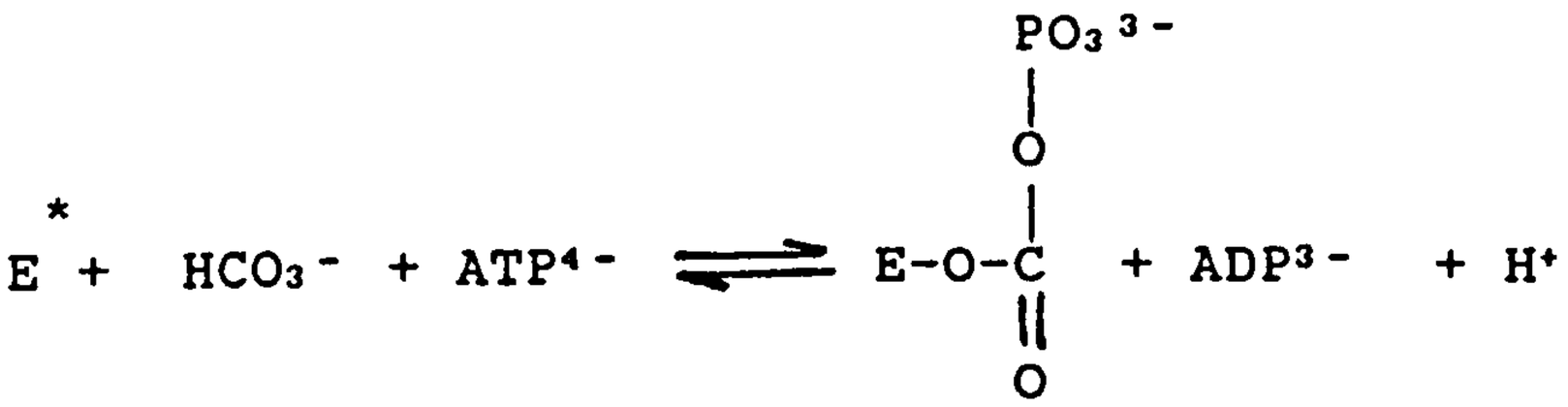

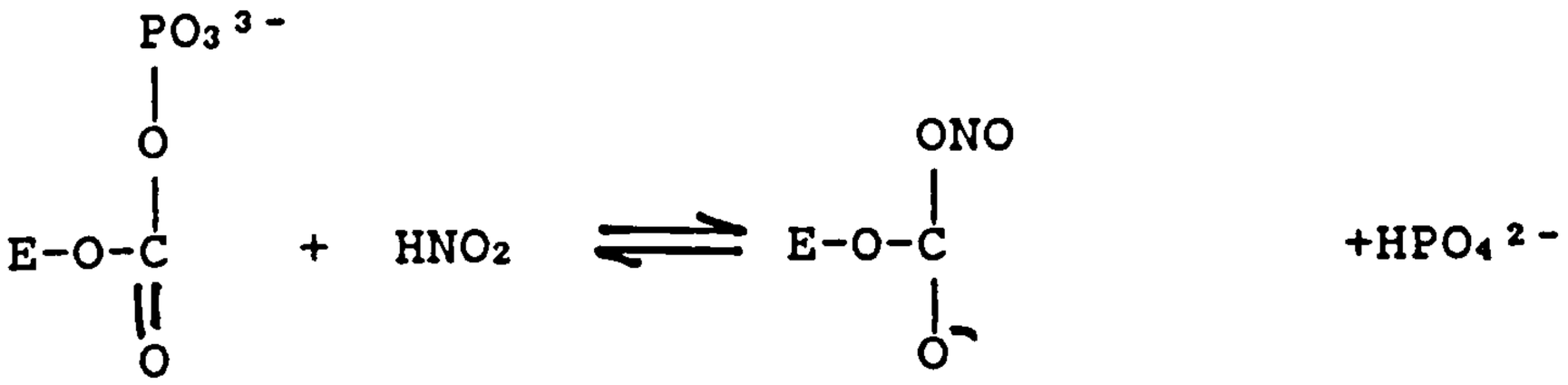

The steps following nitrite ester formation are thought to be similar to the known inorganic chemical reaction below[63]:

brown colourless

Two nitrite esters are proposed to react in the presence of nitrite reductase to yield two nitroso-intermediates and oxygen.

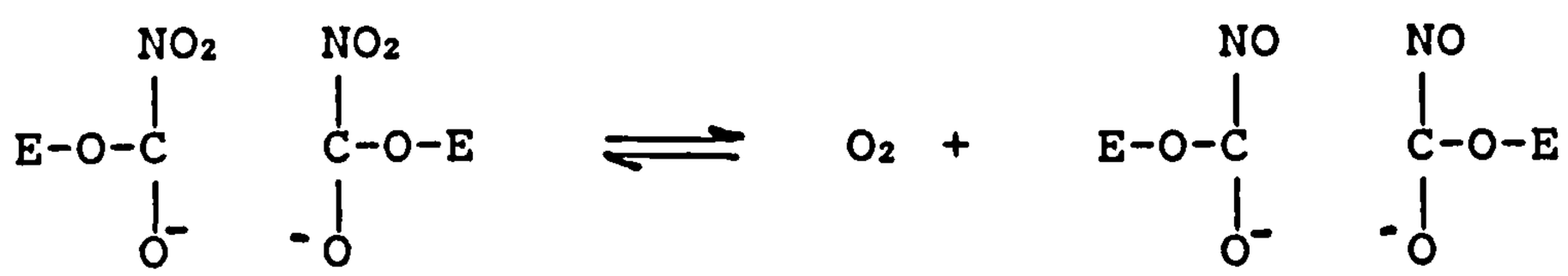

The assumed reason for the reaction is to obtain oxygen under "oxygen stress" conditions. The oxygen from the reaction can then be used for respiration or by ammonia

mono-oxygenase. The oxygen is assumed to be removed by a copper site in the enzyme and this is in agreement with Miller's [91] observations. Miller found that a copper site in nitrite reductase had a "high affinity" for O_2, to such an extent that accurate measurement of its affinity was precluded.

The two nitroso intermediates together should be very reactive, and it is assumed they react to give nitrous oxide. The reaction can only be carried out in low oxygen tensions as it involves the nitroso intermediate. Electrons ($2e^-$ per O_2) are required to make use of the oxygen obtained. This is suggested to limit the extent of denitrification. Goreau et al. [93] observed a yield of only 0.47 ± 0.1 % N_2O from NO_2^- (both expressed as moles of N) with *Nitrosomonas europea*. Ammonia oxidation yields four electrons, but two are used to form hydroxamic acid. The other two electrons are required for respiration to obtain energy for the bacteria. It is assumed that denitrification in *Nitrosomonas* is limited, because only a few electrons can be diverted from respiration. This then prohibits the reduction of nitrates (to nitrites) and nitrites to atmospheric nitrogen.

Nitrous Oxide

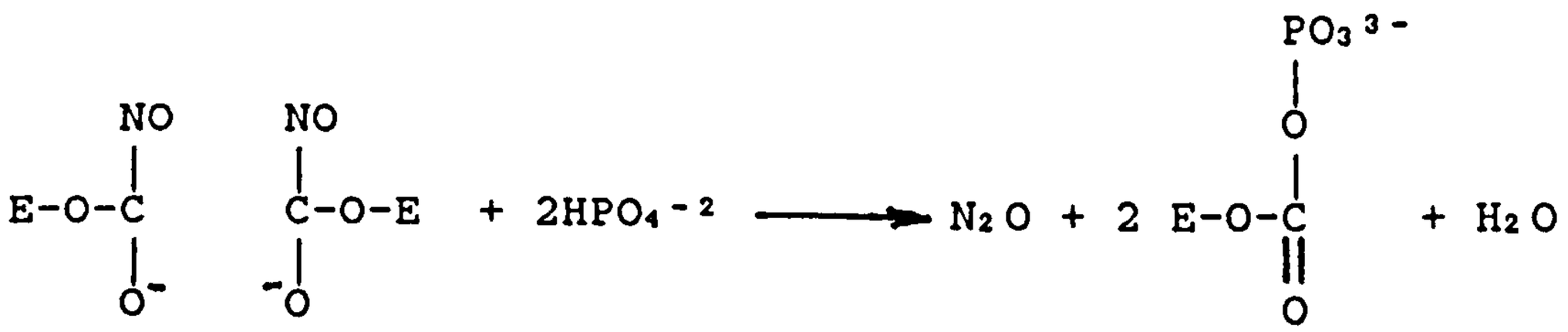

Atmospheric Nitrogen

It is suggested that the reduction of nitrite to atmospheric nitrogen follows the path given above, except for the last step. The nitroso intermediates are possibly brought together and the enzyme aids in the removal of the oxygen.

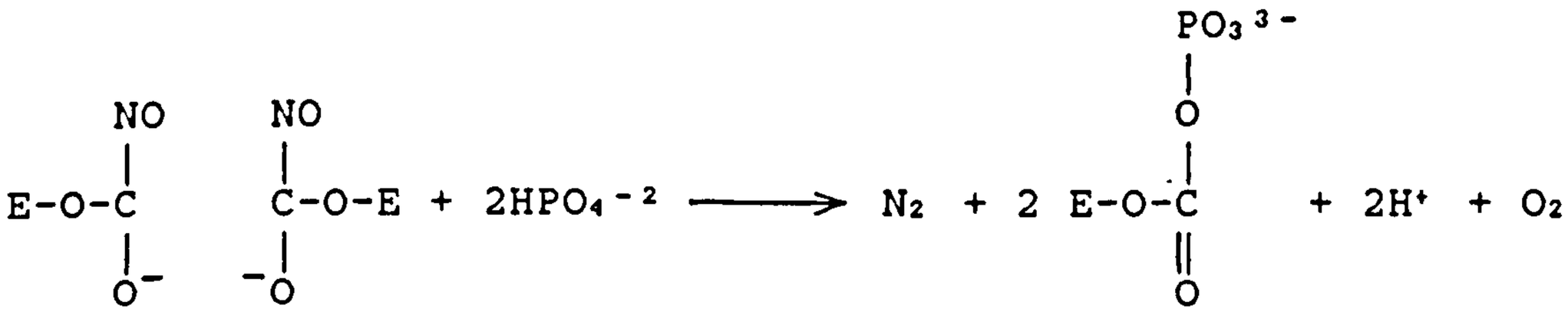

Organic chemistry [60] has a similar overall reaction for the reduction of nitro compounds. Two nitro compounds can react to form Azoxy (-N=N-) compounds. One nitro molecule is reduced to the nitroso and the other to a hydroxylamine. These then combine to yield the azoxy.

It would be surprising if the speculated reaction path represented the entire mechanism for these reactions or the others given later in this chapter. Thus, they are intended to indicate the assumed major steps, rather than the detailed mechanisms. For a more detailed understanding of the possible mechanisms, further studies are required.

As was mentioned by Wood[39], ammonia-oxidizing bacteria "would do much better to oxidize ammonia to nitrogen gas"[39]. The reaction of ammonia with nitrous acid has a Gibbs free energy of negative 360 kJ/mol. This reaction is well known in chemistry. It may be thought that ammonia gas (or a

primary amine) could react with nitrous acid to form nitrogen gas and protons. However, this is speculated not to occur in organisms, because ammonia gas requires a high pH, and the reaction (which involves nitrous acid) requires a very low pH (less than pH3).

More energy is required to reduce nitrite to atmospheric nitrogen than to nitrous oxide. Thus, the reduction of nitrite to atmospheric nitrogen is only worthwhile for bacteria whose substrates contain more energy (electrons) than ammonia. The proposed mechanism also involves the nitroso intermediate which requires the absence of atmospheric oxygen (anaerobic conditions). Methane contains more energy than ammonia and is thought to use the carboxy nitrite ester (see section 6.6).

Denitrification is used in the water treatment industry to reduce nitrates in drinking water supplies. This is conducted under anaerobic conditions, and a source of reductant has to be added. Although many substrates have been tried, only methanol has been found to be satisfactory. Methanol is invariably used as the source of reductant, but it is undesirable in the treated water because of its toxicity. Denitrification with methanol has been shown to require about three methanol molecules for each nitrate molecule[94]. Added methanol is likely to be oxidized by denitrifying bacteria, as is suggested for methanotrophs (see 6.6). The proposed mechanism for ammonia/methane oxidation can explain the problem of the limited reductants for denitrification, i.e. they must react with the carboxy phosphate/nitrite ester to yield the required electrons. The proposed mechanisms also indicate that methane, not

methanol, is the natural substrate and that control problems may exist with using methanol.

6.5.2 Nitrogen Metabolism

The reverse reaction to nitrification is nitrogen metabolism. This reaction is used by plants and most algae (some can use ammonia directly) to obtain inorganic nitrogen. The principle of micro-reversibility indicates that chemical reactions always take the easiest thermodynamic path. This thermodynamic law indicates that the reduction of nitrates should follow the same path as the oxidation of ammonia.

Organic nitrogen is necessary for life. It is found in amino- acids, proteins, and nucleic acids. The source of this nitrogen is ammonia, which is obtained by the reduction of nitrates. It is estimated that 1,000,000,000 tons[64] are produced in the living world each year. Nevertheless, "much less is known about the pathway of NO_3^- reduction than about CO_2 reduction"[64].

The proposed pathway for nitrate reduction is now outlined. Nitric acid is reduced to nitrous acid via NADH in the reverse of the mechanism already given. The mechanism for the oxidation of hydroxamic acid to nitrous acid has also already been given, and the reduction is thought to be the reverse. However, the oxidation of ammonia contains an irreversible step, the addition of oxygen to carbamate.

Thus, the pathway is assumed to be different here:

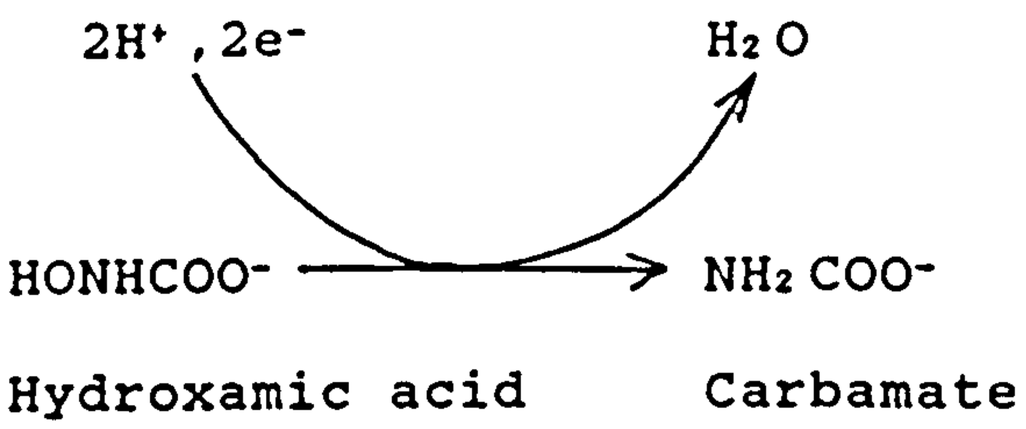

The reduction of hydroxamic acid requires that the oxygen is removed via NADH to form carbamate. Reduction of carbamate then yields ammonia, bicarbonate ion and ATP. This brings us back to similar enzymes and possible intermediates (see 3.7). The enzyme carbamyl phosphate synthetase is unable to reduce carbamate, as the relevant step is irreversible[68]. The enzyme carbamate kinase, however, readily performs the reduction of carbamate, which strongly favours ATP and ammonia production. Carbamate kinase is not involved in the formation of carbamyl phosphate, "since much evidence now indicates that this enzyme does not play a significant metabolic role in the synthesis of carbamate phosphate"[68]. However, it is suggested that carbamate kinase or a similar enzyme is involved in the final step in the reduction of nitrates.

The ammonia from the reduction of nitrates is immediately used to make glutamic acid.

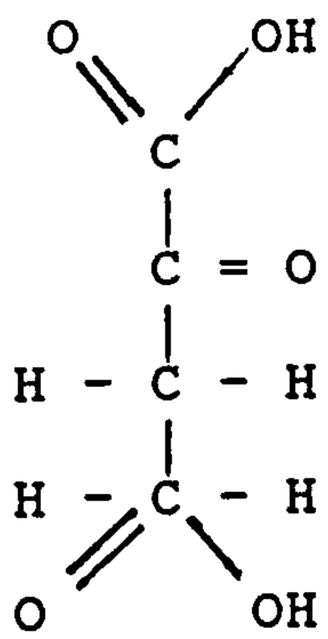

NADH removes the O to form H_2O.

NH_3 replaces it.

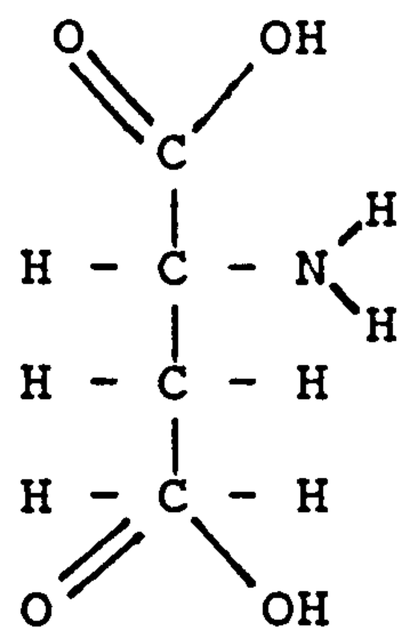

Ketoglutaric acid

Glutamic acid

Glutamic acid then undergoes various enzyme-catalyzed reactions to make the amino-acids required for synthesis. This process is called transamination. Many amino-acids are formed, as is described below:

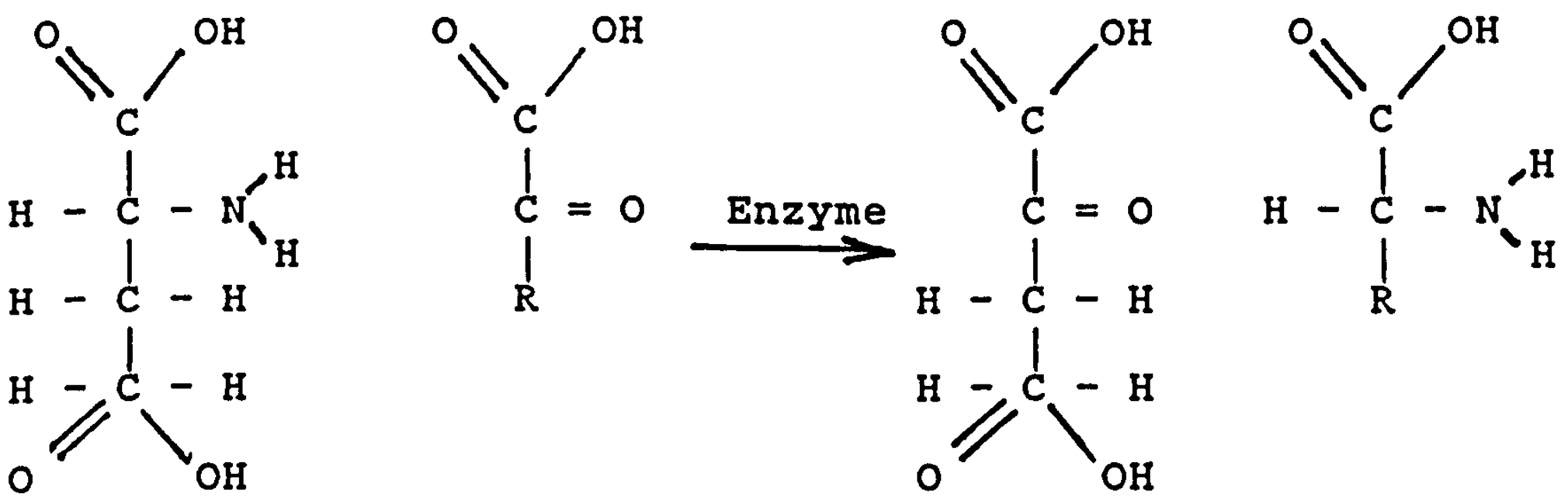

Glutamic acid | Keto-acid | Ketoglutaric acid | New amino acid

Ketoglutaric acid is obtained from the Krebs cycle. Further details can be obtained from biological pathway charts and biochemistry textbooks[95,66].

The above illustrates how organic nitrogen is

assimilated. This process requires energy, which bacteria obtain from a substrate. Algae and plants use the energy from photosynthesis, stored as carbohydrates, which is used to produce the required amounts of NADH and ATP.

6.6 Methane, Methanol and Formate

Nitrifying bacteria can carry out the oxidation of a number of chemicals that are not primary amines (see 5.5). The reactions of most interest are those involving C_1 compounds, that is methane, methanol and formate.

Nitrosomonas europaea is capable of oxidizing methane and methanol to formate[96]. Although methane can be oxidized by Nitrosomonas, it will not grow on methane as a sole substrate. "Methane oxidizing bacteria possess a very similar mono-oxygenase"[39] (to ammonia). It was this property that led Shears and Wood [82] to suggest the oxidizing cycle for ammonia mono-oxygenase (see 5.4.1). It has also been found that methanotrophs can oxidize ammonia to nitrite[39]. "Nevertheless, so far no-one has achieved growth of a methanotroph on ammonia"[39] (as its energy source). "The distinction between nitrifiers and methanotrophs persists, but becomes increasingly fragile"[39]. This then begs the questions of what the differences are and how the reactions proceed.

The implied mechanisms of section 1.2.3 do not give a reaction mechanism for the oxidation of methane, and no insight is offered into the fragile distinction between nitrifiers and methanotrophs. Methane oxidation yields more energy than ammonia oxidation, but nitrifiers cannot grow on

methane. Voysey and Wood[96] speculated that toxic oxime formation (formaldehyde + amine = oxime) resulting from formaldehyde production could be the cause. However, this is not persuasive, as no oxime has been reported without the deliberate addition of either formaldehyde or hydroxylamine.

The proposed mechanisms for ammonia oxidation can answer how the reactions proceed and explain the fragile distinction between nitrifiers and methanotrophs. It is suggested that methane oxidation proceeds in the same way as ammonia oxidation, except for the fact that the nitrite ester, and not the phosphate ester, is used. Methane is first reacted with a nitrite ester (otherwise methane is inert because of a thermodynamic barrier, as is the case with ammonia) to yield nitromethane (methyl nitrite). Ammonium nitrite is probably too unstable to be formed. Nitromethane is then oxidized by the copper-based peroxide to yield nitromethanol ($_2ONCH_2OH$), which yields formate and the nitrite ester (via hydrated nitroformaldehyde). The addition of methanol results in a reaction with the nitrite ester (similar to what happens when hydroxylamine is added to ammonium mono-oxygenase).

In the proposed mechanisms for nitrification, two esters are seen to be involved, the phosphate ester used by Nitrosomonas and a nitrite/nitrate ester used by Nitrobacter. The formation of "active CO_2" would allow either ester to be formed. Carbamate formation and the release of nitrite are performed by two enzymes at different locations. This is in agreement with Nitrosomonas avoiding nitrous acid formation at the ammonia mono-oxygenase reaction site. It is suggested that bacteria can be

classified according to whether they promote the phosphate or the nitrite/nitrate ester. Thus, the suggested difference between methanotrophs and nitrifiers consists in the extent to which they encourage the formation of either the nitrite or the phosphate ester. Nitrifiers and methanotrophs can both oxidize each other's substrates and so both have an ability to form both esters. However, as the formation of the discouraged ester is rare, not enough energy is made to allow growth. Furthermore, the cytochromes which obtain the electrons may not be able to utilize fully the energy from the discouraged substrate.

Sulphur-oxidizing bacteria, like methanotrophs, are closely related to nitrifiers. It is possible that sulphur-oxidizing bacteria also use the nitric/nitrite/nitroso esters. Known reactions in inorganic and organic chemistry would support this view. In organic chemistry nitric acid acts as a catalyst in the oxidation of sulphur compounds to sulphonic acids[60]. In inorganic chemistry[63], NO acts as a catalyst for the oxidation of sulphur dioxide, as is shown below:

$$2NO + O_2 \longrightarrow 2NO_2 \qquad (70)$$

$$NO_2 + SO_2 \longrightarrow SO_3 + NO \qquad (71)$$

6.7 Ultraviolet Light

Both Nitrosomonas and Nitrobacter are known to be inhibited by visible blue and ultraviolet light[72,73,74,75]. The oxygenated copper catalytic cycle based on tyrosinase was chosen by Shears and Wood[82] because of its sensitivity to

ultraviolet light. This could explain the sensitivity of ammonium mono-oxygenase to ultraviolet light, but it does not explain that of Nitrobacter. This "unexplained feature of nitrite oxidation"[39] can be answered by the proposed mechanisms. It is proposed that light interferes with the nitro-nitroso groups in nitrification. The given mechanisms indicate that nitrite oxidation and nitric acid reduction will be affected.

Nitro and nitroso groups as given in the proposed mechanisms undergo many photochemical reactions. Based on the reactions of nitromethane, the carbon-nitrogen-oxygen bonds are known to break, leading to other re-arrangements. Morrison gives a table of reactions in "The chemistry of the nitro and nitroso groups (part 1)"[87]. The photochemical reactions of possible interest to the oxidation and reduction of inorganic nitrogen are:

Dissociation into free radicals:

$$RNO_2 \longrightarrow R\bullet + NO_2 \qquad (72)$$

Nitrogen-oxygen bond cleavage:

$$RNO_2 \longrightarrow R\dot{N}O + O \qquad (73)$$

This type of reaction has been assumed in the proposed mechanism for nitrite oxidoreductase to form a nitroso and a nitrate (see 6.2).

Nitrite formation:

$$RNO_2 \longrightarrow RONO \qquad (74)$$

This is assumed to occur in the breakdown of the nitro group to form nitrite in the oxidation of hydroxamic acid.

Hydrogen abstraction:

$$RNO_2 + R\,H \longrightarrow \dot{R}NO_2\,H + R \qquad (75)$$

Radical anion formation:

$$RNO_2 + e^- \longrightarrow RNO_2^{\dot{-}} \qquad (76)$$

Both hydrogen abstraction and radical anion formation may be involved in removing electrons by a cytochrome and formation of nitrous acid.

CHAPTER 7

NITRIFICATION RATE AND DESIGN EQUATIONS

Earlier in the thesis (see 3.3), many rate equations were tested, but they failed to fit the observed rate data. Having investigated the possible mechanisms, the reaction rate data can now be better understood. The proposed mechanisms suggest that ATP is involved in the reactions, but unfortunately it is not practical to measure the concentration of ATP in this type of experiment. The concentrations of ATP can be measured in growing nitrifying bacteria in a biochemistry lab fermenter, but it poses major difficulties in an unsteady-state biological filter. As a result, various rate equations can be examined and compared with the available data, but the rate equations cannot be statistically tested.

7.1 Michaelis-Menten Kinetics

Saturation kinetics and Michaelis-Menten kinetics have often been referred to in this thesis. The form of the rate equation for both saturation kinetics and Michaelis-Menten kinetics is identical. The difference between the two relates to the branches of science they come from.

Saturation kinetics was developed by chemists investigating solid catalyzed gas reactions. There, the rate of reaction depends on the number of catalytic sites, which is a fixed quantity. These are saturated with reactants or products.

The Michaelis-Menten equation in its original form

describes a reactant (substrate) combining in a reversible step with an enzyme, a step which is followed by an irreversible reaction. The usage has since been widened to cover other enzyme mechanisms which share the same rate equation form. Michaelis and Menten were not the first to develop this form of rate equation. However, they helped develop the experimental methods of controlling pH and of measuring the initial rates of reaction in enzyme reactions. In measuring the initial rates of reaction, "the reverse reaction, inhibition by products, progressive inactivation of the enzyme and other complicating features can be avoided"[76].

The statistical analysis of section 3.3 indicates that ammonia was not oxidized according to Michaelis-Menten kinetics. Related mechanisms will now be examined.

7.2 The Kinetics of Activation

It is worth examining the author's earlier data, figures 27 and 28, which have been reproduced from reference 29. The plots are for saturation (Michaelis-Menten) kinetics, but the residence time in minutes for each point is also given. These plots indicate that there is a systematic trend to the data.

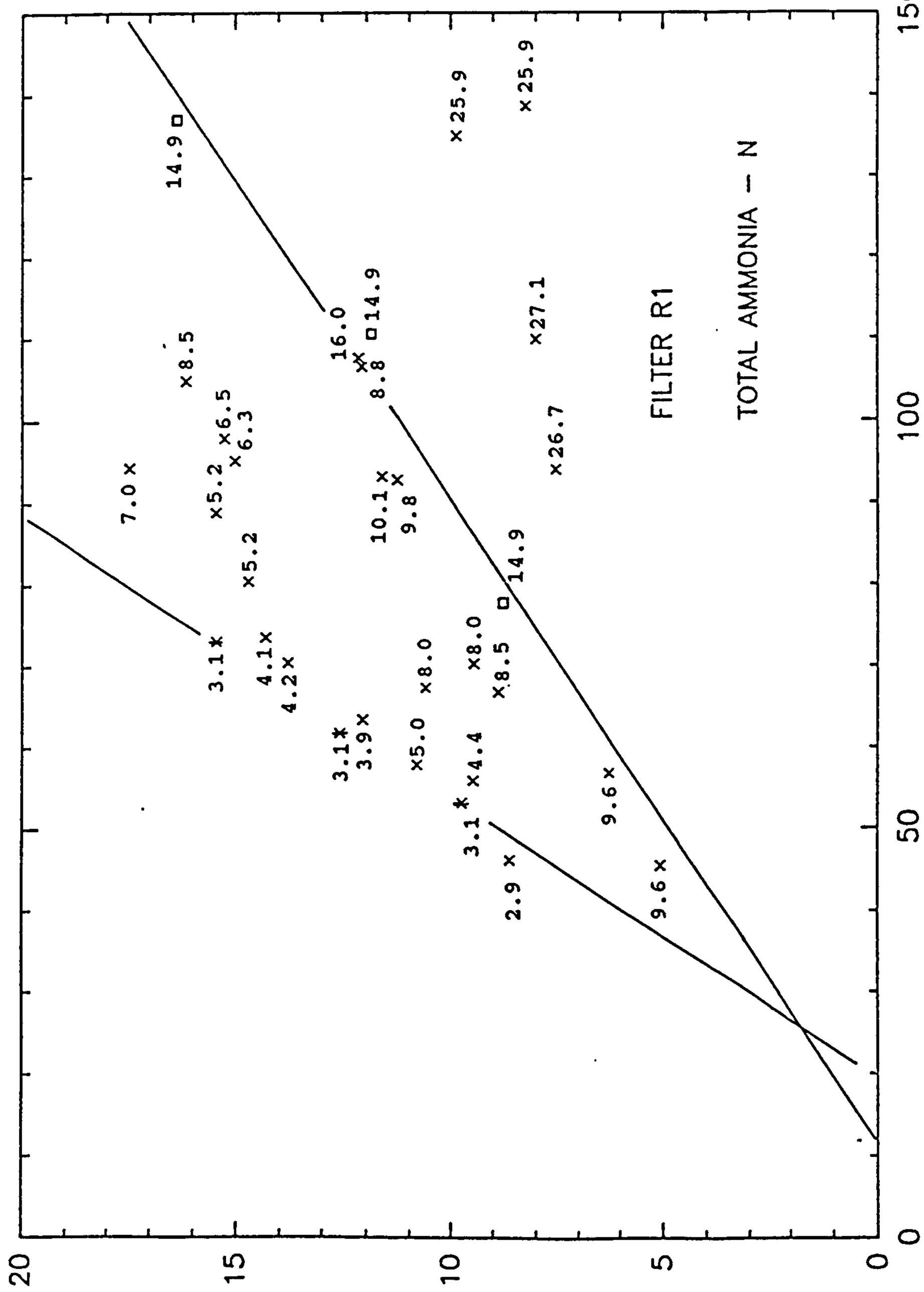

Figure 27. Saturation kinetic plot for filter R1.

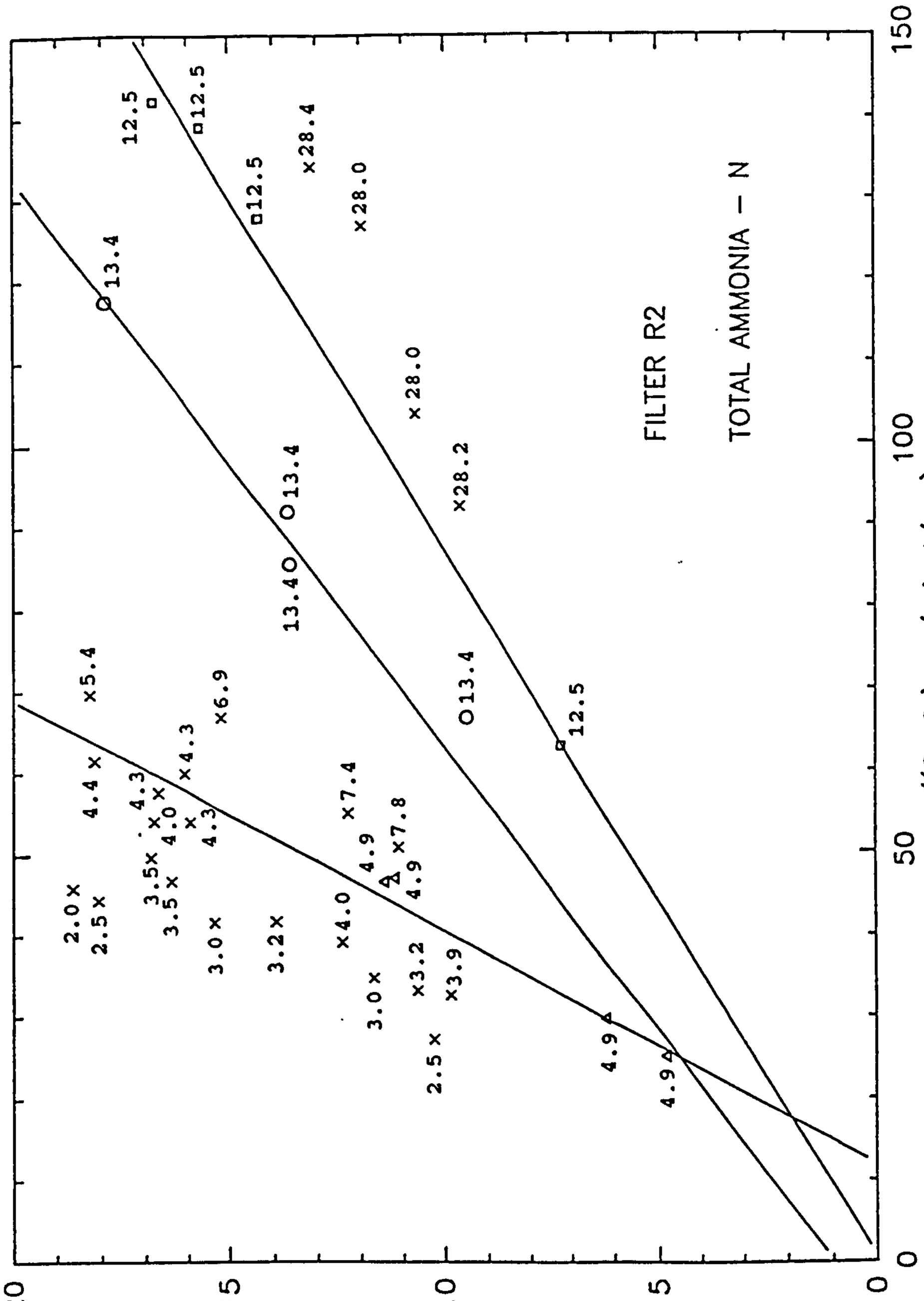

Figure 28. Saturation kinetic plot for filter R2.

The data appear to be of Michaelis-Menten form for the given residence times. However, the slope and intercept vary. From these two graphs it can be seen that the rate of ammonia oxidation increases with decreasing residence time. Filter R2 is seen to show higher reaction rates (see figure 28). This is in agreement with the fact that it has shorter residence times. The variation of the intercepts with residence time indicates that an inhibitor/activator is involved.

It can be argued that a product might be inhibiting the reaction, and several possibilities require re-examination. Nitrite has never been reported as an inhibitor in the low micro g/l Nitrogen range. Hydroxylamine, even if it were an intermediate, has only been detected in very small quantities and only upon addition of hydrazine. The other product, hydrogen ions, remained at a constant concentration in the water during the experiments, and there was no difference observed between the influent and effluent pH. This is assumed to be due to buffering. The implied mechanisms of section 1.2.3 thus cannot explain the observed kinetic data.

This demands a mechanism that can explain the data. The proposed mechanism for ammonia oxidation will now be compared with the steady-state kinetic data examined in section 3.3.

7.3 ATP as an Activator

For ammonia to be oxidized by the proposed mechanism, ATP is required to form the carboxy phosphate ester. The reaction

can be considered to be controlled by the activator $MgATP^{-2}$ (see 5.4.1). Magnesium is assumed to be an integral part of the substrate[76], and it is assumed that its bulk contributes to binding. Using the notation and equations used in the "Fundamentals of Enzyme Kinetics"[76], the kinetics of *compulsory activation* is as follows:

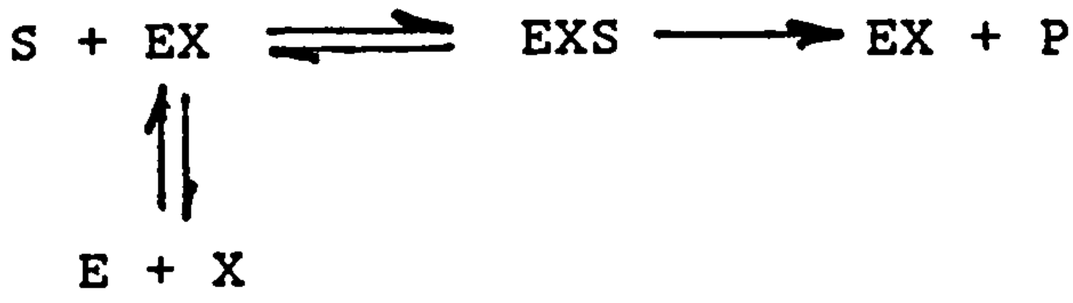

The rate equation is:

$$v = \frac{V' s}{K'_m (1 + K_x/x) + s} \qquad (77)$$

$$K_m^{app} = K_m (1 + K_x/x)$$

Thus the rate is seen to appear to be Michaelis-Menten in nature. However, the Michaelis constant in the equation is only an apparent constant and its value depends on the concentration of activator, $MgATP^{-2}$. This would have the effect of changing the position of the (y-axis) intercept, but, as is observed from the aquaculture system data (see figures 27 and 28), the y-axis intercept can take positive values. Thus it is clear that this form of equation is not suitable.

7.4 Mixed Inhibition and Activation

Mixed inhibition and activation cannot explain the observed positive y-axis intercepts either, but it will be considered because protons have been indicated to activate and inhibit the reaction. A simple mechanism for mixed inhibition/activation which produces both apparent Michaelis constants is:

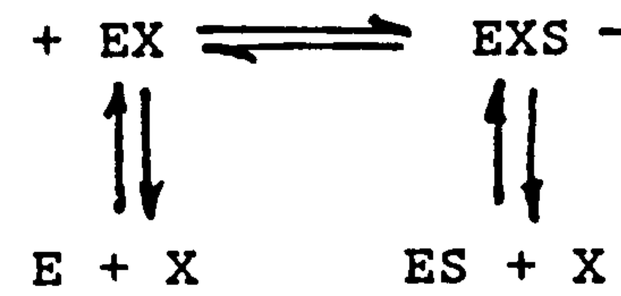

This mechanism has a rate equation of Michaelis-Menten form, but has two apparent constants:

$$v = \frac{V' s}{K'_m (1 + i/K'_i) + s (1 + i/K'_i)} \qquad (78)$$

For mixed inhibition the apparent constants are:

$$K_m^{app} = \frac{K_m (1 + i/K_i)}{1 + i/K'_i} \qquad V^{app} = \frac{V'}{1 + i/K'_i}$$

For activation, the apparent constants are obtained by substitution of i/K'_i with K'_x/x .

Bacteria control enzyme reactions to permit orderly change in the organism and to avoid a rapid return to equilibrium. Biological organisms have developed ways of controlling their metabolism and ATP is often involved.

However, the degree of control that can be achieved by the above mechanism is limited.

The proposed mechanism suggests that ATP and protons activate and inhibit the reaction. The possibility of mixed activation by ATP is examined first. It would require very large changes in the concentration of ATP to control the above reaction mechanism and these changes would disrupt every other ATP-dependent reaction. More significantly, the large variations in the ATP concentrations required by equations 77 and 78 have not been observed in nitrifiers.

The proposed mechanism also suggests that a proton will inhibit the formation of the reaction intermediate at a low pH, but at a high pH it will act as an activator by breaking down the reaction intermediate. Thus protons (pH) can be considered as activators and inhibitors. The problem of protons acting according to the above equation is the opposite to the one for ATP. The range of proton concentrations experienced in biological systems is so great that it is measured using a logarithmic scale (pH). The result is that the reaction could only be controlled over a very narrow pH-range. However, Nitrosomonas oxidizes ammonia over a large pH-range (6 to 9 in the unsteady-state experiments).

The above analysis and the positive y-axis intercepts indicate that the reaction is not controlled by protons and ATP according to equations 77 or 78. This type of equation cannot explain the behaviour of figure 16 either. Furthermore it does not explain the residuals observed in the unsteady-state ammonia and nitrite experiments. The wave like characteristic of the unsteady-state residuals

indicates sigmoidal behaviour and this is discussed in the following section.

7.5 Sigmoidal Behaviour and the Hill Equation

"Clearly, the ordinary laws of enzyme kinetics are inadequate for providing the degree of control that is necessary for metabolism [as discussed in section 7.4]. Instead, many of the enzymes at control points display the property of responding with exceptional sensitivity to changes in metabolite concentrations. This property is generally known as *co-operativity*, because it is thought to arise in many instances from 'co-operation' between the active sites of polymeric enzymes"[97].

A discussion of co-operativity and sigmoidal behaviour requires a short historical summary of biochemical investigations into haemoglobin. Haemoglobin is a protein that binds and transports oxygen in the blood. It is not an enzyme. However, haemoglobin was the first molecule found to exhibit sigmoidal behaviour. Oxygen-binding in haemoglobin is stable and easy to study. As a result, many of the early investigations into sigmoidal behaviour used haemoglobin. Haemoglobin also has a non-sigmoidal analogue, myoglobin, for storing oxygen in muscle.

Sigmoidal behaviour is best illustrated by a plot of the fraction of saturated binding sites versus the substrate concentration (see figure 29 from reference [97]). Haemoglobin gives a curve, termed sigmoidal, whereas myoglobin gives a curve of the Langmuir isotherm type. The chemical nature of haemoglobin has been determined and the difference between

the two molecules is the number of subunits, each with its own oxygen binding site. Haemoglobin has four peptide chains each with a single haem, whereas myoglobin has one. This indicates that the sigmoidal behaviour of haemoglobin is connected (at least in part) with the number of binding sites.

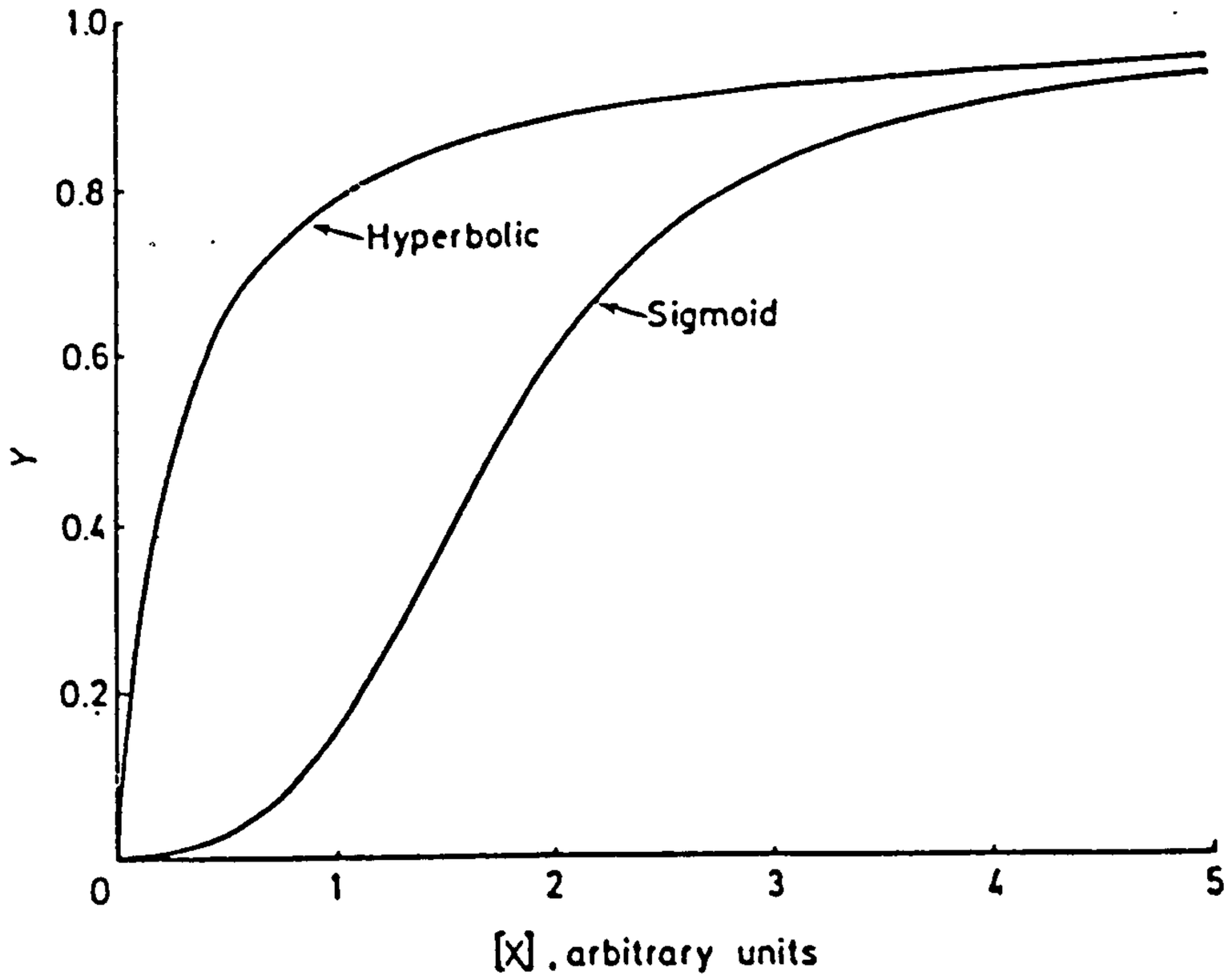

Figure 29. Hyperbolic and Sigmoidal Binding.

In 1910, before the nature of haemoglobin was known, Hill considered oxygen binding at two sites but found that this only fitted some of the available data [98]. Hill realized that his model for two sites would become unmanageable with larger numbers of binding sites and thus proposed a purely empirical equation. It was suggested that an equation of the "type" proposed could describe sigmoidal behaviour. It has since become known as the Hill equation

and is given below:

$$Y = \frac{K_h [X]^h}{1 + K_h [X]^h} \qquad (79)$$

Hill found that the equation fitted all of the available data for haemoglobin very accurately. The exponent h is known as the Hill coefficient and the haemoglobin data gave values of h = 1.0 to 3.2. It should be noticed that when the Hill coefficient has a value of one it is equivalent to the Langmuir isotherm equation. Hill disclaimed any physical meaning to K_h and h. However, it is apparent from the behaviour of haemoglobin that the Hill coefficient is connected with the number of subunits. The value of h is used as a measure of co-operativity, unity represents non-co-operativity. Negative co-operativity exists when h is less than unity and positive co-operativity exists when h is greater than unity. The values for K_h and h can be obtained from a Hill plot as illustrated below:

$$\frac{Y}{1 - Y} = K_h [X]^h \qquad (80)$$

$$\log \frac{Y}{1 - Y} = \log K_h + h \log[X] \qquad (81)$$

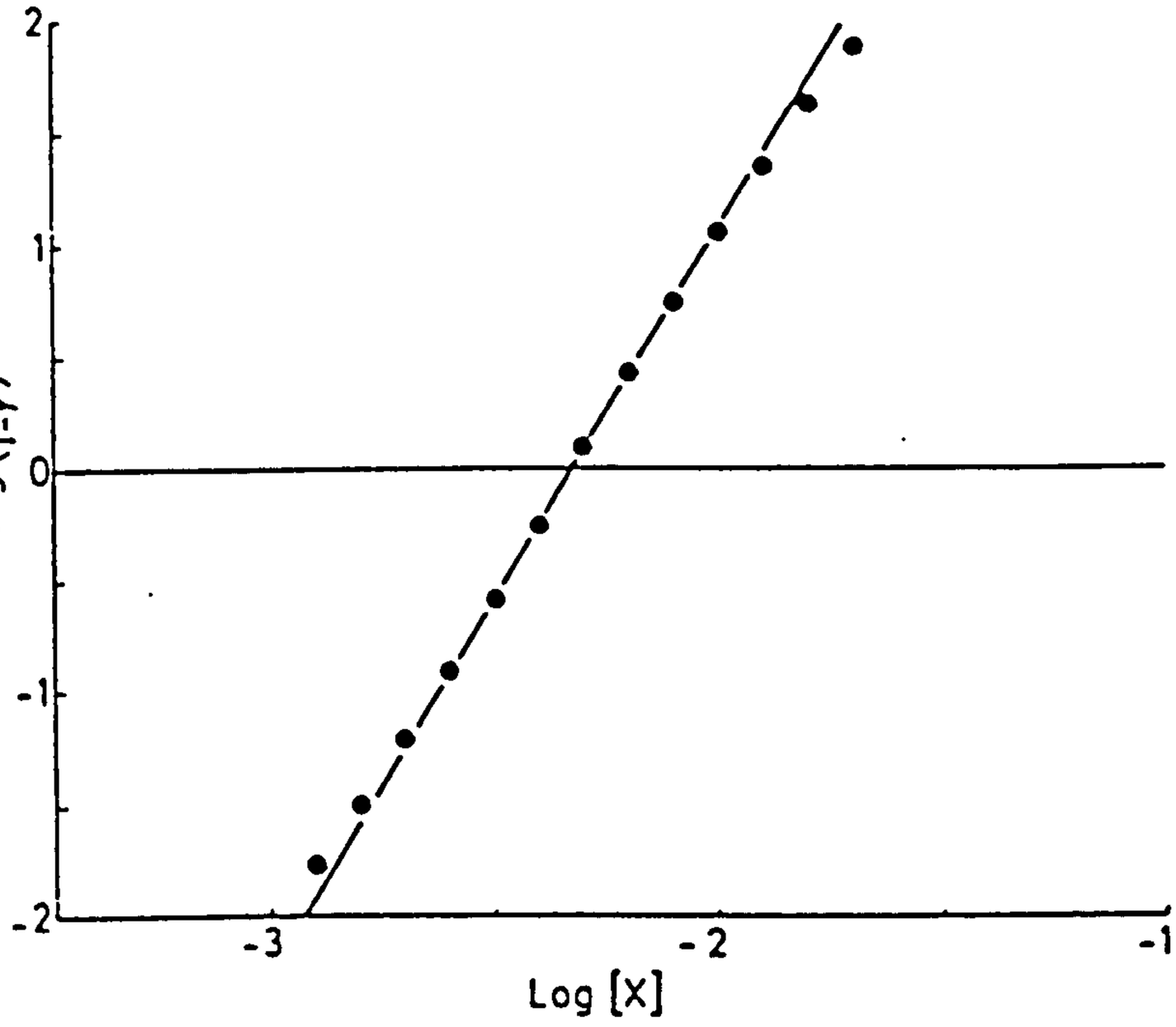

Figure 30. The Hill plot

The Hill plot "has been found to fit a wide variety of binding data remarkably well for values of Y in the range 0.1-0.9, but deviations always occur at the extremes"[97]. A feature of the Hill equation that has been subject to most debate is the non-integer values obtained for the Hill coefficient. The Hill coefficient might be expected to take integer values reflecting the number of bound subunits. This problem is easily illustrated. Even though haemoglobin has four binding sites, the maximum observed Hill coefficient is 3.2. This problem has not been addressed, rather it has been pointed out that the Hill equation is purely empirical. As an empirical equation it is seen as "at best only an approximation of a more complex relationship"[97].

With the discovery of the exact chemical structure of haemoglobin many authors have attempted to develop

non-empirical models. For further information the reader should consult "The principles of Enzyme Kinetics"[97]. These models are much more complex than the Hill equation and have many more variables. The models do not fit the data significantly better than the Hill equation. Many of the models give the Hill equation as a special solution.

To use the Hill equation to describe a sigmoidal enzyme reaction, it must be assumed that the rate of reaction is proportional to the extent of saturation (Y) of the enzyme. In the published literature the enzyme form of the Hill plot (figure 30) has been used to determine the Hill coefficient for sigmoidal enzymes. These experiments have been carried out in the laboratory using batch experiments.

$$\log (v_o / (v - v_o) = h \log s + \log K_h \qquad (82)$$

This method requires the determination of the initial velocity (v_o) and the maximum velocity (v) at several initial substrate concentrations (s). (The initial rate is used because the second substrate concentration can be easily dictated.) The slope of the plot yields the Hill coefficient. This plot has been used to demonstrate sigmoidal behaviour for certain substrates in many enzymes. Anderson and Meister[99] used this method to demonstrate sigmoidal behaviour in carbamate phosphate synthetase (see 3.7). The value of the obtained Hill coefficient for ATP was 1.7 (constant L-glutamine). The proposed mechanism suggests that this enzyme has a similar mechanism to ammonia mono-oxygenase.

Two enzymes that show strong but different degrees of co-operativity are glucokinase and hexokinase. Glucokinase

has two known substrates, ATP and glucose. Indeed, deviations from Michaelis-Menten kinetics have only been observed in enzymes which have more than one substrate. To obtain Hill rate plots the concentration of only one substrate at a time is allowed to vary. The problem with testing the Hill rate plot on the kinetic data collected is that the ATP concentration has not been measured nor held constant.

In developing a design equation it is important to minimize the number of variables that must be evaluated. The main advantage of the Hill equation and the reason for its success can be attributed to it having few variables. However, to use the Hill equation as a design equation some physical meaning to the parameters is desirable. In particular, negative co-operativity needs to be understood. Negative co-operativity has been observed in numerous enzymes but the puzzle of non-integer values for the Hill coefficient remains. Alternative models to the Hill equation also fail to explain accurately negative co-operativity. Whilst considering this problem the author realized an analogy between sigmoidal enzymes and process control valves. The power of this analogy may not be self-evident at first, but it will be used to illustrate a proposed equation. This equation is discussed and compared to the one for control valves in the following sections.

7.6 Sigmoidal Enzymes and Control Valves

In section 5.8 the oxidation of ammonia is discussed as if it were a chemical process. It was also suggested that

(sigmoidal) enzymes could be equated with process control valves. To develop the analogy, the various types of control valves require discussion. Readers who are not familiar with control valves are encouraged to read sections 22-79 to 22-84 in "Perry's Chemical Engineers' Handbook"[58].

There are three basic types of control valve, showing decreasing sensitivity, linear (constant) sensitivity and increasing sensitivity to the valve stem travel. This equates to enzymes exhibiting negative co-operativity, non-co-operativity and positive co-operativity to substrate concentration.

There are two other valve properties, the rangeability and the turndown. To discuss the equivalent property in enzymes, the Hill plot of figure 30 should be consulted. The rangeability of a valve is the ratio of the maximum to the minimum controllable flow. The enzyme equivalent is the ratio of maximum to minimum enzyme saturation (Y) that can be obtained. Valve turndown is given by the normal maximum flow divided by the minimum controllable flow. It is proposed that the normal maximum flow equivalent would be the enzyme saturation value at which deviations from Hill-type plots begin.

A control valve's inherent characteristics are given at constant pressure. When control valves are installed their characteristics alter because of pressure drops, mostly across other equipment. The enzyme equivalent to pressure drop is proton concentration (pH) differences and an enzyme's 'inherent' characteristics are defined at its optimum pH. As part of a biological control system an enzyme is influenced by all the other processes. Thus to compare

enzymes in situ with control valves the equivalent equation for installed control valves is required. This equation is now given from reference 58:

$$Q = \frac{L^{n}}{(\alpha + (1-\alpha) L^{2n})^{1/2}} \qquad (83)$$

"Q and L are the fractions of maximum flow and stem travel respectively; the term α is defined as"[58]:

$$\alpha = \frac{\text{valve head differential at maximum flow}}{\text{valve head differential at zero flow}}$$

The exponent for the denominator results from the nature of fluid flow through restrictions, and as such it is predetermined. On the other hand, the geometry of the valve plug and seat is altered to obtain the desired stem travel exponent. This exponent (n) is the single most important factor in determining the characteristics of a control valve. It is normally specified to be either one (linear control valve) or two (equal-percentage). The type of valve specified depends on the characteristics of the process.

Having outlined the characteristics of control valves, a proposed equation describing sigmoidal behaviour, analogous to the one for control valves, is now given:

7.7 A Proposed Equation to Describe Sigmoidal Binding

$$Y = \frac{K_{ps}[s]^{n}}{\left(\lambda + (1-\lambda) K_{ps}[s]^{mn}\right)^{1/m}} \qquad (84)$$

The enzyme fractional saturation (Y) is noted to equate to the fraction of maximum flow (Q). The fractional stem travel (L) is noted to equate to the product of a constant (K_{ps}) and the substrate (ligand [X]) concentration (s). K_{ps} is related to the association of substrate with enzyme to form a complex. The substrate concentration has an exponent. It is proposed that the exponent (n) is a product of a pseudo-order and the number of subunits (haems). This exponent is equal to the Hill coefficient (*h*). As a pseudo-order it does not have to take integer values. A more detailed explanation of both K_{ps} and the exponent is given later.

The equivalent to λ is given by:-

$(1-\lambda)$ = fraction of enzyme in singly protonated form

This parameter accounts for the influence of ionization (pH) on the large number of acid and basic groups on the enzyme. A plot of the reaction rate versus pH for many enzymes shows a 'bell shaped' curve. A sketch is given in figure 31 from reference 64.

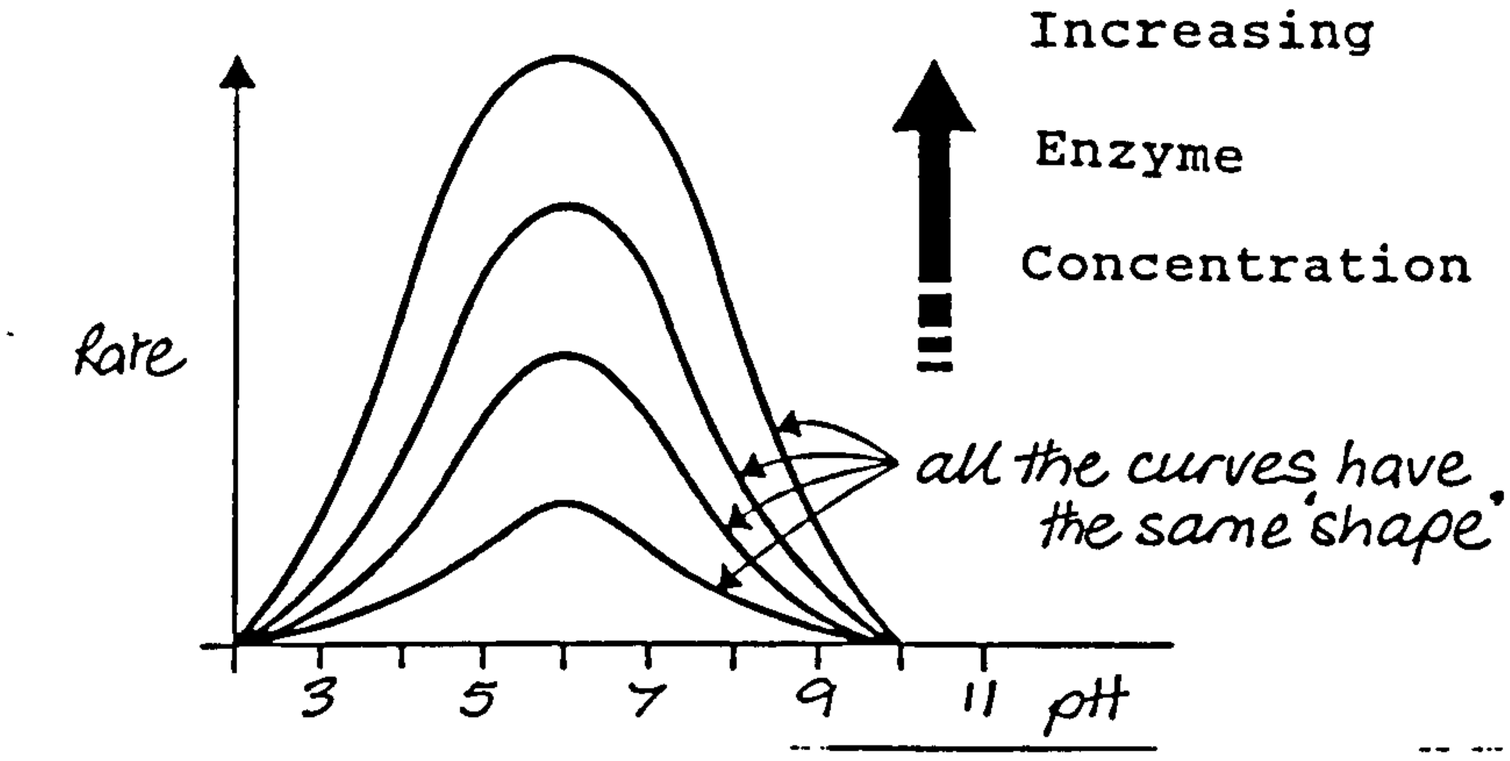

Figure 31. Reaction rate versus pH.

The denominator exponent (1/m) represents the 'molecularity' of the binding involved and thus can only take numbers that are integers or fractions of integers. For a single substrate combining at a subunit, it equals one. It is assumed that two substrates (bi-substrate) binding at a single subunit or a single substrate binding with two subunits is rarer.

The non-integer values of the substrate exponent will now be discussed. No suitable explanation for negative co-operativity, as appears to occur in ammonia mono-oxygenase, could be found in the literature. However, an explanation is now offered that is compatible with the proposed nitrification mechanisms. The explanation offered could also apply to other enzymes and subunits in which negative co-operativity or non-integer values of the Hill coefficient have been observed.

It is possible that the binding (reactions) of many

substrates occurs by chain mechanisms. The main feature of a chain mechanism is that it contains a propagation step. In this step an intermediate is not consumed but acts as a catalyst. This intermediate can then catalyze a large number of reactions before being destroyed. It is proposed that protons perform a related function in the nitrification mechanisms. The role of protons is of importance because they change the pH of the reaction site, i.e. the pH of the reaction site is no longer the same as the bulk fluid pH. This pH difference can then influence nearby substrates and the enzyme's amino-acids (their acid and basic groups) that make up the enzyme's binding site(s). This pH difference, it is proposed, alters the geometry of the enzyme binding site or the ionic form/shape of the substrate. The amino-acids used and their order in the enzyme would determine the enzyme's control characteristics. In the control valve analogy, the geometry of the valve seat and plug is altered. The result of the structural changes is that the reaction rate can be altered with great sensitivity. Thus, the Hill coefficient takes its value from the geometry of the substrate/enzyme and not only from the number of binding sites. As its value depends on the geometry of the enzyme, there is no reason for it to assume integer values. In control valves, engineers construct the valve plug and seat to give integer values, i.e. linear or equal percentage.

The idea that the geometry of co-operative enzyme sites changes is already contained in another theory, the *theory of induced fit* [100]. Interestingly a *lock and key* analogy is often used to describe the theory, i.e. the key (substrate) must fit the lock (enzyme) and realign the tumblers (as in

Yale locks) before it will turn. This theory suggests that a part of the substrate induces a conformational change in the enzyme binding site. An enzyme which is often used to explain this theory is hexokinase. This enzyme catalyzes the phosphorylation of glucose. It not only reacts with glucose, but also with fructose, mannose and other sugars. However, water does not react even though it cannot fail to saturate the enzyme. The theory of induced fit suggests that only the *bulk* of glucose brings about the proper alignment for binding.

The theory of induced fit might explain the behaviour of ATP that requires the *bulk* of $MgATP^{-2}$ to bring about binding. However, the theory of induced fit cannot explain the sigmoidal behaviour in nitrifiers. The substrates ammonia gas and nitrogen dioxide are almost as small as water molecules and they have little or no *bulk*.

Protons can affect the local reaction site in both the proposed reaction mechanisms. In the proposed mechanism for the overall formation of hydroxamic acid (see 5.4.1), a proton is removed. Thus, ammonium ion can be converted to ammonia gas and the reaction propagated. However, the hydrolysis of hydroxamic acid yields 5 protons, which can be used to give feedback control halting the propagation of ammonia gas. The protons can either be used in respiration giving no feedback, or they can travel between the two enzymes to slow the reaction.

According to the proposed mechanism the formation of nitrous acid in the oxidation of nitrite can also be activated (propagated) by protons. The protons can come from the hydrolysis of the nitroso group.

The single most important factor determining the characteristics of a sigmoidal enzyme is the substrate exponent (n). In control valves the stem travel exponent is the single most important factor and a process engineer would specify a linear or equal percentage valve to best suit the process. It is suggested that evolution determines the equivalent decision in organisms. To change an enzyme's co-operativity, the number of subunits can be increased or decreased, dramatically changing the enzyme's characteristics. Evolutionary pressures would give enzymes the number of subunits suitable for their different purpose and environment. Thus molecules such as haemoglobin (4 subunits) and myoglobin (1 subunit) reflect their different environments and tasks.

It is possible that molecularity can explain the behaviour of known enzymes that show sigmoidal binding but fail to fit the standard Hill plot. This could be tested by plotting $\log(v_o^m / v^m - v_o^m)$ versus log(s) for different values of m. Many sigmoidal enzymes do fit the standard Hill plot (m = 1) and thus it is proposed that they involve a single substrate at each subunit. The proposed binding equation can be manipulated to form a Hill type equation and is given below:

$$Y_{Hill} = (1-\lambda)Y^m = \frac{K_{ps}[s]^{nm}(1-\lambda)/\lambda}{(1+K_{ps}[s]^{nm}(1-\lambda)/\lambda))} \qquad (85)$$

A significant difference between the proposed equation and Hill's is evident. The inclusion of the λ term indicates that K_h ($K_h = K_{ps}(1-\lambda)/\lambda$) and the fractional binding ($Y_{Hill} = (1-\lambda)Y^m$) are functions of pH. K_h equals K_{ps} at the mid-range value of $\lambda = 0.5$. This corresponds to known enzymes showing "half-of-the-sites-reactivity"[101]. The advantage of operating around $\lambda = 0.5$ is that it gives the most responsive (optimal) control, but the binding (reaction) rate is sub-optimal. The upper ($\lambda = 1$) and lower ($\lambda = 0$) limits of λ cause numerical difficulties in the Hill type equation form. The case of $\lambda = 1$ corresponds to the denaturing of the enzyme by extreme of pH. The value $\lambda = 0$ is assumed to be approached, but is never met in practice because the reactions always alter the pH of the enzyme's binding site. It is analogous to a control valve which has no pressure drop across itself.

Blood is kept at a pH close to 7.4 by the buffering action of the bicarbonate system[63]. The sigmoidal experiments into haemoglobin have been carried out over a narrow pH-band and thus any pH effect would not be very evident.

Sigmoidal enzymes in common with non-sigmoidal enzymes show pH-dependent activity. The proposed equation accounts for this known behaviour. The λ term separates the effect pH has on the enzymes acid and basic groups away from the binding site from the pH at the binding site.

The parameters of the proposed equation are pseudo-constants and they are an approximation to a more complex relationship. The methods used to alter the local pH and thus the enzyme geometry could involve many substrates, co-

enzymes and other biological chemicals. It may be more pragmatic to acquire a knowledge of the pseudo-constants' values under various conditions rather than develop equations to explain the change in geometry. A method by which the pseudo-constants can be obtained over the operational range of conditions is now outlined.

7.8 Determining Hill Type Pseudo-Constants

The Hill plot is not suitable for continuous processes in which the available data are often limited to effluent and influent concentrations. It is also desirable to use an unbiased statistical method to obtain the pseudo-constants. The following method is suggested, which has an advantage in that it can be represented graphically.

The method by which data from plug flow reactors can be analyzed is now given. Batch reactors can be studied by substituting the space time with the elapsed reaction time and substituting the influent concentration with the initial concentration. Deviations from plug flow to mixed flow can be examined by treating the plug flow reactor as having a recycle stream. This is explained in "Chemical Reaction Engineering"[51]. In common with using the Hill plot it is assumed that the reaction rate is proportional to the fractional saturation of the enzyme. Thus the rate of

reaction is given by:

$$-\frac{ds}{dt} = \frac{N K_{ps} s^{n}}{(\lambda + (1-\lambda) K_{ps} s^{mn})^{1/m}} \qquad (86)$$

where N is a constant related to the moles of enzyme (and the fraction of enzyme saturated by other substrates).

The method is also restricted to enzymes that bind a single substrate (at a time) to a subunit, that is m = 1. It must also be assumed that the concentrations of the other substrates in the reaction do not alter.

Separating the rate equation variables in the same manner as for the integrated Michaelis-Menten plot and integrating one obtains:

$$\frac{\int_{C_F}^{C_I} \frac{1}{C^{n}}\, dc}{(C_I - C_F)} = NK_{ps}/\lambda \; \frac{\tau}{(C_I - C_F)} - K_{ps}(1-\lambda)/\lambda \qquad (87)$$

This yields an integral on the L.H.S. that has to be evaluated. The integral is easy to evaluate for integer values of co-operativity, but in most cases it will require numerical integration, using a calculator or computer. A search procedure such as golden section is then required to determine the optimum Hill coefficient. A value for the Hill

coefficient is first estimated, non-co-operativity being a reasonable starting point. The integral is then calculated and the L.H.S. plotted against $\tau/(C_I - C_F)$. This plot should ultimately be a straight line in which the slope and intercept yield $N K_{ps}/\lambda$ and $K_{ps}(1 - \lambda)/\lambda$ respectively. The least-squares-fit of this line is then statistically evaluated. The search is continued to find the value of Hill coefficient that produces the best-least-squares- fit.

The slope divided by the intercept then gives $N/(1-\lambda)$. Through carrying out experiments at various pHs the 'bell-shaped' curve for the enzyme is then determined. With the pH-dependence of the enzyme described, both N and K_{ps} can be evaluated.

The above procedure then yields the pseudo-constants for a single substrate binding at one enzyme. The chemical process analogy would be that the behaviour of a control valve adding a single reactant has been described. Unfortunately, sigmoidal enzymes have been observed to have multiple substrates. Thus, in practice the reaction rate is determined by the other substrates and to what extent they contribute to enzyme saturation. For a complete description of the process, each substrate's contribution must be included.

In the oxidation of ammonia the concentration of ATP, ammonia, bicarbonate ions and dissolved oxygen appear to determine the reaction rate. This does not take into account other factors such as temperature, which will alter the constants. In aquaculture, dissolved oxygen and bicarbonate ion concentrations should not normally influence the reaction rate. However, the concentration of ATP will

determine the enzyme saturation. Thus N would be a pseudo-constant reflecting the fraction of enzyme sites saturated by ATP as well as the moles of enzyme.

Figures 27 and 28 can now be explained. The y-axis intercept can take positive values because the reaction does not follow Michaelis-Menten kinetics. As can be inferred from the above equations, the intercept varies with different values of n (which equals the Hill coefficent). The increasing slopes of the plots indicate that the amount of ATP increases with decreasing residence time. However, the amount of ATP can be observed to approach saturation at the shortest residence times.

The oxidation of ammonia by nitrifying bacteria is a complex process and the control of the reactions has features found in chemical plants. Nitrifying bacteria are well equipped to oxidize ammonia efficiently. It remains for the process engineer to promote conditions that make maximum use of the bacteria's own control system. A principal feature of nitrifiers appears to be that they show sigmoidal behaviour. As a result of this, nitrification is best conducted at low substrate concentrations and short residence times, as suggested by figures 27 and 28.

CHAPTER 8

CONCLUSIONS AND FURTHER RECOMMENDATIONS

Literature Review

Previous literature, as indicated in chapter 1, has established the stoichiometry of nitrification. However, no detailed mechanisms have been given. Experiments conducted trying to establish previously-theorized intermediates have failed to produce unequivocal evidence for any of them. Many rate and design equations, assuming various rate influencing steps, have been proposed in the literature. However, there is not a consensus on what the rate-determining steps are and on how nitrification data should be treated or presented. The aquacultural designer is faced with a wide range of variables for which the degrees of influence have not yet been established. In consequence, filter design has been seen as an art[11,102] rather than a science.

The Effect of Diffusion

In earlier work on kinetic data from an aquaculture nitrification filter[29], the influence of diffusion on nitrification in aquaculture was evaluated. It was observed that the rate of ammonia oxidation approximated Michaelis-Menten kinetics for a given residence time, but that large variations occurred at different residence times. However, as Jennings[4] noted, diffusion resistance only produces limited deviations from first order kinetics. It was apparent from the data that first order kinetics was not

approached and that correlations for film diffusion yielded faster reaction rates than observed. Thus diffusion was eliminated as the cause of the deviations from Michaelis-Menten kinetics and as a major influence to ammonia oxidation in aquaculture.

The Effect of Fluid Mixing

The influence of fluid mixing on the oxidation of ammonia has been examined, as has been discussed in chapter 2. The analysis of the mixing data is complicated by the presence of deadspace and the lack of a suitable mixing model. However, a mixing model has been developed to describe both dispersion and deadspace. The kinetic data have been corrected for fluid mixing effects. However, these corrections have proved to be minor and fail to account for the deviations from Michaelis-Menten kinetics.

Statistical Evaluation of Rate Equations for the Direct Oxidation of Ammonia

The elimination of diffusion and dispersion indicates that it is the nitrification reactions themselves that are responsible for the deviations. The kinetic data have been tested against every possible mechanism for the oxidation of ammonia with oxygen, as described in chapter 3. The resulting rate equations include all previous equations suggested in the literature. However, the statistical analysis of the kinetic data overwhelmingly indicates that the ammonia is not oxidized to hydroxylamine and that none

of the previously suggested rate equations fits the data. The very large discrepancies cannot be attributed to any experimental error. This implies that hydroxylamine is not an intermediate and that the ammonia oxidation reaction mechanism requires examination.

Bicarbonate Ions

Unsteady-state nitrification experiments have been conducted over a wide pH-range. These experiments have produced a series of unexpected observations. The only explanation consistent with the observations is that bicarbonate ions are, in all probability, involved in both nitrification reactions.

Ammonia Oxidation

The pathways by which ammonia might be oxidized are very limited. The involvement of bicarbonate ions suggests a single pathway. This pathway and the proposed reaction mechanism are given in chapter 5. The involvement of bicarbonate ions suggests that a carboxy phosphate ester is made, presumably with ATP. The proposed mechanisms indicate that ammonia reacts with the ester to form carbamate which is oxidized to hydroxamic acid and then hydrolyzed. This mechanism for the oxidation of ammonia is entirely compatible with the previous experimental observations. Indeed, it answers major questions that had not been dealt with in the previous literature.

The mechanism implied by hydroxylamine as an

intermediate fails to explain either the unsteady-state kinetic data or the earlier data. However, the proposed mechanisms do and they indicate where the difficulties in analyzing nitrification data lie. The concentration of a major reactant, ATP, has not been recorded. Thus the data can appear to be perplexing and the development of a design equation has been hindered.

Nitrite Oxidation

The unsteady-state nitrite experiments indicate that, in all probability, bicarbonate ions are involved in the reactions. The mechanisms proposed in chapter 6 are the first detailed mechanisms to be offered for the oxidation of nitrite and denitrification. The mechanisms are all related to known mechanisms in inorganic and organic chemistry. The main feature of the proposed reactions is that they involve a carboxy nitrite ester formed from a carboxy phosphate ester. Once again it is proposed that ATP is used to overcome the thermodynamic barriers involved. The proposed intermediates are unstable and vulnerable to oxygen. It is unlikely that they could be observed. The proposed mechanisms explain three major previously unanswered questions. These questions are: How is formate oxidized; why are nitrifiers vulnerable to ultraviolet light; and why are they influenced by high oxygen tensions?

The proposed mechanism for nitrite oxidation is compatible with the unsteady-state kinetic data. Sigmoidal behaviour is observed, and this has only been observed in enzymes with multiple substrates. This indicates that the

problem of analyzing nitrite oxidation data is that the concentration of a major reactant, assumed to be ATP, has not been recorded.

The Kinetics and Mechanisms of Nitrification

The unsteady-state kinetic data for ammonia and nitrite oxidation suggests sigmoidal behaviour. This implies that ammonia mono-oxygenase and nitrite oxidoreductase are sigmoidal enzymes, i.e. both oxidations are sensitively controlled over a wide range of substrate concentrations. Indeed, it would be surprising, with the benefit of hindsight, if nitrifying bacteria did not use sigmoidal enzymes at such critical metabolic positions. Sigmoidal behaviour indicates that a rate equation of the Hill type is appropriate. A rate equation of this type which also compensates for pH has been developed in section 7.7.

All the proposed mechanisms in the thesis are compatible with the stoichiometric equations given by the United States Environmental Protection Agency[26] and all the isotope studies contained in the literature. The actual source and destination of the various atoms can be obtained from the proposed mechanisms.

Sizing Nitrification Filters

A rate equation suitable for designing nitrification filters is proposed in section 7.7 and it has a similar form to the well-known Hill equation. The problem for nitrification filter designers is that the concentration of a chemical

inside the bacteria influences the reaction rate. It is currently not practical to measure the concentrations of chemicals, such as ATP, inside nitrifying bacteria. This suggests that the way forward lies in developing a knowledge of the control behaviour of nitrifiers. The kinetic data indicate that short residence times at low substrate concentrations increase the reaction rate.

Filter Design Recommendations

The main recommendation for fluid mixing in submerged biofilters is that rapid expansion and contraction inside a filter should be avoided, because this causes deadspace. This is most important at the filter's entrance and exit, and a gradual expansion and contraction of the flow is desirable. The diameter of the vessel should be more than twenty times the equivalent particle diameter and the filter length should be over one hundred times the equivalent particle diameter. Plastic packings have large voidages, which means that they are less vulnerable to blockage. However, the high voidage increases the fluid residence time for a given volume and this is not desirable. It is suggested that loose packing, large enough to avoid blockage, is used. The choice of the volumetric flowrate through the filter depends on the desired fluid residence time. Short residence times give faster reaction rates and higher water quality, but this increases the pumping costs.

In the experiment to determine the nature of the curve of ammonia concentration versus time, it is apparent that the nitrite concentration remains very low (figure 12). This

indicates that nitrite oxidation, as opposed to Nitrobacter growth, is faster than ammonia oxidation. The low nitrite concentrations are probably due to it being an intermediate in a series of reactions. Chemical reaction kinetics indicate that to reduce the concentration of an intermediate in a series reaction, the residence time should be reduced. Thus, to keep nitrite concentrations to a minimum, the residence time should be low, as it was in the experimental rig.

In the author's MSc it was indicated that, on the basis of process economics, fluidized bioreactors were the preferred type of filter because they have a lower pressure drop and a reduced filter volume for a given active area. The observed nitrification kinetics compound the advantages. As mentioned before, a feature of the bacteria's control system is the fact that lowering the residence time increases the reaction rate. In the waste water industry, the increased oxygen requirement may cause problems if a three-phase fluidized filter is used.

Presentation and Analysis of Nitrification Data

The nitrification studies indicate that the oxidation of inorganic nitrogen by bacteria is a complex process. The rate of oxidation is a function of the ammonia nitrogen supplied per day, residence time, pH, temperature, oxygen, alkalinity and the filter's recent "history" (ATP concentration).

To obtain design data for a variety of systems and filter designs, aquaculturists must provide the data

themselves. To be of use, the data presented in the literature must be in a form which allows data evaluation. The proposed plot suggested in section 7.8 is recommended. The pseudo-constants from equation 86 must be given along with the filter and the system fluid residence times. The inorganic nitrogen supplied per day, available surface area, filter volume, pH, temperature, alkalinity, oxygen concentration and the recent filter history must also be defined.

Presentation of nitrification data as a percentage of the substrate oxidized is not useful. The rate of oxidation is <u>not</u> given by the influent-minus-effluent concentration divided by the flowrate.

The performance of a filter is dynamic. Therefore, the amount of ammonia nitrogen supplied per day cannot be obtained from taking a water sample, determining the ammonia removed and dividing by the filter residence time. If this method were to be used, a continuous measurement over 24 hrs would be required. The ammonia nitrogen supplied per day can alternatively be calculated from the nitrogen contained in the feed and its estimated conversion to dissolved ammonia-N.

<u>Bacteria Growth and Rate Equations</u>

The observation that nitrification enzymes are sigmoidal has implications for describing bacterial growth. In growth studies it is often assumed that Monod kinetics is followed, i.e. growth is dictated by the concentration of a single limiting nutrient. However, this equation is not suitable to

describe nitrification because kinetic limitations apply. The reactions are controlled by the enzymes within the bacteria. The rate of growth relies upon the energy obtained from the oxidation reactions, carried out by the enzymes. Therefore growth depends upon the co-operativity of the enzymes and this varies with substrate concentration.

Adaption to Conditions and Competition

Heterotrophic growth affecting nitrification is not evident in this work. It is suspected that some authors have wrongly attributed effects of the bacteria's control system to heterotrophic bacteria growth or diffusion limitation. On the whole, the nitrification data seem to be remarkably free from transient effects and this is believed to be due to the type of control system used.

Nitrifying bacteria have a sophisticated control mechanism. It appears that by adjusting the ATP "pool", nitrifying bacteria can adapt to different pHs and variations in substrate concentration. However, once all the binding sites are saturated in making the carboxy phosphate ester, further increases in the ATP "pool" would have no effect. This can explain the discrepancies in the reported effects of pH upon nitrification (see figure 23).

Nitrifying bacteria are primeval bacteria. It seems probable that nitrifying enzymes have evolved to suit their natural environment, i.e. the number of subunits and the type of co-operative binding. Nitrifying bacteria appear to show negative co-operativity (the enzymes react with decreasing sensitivity to rising substrate concentrations).

This implies that their natural environment is low substrate concentrations. These conditions would match those found in natural seas, streams and rivers.

Recommendations for High Substrate Concentrations

The concentrations of ammonia found in settled fish farm waste or domestic waste water are unnaturally high. However, the higher concentrations are easier to monitor continuously. This means that it should be possible to develop an expert system that uses information about the bacteria's control system to anticipate effluent concentrations. The expert system would co-operate with the bacteria's own control system to meet effluent concentration standards. High concentrations of nitrates in water can now be measured with probes and this offers possibilities for water treatment. Nitrate influent minimization is preferred to denitrification, but, where this is not practical, an expert system could calculate the precise quantities of the carbon source that have to be added, for example methane or methanol, which is potentially toxic.

Modelling Fluid Flow in Aquaculture Systems

The recycled crossflow mixing model, as developed in chapter 2, is very suitable for describing real stirred tanks, such as fish tanks. However, to describe deadspace in biological filters, the tanks in series model must be combined with it. If possible, the analytical solution to this model should be obtained. The mixing model is essentially a statistical

model for describing skewed distributions with long tails. The model could be extended so that the number of tanks does not have to be an integer. The model would then become an extension to the incomplete gamma (function) distribution.

Recommended Biochemistry Experiments and Investigations

The discovery of a chemical intermediate during the "normal" oxidation of ammonia would confirm the pathway of ammonia oxidation. What then is the prospect of observing the intermediates in the proposed mechanisms? The observation of either carbamate or hydrated hydroxamic acid is very unlikely. However, it may be possible to observe a ferric stabilized form of hydroxamic acid. Hydroxamic acid is unstable and therefore the detection method must avoid breaking it down to hydroxylamine. It is proposed that use be made of the fact that hydroxamic acid forms coloured complexes with iron. It might be possible to transfer hydroxamic acid, from its ferric carrier, under the right pH conditions to ferric ions. The stabilized hydroxamic acid could then be concentrated by the use of magnetism.

Many soluble haems described as "proteins with no known role"[39] have been found in nitrifiers, and these are thought to carry the substrates and products. The proposed mechanisms include many chemicals previously not considered to be involved in nitrification. More work is required to determine which substrates and products are carried by which haems. The haems may also be closely linked with transporting protons and altering the local proton concentration at the reaction sites. Using the mechanisms,

the locations of the various binding and reaction sites might be determined.

In the proposed mechanisms, it is suggested that ATP is used to control the reactions. This naturally begs the question of how the ATP is generated. This problem has already been addressed in the literature, as ATP is used for growth. However, the author would strongly caution future investigators against assuming that this must occur by proton pumping. It is possible that a chemical reaction is involved, and, therefore, attention must be given to possible chemical reactions. In sulphite-oxidizing bacteria, for example, ATP is generated via adenosine-5'-phosphosulphate. It has been suggested that in nitrobacter proton pumping occurs because cell-free systems oxidize nitrite without the presence of ADP [39]. This does not logically follow as implied. The proposed mechanism indicates that ADP is not involved once the phosphate esters are formed, as the esters act as true catalysts. A chemical intermediate would also match Hollocher's conclusions from experiments on *Nitrobacter agilis*[103]. Measurements of H^+/O ratios in Nitrosomonas[104] have observed that the H^+/O ratio falls with increasing substrate concentrations. The kinetic data in this thesis indicate that this is due to the sigmoidal nature of the enzymes.

A consequence of the proposed use of ATP in the reactions is that the redox potentials for the oxidations are lowered. This suggests that the activity of the cytochromes involved does not have to be as high as previously assumed. As a result, the electrons may be able to take different paths from those currently suggested.

The toxicity of nitrous acid is well known, not only in fish, but in all animals. Nitrates in food and water have also been suspected of posing health risks. The nitrite ester in the proposed mechanisms is very reactive. It is possible that the nitrite ester (contained in bacteria present in the gut) could provoke undesirable reactions.

APPENDICES

APPENDIX 2.a

FLUID MIXING IN SUBMERGED PACKED BED BIOFILTERS FOR INTENSIVE AQUACULTURE

A.P.G.Newton and L.R.Weatherley*

Systematic mixing experiments were conducted on a set of 150 mm diameter horizontal packed bed biofilters. Impulse tracer response analysis was used to fit a number of single and multiple parameter models. The moments of the curve were found to give poor fits and curve fitting is recommended. The relationships between flow velocity, mixing regime and deadspace were determined. Deadspace was found to be a significant parameter at low superficial velocities.

INTRODUCTION

The use of biological filtration as a water treatment technique for the removal of ammonia from fish farm waste water and from municipal waste water is well known, and in the latter case a considerable body of design data based on research and operating experience has been established. By contrast a consistent design methodology for the application of biological filtration to the emerging technology of intensive aquaculture has yet to be properly defined. Published work to date comprises largely of descriptive accounts of particular commercial systems to which biological filtration has been applied. No detailed modelling studies are evident in the literature. The objective of the currently described work was to undertake specific experiments to examine the two most important processes which are perceived as exercising the major control over the performance of submerged packed bed biofilters, namely:- Fluid Mixing, and Reaction Kinetics. The philosophy which was adopted stems directly from the design methods widely used in the sizing and specification of conventional packed bed chemical reactors.

Experimental definition of the hydraulic flow regime within the reactor allows kinetic data to be used to accurately model the concentration (and temperature) profiles and thus quantify the required reactor size for a particular specified performance. A second benefit from such an approach is that control of reactor performance may be predicted with some confidence and this may be particularly useful in the context of intensive recycle systems where small perturbations in external parameters can have drastic results.

*Dept. of Chemical & Process Engineering, Heriot-Watt University.

The work described in this paper is confined to a series of mixing experiments conducted on a set of horizontal 150mm diameter, submerged packed bed biofilters which had been used in service on a smolt hatchery recycle system.

Tracer response analysis techniques were used to quantify the hydraulic performance of the filters and alternative mathematical models used to analyse the experimental data.

THEORY

The biological oxidation of ammonia to nitrate by nitrifying bacteria is generally given by the two stage reaction scheme thus:-

$$NH_4^+ + 1.5\ O_2 \longrightarrow 2H^+ + H_2O + NO_2^- \quad (1)$$

and:-

$$NO_2^- + 0.5\ O_2 \longrightarrow NO_3^- \quad (2)$$

It is also generally accepted that two genera of bacteria are involved, Nitrosomonas and Nitrobacter respectively and the kinetics of these reactions at concentrations pertinent to intensive aquaculture have been evaluated in flocculent and film based bioreactor systems Srna and Baggaley (1),Weatherley (2),Knowles et al (3),Lawrence and McCarty (4), and in both marine and freshwater systems. Many of the kinetic models centre around a pseudo first order approach and assume a steady biomass concentration. Much remains to be properly understood and evaluated in this area and kinetic studies are the subject of a follow up paper.

Successful operation of packed bed submerged filters on the commercial scale depends not only upon favourable kinetic conditions but also upon the attainment of efficient fluid flow conditions. In the majority of intensive aquaculture situations the parameters which affect reaction kinetics will be dictated by external factors such as pH, temperature, metabolite concentration, and the filter history, and so the designer has little flexibility. By contrast, the hydraulic performance of the filter is highly dependant upon parameters over which the designer has a significant degree of control, for example in the choice of filter diameter, flow velocity, packing shape and size, and internal construction of the filter.

Levenspiel (5) defines two limiting flow patterns for continuous flow in vessels:-

Plug Flow. Which is characterised by an entirely orderly flow pattern in which no element of fluid overtakes or mixes with any other element of fluid. Thus all elements of fluid leaving the reactor have the same residence time.

Ideal Mixing. Which is, characterised by an entirely uniform composition in the vessel and all elements of fluid in the exit

stream from the reactor have the same composition as each other and as the fluid in the vessel.

Reactor design and prediction of steady state performance is straightforward if either of these flow regimes prevail within the reactor. Significant deviations can be caused by channelling, by short circuiting, and by stagnant regions, thus giving rise to a flow regime different from either of the two ideal limiting cases. Neglect of flow regime considerations in either filter design or operation can lead to gross errors with consequent financial penalties. Much information can be gathered about the mixing regime within a biological filter of a particular design and operating under a specific set of conditions by tracer response techniques. Tracer response methods are described quantitatively elsewhere (Nauman and Buffham (6)). The basic elements of the technique may be summarized as follows. Consider the input of an instantaneous pulse of tracer into the inlet stream of a biological filter, for example the tracer may be an electrolyte solution, or a dye. The tracer concentration in the outlet stream from the vessel can be readily measured as a function of time, and typical concentration versus time data are shown in figure 1. We can show how the nature of mixing within the vessel can be quantified using this data. In summary, the concentration-time data is normalised and then made dimensionless using the mean residence time. Direct comparison of the measured data with mathematical mixing models allows determination of the parameters characterizing the degree of mixing. The dimensionless concentration and dimensionless time are given by

$$C_\theta = C\,\bar{t} \qquad \theta = \frac{t}{\bar{t}} \tag{3}$$

It is also possible to calculate the moments of the curve, the first moment giving the mean residence time, the second the variance. Such methods are often given in text books eg. (5).In many cases the moments of a particular model can be obtained but its analytical solution can not be.

The two single parameter models often used are as follows;-

The Dispersion Model. This is derived by superimposing Ficks law of diffusion on to a plug flow system. This gives a partial differential equation in which the boundary conditions must be defined. The dispersion model thus suffers from problems associated with the boundary conditions. The only analytical solution is for open vessels as defined and given by (5), although the moments have been calculated for several others. The dispersion number, (D/uL), defines the degree of mixing between the two ideal cases. The solution for open vessels is as follows;-

$$C_\theta = \frac{1}{2\sqrt{\pi\theta(D/uL)}} \exp\left[\frac{-(1-\theta)^2}{4\theta(D/uL)}\right] \quad (4)$$

The Tanks in Series Model. This model represents a vessel as a number of equally sized perfectly mixed tanks in series, with an infinite number corresponding to plug flow. Since the equations are of the initial value type the problems of boundary conditions does not occur. The number of tanks defines the degree of mixing between the two ideal cases.

$$C_\theta = \frac{n(n\theta)^{n-1}}{(n-1)!} \exp(-n\theta) \quad (5)$$

When the flow tends towards plug flow the solutions for the different boundary conditions and that for the tanks in series model converge to give the approximation.

$$D/uL = \frac{1}{2n} \quad (6)$$

Multi Parameter Models. Often in packed beds it is found that the single parameter models do not completely represent the flow. Single parameter models do not account for channelling, short circuit flow or the presence of stagnant regions. In the case of packed beds slow moving regions are often evident by the existence of a long tail on the tracer curve. Many models have been proposed to represent this type of flow and they are often largely based on single parameter models. They are often related as shown by Buffham and Gibilaro (7). Two such models are the "tanks in series with deadspace" and the "tanks in series with crossflow" models.

Tanks in Series with Deadspace. This model is identical to the tanks in series model differing only in the fluid volume used, part of the fluid volume is considered completly stagnant,and no fluid enters or leaves this stagnant region. This is illustrated in figure 2.

Tanks in Series with Crossflow Model. This model was first proposed by Deans (8) and latter the analytical solution was given by Buffham and Gibilaro (9). This cell model has as its basis a stirred tank from which fluid flows into a 'stagnant' region from which it cannot leave directly (termed crossflow). A number of these cells are connected in series as illustrated in figure 3.

EXPERIMENTAL

The tracer experiments were conducted on a pair of fixed bed filters which had been in service in a salmon hatchery system. The filters were arranged in series and each comprised of a 150 mm diameter shell with a total length of 2080 mm. The main packing consisted of limestone chips, with a characteristic length of 12 mm. In order to improve flow distribution, at the entrance and exit, Raschig rings were incorporated into each of the end sections(80x1¼ inch rings per section, 10 cm deep). Water circulation was achieved by a pair of centrifugal Chem pumps and the flowrate measured by variable area flowmeters incorporated into the exit line from the filters. The feed line to the filter system was equipped with a tracer injection point for introduction of controlled amounts of sodium chloride solution. In the final exit line from the filters a small offtake point into a conductivity flow cell was installed to allow in line measurement of the conductivity of the exit water. The cell was connected to a Pye Unicam conductivity meter and chart recorder.

The volumetric hold up within the filter was measured by filling the dry filter with measured amounts of water. Care was taken during the experiments to exclude air locks within the system and vent points were located along the upper surface of the filter to allow escape of air during start up.

A total of fifteen runs were undertaken covering a range of flowrates 2 to 20 litres per minute with reproducibility checks. A series of preliminary tracer injections was conducted to establish the optimum injection dose to yield a satisfactory response in the outlet stream. A linear relationship between output voltage from the conductance meter and tracer concentration was confirmed and the response data were treated to obtain a normalised curve or C curve.

RESULTS

The analysis of tracer data requires an accurate definition of the mean residence time. In general terms mean residence time is defined as the effective volume of the fluid hold up in a vessel divided by the volumetric flowrate. This definition is only accurate if either there is zero dead space in the vessel, or, if the volume used truly corresponds to the 'moving hold up' of the vessel. Independent measurement of the latter is virtually impossible and therefore mean residence time is generally only determined from analysis of the tracer data.

A problem often encountered, as in these experiments, is that of accuracy in determining the fluid hold up volume or the volumetric flowrate. The volumetric flowrate was measured using a rotameter with an accuracy of ±3% F.S.D. Whilst this is not excessive at higher flows, at lower flows this represents ±50%. In measuring the fluid volume(41 l) it is difficult to completely fill or drain a packed bed and thus errors are enlarged. If the filter was a trickling filter the problem would be more difficult. The mean of the tracer curve, along with other properties, can be obtained using the moments of the tracer curve. Figure 4

shows a dimensionless C curve for Run 15, where the mean residence time was calculated from the first moment. The fit is for the "tanks in series with crossflow" model and was obtained by curve fitting the data.

TABLE 1 - Tanks in series model

Run No	flowrate q (l/min)	Mean $\bar{t}$ (min)	Variance σ^2 $(min)^2$	Tanks n
1	12.8	3.75	0.42	33
2	19.4	2.44	0.165	36
3	18.2	2.57	0.206	32
4	16.6	2.82	0.298	27
5	14.7	3.11	0.295	33
6	13.2	3.63	0.478	28
7	11.7	3.96	0.640	25
8	10.2	4.47	0.877	23
9	8.9	5.03	1.037	24
10	7.5	6.06	1.638	22
11	6.2	7.38	2.357	23
12	5.0	9.42	3.379	26
13	3.8	13.43	9.999	18
14	2.6	20.38	34.907	12
15	13.2	3.59	0.438	29

TABLE 2 - Tanks in series with crossflow model

Run No	Flowrate q ($l\ min^{-1}$)	Tanks n	% Dead Vol 100α	Crossflow p/q
1	12.8	39	3.4	0.1
2	19.4	41	3.4	0.12
3	18.2	40	4.6	0.15
4	16.6	37	5	0.16
5	14.7	40	4	0.13
6	13.2	37	4.6	0.14
7	11.7	37	4.9	0.15
8	10.2	35	5.8	0.17
9	8.9	35	5.2	0.15
10	7.5	34	5.1	0.15
11	6.2	34	4.6	0.12
12	5.0	32	6.3	0.16
13	3.8	28	7.8	0.18
14	2.6	21	16.7	0.19
15	13.2	38	3.6	0.12

Run 15 is a repeat of Run 6. Direct comparison of the two chart recorder curves revealed an excellent match, however the mean residence times differ by a few seconds. This can be explained by a small difference in flowrates which the rotameter would not show. The variances of the two curves are more markedly different and this confirms that the second moments have been markedly increased by the long tails.

The statistical data from the moments of the curves are given in table 1. The number of tanks in series estimated from the tanks in series model using the variance is also shown. The results from curve fitting the tanks in series model with crossflow are given in table 2.

DISCUSSION

Examination of the tracer curves showed that they all had long tails, this indicates stagnant regions and channelling occuring in the filters. This affects the moment values since the fluid elements with low concentrations but long residence times disproportionately increase the magnitude of the moments. The error involved increases as moments of higher order are taken, often the second moment is inaccurate and accurate third moments are rarely reported. To compensate the curve should be weighted (6). From the tracer curves it was found that this was insufficient, other alternatives involving truncation of the curve are possible but tend to be subjective. The tracer data indicates that all moments higher than the first contain unacceptable error. This is most marked when the variance is used to model the curves. This resulted in curves which are too broad and flat. The only truly acceptable way to fit models with long tails is to directly curve fit the data. This requires computation of the curves for each model. The method of least squares is recommended however care must be exercised in the choice of optimizing routine used(6).

Curve fitting the data using the tanks in series model with deadspace or with crossflow gave the same number of tanks. The number of tanks coincided with that obtained from the peak value. Thus the peak is deemed to give better fits than the variance. The percentage dead volume was obtained through the shift of the dimensionless C curve mean and its accuracy is ±1 estimating from Run 6 and Run 15. It can be seen that the dead volume increases as the flowrate decreases and this is illustrated in figure 5. At flowrates below 5 l/min the amount of dead volume increases significantly. At these lower flowrates it was found that all the models gave poor fits, the principal reason being the size of the tail. The number of tanks in series increases as the flowrate increases, this can be seen in figure 6. Thus the flow tends to become more plug like in behaviour, which is to be expected, as the velocity profile flattens with increasing Reynolds numbers.

The crossflow ratio was found to remain fairly constant, this agrees with other similar work by Buffham et al (10). The fitted curve was weighted to favour dimmensionless concentrations above 0.1. The crossflow ratio was found to be to a small extent dependent on the weighting of the curve.

In fitting the "tanks in series with crossflow" model it was found that the solution required significantly more processing time, especially for large numbers of tanks, than without crossflow. It was also found that the solution was only slightly different from the much simpler tanks in series with deadspace model. As the number of tanks increases the difference between the two decreases and the tanks in series with crossflow model fails to give substantial tails. The suggested methods of fitting the curve as given by Levich et al (11) were found to be unworkable, the tail, in practice, was far more pronounced than indicated by the model. As mentioned before the multi-parameter dispersion models are very similar and thus it is concluded that these models also will not accurately represent the curve's tail.

The most satisfactory solution was to obtain the active residence time from the peak height and time, assuming the flow to be represented by the tanks in series with deadspace model, as given below.

$$C_p t_p = \frac{(n-1)^n}{(n-1)!} \exp\{-n(n-1)\} \qquad t_a = t_p \frac{n}{(n-1)} \qquad (7)$$

The number of tanks and the active residence time can then be used to estimate the filters performance. For first order reaction kinetics and a large number of tanks the performance can be compared to the ideal case of plug flow.

$$\frac{V_n}{V_{plug}} = 1 + \frac{kt_a}{2n} \qquad (8)$$

If the second term is small the filter kinetics can confidently be modelled by a plug flow reactor with a residence time equal to the active residence time. The magnitude of the rate constant from current data suggests that the active residence time often determines the size of the second term. The contribution from the dead volume to the conversion is normally small and can be ignored.

Haug and McCarty (12) using an alkali tracer performed some step input tracer experiments, the results being presented in the form of I curves, which are defined in standard text books (5) and are related to C and F curves (I = 1-F). The curves were interpreted using a single parameter model but took no account of stagnant regions or channelling. The use of I curves tends to reduce the visual effect of stagnant regions on the curves, in comparison to C curves, however from their results it is evident that such regions existed in their filters. The parameters of the model were obtained from the second moments and, because of the

tail, could be erroneous.

The tail is caused by regions of slow moving fluid which are normally at the contact points of the packing, being associated with the packing itself or with adhering biomass (from which slow diffusion may occur). The effect of the tail was found to be most serious at the very low flowrates. This can be explained in that the fluid velocity was too low to create a uniform profile and additional dead volumes formed in the "corners" of the filter. Thus the main stream of the fluid "channels" through the centre of the filter.

Filter design should minimise dead space wherever possible. These experiments, valid for 12 mm limestone packing, indicate that a superficial velocity of greater than 280 mm/min should be used to avoid excessive dead volumes.

In the process industry it is usual to have packed beds in which the diameter is over twenty times that of the packing diameter and the length at least one hundered times greater. Thus, vessel diameter is chosen to ensure that the voidage at the walls is not greatly increased, causing channelling. Whilst the length ensures complete contact with the packing and plug flow behaviour, it is suggested that these limits should be adhered to for both trickling filters and submerged filters. It is concluded that larger packing sizes require larger vessel diameters to ensure good flow characteristics. In large packed beds re-distributors should also be used.

The minimum packing diameter required to avoid blockage due to biomass growth in the literature (Muir and Roberts (13)) is 12 mm and thus lower limits on the filter dimensions for good fluid flow can be determined. If the total length exceeds practical limits then the filter can be split giving two smaller filters in series. Some authors claim that two filters in series are better than a single one of larger diameter. Fluid mixing can explain some of this, since, as the flowrate was not altered, the effect was to increase the superficial velocity, thus reducing dead volume.

CONCLUSION

In using a model to describe the flow in a filter, curve fitting should be used, moments other than the first moment are unreliable. The filters investigated were found to contain stagnant regions which decreased with increasing fluid velocity. Using the peak of the C curve the active residence time can be estimated and this can be used to evaluate filter performance instead of the mean residence time. A filter can be approximated to a plug flow reactor using the active residence time depending on the magnitude of the rate constants.

SYMBOLS USED

C = C curve tracer response to an ideal pulse input (min^{-1})

C_p = Value of the C curve at its peak (min^{-1})

C_θ = Dimmensionless concentration

c_a = Concentration of reactant A

D = Dispersion Coefficient (mm min^{-1} ^{2})

k = First order rate constant, unit must match c_a

L = Length of vessel ,filter, (mm)

n = Number of cells or tanks in series

p = Flowrate into stagnant part of cells (l min^{-1})

q = Flowrate through vessel (l min^{-1})

t = Time (min)

t_a = Active residence time $(1-\alpha)nv/q$ (min)

t_p = Time at the peak of the impulse response curve (min)

t = Mean residence time as obtained from the first moment. (min)

u = Superficial velocity (mm min^{-1})

v = Cell volume (l)

V_n = Volume of vessel obtained for n number of tanks (l)

V_{plug} = Volume of vessel obtained for plug flow (l)

α = Fraction of cell volume regarded as stagnant

θ = Dimensionless time

REFERENCES

1. Srna,R.F and Baggaley,A.,1971,J.Water.Pollut.Control .Fed. 47(3),472.

2. Weatherley,L.R.,1984,Aquacultural Engineering 3 No 1,15.

3. Knowles,G.,Downing,A.L. and Barrett,M.J.,1965, J.Gen.Microbiol,38,263.

4. Lawrence,A.W. and McCarty,P.L.,1970, Am.Soc.civil. Engineers.Proc Jour Sanitary Eng Div,96(SA 3),757.

5. Levenspiel,O.,1972,"Chemical Reaction Engineering",John Wiley & Sons,U.S.A.

6. Nauman,E.B. and Buffham,B.A.,1983,"Mixing in Continuous flow systems",John Wiley & Sons,U.S.A.

7. Buffham,B.A. and Gibilaro,L.G.,1970,Chem.Eng.J 1,31.

8. Deans,H.A.,1963,Soc. Petroleum. Engineers. Jour.3,49.

9. Buffham,B.A. and Gibilaro,L.G.,1968,Chem.Eng.Sci. 23,1399.

10. Buffham,B.A.,Gibilaro,L.G. and Rathor.M.N.,1970,AIChE J,16, ,218.

11. Levich,V.G.,Martin,V.S. and Chismadzhev,Yu.A.,1967, Chem.Eng.Sci. 22,1357.

12. Haug,R.T. and McCarty,P.L.,1971,"Nitrification with the Submerged Filter".Technical Report No.149,Dept of Civil Engineering,Stanford University.

13. Muir,J.F. and Roberts,R.J.,1982,"Recent advances in aquaculture",Croon Helm.

Run 3

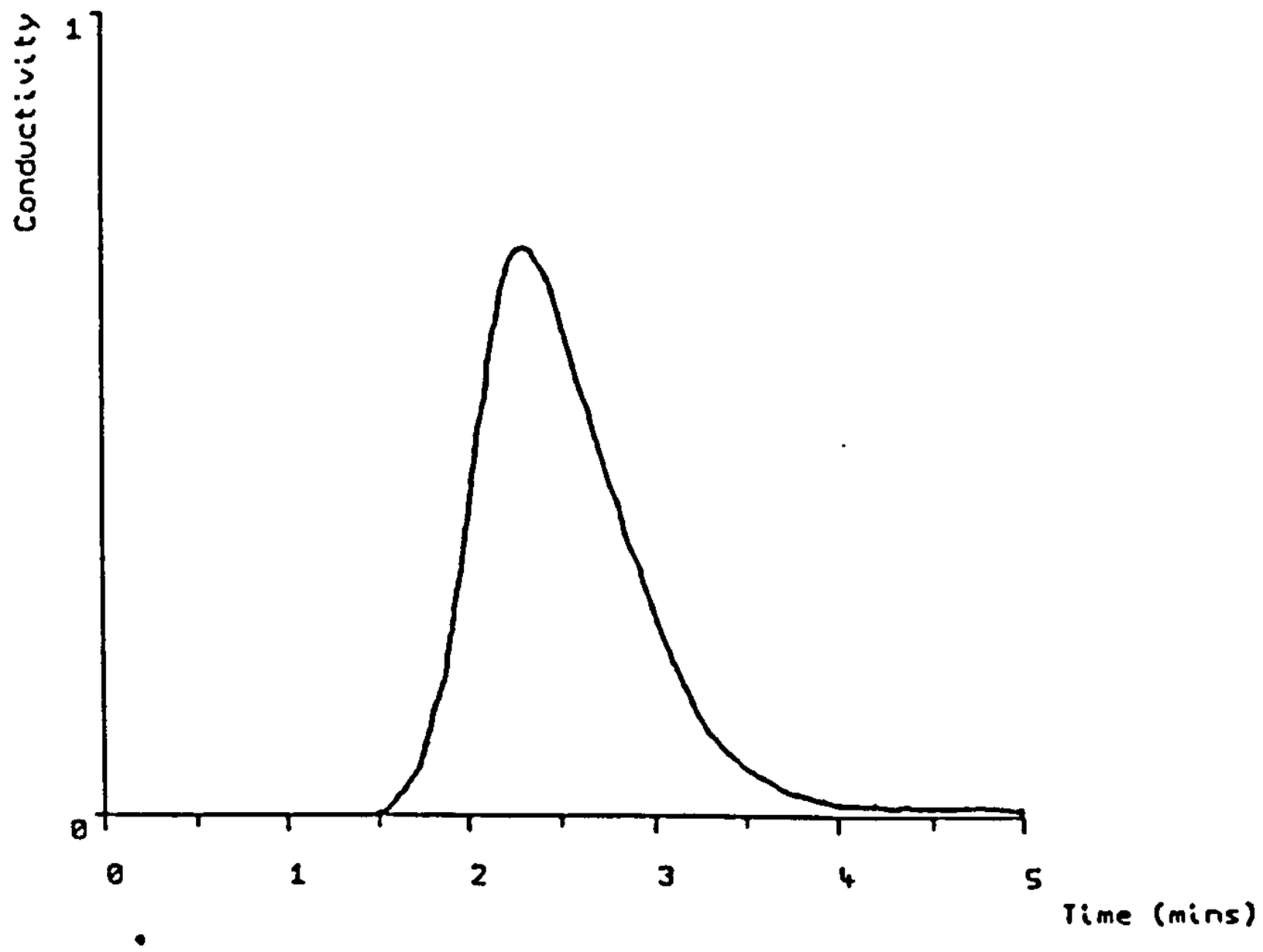

Figure 1 Tracer concentration versus time curve for Run 3

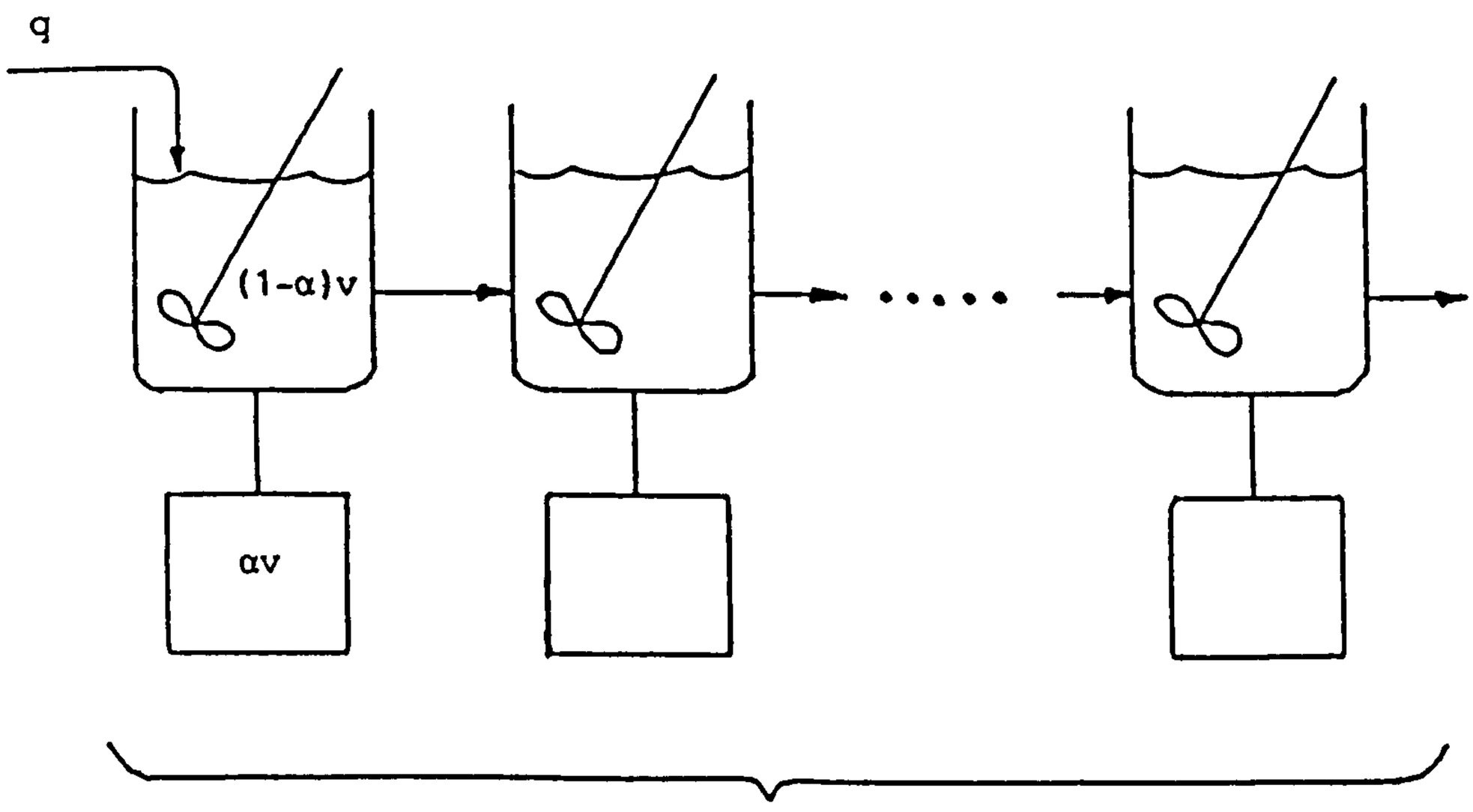

Figure 2 Tanks in series with deadspace model

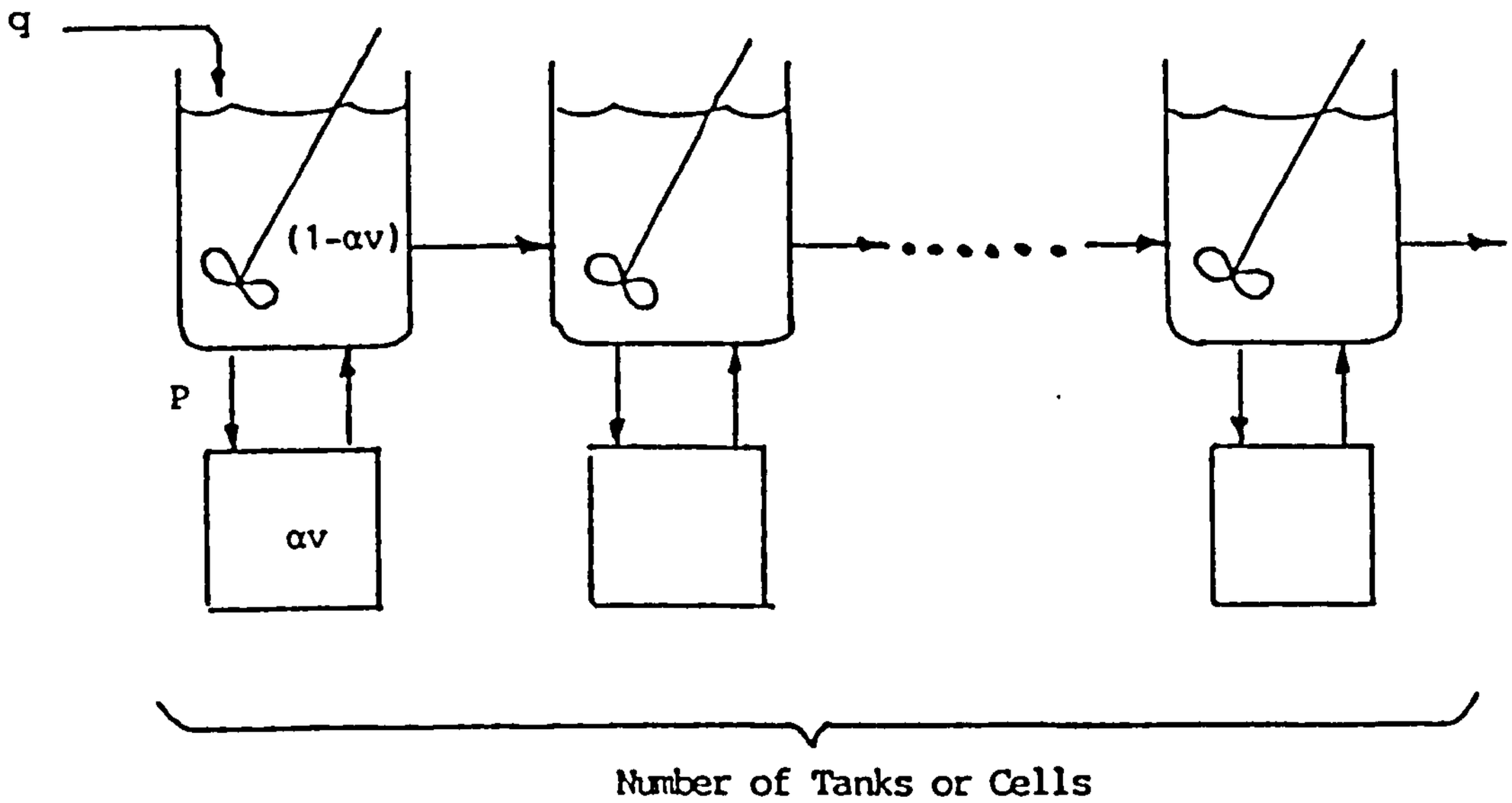

Figure 3 Tanks in series with crossflow model

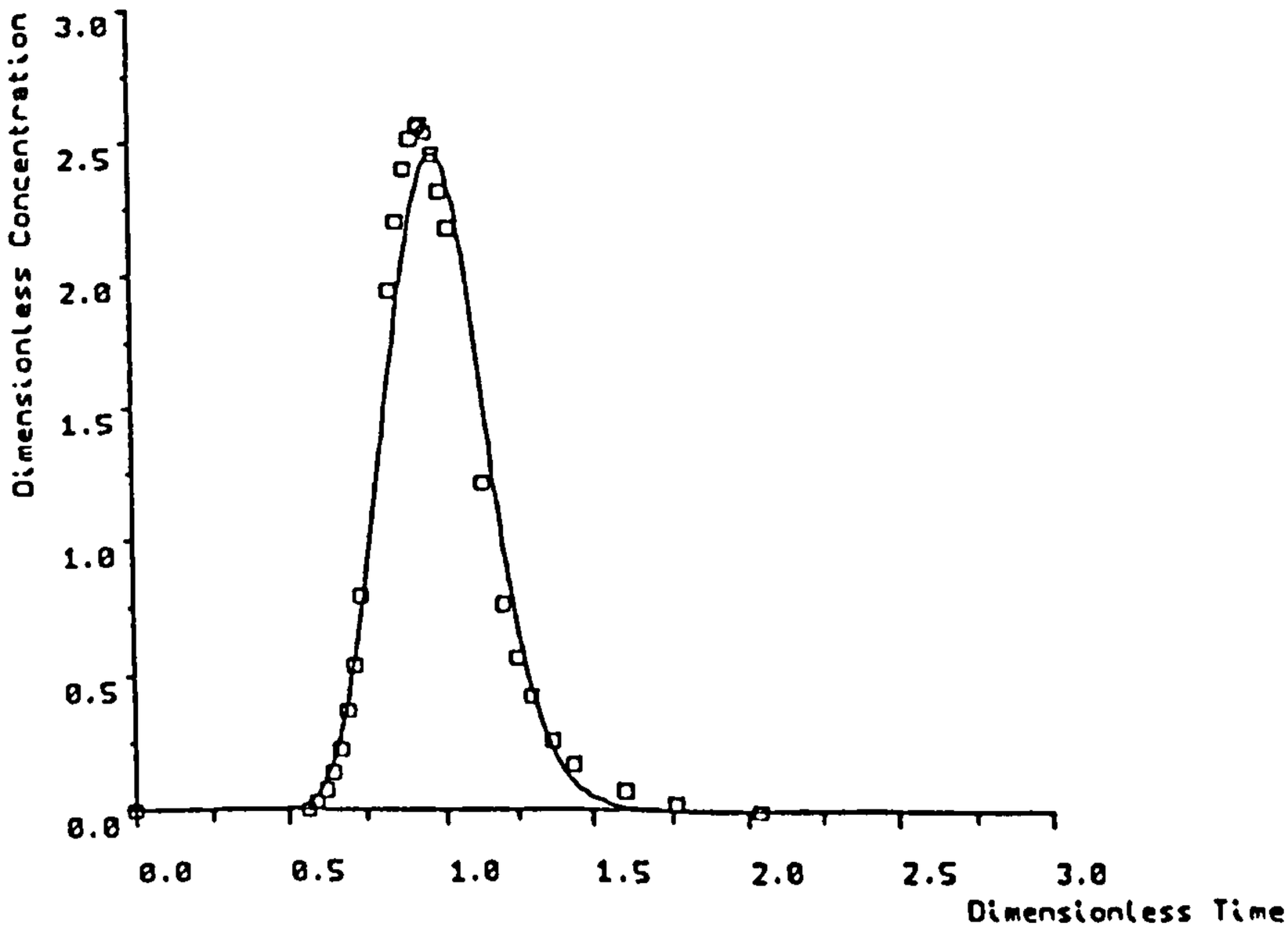

Figure 4 Dimensionless concentration versus dimensionless time curve for Run 15

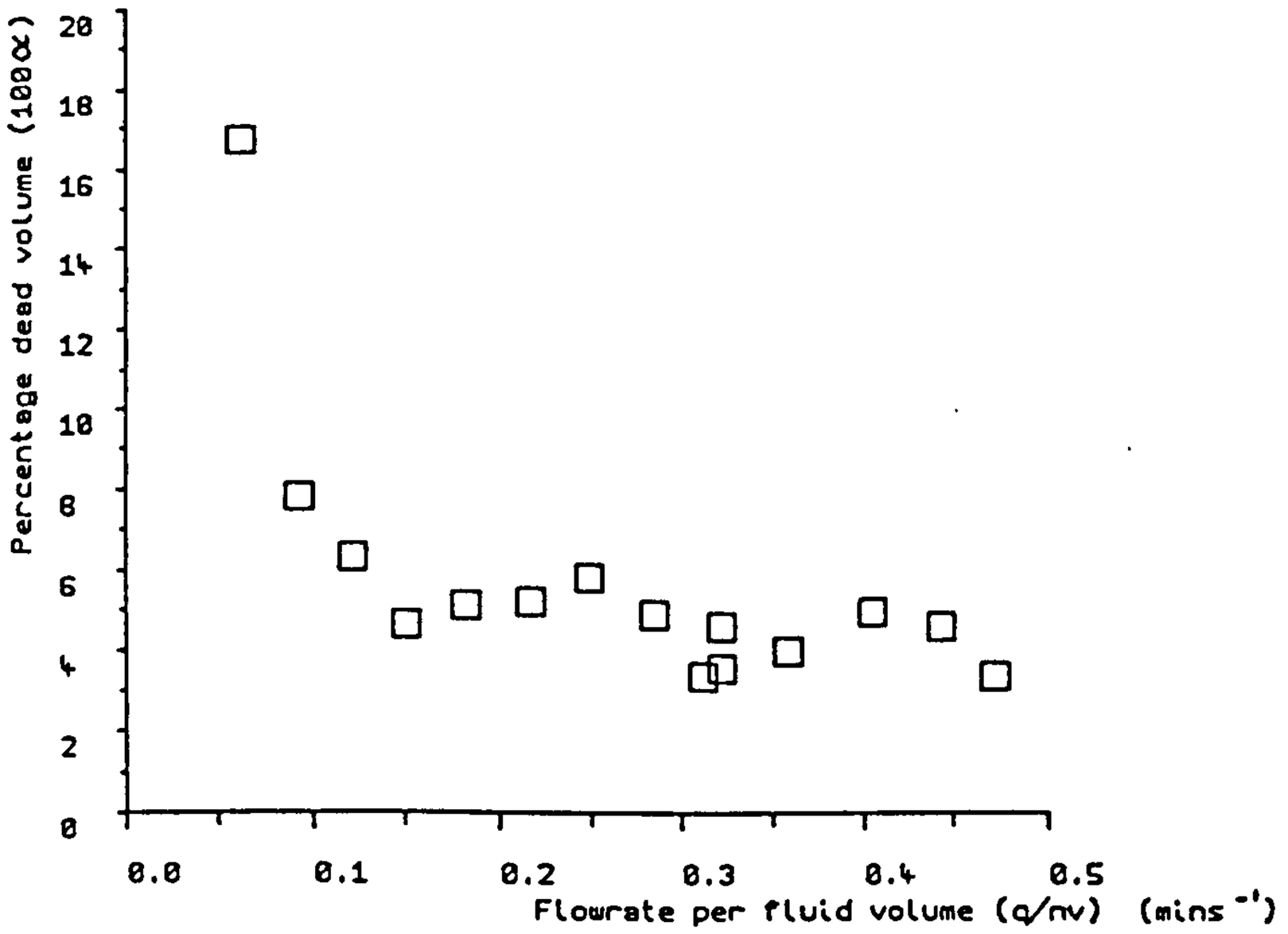

Percentage dead volume versus flowrate per fluid volume

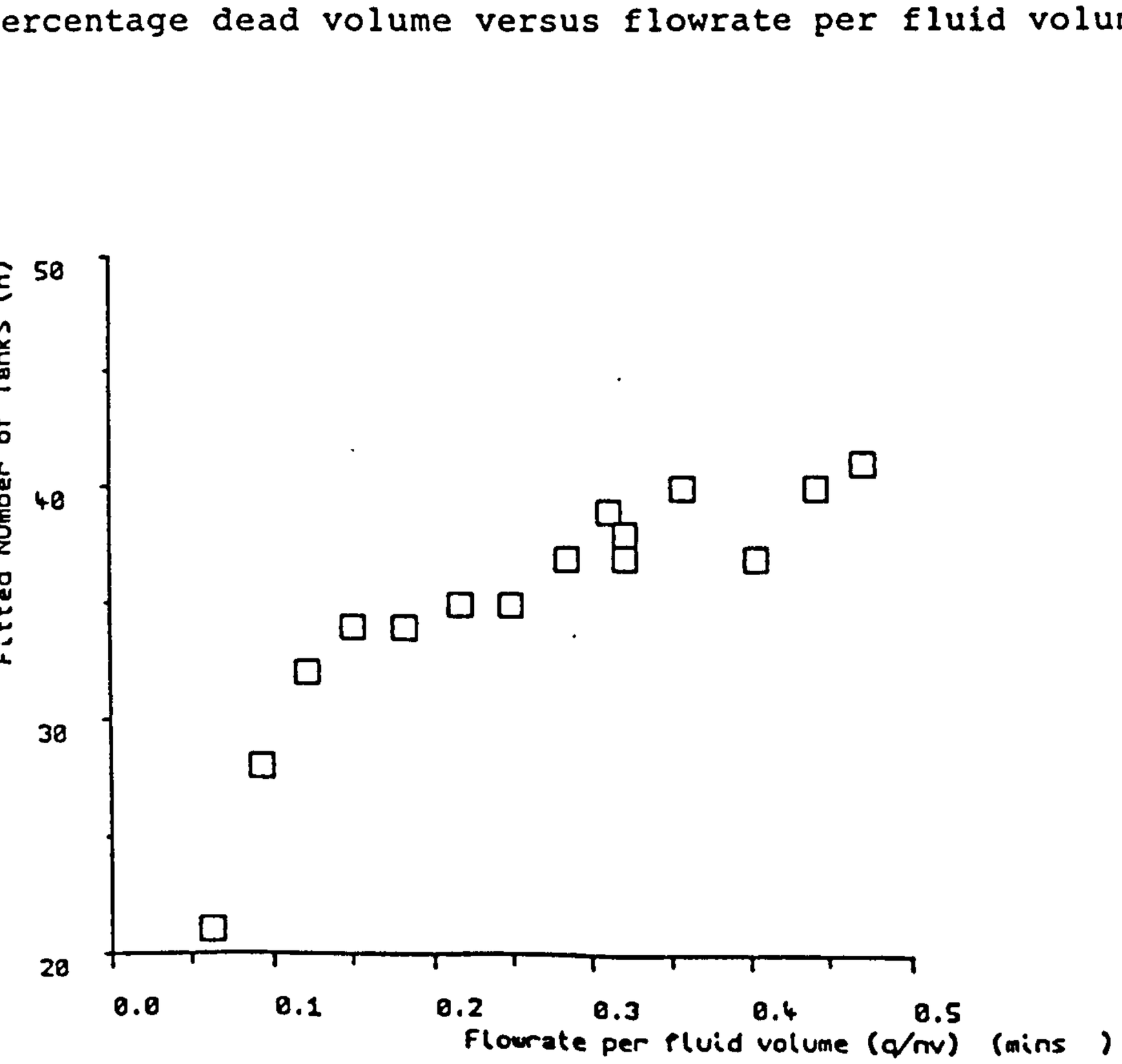

Number of tanks in series versus flowrate per fluid

APPENDIX 2.b

```
{ $D DP := true }
PROGRAM MixingModel(InFile,input,output);

{ Fits a multiple cells in series mixing model to impulse tracer data obtained by
experiment. The model consists of a number of cells in series. Each cell
consists of two ideal mixing tanks, fluid crossflows between the two. In
addition part of the crossflow is recycled. The model is an extention to the
Deans and Levich model, which is a special case in which the recycle ratio
equals zero. The program illustrates the problems with fitting the Deans-Levich
model. It is not suitable for packed bed modelling. A more suitable model is
given in the authors PhD.
            A.P.G. Newton  August 1988 }

type
     DataFile = text;                              { data to be read from disk }
     FactorialType = array [0..100] of real;  { factorial }
     DataType = array [1..50] of real;
var
   InFile : DataFile;
   NoPoints,NoCells : integer;
   Tpeak,MeanRT : real;
   factorial : FactorialType;
   Time,Conductivity,Ecurve : DataType;

 {************************************************************************** }

procedure CalcFactorial;

  var
     i,Precision : integer;

  begin
   Precision:=33;      { 33 (16 Cells) max single precision can handle }
   { $B DP }
   Precision:=100;     { Allows a maximum of 50 Cells in Series }
   { $E DP }
     factorial[0]:=1;
     for i:=1 to Precision do
     factorial[i]:=factorial[i-1]*i;
  end; { of procedure factorial }

{************************************************************************** }

procedure GetDataFromDisk ;

var
   i : integer;

begin
   reset (InFile);
   Readln (InFile,NoPoints);
   for i:=1 to NoPoints do
      Readln (InFile,Time [i],Conductivity [i]);
   for i:=2 to NoPoints do
    if ( Conductivity[i] > Conductivity[i-1] ) then Tpeak:= Time[i];
end; { of procedure GetDataFromDisk }
```

```
 {*************************************************************************** }

function pow (number:real;exponent:integer):real;

var
   i : integer;
   result : real;

begin
  result:= exp(exponent*ln(abs(number)));
      if ( number < 0) and (odd(exponent)) then result:= -result;
    pow := result;
end; { of function pow }

 {*************************************************************************** }

function Trapezoidal( x,y : Datatype): real;

var
   j: integer;
   totalarea : real;

begin
     totalarea:=0;
     for j:=2 to NoPoints do
     totalarea:=totalarea+(x[j]-x[j-1])*(y[j]+y[j-1])/2.0;
     Trapezoidal:=totalarea;
end; { of function Trapezoidal rule }

 {*************************************************************************** }

procedure Normalise;

var
   i: integer;
   normalized : Real;

begin
   Normalized:=Trapezoidal(time,conductivity);
   for i:=1 to NoPoints do
   Ecurve[i]:=conductivity[i]/normalized;
end;  { of procedure Normalise }

 {*************************************************************************** }

procedure MeanResidenceTime;

   var
      i: integer;
      ct : DataType;

   begin
      for i:=1 to NoPoints do
         ct[i]:=conductivity[i]*time[i];
      MeanRT:=Trapezoidal(time,ct)/Trapezoidal(time,conductivity);
   end;

{ *************************************************************************** }
```

```
Procedure ComplexMethod ;
{ finds the minimum of a function using the complex method of Box

 Program adapted from "Basic Optimisation Methods" by B.D.Bunday
 notation is as in the Basic program given above.
 Sorry Pascal purists! I have kept the limited basic variable names for
reasons of compatability with the above.I have tried to banish the dreaded
GOTO statement and I hope this is readable }

   const
      n = 4;    { number of variables }
      m = 2;     { number of constraints }
      k = 8;     { 2n as suggested by Box }
      alpha = 1.3; { reflection factor }
      sdacc = 0.01; { standard deviation accuracy required on test }
      dmacc = 0.01;     { max distance between points allowed in test }
   type
      indices = 1..k;     { number of points }
      narraytype = array [1..n] of real;
      karrayType = array [1..k] of real;
      ecarraytype = array [1..k] of boolean;
      icarray = array [1..m] of boolean;
      marraytype = array [1..m] of real;
      complexarray = array [1..k,1..n] of real;
   var
      i,j,l : indices;
      seed,                    { seed for random number generator }
      fe : integer;            { number of function evaluations   }
      im,                      { test only implicit constraints in
                                     CHECKCONSTRAINTS                    }
      ecviolated,              { explicit constraints violated ? }
      icviolated : boolean;    { implicit constraints violated ? }
      z,                       { function evaluated }
      rnd,                     { random number between 0 and 1 }
      s1,s2,                   { part of sd calculation }
      sd,                      { standard deviation of points }
      dm,                      { maximum distance }
      d,                       { distance between points in complex }
      fm,                      { lowest function value }
      fval,                    { used to order function values }
      fr : real;               { reflected function value }
      x,                       { variable values }
      y,                       { used to order point values }
      xr,                      { reflected points }
      xc,                      { centroid of x points }
      xo,                      { centroid of best points }
      xh,                      { worst point }
      lowerlimit,              { explicit lower limits }
      upperlimit : narraytype; { explicit upper limits }
      ic : icarray;            { implicit constraints }
      g : marraytype;          { implicit constraints evaluated }
      f :  karrayType;         {  objective function values }
      ec : ecarraytype;        { explicit constraints }
      c : complexarray;        { complex array }

{ ********************************************************************** }

procedure initialise;
```

```
   begin
        fe:= 0;
   end; { of procedure Initialise }

{ ********************************************************************** }

procedure MixingModel(var fit : real );

var
   i,j,k : integer;
   b1,b2,b3,b4,r1,r2,k1,k2,sumB,sumC,BC : real;
   sumBnjt,sumCnjt : array[1..50] of real; { 1..NoCells max 50 }
   Model : DataType;

begin
  b1:=x[1]/(1.0-x[2]);
  b2:=x[3]*b1;
  b3:=b2*(1.0-x[2])/x[2];
  b4:=b3*(1.0-x[4]);
   r1:=((b1+b2+b4)-sqrt((b1+b2+b4)*(b1+b2+b4)-4.0*(b4*(b1+b2)-b2*b3)))/2.0;
   r2:=((b1+b2+b4)+sqrt((b1+b2+b4)*(b1+b2+b4)-4.0*(b4*(b1+b2)-b2*b3)))/2.0;
  k1:=b1*(b4-r1)/(r2-r1);
  k2:=b1*(b4-r2)/(r1-r2);
    for i:=2 to NoPoints do
        begin
        sumBnjt[i]:=0.0;
        sumCnjt[i]:=0.0;
        end;
    for j:=0 to NoCells-1 do
        begin
        sumB:=0;sumC:=0;
      for k:=0 to (NoCells-1-j) do
        begin
        BC:=factorial[2*NoCells-2-j-k]/
         (factorial[k]*factorial[NoCells-k]*factorial[NoCells-1-j-k]);
        if odd(NoCells-1-j-k) then BC:=-BC;
        sumB:=sumB+BC/(pow(b4-r1,k)*pow(r2-r1,NoCells-1-j-k));
        sumC:=sumC+BC/(pow(b4-r2,k)*pow(r1-r2,NoCells-1-j-k));
        end;
      for i:=2 to NoPoints do
        begin
       sumBnjt[i]:=sumBnjt[i]+NoCells/factorial[j]*sumB*exp(j*ln(time[i]));
        sumCnjt[i]:=sumCnjt[i]+NoCells/factorial[j]*sumC*exp(j*ln(time[i]));
        end;
    end;
fit:=0.0;
for i:=2 to NoPoints do
        begin
        Model[i]:=exp(NoCells*ln(k1))*sumBnjt[i]*exp(-r1*time[i])+
         exp(NoCells*ln(k2))*sumCnjt[i]*exp(-r2*time[i]);
        fit:=fit+sqr(Ecurve[i]*MeanRT-Model[i]);
        end;
     writeln(output,'q/v ',x[1]:10,' deadfrac ',x[2]:10,' p/q ',x[3]:10,' R ',x[4]:10);
     writeln(output,'The least squares fit is ',fit:10,' Function evaluations',fe);
     fe:=fe+1;

end; { end of procedure mymodel }

{ ********************************************************************** }
```

```
procedure CheckConstraints ;

   var
      ii : indices;
    b1,b2,b3,b4 : real;

   begin
      for ii:= 1 to k do ec[ii]:=false;
      ecviolated:= false;
      for ii:= 1 to m do ic[ii]:=false;
      icviolated:=false;
      if im = false then
            begin
               for ii:= 1 to n do
                  begin
                     if x[ii]<lowerlimit[ii] then
                        begin
                        ec[ii]:=true;
                     ecviolated:= true;
                        end;
                     if x[ii]>upperlimit[ii] then
                        begin
                     ec[n+ii]:=true;
                       ecviolated:= true;
                        end;
                  end;
            end;
     g[1]:=(sqr(x[4]-1.0)+x[2]*x[4]*(2.0-x[4]))/(sqr(x[4]-1.0)+x[3]*x-
[4]*(x[4]*x[3]+2.0*x[4]-2.0));
      b1:=x[1]/(1.0-x[2]);
    b2:=x[3]*b1;
      b3:=b2*(1.0-x[2])/x[2];
      b4:=b3*(1.0-x[4]);
     g[2]:= sqr(b1+b2+b4)-4.0*(b4*(b1+b2)-b2*b3);
      if g[1]< 1.0 then begin ic[1]:=true;icviolated:=true; end;
      if g[2]< 0 then begin ic[2]:=true;icviolated:=true; end;
   end; { of procedure CheckConstraints }

{ ********************************************************************** }

procedure  Random ;
 { produces a random number between 0 & 1 }

begin
   rnd := seed/65536;
   seed := (25173 * seed + 13849) mod 65536
end; { of function rnd }

{ ********************************************************************** }

procedure Constraints;

   begin
    writeln;
      write (output,'The mean residence time from the tracer curve is');
      writeln (output,MeanRT:10);
      write (output,'The peak time from the tracer curve is');
      writeln (output,Tpeak:10);
      writeln;
      writeln (output,'Enter the number of cells');
```

```
  read (input,NoCells);

  { Explicit Constraints }
{ The limits for q/v are taken so that any value is possible }
  lowerlimit[1]:= NoCells/MeanRT; upperlimit[1]:=NoCells/Tpeak;
  { Deadfraction }
  lowerlimit[2]:= 0; upperlimit[2]:= (MeanRT-Tpeak)/MeanRT;
  { Crossflow ratio }
  lowerlimit[3]:= 0; upperlimit[3]:= 1.0;
  { RecycleRatio }
  lowerlimit[4]:= 0; upperlimit[4]:= 1.0;

{ Initial Values based on the Deans-Levich Model }
{ RecycleRatio and MeanRT as for Deans-Levich Model }
    { q/v }
    x[1]:= NoCells/MeanRT;
    { Recycle Ratio =0 }
    x[4]:= 0;

      writeln;
      writeln (output,'Enter initial values');
      writeln (output,'Deadfraction. note:- to be less than ',(MeanRT-Tpeak)/MeanRT:10);
      read (input,x[2]);
      writeln (output,'Crossflow Ratio p/q. Use same as deadfraction if in doubt');
      read (input,x[3]);

  end; { of procedure constraints }

{ ********************************************************************** }

procedure InitiateComplex ;

var i,j,l : indices;

begin
Constraints;
   for j:= 1 to n do
      begin
      c[1,j]:=x[j];
      xc[j]:=x[j];
      end;

   { set random generator }
   writeln (output,'Enter seed for random number generator (integer)');
   readln (input,seed);
   i:=1;
   MixingModel(z) ;
f[1]:=z;
repeat
   i:=i+1;
   for    j:=1 to n do
      begin
      Random ;
      c[i,j]:=lowerlimit[j]+rnd*(upperlimit[j]-lowerlimit[j]);
      x[j]:=c[i,j];
      end;
   im:=true;
   CheckConstraints ;
   while icviolated = true do
       begin
```

```
            for j:=1 to n do
               begin
                 c[i,j]:=(c[i,j]+xc[j])/2.0;
                 x[j]:=c[i,j];
               end;
            im:=true;
            CheckConstraints
         end;
      { UPDATE CENTROID }
      for j:=1 to n do
         xc[j]:=((i-1)*xc[j]+c[i,j])/i;
      MixingModel(z) ;
      f[i]:=z;
      { writeln (output,z); }
   until i=k;
   { PUT FUNCTION VALUES AND POINTS IN ORDER }
   for j:=1 to k-1 do
      begin
         for i:=j+1 to k do
            begin
               if f[j]>f[i] then
                  begin
                     fval:=f[j];
                     f[j]:=f[i];
                     f[i]:=fval;
                     for l:=1 to n do
                        begin
                        y[l]:=c[j,l];
                        c[j,l]:=c[i,l];
                        c[i,l]:=y[l];
                        end;
                  end;
            end;
         { NOTE LOWEST VALUE }
      fm:=f[1];
      writeln(output,'First point');
      writeln(output,'Min.Value=',f[1]);
      writeln(output,'Min point');
      for l:=1 to n do
         writeln(output,'x',l,c[1,l]);
      writeln;

end; { procedure iniatecomplex }

{ ********************************************************************** }

procedure CheckFeasibility ;

var
   j,l : indices;
   k1 : integer;

   begin
   k1:=1;
   while k1<>10 do
   case k1 of

   1 : begin im:=false;CheckConstraints ;k1:=2;   end;
```

```
2 : begin if (ecviolated = false) AND (icviolated = false) then k1:=5
    { POINT IS FEASIBLE CALCULATE FUNCTION }
                              else k1:=3   end;

3 : begin if ecviolated = false then k1:=4
                else
                    begin { EXPLICIT CONSRAINTS VIOLATED }
                          { RESET JUST INSIDE BOUNDARY }
                        for j:=1 to n do
                           begin
                               if ec[j]=true then
                                   begin
                                       xr[j]:=lowerlimit[j]+1.0E-6;
                                       x[j]:=xr[j];
                                   end;
                               if ec[j+n]= true then
                                   begin
                                       xr[j]:=upperlimit[j]-1.0E-6;
                                       x[j]:=xr[j];
                                   end;
                           end;
                        k1:=4;
                    end;
        end;

4 : begin
        if icviolated = false then k1:=5 { FEASIBLE POINT CALCULATE FUNCTION }
            else { IMPLICIT CONSTRAINTS VIOLATED }
                begin
                    { MOVE HALFWAY TO CENTROID XO }
                    for l:=1 to n do
                        begin
                            xr[l]:=(xr[l]+xo[l])/2.0;
                            x[l]:=xr[l];
                        end;
                    k1:=1;
                end;
    end;

5 : begin MixingModel(z);fr:=z ;k1:=6 end;

6 : begin
        if fr < f[k] then k1:=10
             else
                 begin
                     { NEW VALUE IS THE WORST MOVE
                       HALFWAY TO XO AND TRY AGAIN }
                     for l:=1 to n do
                         begin
                             xr[l]:=(xr[l]+xo[l])/2.0;
                             x[l]:=xr[l];
                         end;
                     k1:=1;
                 end;
        end;

    end;

end; { of procedure CheckFeasibility }
```

```
{ ********************************************************************** }

procedure TestConvergence;

   var
   i,j,l : indices;

   begin
      { FIND VARIANCE OF FUNCTION VALUES }
   s1:=0;s2:=0;
   for i:=1 to k do
       begin
           s1:=s1+f[i];
           s2:=s2+f[i]*f[i];
       end;
    sd:=s2-s1*s1/k;
    sd:=sd/k;
    { FIND MAX. DIST. BETWEEN POINTS OF COMPLEX }
    dm:=0;
    for i:=1 to k-1 do
        for j:=i+1 to k do
            begin
               d:=0;
               for l:=1 to n do
                   d:=d+(c[i,l]-c[j,l])*(c[i,l]-c[j,l]);
               d:=sqrt(d);
               if d>dm then dm:=d;
            end;

end; { of procedure TestConvergence }

{ ********************************************************************** }

procedure ImprovedPrint;

   var
      l : integer;

   begin
   writeln(output,'New Point');
   writeln(output,'Min.Value=',f[1]);
   writeln(output,'Min.Point=');
   for l:=1 to n do
       writeln(output,'X',l,c[1,l]);
   writeln;
   fm:=f[1]
   end; { of procedure ImprovedPrint }

{ ********************************************************************** }

procedure IterativeRoutine ;

   var
   i,j,l : indices;

   begin
       repeat
       { FORM CENTROID OF BEST (K-1) POINTS AND RECORD WORST POINT}
       for l:=1 to n do
           begin
```

```
            xh[l]:=c[k,l];
            xo[l]:=(k*xc[l]-xh[l])/(k-1);
        end;
{ FORM REFLECTED POINT }
for l:=1 to n do
    begin
        xr[l]:=(1+alpha)*xo[l]-alpha*xh[l];
        x[l]:=xr[l];
    end;
{ TEST NEW POINT FOR FEASIBILITY }
CHECKFEASIBILITY;
{ UPDATE XC AND REPLACE WORST POINT BY NEW POINT }
f[k]:=fr;
for l:=1 to n do
    begin
        xc[l]:=k*xc[l]-c[k,l]+xr[l];
        xc[l]:=xc[l]/k;
        c[k,l]:=xr[l];
    end;
{ PUT FUNCTION VALUES AND POINTS IN ORDER }
for j:=1 to k-1 do
    for i:=j+1 to k do
       if f[j]>f[i] then
           begin
               fval:=f[j];
               f[j]:=f[i];
               f[i]:=fval;
               for l:= 1 to n do
                   begin
                       y[l]:=c[j,l];
                       c[j,l]:=c[i,l];
                       c[i,l]:=y[l];
                   end;
           end;
       TestConvergence;
       if f[1]<fm then ImprovedPrint; { IF LOWEST VALUE NOT REDUCED SKIP
                        PRINT }
                      { TEST OF CONVERGENCE }
       until (sd<sdacc) AND (dm<dmacc);
       writeln(output,'Minimum Found');
       writeln(output,'Minimum Point');
       for l:=1 to n do
           writeln(output,'X',l,c[1,l]);
       writeln(output,'Function Minimum=',f[1]);
       writeln(output,'Function Evaluations=',fe);

end; { of procedure IterativeRoutine }

{ ********************************************************************** }

BEGIN
   Initialise ;
   InitiateComplex ;
   IterativeRoutine ;
END; { Procedure ComplexMethod }

{ ********************************************************************** }
```

```
BEGIN
   CalcFactorial;
   GetDataFromDisk;
   Normalise;
   MeanResidenceTime;
   ComplexMethod;
END. { The main program }

 {************************************************************************** }
```

APPENDIX 2.c

IMPULSE TRACER DATA

Time measured in minutes and flowrate in litres/min.

All flowrates are accurate to ± 0.6 litres/min.

Run 1		Run 2		Run 3	
Flowrate	12.8	Flowrate	19.4	Flowrate	18.2
Time	Cond	Time	Cond	Time	Cond
0	0	0	0	0	0
2.2	0	1.42	0	1.55	0
2.33	1	1.5	1	1.63	1.5
2.5	4.5	1.58	3	1.7	4.5
2.58	7	1.67	6	1.75	7
2.67	11	1.75	12.5	1.83	15
2.75	17	1.83	22.5	1.92	26
2.83	23	2.08	64	2.17	70
2.92	31	2.17	74	2.25	81
3.17	55	2.24	79	2.33	87
3.25	62	2.3	80	2.39	88
3.33	67	2.35	79	2.44	87
3.45	70	2.42	75	2.5	84
3.53	71	2.5	67.5	2.58	77
3.62	70	2.75	40	2.83	49
3.67	69	2.83	32	2.92	40
3.75	65	2.92	26	3	33
4.25	35	3	20.5	3.17	21
4.5	23	3.08	15.5	3.33	13
4.67	17.5	3.25	10	3.5	8.5
4.92	11	3.42	6	3.75	4.5
5.25	6	3.75	2.5	4.08	2
5.75	2.5	4.33	0	5.33	0
6.75	0				

Run 4		Run 5		Run 6	
Flowrate	16.6	Flowrate	14.7	Flowrate	13.2
0	0	0	0	0	0
1.58	0	1.83	0	2	0
1.67	1	1.92	1	2.17	1
1.75	2.5	2	3	2.33	3.5
1.83	5	2.08	6	2.42	6.5
1.92	9	2.17	11	2.5	10
2	16	2.25	18	2.58	16
2.08	26	2.33	22	2.67	23
2.33	65	2.58	62	2.75	32
2.42	76	2.67	72	3	61
2.47	80.5	2.72	77	3.08	69
2.53	84.5	2.79	82.5	3.17	75
2.61	85.5	2.84	84	3.25	79
2.67	84	2.91	84.5	3.3	80
2.75	79	2.98	83	3.37	81
2.92	64	3.05	80	3.42	80.5
3.08	47.5	3.17	71	3.5	78
3.25	33	3.5	41	3.67	69
3.42	22	3.58	35	3.92	50
3.58	15	3.75	25	4.08	39
3.75	11	3.92	17	4.25	29.5
4	6.5	4.17	10	4.42	22
4.5	3	4.42	6	4.58	16
6	0	4.83	2.5	4.83	10.5
		5.08	7		

Run 7		Run 8		Run 9	
Flowrate 11.7		Flowrate 10.2		Flowrate 8.9	
0	0	0	0	0	0
2.25	0	2.5	0	2.83	0
2.42	1	2.58	.5	3	1
2.58	5	2.67	1	3.17	3
2.67	7.5	2.83	3.5	3.33	6
2.75	11.5	2.92	5.5	3.5	11.5
2.83	17	3	8	3.67	21
2.92	23	3.08	12	3.75	26
3	31	3.17	17	3.83	31.5
3.25	58	3.25	22.5	4.08	50
3.33	66	3.33	30	4.17	56
3.42	72	3.67	60	4.25	61
3.5	77	3.75	66	4.33	65
3.56	79	3.83	72	4.42	69
3.67	80.5	3.92	75	4.5	71
3.75	79.5	4	78	4.56	72
3.85	75	4.09	79	4.63	72.5
4	68	4.17	78.5	4.73	72
4.42	40.5	4.25	77	4.83	70
4.58	31	4.33	74	5	64.5
4.75	24	4.42	70.5	5.58	38
5	15.5	5	38	5.83	28
5.25	10.5	5.25	27	6.08	21
5.58	6	5.42	21	6.25	17
6	3	5.67	15	6.5	12.5
6.83	1.5	6	10	6.83	8
8	0.5	6.25	6.5	7.17	5.5
9.5	0	6.67	4	7.67	3.5
7.5	2	8.5	1.5		
8.42	1	9.5	1		
10.58	0	10.58	0		

Run 10		Run 11		Run 12	
Flowrate 7.5		Flowrate 6.2		Flowrate 5.0	
0	0	0	0	0	0
3.42	0	4.17	0	5.33	0
3.5	1	4.33	1	5.67	1.5
3.67	1.5	4.58	2.5	6	4
3.83	3.5	4.92	7	6.33	9
4	7	5.08	11	6.67	13
4.17	11	5.25	16	7.33	41
4.33	18	5.5	25	7.67	52
4.5	27	6	47	7.83	57
4.83	47	6.25	56	8	61
5	56	6.5	62	8.23	64.5
5.17	63	6.67	63.5	8.37	66
5.25	66	6.83	64	8.55	66.5
5.42	69	7	62.5	8.7	66
5.58	70	7.25	58	9	63
5.75	68	8.17	34	9.33	57
5.92	64	8.5	26.5	10	43
6.25	53	8.92	19	10.67	30
6.67	38	9.33	13	11.33	20
7	27	9.75	10	11.67	16
7.33	20	10.25	7	12	13
7.58	15	11	4	12.33	11
8.08	9	12	2	13	7
8.5	6	13.42	1	14	4
9.17	4	15	0.5	15.33	2.5
9.83	2.5		20.33	0	
11	1				
12.17	0.5				
13	0.5				

Run 13		Run 14		Run 15	
Flowrate 3.8		Flowrate 2.6		Flowrate 13.2	
0	0	0	0	0	0
7.33	0	10.33	0	2.04	0
7.67	.5	11	1	2.13	1
8	2	11.67	3	2.25	2.5
8.33	4	12.33	6	2.33	5
8.67	7	13	12	2.42	8
9	11	13.67	20	2.5	13
9.33	21.5	15.15	38	2.58	19
9.67	23	15.67	43	2.67	28
10.4	40	16	45	3	69
10.8	48	16.33	47	3.08	78
11.1	52.5	16.78	48	3.17	85
11.33	55	17.13	48.5	3.25	89
11.5	56	17.5	47.5	3.33	90.5
11.77	57	18	46	3.37	91
11.93	57.5	18.67	43	3.42	90
12.17	57	21.33	28	3.5	87
12.67	54	22	24	3.58	82
13	50	22.67	21	3.67	77
14.33	34	24.6	14	4.08	43
15	27	26	10.5	4.33	27
15.67	21	28.33	7	4.5	20
16.33	16	31.33	4.5	4.67	15
17.33	11	36.33	2.5	4.92	9
18.33	8	41.67	1	5.17	6
20	4.5	47.67	0.5	5.75	2.5
21.67	3		6.33	1	
24	2		7.33	0	
29.33	0				

```
{ $D debug:= true; }
PROGRAM Deconvolution(InFile,Outfile,input,output);
{ This program removes a number of tanks in series from the E curve
            A.P.G.Newton  October 1989 }
type
     DataFile = text;                              { data to be read from disk }
   PlotArray = array [1..100,1..2] of real;
var
   InFile,Outfile : DataFile;
   NoPoints,NoTanks,SplinePnts : integer;
   MeanRT,TankRT,Tpeak : real;
   CondData,Ecurve,NewEcurve,DimEcurve : PlotArray;

{ ********************************************************************** }

procedure GetDataFromDisk ;
var
   i : integer;
begin
   reset (InFile);
   Readln (InFile,NoPoints);
  for i:= 1 to NoPoints do
            begin
            Readln (InFile,CondData[i,1],CondData[i,2]);
            end;

end; { of procedure GetDataFromDisk }

 {********************************************************************** }

function Trapezoidal( xy : PlotArray): real;
var
   j: integer;
   totalarea : real;
begin
     totalarea:=0;
     for j:=2 to NoPoints do
     totalarea:=totalarea+(xy[j,1]-xy[j-1,1])*(xy[j,2]+xy[j-1,2])/2.0;
     Trapezoidal:=totalarea;
end; { of function Trapezoidal rule }

 {********************************************************************** }

procedure Normalise;
var
   i: integer;
   normalized : Real;
begin
   Normalized:=Trapezoidal(CondData);
   for i:=1 to NoPoints do
            begin
            Ecurve[i,1]:=CondData[i,1];
        Ecurve[i,2]:=CondData[i,2]/normalized;
   { $B debug }
            writeln(output,Ecurve[i,1],Ecurve[i,2]);
   { $E debug }
```

```
            end;
end;  { of procedure Normalise }

 {************************************************************************** }

procedure MeanResidenceTime;
   var
      i: integer;
      ct : PlotArray;
   begin
      for i:=1 to NoPoints do
            begin
            ct[i,1]:=CondData[i,1];
         ct[i,2]:=CondData[i,2]*CondData[i,1];
             end;
      MeanRT:=Trapezoidal(ct)/Trapezoidal(CondData);
    end;

{ ************************************************************************ }

Procedure OtherCurveProperties;

  var
           i : integer;
  begin
  for i:=2 to NoPoints do
           if (CondData[i,2] > CondData[i-1,2]) then Tpeak:=CondData[i,1];
  { This assumes that the peak is a measured point on the tracer data }
  { If this is not the case the spline produced data might be used }
           end; { procedure OtherCurveProperties }

{ ************************************************************************ }

procedure spline(A:PlotArray;
                 N:integer;
                 X1,XM:real;
                 var B:PlotArray;
                 M:integer);
  const MaxSpline=100;
  type Vector = array [1..MaxSpline] of real;
  var x,y,z:Vector;
      i:integer;
      DeltaX:real;

{ ************************************************************************ }

procedure stg(Vector1,Vector2,Vector3:Vector;
              var Vector4:Vector;
              NPts:integer);
  var i:integer;
      Factor:real;

  begin
    for i:=2 to NPts do
     begin
      Factor:=Vector1[i-1]/Vector2[i-1];
      Vector2[i]:=Vector2[i]-Factor*Vector3[i-1];
      Vector4[i]:=Vector4[i]-Factor*Vector4[i-1];
```

```
      end;
    Vector4[NPts]:=Vector4[NPts]/Vector2[NPts];
    for i:=1 to NPts-1 do
      Vector4[NPts-i]:=(Vector4[NPts-i]-Vector3[NPts-i]*Vector4[NPts-i+1]) /
                       Vector2[NPts-i];
  end;

{ ********************************************************************** }

  procedure sc(X,Y:Vector;
               var Z:Vector;
               NPts:integer);
    var i:integer;
        D,C:Vector;

  begin
    D[1]:=1.0;
    C[1]:=0.5;
    Z[1]:=0.5;
    for i:=2 to NPts-1 do
     begin
      D[i]:=2.0*(X[i+1]-X[i-1]);
      C[i]:=X[i+1]-X[i];
      Z[i]:=6.0*((Y[i+1]-Y[i])/(X[i+1]-X[i])-(Y[i]-Y[i-1])/(X[i]-X[i-1]));
     end;
    D[NPts]:=1.0;
    C[NPts-1]:=0.0;
    C[NPts]:=0.0;
    Z[NPts]:=0.0;
    stg(C,D,C,Z,NPts);
  end;

{ ********************************************************************** }

  function si(V:real;
              X,Y,Z:Vector;
              NPts:integer):real;
    var i,j:integer;
        dummy,ai,hi:real;

    begin
      if (V>X[1]) and (V<X[NPts]) then
       begin
        j:=1;
        repeat
          j:=j+1;
          i:=NPts-j;
          dummy:=V-X[i];
        until (dummy>=0.0) or (i=2);
        hi:=X[i+1]-X[i];
        ai:=dummy*(Z[i+1]-Z[i])/(6.0*hi)+0.5*Z[i];
        ai:=dummy*ai+(Y[i+1]-Y[i])/hi-hi*(2.0*Z[i]+Z[i+1])/6.0;
        si:=dummy*ai+Y[i];
       end
      else if V=X[1] then si:=Y[1]
      else si:=Y[NPts];
    end;

{ ********************************************************************** }
```

```
  procedure sia(X,Y:Vector;
                NPts:integer;
                XInt:Vector;
                var YInt:Vector;
                N:integer);
    var i:integer;
        V3:Vector;

    begin
      sc(X,Y,V3,NPts);
      for i:=1 to N do YInt[i]:=si(XInt[i],X,Y,V3,NPts);
    end;

{ ********************************************************************** }

begin { Spline :fits a cubic spline which has a continuous first derivative
              and the second derivative equals zero }
  if (abs(N)>=2) and (abs(M)>=2) then
   begin
    if ((X1>=A[1,1]) and (XM<=A[N,1])) and (M>=2) then
     begin
      DeltaX:=(XM-X1)/(M-1);
      for i:=1 to N do
       begin
        X[i]:=A[i,1];
        Y[i]:=A[i,2];
       end;
      for i:=2 to M-1 do Z[i]:=X1+(i-1)*DeltaX;
      Z[1]:=X1;
      Z[M]:=XM;
      sia(X,Y,N,Z,Y,M);
      for i:=1 to M do
        begin
         B[i,1]:=Z[i];
         B[i,2]:=Y[i];
        end;
      end
     else writeln(output,'Error in defining the limits of the spline points');
    end
   else writeln(output,'Too few base and spline points');
  end;

{ ********************************************************************** }

Procedure Deconvolution;
{ Removes a number of tanks in series using deconvolution }

var
        i,j,k : integer;
        TwoH : real;
        slope : array[0..4] of real;

begin
 { $B debug }
        for i:=1 to SplinePnts do
                writeln(output,NewEcurve[i,1],NewEcurve[i,2]);
 { $E debug }

writeln (output,'Enter the number of tanks to be removed from the curve');
Readln (input,NoTanks);
```

```
  TankRT:=Tpeak/(NoTanks-1); { mean residence time of a single tank }

  { differentiating using Three-Point Lagrange Formulae }
          TwoH:=2*(Ecurve[NoPoints-1,1]-Ecurve[3,1])/(SplinePnts-1);

  for i:=1 to NoTanks do
  begin
           NewEcurve[1,2]:=NewEcurve[1,2]+TankRT*(-3*NewEcurve[1,2]+4*NewEc-
urve[2,2]-NewEcurve[3,2])/TwoH;
          for j:=2 to (SplinePnts-1) do
                  NewEcurve[j,2]:=NewEcurve[j,2]+TankRT*(-NewEcurve[j-1,2]+NewEcur-
ve[j+1,2])/TwoH;
           NewEcurve[SplinePnts,2]:=NewEcurve[SplinePnts,2]+TankRT*(NewEcur-
ve[SplinePnts-2,2]-4*NewEcurve[SplinePnts-1,2]+3*NewEcurve[SplinePnts,2])/TwoH;
      { $B debug }
                  for k:=1 to SplinePnts do

writeln(output,NoTanks-i+1,k,NewEcurve[k,1],NewEcurve[k,2]);
          { $E debug }
          { The differentiated curve now must be smoothed otherwise the process F.. up
}
           NewEcurve[1,2]:=(5*NewEcurve[1,2]+2*NewEcurve[2,2]-NewEcurve[3,2])/6;
          for j:=2 to (SplinePnts-1) do

NewEcurve[j,2]:=(NewEcurve[j-1,2]+NewEcurve[j,2]+NewEcurve[j+1,2])/3;
           NewEcurve[SplinePnts,2]:=(-NewEcurve[SplinePnts-2,2]+2*NewEcurve-
[SplinePnts-1,2]+5*NewEcurve[SplinePnts,2])/6;
  end;
  for i:= 1 to SplinePnts do
          begin
           DimEcurve[i,1]:=NewEcurve[i,1]/(meanRT*(NoTanks-1)/NoTanks-Tpeak);
           DimEcurve[i,2]:=NewEcurve[i,2]*(meanRT*(NoTanks-1)/NoTanks-Tpeak);
          end;
          rewrite(outfile);
          for i:= 1 to SplinePnts do
                  writeln(OutFile,DimEcurve[i,1]:10 ,DimEcurve[i,2]:10 ,'
',ln(DimEcurve[i,2]):10);
  end; { of procedure Deconvolution }

{ ********************************************************************** }

BEGIN
   GetDataFromDisk;
   Normalise;
   MeanResidenceTime;
   OtherCurveProperties;
   writeln(output,'Enter the number of spline Points ( max 100)');
   readln (input,SplinePnts);
   Spline (Ecurve,NoPoints,Ecurve[3,1],Ecurve[NoPoints-1,1],NewEcurve,SplinePnts);
   Deconvolution;
END. { The main program }

{********************************************************************** }
```

APPENDIX 3.a

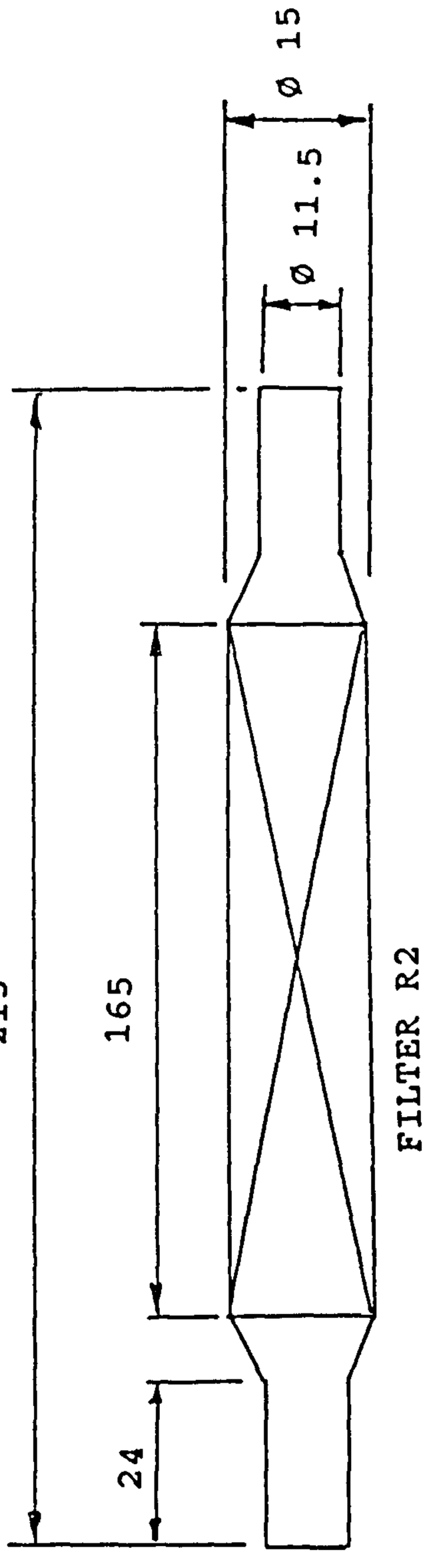

Dimensions in cm

Ends contain 80 pieces of 1 1/4" plastic rashig rings

ONE HALF OF EACH FILTER USED FOR KINETICS DATA

```
{$D debug:=true; }
PROGRAM ContinAmm(InFile,OutFile,input,output);

{ This program is designed to fit a given reaction kinetic model to given
kinetic data. The data is required in the form of initial and final
concentrations for reactant 'a' along with the residence time. The kinetic
model is integrated and the calculated residence times and the actual times
are compared. Using the least squares fit, the kinetic constants are altered
to obtain the best fit possible.
            A.P.G.Newton  October 1988 }

INCLUDE 'Rate.inc';

FUNCTION NoVariables:indices;import;

PROCEDURE NamesofVar;import;

FUNCTION InvRate(x : real):real;import;

{ ********************************************************************** }


procedure GetDataFromDisk ;

var
   i : integer;
   Flowrate : DataType;
   ExperType,TotalSubs : string[10];

begin
   reset (InFile);
   {$B debug }
   Expertype:='expertype';
   totalsubs:='substrate';
   {$E debug }
   Readln (InFile,ExperType);
   Readln (InFile,TotalSubs);
   writeln (output,expertype,' Experiment Substrate ',totalsubs);
   if (ExperType = 'CONTINUOUS') and (TotalSubs = 'AMMONIA') then
   begin
      Readln (InFile,pH,Temp,ActiveVol);
      i:=1;
    while not eof(InFile) do
       begin
                Readln (InFile,Sample[i],Flowrate[i],CAI[i],CAF[i]);
                i:=i+1;
             end;
      NoPoints:=i-1;
      for i:= 1 to NoPoints do Time[i]:=ActiveVol/FlowRate[i];
   end
   else writeln (output,'Incorrect data file being used');
end; { of procedure GetDataFromDisk }

 {********************************************************************** }

procedure EquilibCorrection;

var
```

```
    j : integer;
    pKa,NH4Frac,Dielectric,Acoeff,IonicCorr,Conduct,IonicStrength : real;
    answer : char;

begin
    pKa:=2.804E3/(273.16+Temp)+0.88E-3*(273.16+Temp)-0.4227;
    Dielectric:=87.74-0.4008*Temp+9.398E-4*sqr(Temp)-1.41E-6*Temp*sqr(Temp);
    Acoeff:=1.82483E6*exp(-1.5*ln(Dielectric*(Temp+273.16)));
    writeln(output,'Enter the Measured or Estimated Conductivity ');
    writeln(output,'Units:- micro Siemens per centemeter');
    readln(input,conduct);
    { The ionic dissolved solids can be estimated by multiplying by 0.01.
      This ignores any contribution by carbon dioxide and ammonia gas, that a
      change in pH might bring. Nitrate, sodium and calcium ions are present
      in much larger quantities and the error is likely to be small.  }
IonicStrength:=Conduct*0.01*0.001;
IonicCorr:=Acoeff*sqrt(IonicStrength)/(1+sqrt(IonicStrength));
NH4Frac := 1/(1+ exp((pH-pKa-IonicCorr)*ln(10)));
{$B debug }
writeln(output,IonicCorr,NH4frac);
{$E debug }
writeln (output,'Choose substrate to be tested');
writeln (output,'(T)otal Ammonia / Ammonia (G)as / Ammonium (I)on');
readln (input,answer);
case ord(answer) of

        73,105    :for j:= 1 to NoPoints do
                   begin
                      CAI[j]:= NH4Frac*CAI[j];
                      CAF[j]:= NH4Frac*CAF[j];
                   end;
  71,103           :for j:= 1 to NoPoints do
                   begin
                      CAI[j]:= (1-NH4Frac)*CAI[j];
                      CAF[j]:= (1-NH4Frac)*CAF[j];
                   end;
  otherwise : writeln(output,'Using Total Ammonia');
  end;

end; { procedure EquilibCorrection }

 {*************************************************************************** }

Procedure FractionConverted;

var
   i : integer;

begin
   for i:=1 to NoPoints do
        XAF[i]:=1.0-CAF[i]/CAI[i];
   {$B debug }
   writeln(output,XAF[i],CAI[i],CAF[i],Time[i],ph,temp);
   {$E debug }
end;  { of procedure FractionConverted }

 { *************************************************************************** }

Procedure SimplexMethod(n : indices);
   { finds the minimum of a function using the simplex method of Nelder &
```

```
Mead }

 { Program adapted from "Basic Optimisation Methods" by B.D.Bunday
notation is as in the Basic program given above.
Sorry Pascal purists! I have kept the limited basic variable names for
reasons of compatability with the above.I have tried to banish the
dreaded GOTO statement and I hope this is readable }
 { This program now has some of its definitions in an include file this is
    so different rate equations can be tested without recompilation }

 const
    alpha = 1.0;          { reflection factor }
    beta = 0.5;           { contraction coefficient }
    gamma = 2.0;          { expantion factor }
    maxvalue = 1.0E20;
    minvalue = -1.0E20;
 var
    i,j : integer;        { counting integer }
    h,                    { heighest function index }
    g,                    { second greatest function index }
    l : indices;          { lowest function index }
    fh,                   { heighest function value }
    fg,                   { second greatest function value }
    fl,                   { lowest function value }
    fr,                   { reflected function value }
    fe,                   { expanded function value }
    fo,                   { centroid function value }
    fc,                   { contracted function value }
    z:real;               { evaluated function }
    s:SArrayType;                    { simplex vertices,[1..n+1,1..n] }
    xh,                              { point with heighest function }
    xg,                              { point with next heighest function }
    xl,                              { point with lowest function }
    xo,                              { centroid of points }
    xr,                              { reflected xh }
    xc,                              { contracted xh-xr }
    xe:NArrayType;                   { expanded xh-xr }
    f:FArrayType;                    { evaluated function }

 {*************************************************************************}

procedure Initialize;

var
   i,j : integer;

begin
m:=n+1;
{$B debug }
for j:=1 to n do
  name[j]:='initialized         ';
{$E debug }
for i:=1 to n do
  begin
  x[i]:=0.0;
  xh[i]:=0.0;
  xg[i]:=0.0;
  xl[i]:=0.0;
  xo[i]:=0.0;
  xr[i]:=0.0;
```

```
      xc[i]:=0.0;
      xe[i]:=0.0;
      end;
   for i:=1 to m do
      begin
         f[i]:=0.0;
         for j:=1 to n do
         s[i,j]:=0;
      end;
   Tev := 0;fl:=0.0;fg:=0.0;fh:=0.0;
end; {of procedure Initialize}

{ ********************************************************************** }
Procedure KineticModel;

var
  i : integer;


{ ********************************************************************** }

function Romb(a,b,eps,eta: real;
           min,max: integer;
                     function f(x : real):real): real;

{ This function is as contained in "Scientific Pascal" by Harley Flanders }
{ It integrates between the limits a and b                                 }

  { eps: absolute error                    }
  { eta: relative error                    }
  { min: least number of bisections        }
  { max: greatest number of bisections     }
  { choose 3 <= min < max <= 15            }

var
    h,          { subinterval length       }
   fa,fb,       { F(a), F(b)               }
   vi,          { integral of |F|          }
   t1,t2,       { previous two estimates   }
   p,           { power of 4               }
   midsum,mv,       { midpoint sums for f, |F| }
   err : real; { closeness of 3 successive estimates }

         d: array[0..15] of real;
   j,nthDiag,r : integer;
   { n-th diagonal of Romberg table ;
     r =2**nthDiag; j is for index          }

    quit: boolean;

{ ********************************************************************** }

  procedure Mid(var r: integer; var h,midsum,mv: real);

    var
           k : integer;
           fk,re,ss: real;

    begin
    h:= h/2; re:=0; midsum:=0; mv:=0;
```

```
    for K:= 1 to r do
            begin
            fk:=F(a+(2*k-1)*h);
            mv:=mv+abs(fk);
            fk:=fk+re;
            ss:=midsum+fk;
            re:=(midsum-ss)+fk;
            midsum:=ss;
            end; { of k}
    r:=2*r
    end; { mid }

{ ********************************************************************** }

  begin     { Romb }
       h:=b-a;  fa:=f(a); fb:=f(b);
t1:=0; t2:=0; quit:= false;
d[0]:=h*(fa+fb)/2;
vi:=abs(h)*(abs(fa)+abs(fb))/2;
nthDiag:=1; r:=1;
repeat
   Mid(r,h,midsum,mv);
   d[nthDiag]:=d[nthDiag-1]/2 +h*midsum;
   vi:=vi/2+abs(h)*mv;
   p:=1;
   for j:= nthDiag-1 downto 0 do
            begin
               p:=4*p;
        d[j]:=d[j+1]+(d[j+1]-d[j])/(p-1);
            end;
        if nthDiag>= min then
           begin
           err:=abs(d[0]-t1)+abs(t1-t2);
                  quit:=quit or (err < 2*eta*vi);
                  quit:=quit or (err < 2*eps)
           end;
        nthDiag:=nthDiag+1;
        quit:=quit or (nthDiag > max);
        t2:=t1;
        t1:=d[0]
    until quit;
           Romb:=t1
end;    { Romb }

{ ********************************************************************** }

Begin
z:=0;
for i:=1 to NoPoints do
           begin
           pointnumber:=i;
           { Since the rate eqn is integrated wrt fractional conversion
             one must multiply by CAI  }
           Tfit[i]:=CAI[i]*Romb(0,XAF[i],0.000001,1,3,15,InvRate);
           z:=z+sqr(Tfit[i]-Time[i]);
           end;
end; { of procedure KineticModel }

{ ********************************************************************** }
```

```
procedure StartWith;

var
   i,j : Integer;
   steplength : real;

begin
     NamesofVar;
     writeln;
     for j:=1 to n do
      begin
        writeln (output,'Enter initial estimate for ', Name[j]);
        readln (input,s[1,j])
      end;
     writeln (output,'Enter the step length');
     readln (input,steplength);
     for i:=2 to m do { set up first simplex around inital points }
        begin
        for j:=1 to n do
           begin
             if (j=i-1) then s[i,j]:=s[1,j]+steplength
             else
             s[i,j]:=s[1,j];
           end;
        end;
     for i:=1 to m do { find function values }
        begin
           for j:=1 to n do
           x[j]:=s[i,j];
           KineticModel;
           f[i]:=z;
        end;
end; { of procedure StartWith }

 {*************************************************************************** }

procedure FindXnFn;

var
   i,j : integer;

begin
   fh:=minvalue;
   fl:=maxvalue;
   for i:=1 to m do
      begin
      if (f[i]>fh) then
      begin
      fh:=f[i];
      h:=i;
      end;
    if f[i]<fl then
      begin
      fl:=f[i];
      l:=i;
      end;
   end;
{ find second greatest value and point }
fg:=minvalue;
for i:=1 to m do
```

```
      begin
      if ((i<>h) AND (f[i]>fg)) then
         begin
         fg:=f[i];
         g:=i;
         end;
      end;
   for j:=1 to n do
      begin
      xo[j]:=0;
      for i:=1 to m do
         if (i<>h) then xo[j]:=xo[j]+s[i,j];
         xo[j]:= xo[j]/n;
         xh[j]:=s[h,j];
         xg[j]:=s[g,j];
         xl[j]:=s[l,j];
       end;
end; { of procedure FindXnFn }

 {************************************************************************** }

procedure FindXoFo;

var
   j : integer;

begin
     for j:=1 to n do
      begin
         x[j]:=xo[j];
      end;
      KineticModel;
      fo:=z;
end; { of procedure FindXoFo }

 {************************************************************************** }

procedure FindXrFr;

var
   j : integer;

begin
      for j:=1 to n do { Reflection }
      begin
         xr[j]:=xo[j]+alpha*(xo[j]-xh[j]);
         x[j]:=xr[j];
      end;
      KineticModel;
      fr:=z;
end; { of procedure FindXrFr }

 {************************************************************************** }

procedure FindXeFe ;

var
   j : integer;

begin
```

```
      for j:=1 to n do
      begin { Expantion }
         xe[j]:=gamma*xr[j]+(1.0-gamma)*xo[j];
         x[j]:=xe[j];
      end; { Expantion }
      KineticModel;
      fe:=z;
end; { of procedure FindXeFe }

 {************************************************************************** }

procedure FindXcFc;

var
   j : integer;

begin
   for j:=1 to n do
      begin { contraction }
         xc[j]:=beta*xh[j]+(1.0-beta)*xo[j];
         x[j]:=xc[j];
      end; { contraction }
   KineticModel;
   fc:=z;
end; { of procedure FindXcFc }

 {************************************************************************** }

procedure ReplaceXhbyX1 (var X1 : NArrayType;
                         var  F1 : real);
var
   j : integer;

begin { replace xh by x1 }
   for j:=1 to n do
      s[h,j]:=X1[j];
      f[h]:=F1;
end; { replace xh by x1 }

 {************************************************************************** }
procedure SetXhXr;

var
   j : integer;

begin {set xh=xr }
   for j:=1 to n do
   xh[j]:=xr[j];
   f[h]:=fr;
end; { set xh=xr }

 {************************************************************************** }

procedure SetAllXi;

var
   i,j : integer;

begin
      for i:=1 to m do
```

```
      begin
         for j:=1 to n do
            begin
               s[i,j]:=(s[i,j]+xl[j])/2.0;
               x[j]:=s[i,j];
            end;
            KineticModel;
            F[i] := z;
      end;
end; { of SetAllXi }

 {*************************************************************************** }

function  Converged : Boolean;

var
   s1,s2,sig : real;
   i : integer;

begin
   Converged := FALSE;
   s1:=0;
   s2:=0;
   for i:=1 to m do
      begin
      s1:=s1+F[i];
      s2:=s2+F[i]*F[i];
      end;
   sig:=s2-s1*s1/m;
   sig:=sig/m;
   IF sig<1.0E-10 then Converged := TRUE;
end; { of function Converged }

  {*************************************************************************** }

procedure DisplayResult;

var
   j : integer;

begin
   writeln (output,'Minimum obtained');
   for j:=1 to n do
  begin
            XLeastSquares[j]:= abs(xl[j]);
        writeln (output,Name[j],'=',XLeastSquares[j]);
  end;
   writeln (output);
   SumLeastSquares:=F[1];
   writeln (output,'Function minimum = ',F[1]);
   writeln (output,'No of Function Evaluations = ',Tev);
end; { of procedure DisplayResult }

 {*************************************************************************** }

{ SIMPLEX METHOD MAIN PROCEDURE BEGINS HERE }
Begin
Initialize;
StartWith ;
REPEAT
```

```
FindXnFn;
FindXoFo;
FindXrFr;
IF (fr<fl) THEN
   begin
     FindXeFe;
     IF (fe<fl) then ReplaceXhbyXl (xe,fe)
      else  ReplaceXhbyXl (xr,fr);
   end
ELSE
   begin
   IF (fr>fg) THEN
      begin
      IF (not (fr>fh)) then SetXhXr;
      FindXcFc;
      IF (fc>fh) then
         SetAllXi
      else
         ReplaceXhbyXl (xc,fc);
      end
     ELSE
         ReplaceXhbyXl (xr,fr);
    end;
UNTIL Converged = true ;
DisplayResult ;
END; { of Procedure Simplex Method }

{ ********************************************************************** }

procedure PutDataToDisk ;

var
   i,j : integer;
   Slope,Corr : real;

{ ********************************************************************** }

Procedure SlopeCorr (x,y : DataType);
  { Calculates the slope and correlation of a straight line forced through the
    origin }

var
  i : integer;
  Sumx,Sumxy,Sumxx,Sumy,Sumyy,SSE,SSTO,RR : real;

  begin
  Sumx:=0;Sumy:=0;Sumxy:=0;Sumxx:=0;Sumyy:=0;
  for i:=1 to NoPoints do
          begin
                  Sumx:=Sumx+x[i];
                  Sumy:=Sumy+y[i];
                  Sumxy:=Sumxy+x[i]*y[i];
                  Sumxx:=Sumxx+x[i]*x[i];
                  Sumyy:=Sumyy+y[i]*y[i];
          end;
Slope:=Sumxy/Sumxx;
SSTO:= Sumyy-(Sumy*Sumy/NoPoints);
for i:=1 to NoPoints do
          SSE:= SSE + sqr(y[i]-slope*x[i]);
RR:=1-SSE/SSTO;
```

```
  if RR < 0 then RR:=0;
  If RR > 1 then RR:=1;
  Corr:=sqrt(RR);
  writeln(output,'The Slope is ',Slope);
  writeln(output,'The Correlation is  ',Corr);
  end; { of procedure SlopeCorr }

 { ********************************************************************** }

begin
   rewrite (outFile);
   for j:=1 to NoVariables do
      writeln (OutFile,XLeastSquares[j] : 8 : 4 );
   writeln (OutFile,SumLeastSquares : 8 : 4 );
   SlopeCorr(Time,Tfit);
   writeln (OutFile,Slope : 8 : 4 ,Corr : 8 : 4 );
   for i:=1 to NoPoints do
      writeln (OutFile,Time[i] : 8 : 4 ,TFit[i] : 8 : 4 ,TFit[i]/Time[i]-1 : 8 : 4 );
end; { of procedure PutDataToDisk }


 { ********************************************************************** }

BEGIN
   GetDataFromDisk;
   EquilibCorrection;
   FractionConverted;
   SimplexMethod(NoVariables);
   PutDataToDisk;
END. { The main program }
```

{**********}

```
MODULE RateEqnB(InFile,OutFile,input,output);
INCLUDE 'Rate.inc';

Function NoVariables: indices;Export;
{ This function contains the number of variables, max 5 }
  begin
  NoVariables:=2;
  end; { of function NoVariables }

{ ********************************************************************** }

procedure NamesOfVar;Export;
{ This contains the prompts for the Variables }
  begin
  {         'the names below must be less than 20 char   }
  {         'thats to here------>'                       }
  Name[1]:= 'K';
  Name[2]:= 'K1';
  end; { of procedure NamesOfVar }

{ ********************************************************************** }

function InvRate(Xa : real):real;Export;

{ This function contains the rate equation to be integrated and tested }
  var
  Ca,K,K1,Rate : real;
    begin
  tev:= tev+1;
  Ca:= CAI[pointnumber]*(1-XAF[pointnumber]);
  k:= abs(x[1]);
  K1:= abs(x[2]);
  Rate:=K*Ca/(1+K1*Ca);
  InvRate:=1/Rate;
    end;

 { ********************************************************************** }

BEGIN
END.

RATE.INC { Include file }

type
     DataFile = text;                          { data to be read from disk }
     DataType = array [1..50] of real;
     indices = 1..8;     { 1..NoVar+1, max 8 }
     SampleType = array [0..50] of integer; { Sample Number identifier }
     NarrayType = array [1..7] of real; { max 7 Variables }
     SArrayType = array [1..8,1..7] of real; { Simplex vertices }
     FArrayType = array [1..8] of real; { Functions Evaluations }
     NameArray = array [1..7] of String[20]; { Names of the variables }
```

```
var
   InFile,OutFile : DataFile;
   CAI,CAF,Time,Tfit,XAF : DataType;
   NoPoints,Pointnumber,          { number of data points, one point}
   tev:integer;                { number of evaluations }
   SumLeastSquares,pH,Temp,ActiveVol,PA,TA : real;
   Sample : SampleType;
   n,m : Indices;              { number of variables, plus one }
   x,XLeastSquares : NarrayType;              { variable values }
   Name : NameArray;           { names of the variables }
 {*************************************************************************}
```

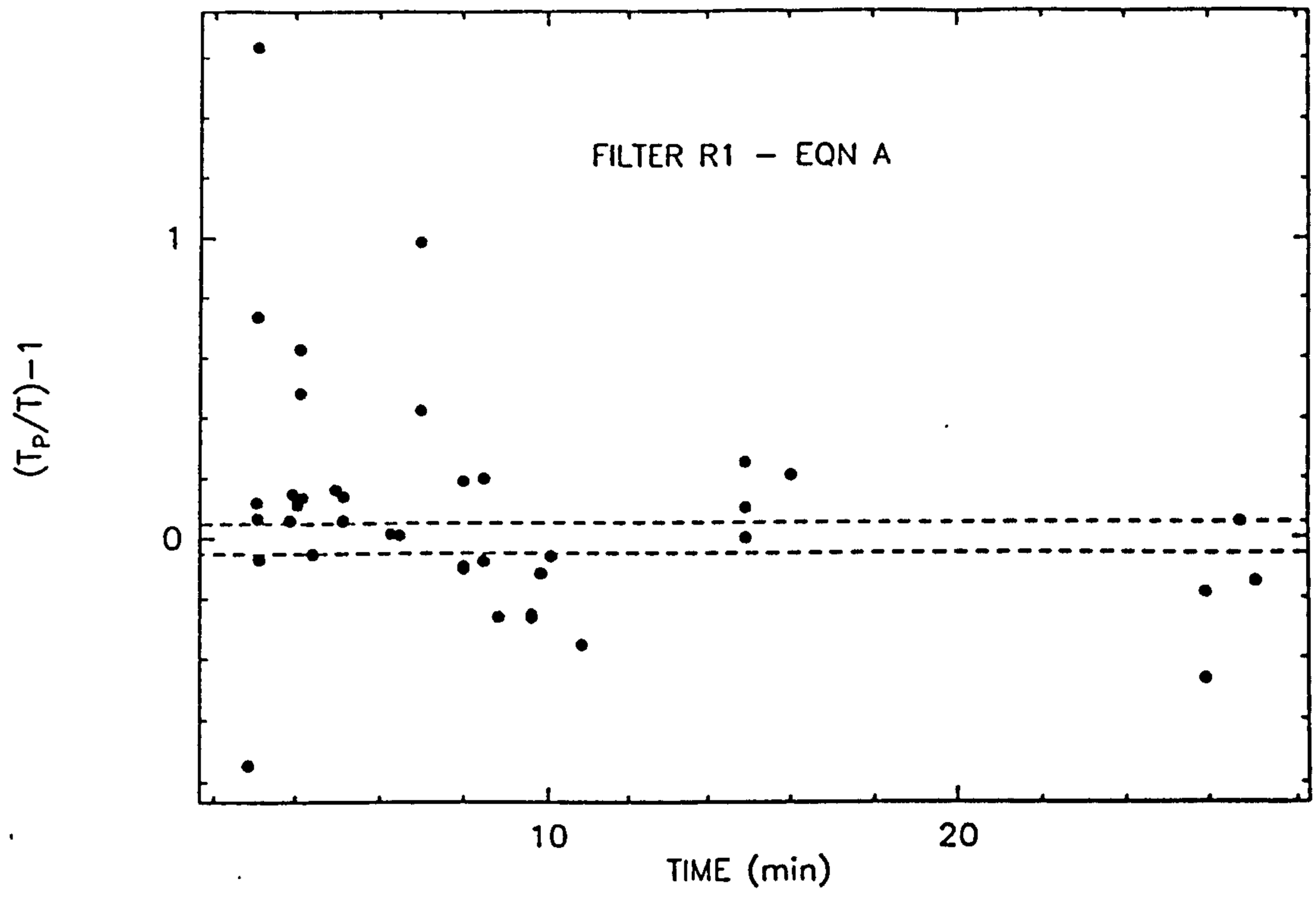
FILTER R1 – EQN A
1
0
$(T_P/T)-1$
10
20
TIME (min)

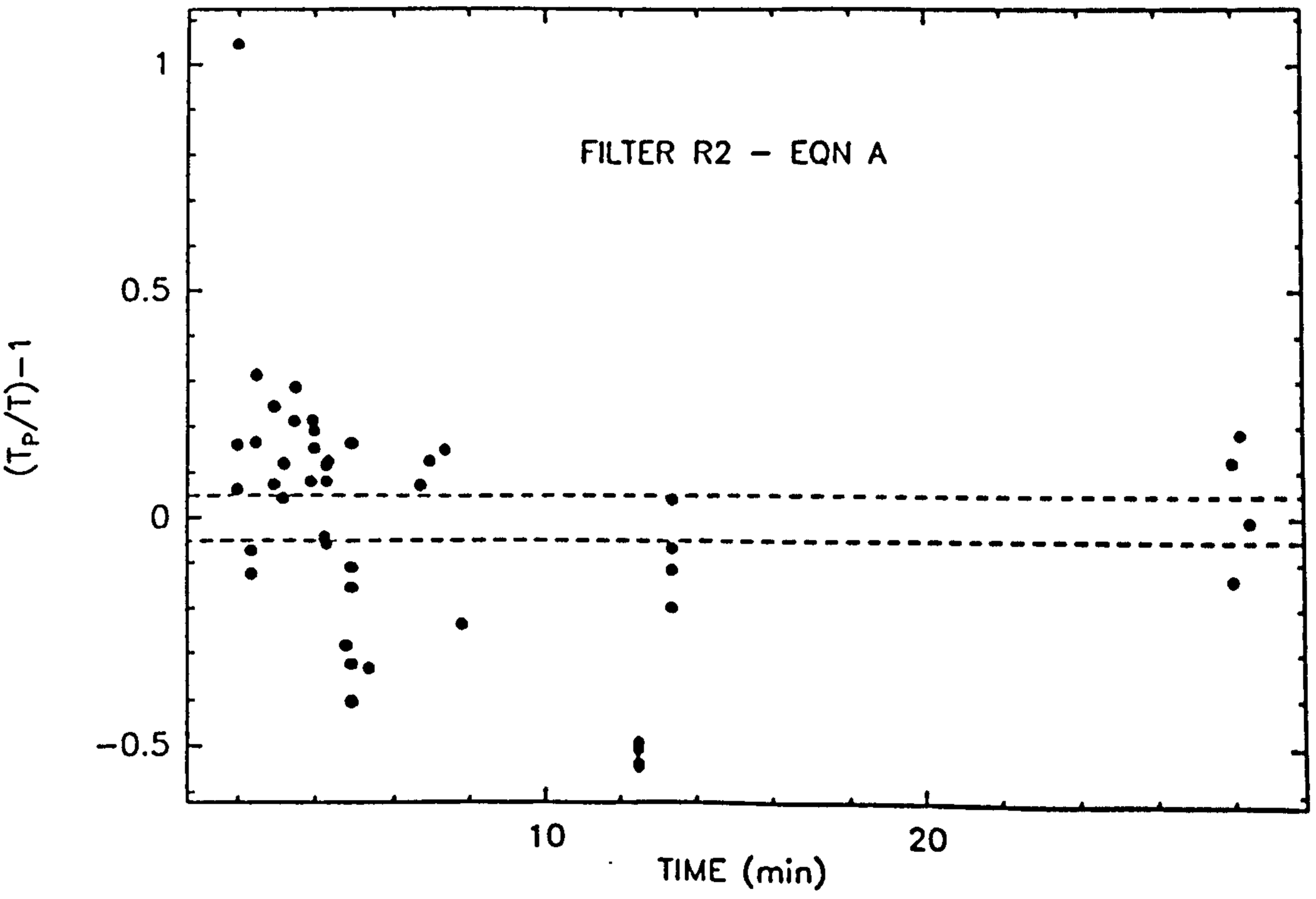
FILTER R2 – EQN A
1
0.5
0
−0.5
$(T_P/T)-1$
10
20
TIME (min)

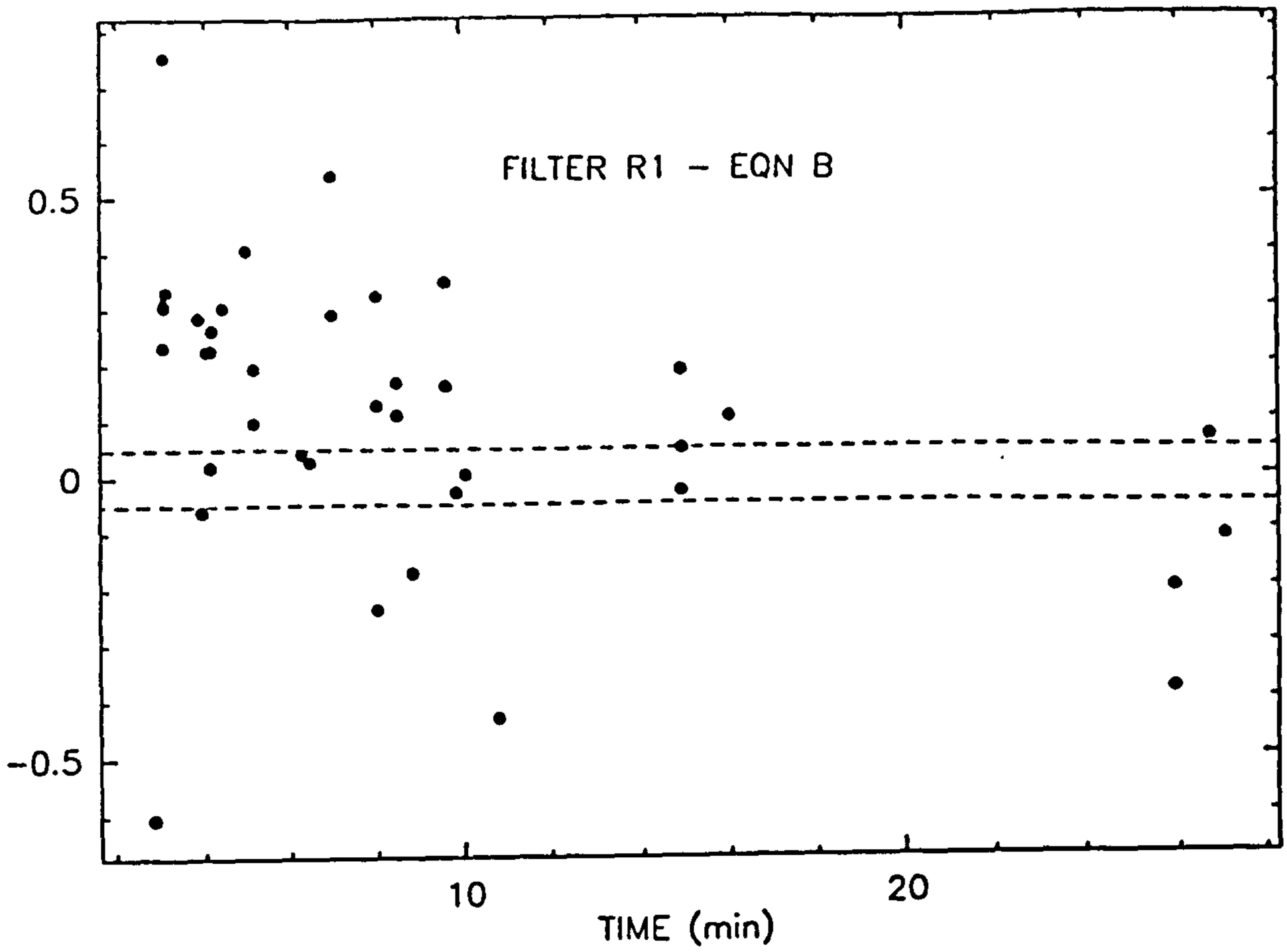
FILTER R1 – EQN B
0.5
0
−0.5
(Tp/T)−1
10
20
TIME (min)

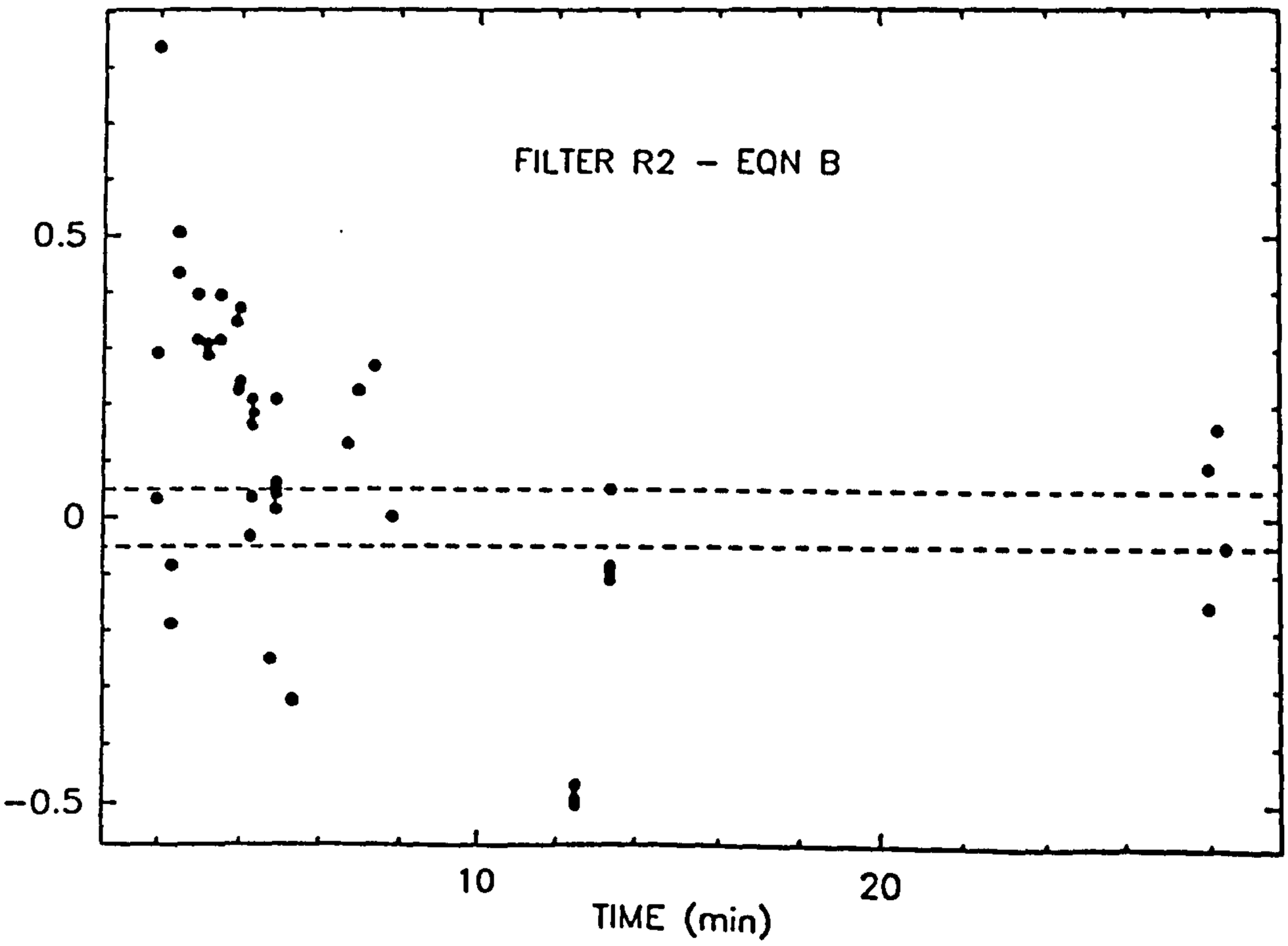
FILTER R2 – EQN B
0.5
0
−0.5
(Tp/T)−1
10
20
TIME (min)

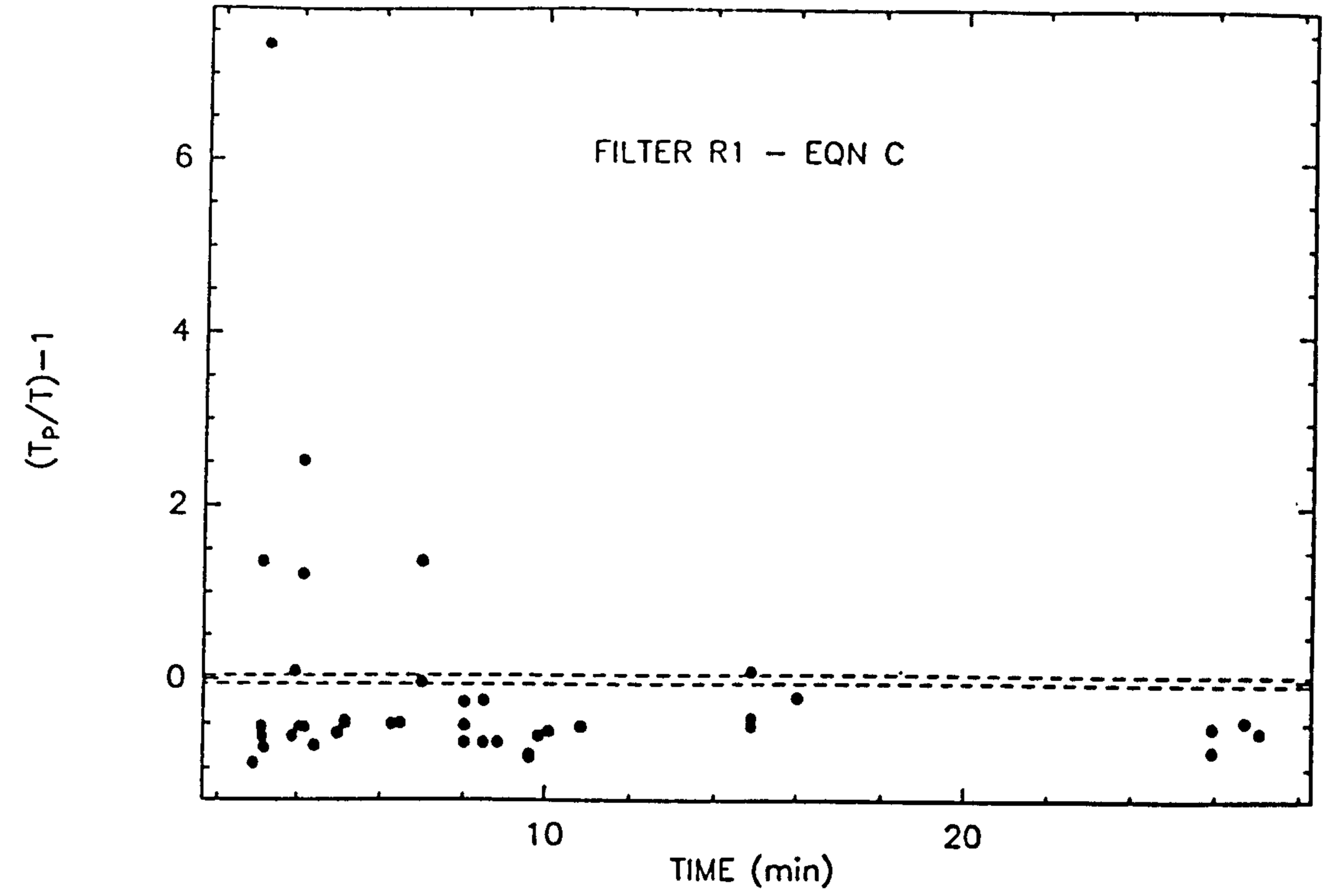
FILTER R1 – EQN C
$(T_p/T)-1$
6
4
2
0
10
20
TIME (min)

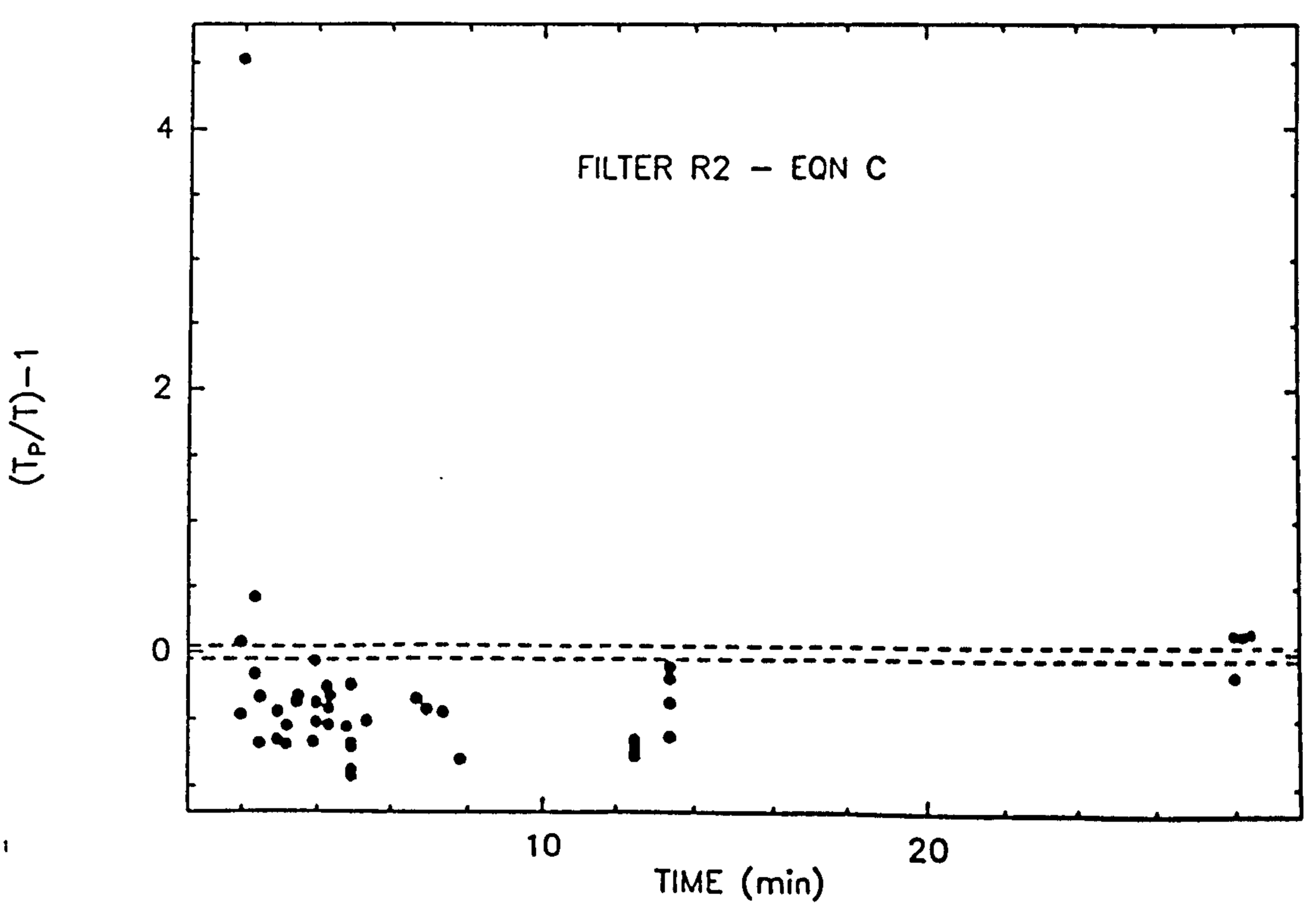
FILTER R2 – EQN C
$(T_p/T)-1$
4
2
0
10
20
TIME (min)

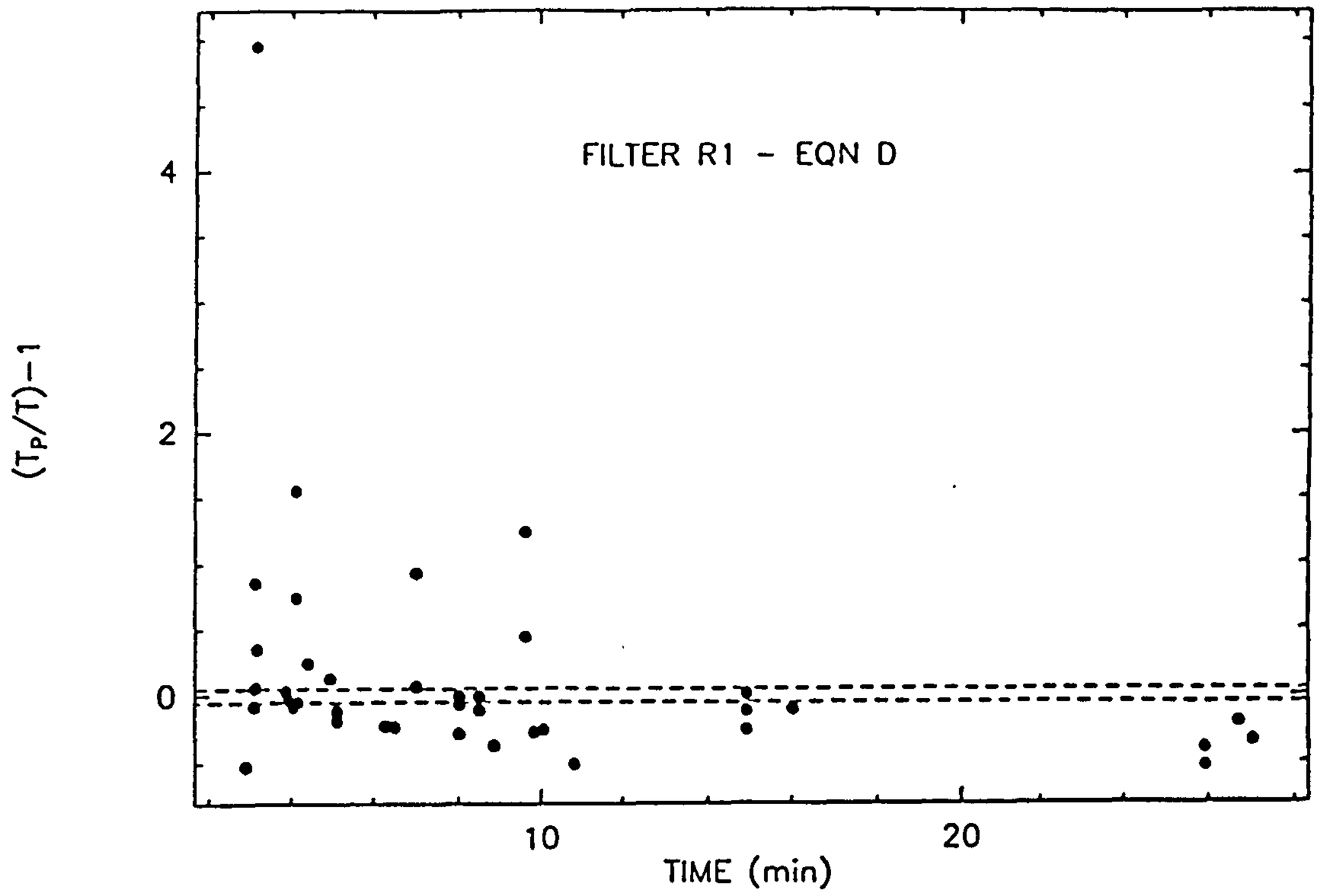
FILTER R1 – EQN D
4
2
0
10
20
TIME (min)
$(T_P/T)-1$

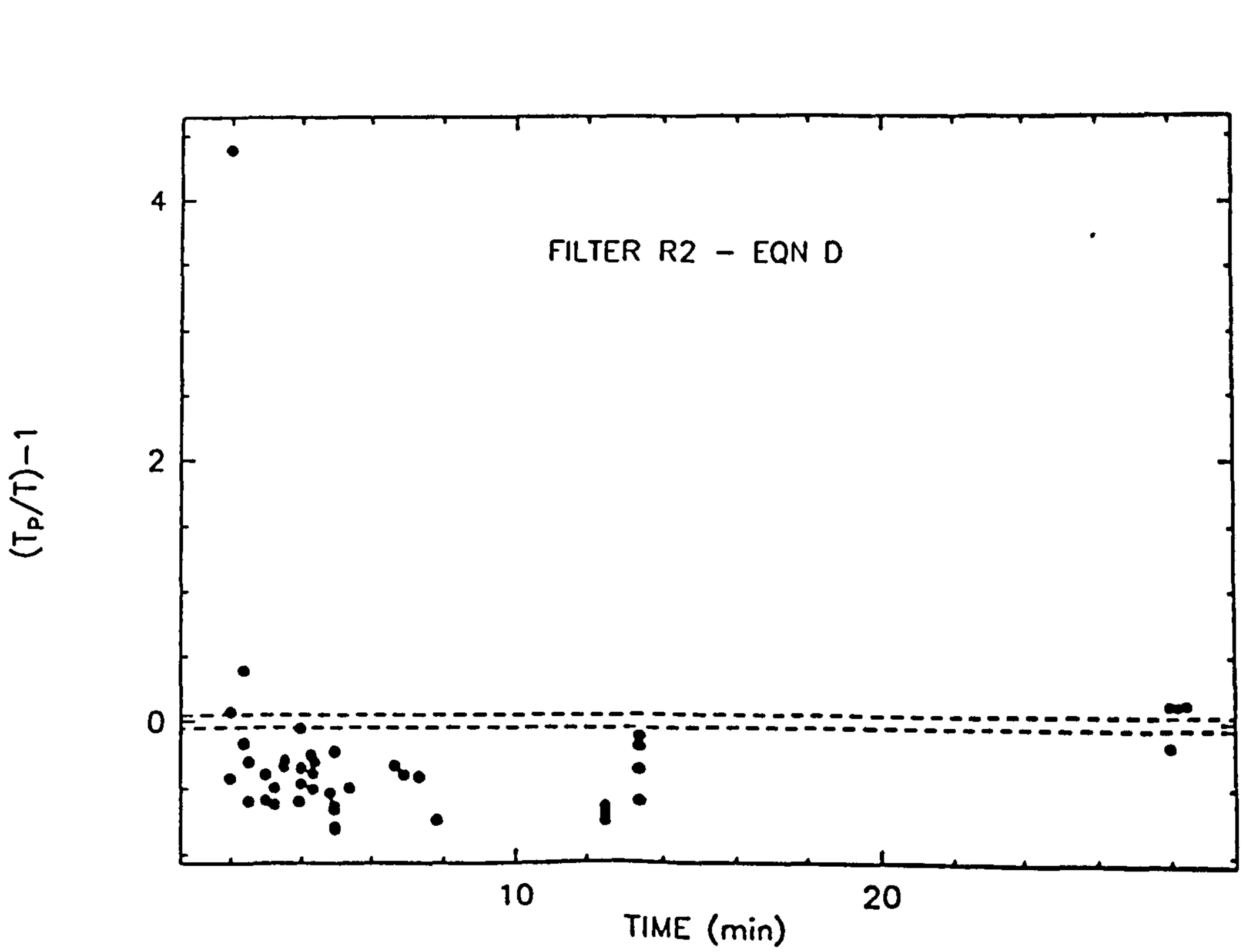
FILTER R2 – EQN D
4
2
0
10
20
TIME (min)
$(T_P/T)-1$

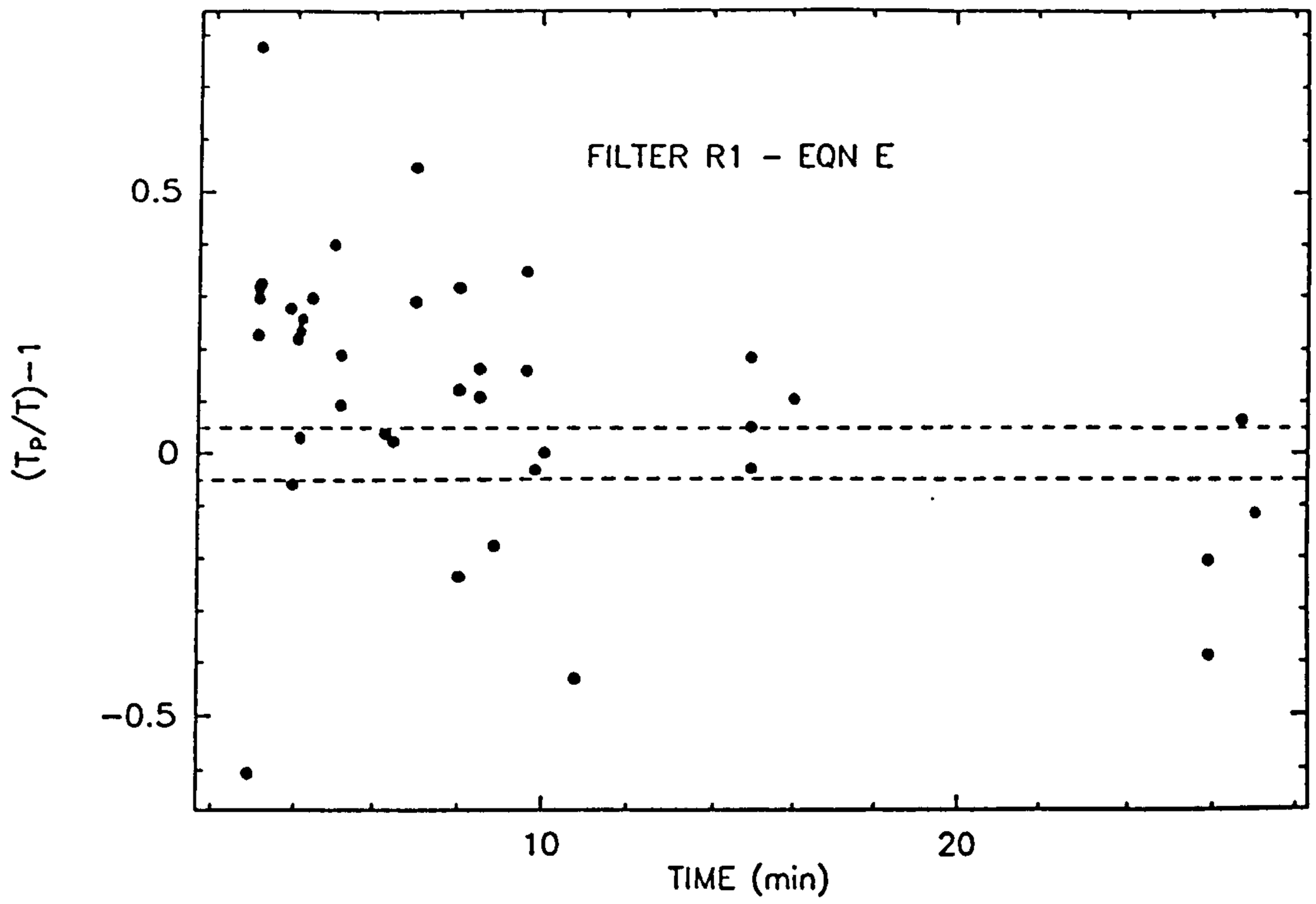
FILTER R1 – EQN E
0.5
0
−0.5
$(T_P/T)-1$
10
20
TIME (min)

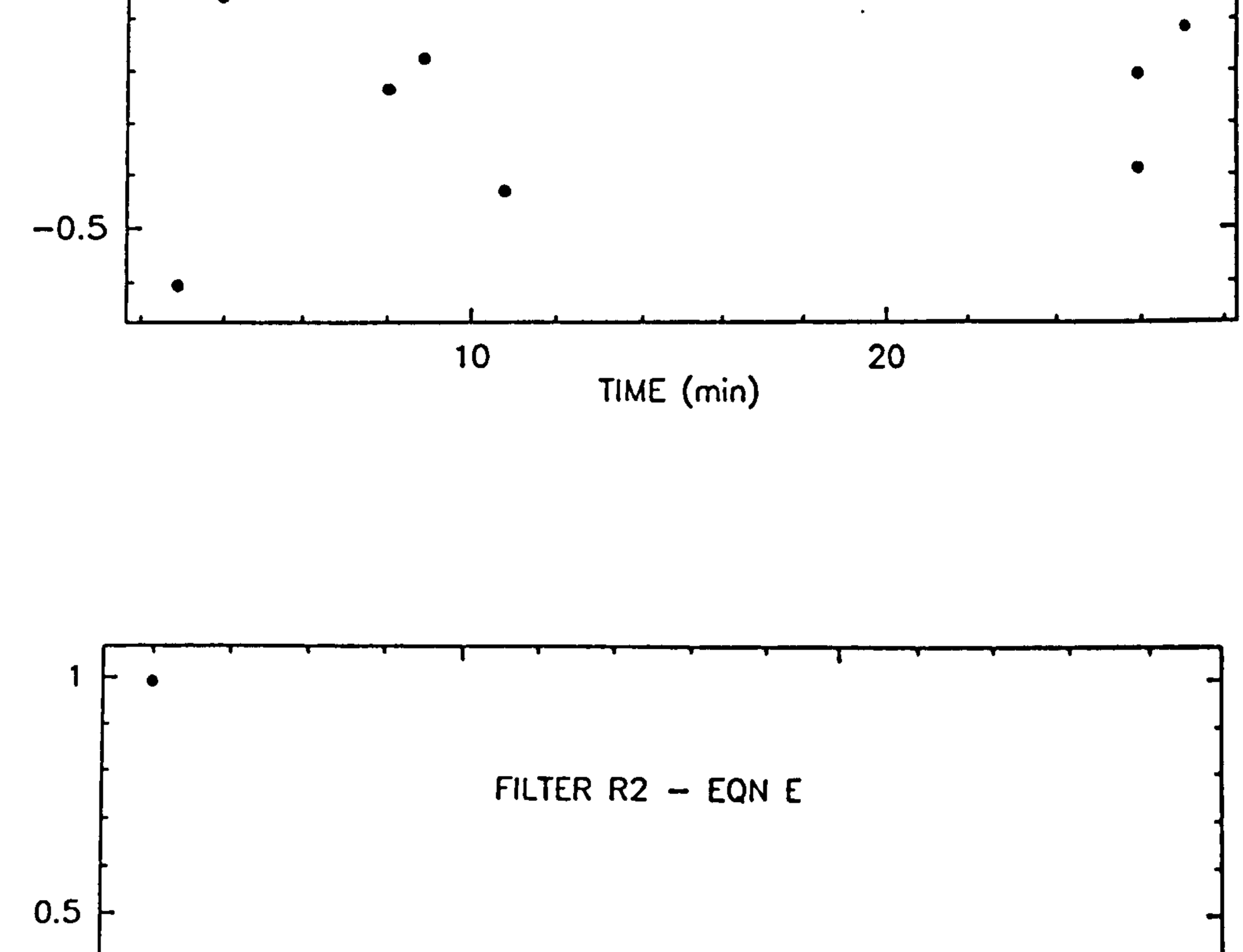
FILTER R2 – EQN E
1
0.5
0
−0.5
$(T_P/T)-1$
10
20
TIME (min)

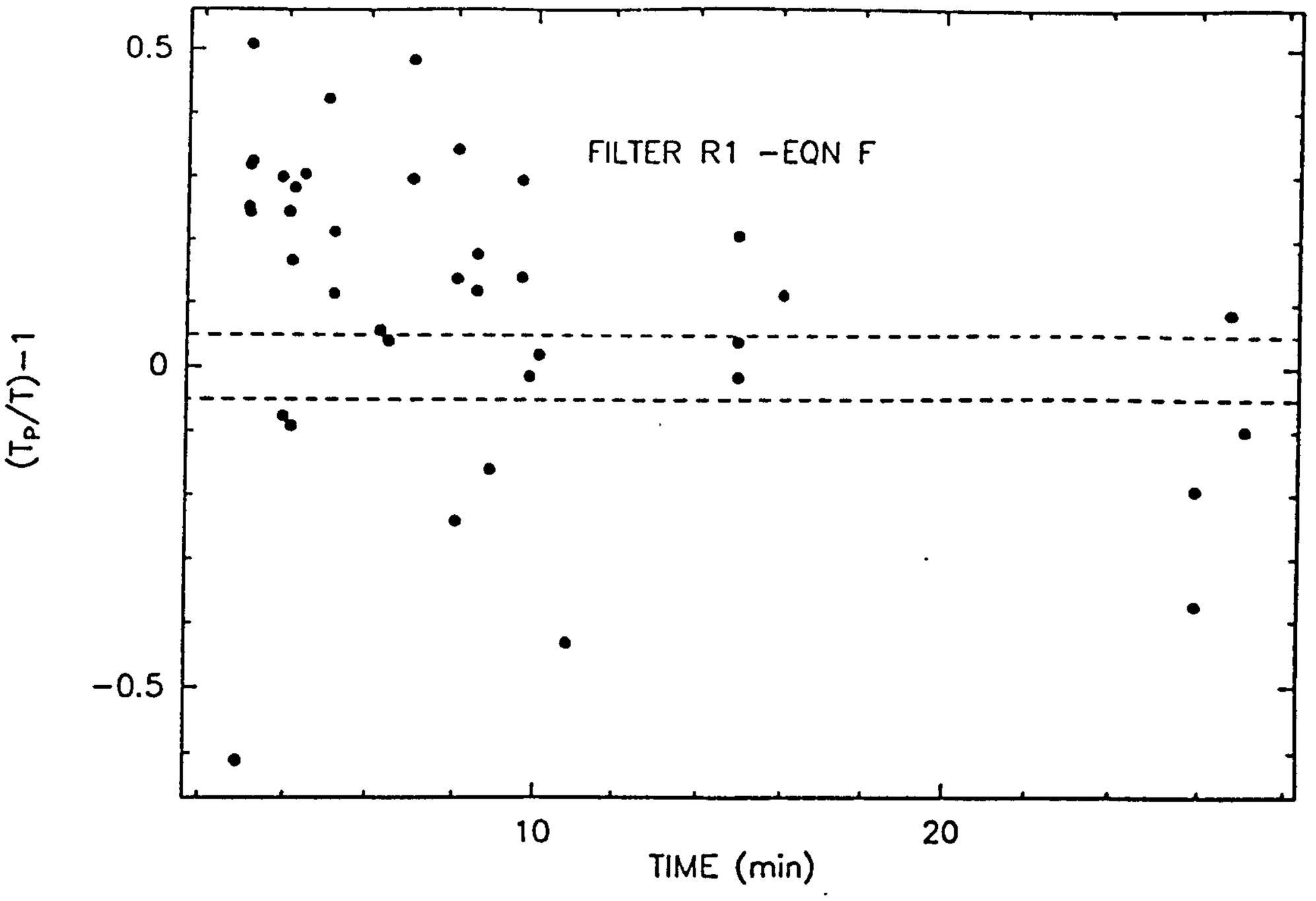
FILTER R1 –EQN F
0.5
0
−0.5
(Tp/T)−1
10
20
TIME (min)

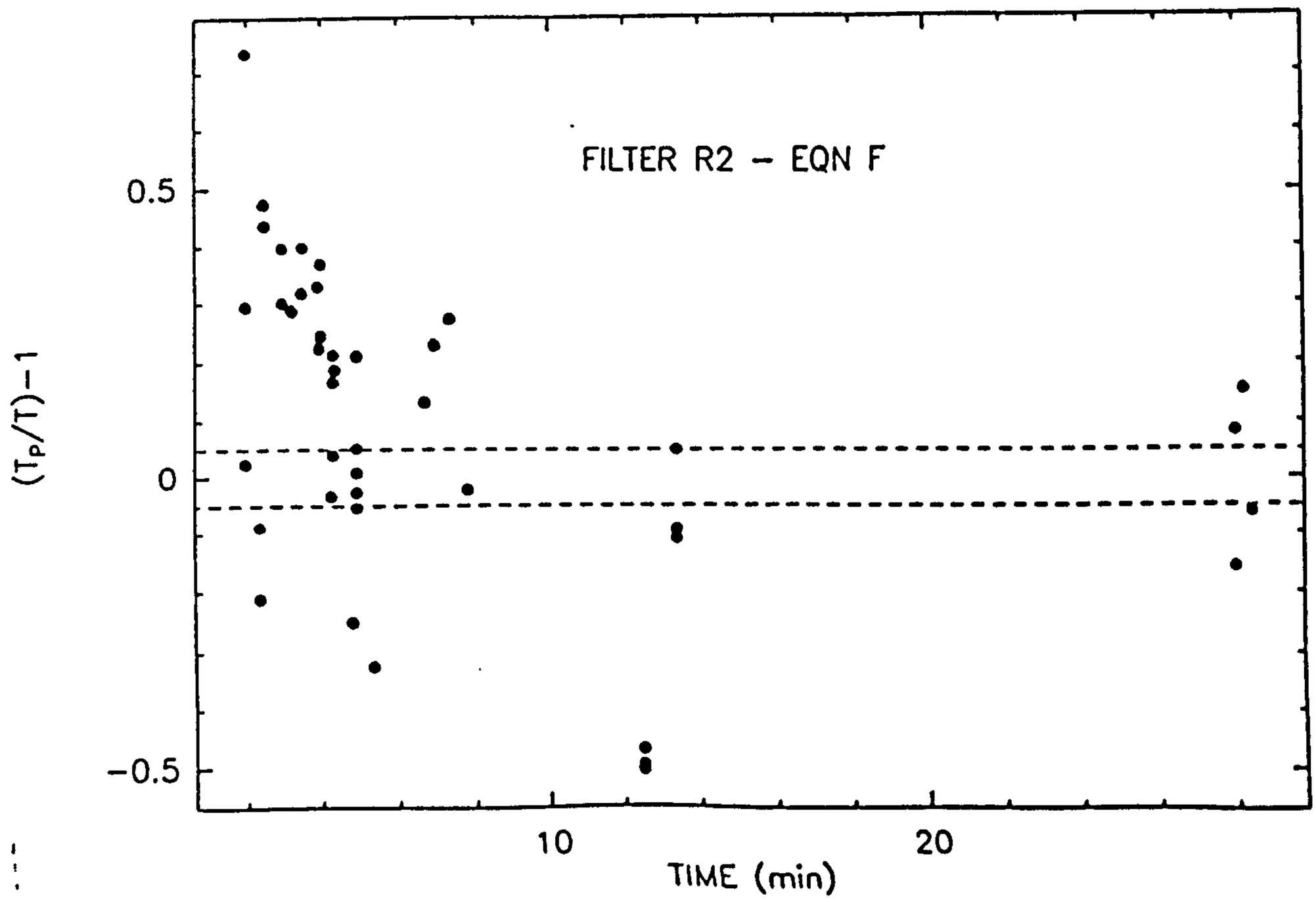
FILTER R2 – EQN F
0.5
0
−0.5
(Tp/T)−1
10
20
TIME (min)

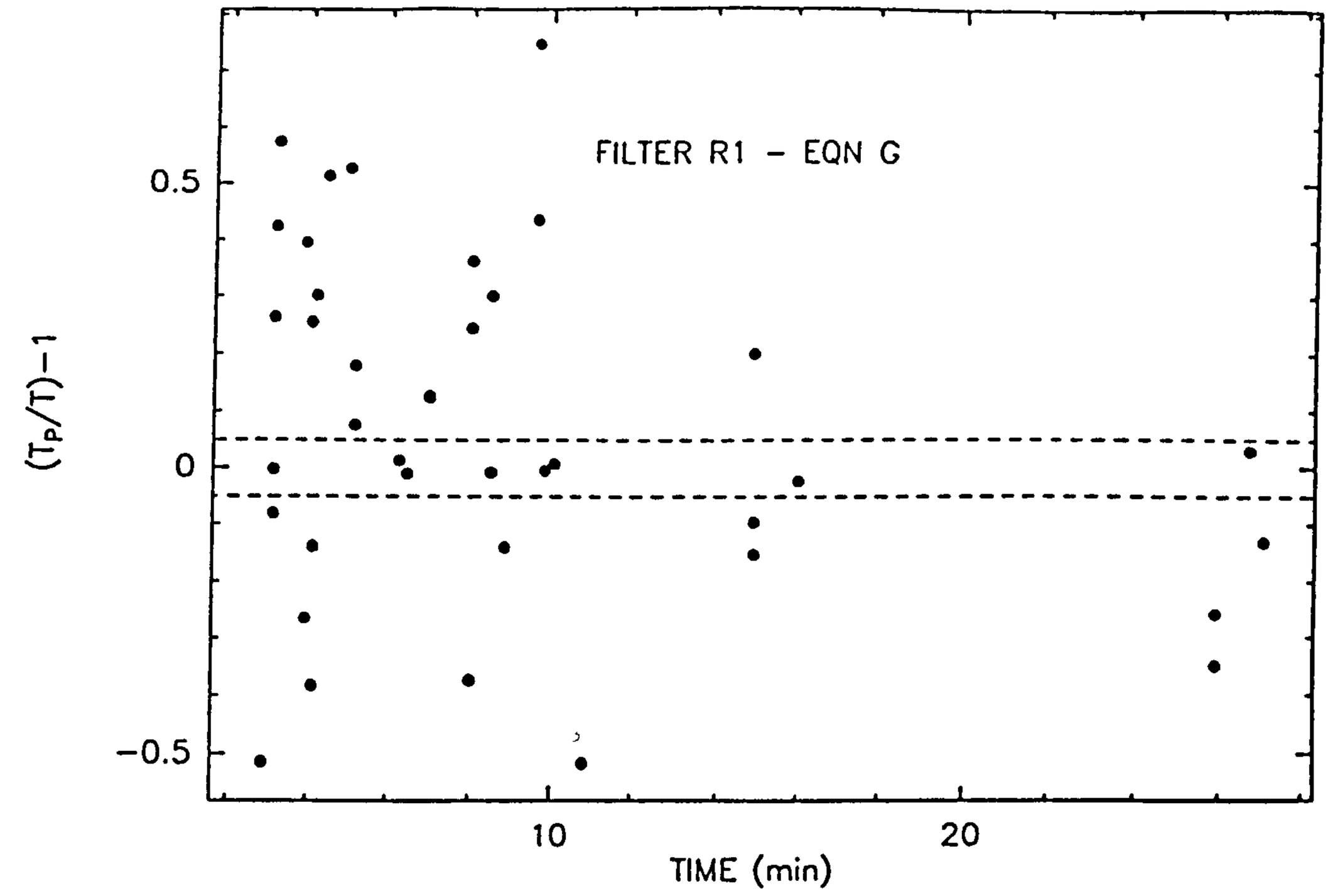
FILTER R1 – EQN G
0.5
0
−0.5
$(T_P/T)-1$
10
20
TIME (min)

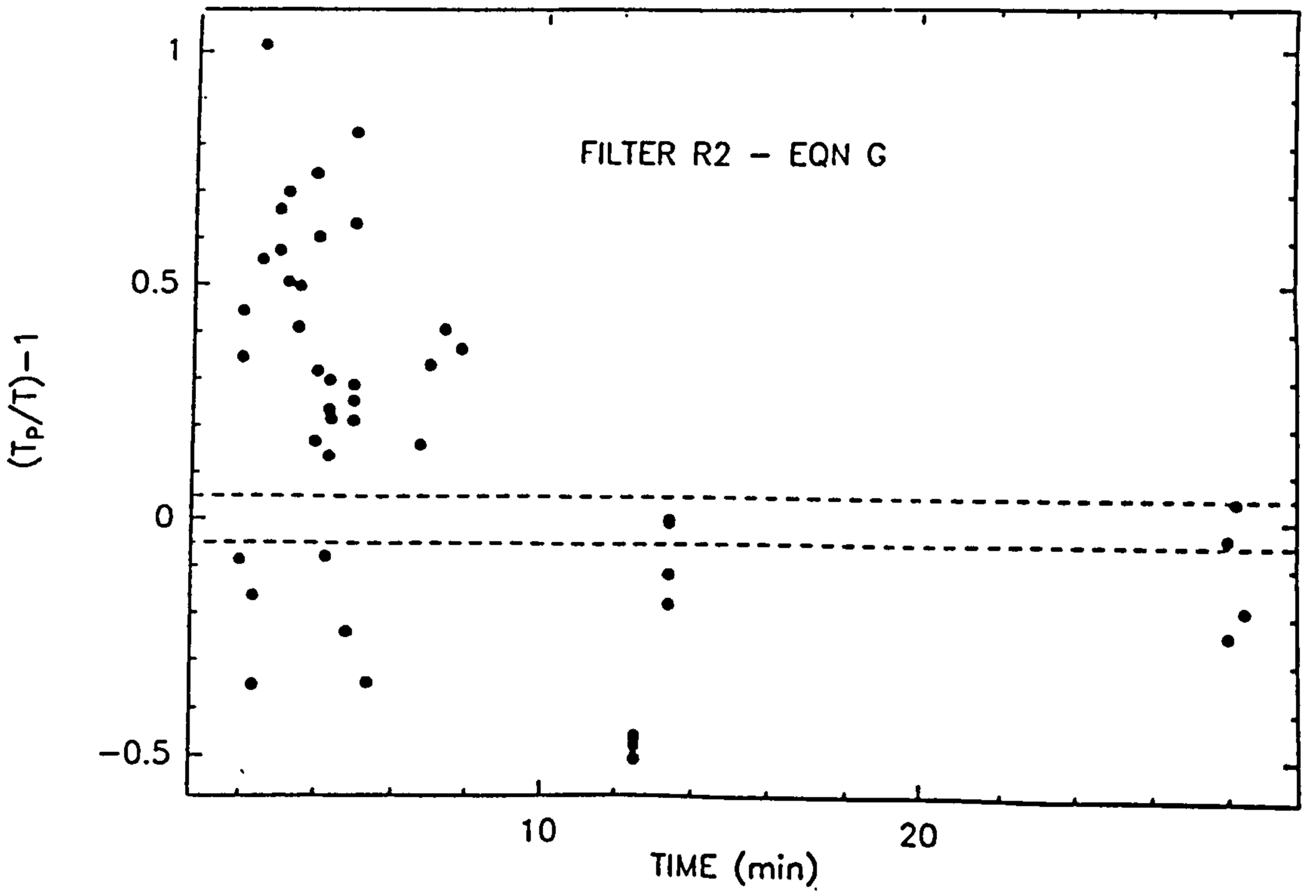
FILTER R2 – EQN G
1
0.5
0
−0.5
$(T_P/T)-1$
10
20
TIME (min)

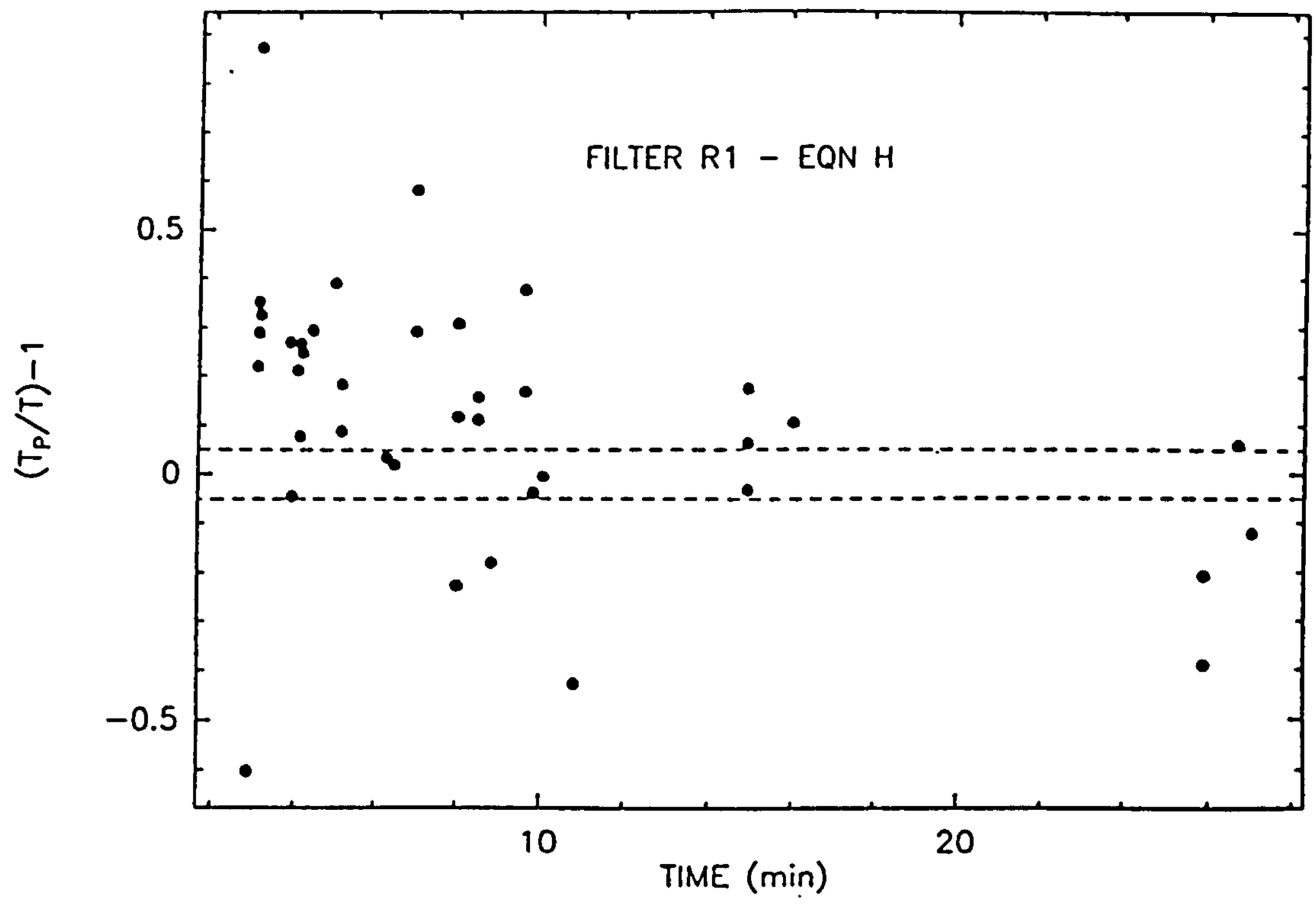
FILTER R1 – EQN H
0.5
0
−0.5
$(T_P/T)-1$
10
20
TIME (min)

FILTER R2 – EQN H
1
0.5
0
−0.5
$(T_P/T)-1$
10
20
TIME (min)

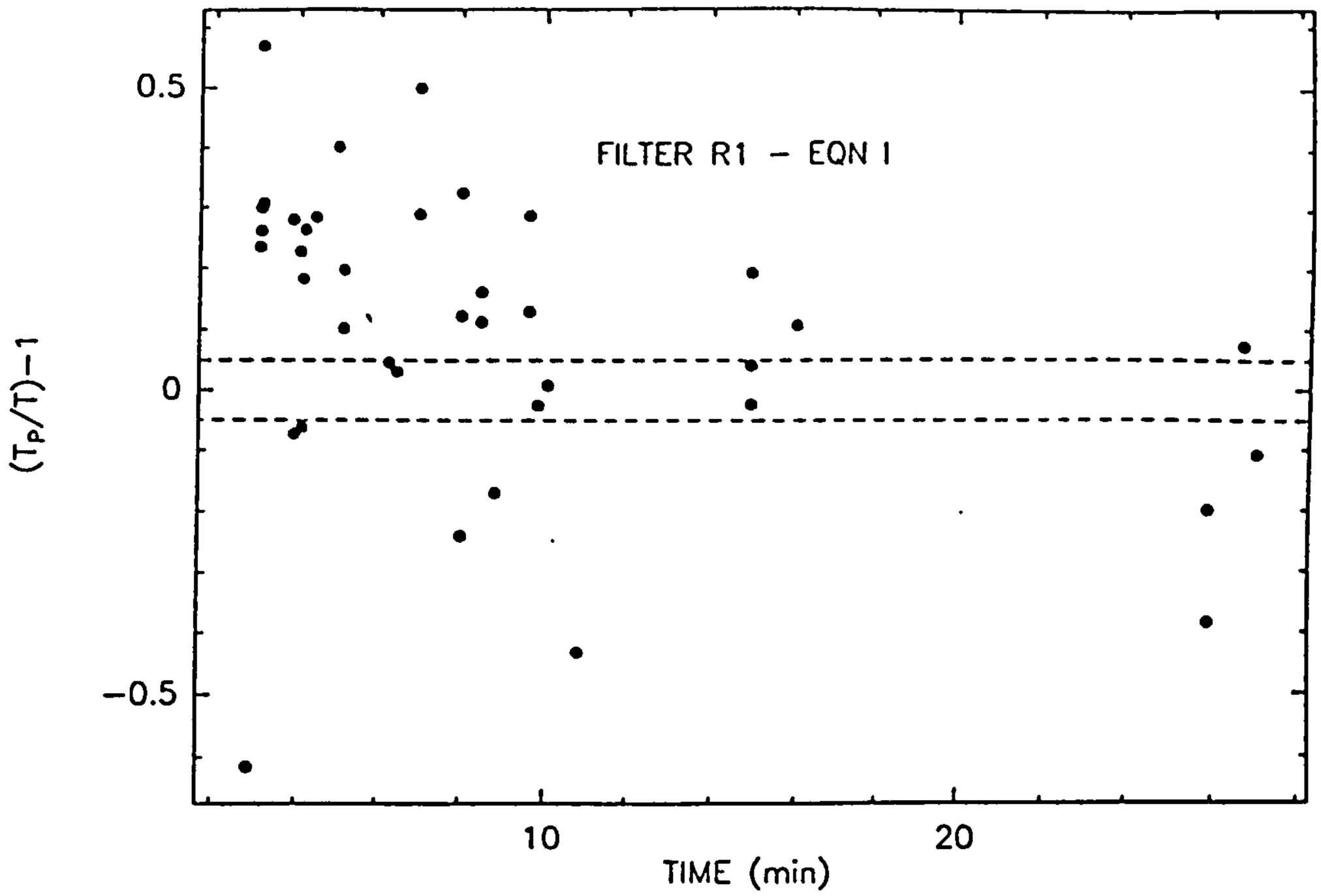
FILTER R1 – EQN 1
0.5
0
−0.5
(Tp/T)−1
10
20
TIME (min)

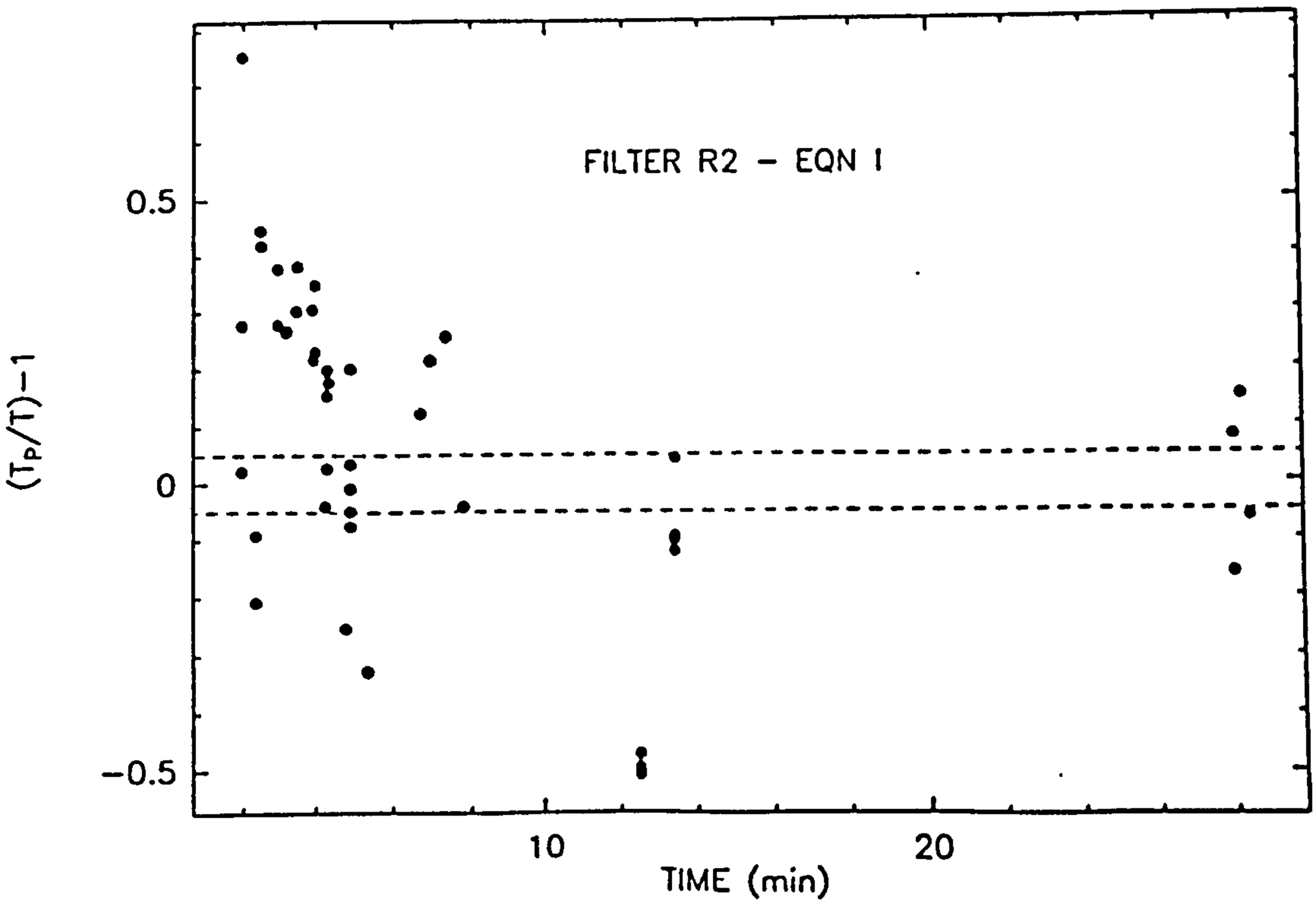
FILTER R2 – EQN 1
0.5
0
−0.5
(Tp/T)−1
10
20
TIME (min)

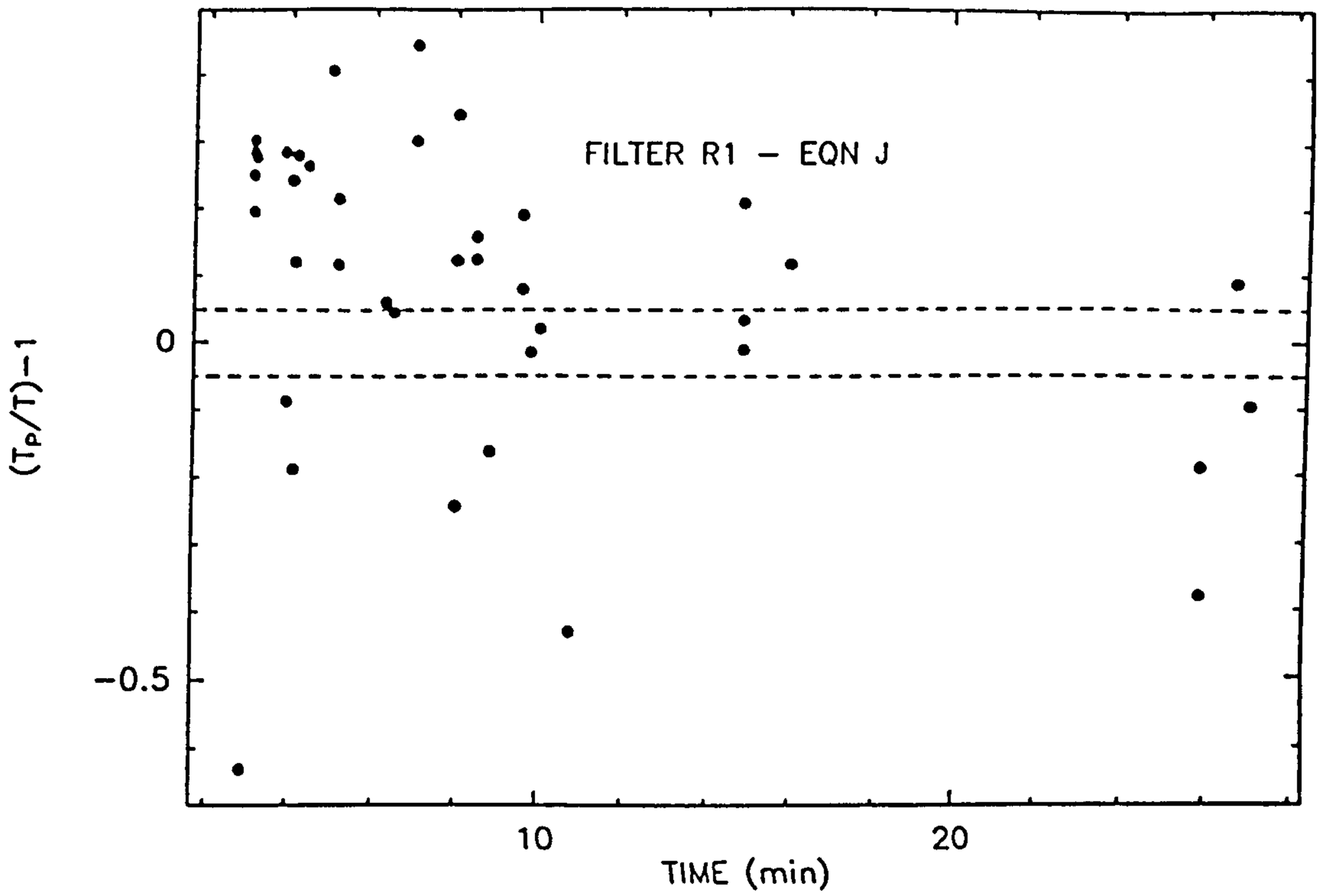
FILTER R1 – EQN J
0
-0.5
$(T_P/T)-1$
10
20
TIME (min)

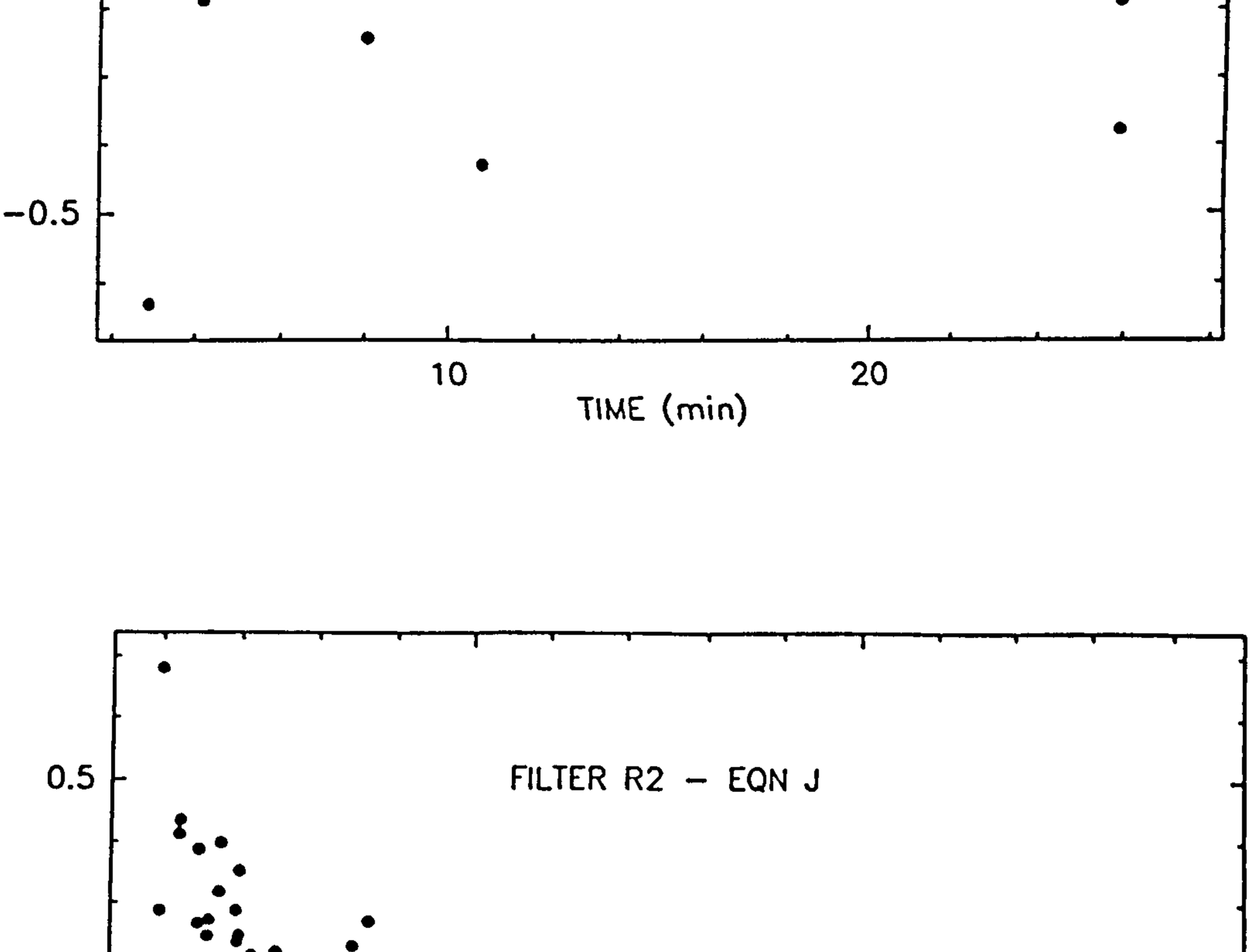
FILTER R2 – EQN J
0.5
0
-0.5
$(T_P/T)-1$
10
20
TIME (min)

APPENDIX 4.a

PLAN VIEW

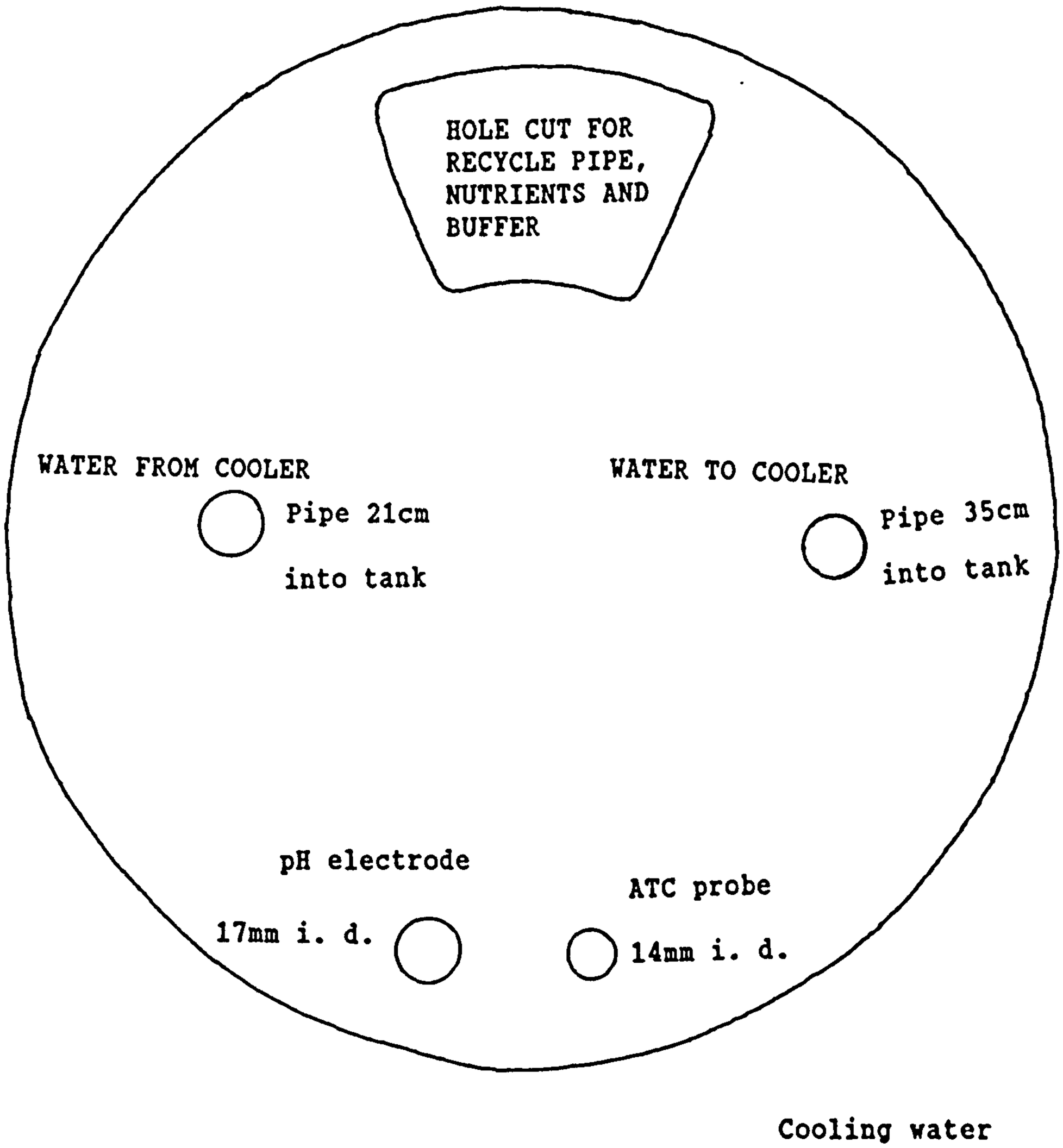

Cooling water pipes 17mm i. d.

Scale 10cm

APPENDIX 4.b

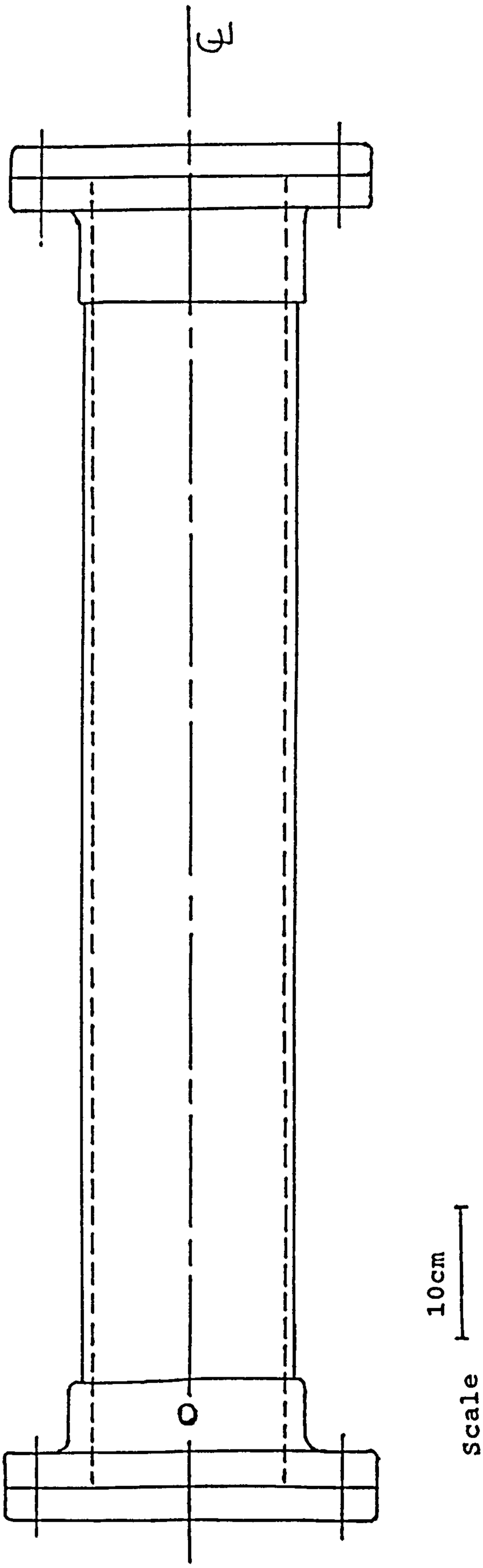

APPENDIX 4.c

FILTER MEDIA PARTICLE SIZE DISTRIBUTION

N	Xm (mm)	NXm^2 (mm^2)	NXm^3 (mm^3)
1	2.25	5.1	11.4
7	2.70	51.0	137.8
9	3.15	89.3	281.3
18	3.60	233.3	839.8
30	4.05	492.1	1992.9
55	4.50	1113.8	5011.9
40	4.95	980.1	4851.5
56	5.40	1633.0	8818.0
47	5.85	1608.5	9409.5
35	6.30	1389.2	8751.6
24	6.75	1093.5	7381.1
21	7.20	1088.6	7838.2
9	7.65	526.7	4029.3
4	8.10	262.4	2125.8
4	8.55	292.4	2500.1
10	9.00	810.0	7290.0
1	9.45	89.3	843.9
2	9.90	196.0	1940.6
373		11954.3	74054.7

$$\text{Volume average size} = \frac{74054.7}{373} = 5.8 \text{ mm}$$

$$\text{Specific surface average size} = \frac{74054.7}{11954.3} = 6.2 \text{ mm}$$

APPENDIX 4.d

Medium for Nitrosomonas

$(NH_4)_2SO_4$	0.235 g
KH_2PO_4	0.200 g
$CaCl_2.2H_2O$	0.040 g
$MgSO_4.7H_2O$	0.040 g
$FeSO_4$	0.5 mg
Na EDTA	0.5 mg
Phenol Red	0.5 mg
Distilled Water	1000 ml

Medium for Nitrobacter

As above but $NaNO_2$ replacing $(NH_4)_2SO_4$.

$NaNO_2$	0.246 mg

Only a small amount of ammonia was added to the filter to avoid clogging the small filter media. However, the amount of ammonia handled could be very much higher in an operational filter. The small experimental rig size meant that the packing size also had to be scaled down. The media size corresponds to the recommendation made in chapter 8.

The total ammonia - nitrogen supplied was:

50 mg/l - N added at 270 ml/hr = 0.324 g/day

APPENDIX 5.a

THE SHAPE OF THE AMMONIA CONCENTRATION v TIME CURVE

pH 8.0 Temperature 24 C

2.01 g NH_4SO_4 added 13 minutes before the first sample was taken.

TOTAL AMMONIA

Measured Extinction

Time	Sample	*10	*25	*50
0.0	I1			0.482
121.0	I2			0.422
240.0	I3		0.590	0.371
450.0	I4		0.360	
540.0	I5		0.272	
580.0	I6	0.582	0.275	

Time	Sample	*10	*25	*50
0.0	O1			0.483
121.0	O2			0.395
240.0	O3		0.560	0.350
450.0	O4		0.365	
540.0	O5		0.316	
580.0	O6	0.577	0.262	

Blank	Standards	F
0.088	0.204	25.862

Calculated Ammonia

Time	Sample	*10	*25	*50
0.0	I1			7137.9
121.0	I2			6045.4
240.0	I3		4547.2	5132.4
450.0	I4		2463.8	
540.0	I5		1664.0	
580.0	I6	1788.8		

Time	Sample	*10	*25	*50
0.0	O1			7156.0
121.0	O2			5561.7
240.0	O3		4275.5	4746.5
450.0	O4		2509.1	
540.0	O5		2062.6	
580.0	O6	1771.8		

TOTAL NITRITE

Measured Extinction

Time	Sample	NoDil	Sample	NoDil
0.0	I1	0.920	O1	0.930
121.0	I2	0.070	O2	0.046
240.0	I3	0.075	O3	0.074
450.0	I4	0.064	O4	0.082
540.0	I5	0.105	O5	0.061
580.0	I6	0.075	O6	0.069

Blank	Standard
0.035	0.431

5.054

Calculated Nitrite

Time	Sample	NoDil	Sample	NoDil
0.0	I1	62.6	O1	63.4
121.0	I2	2.46	O2	0.76
240.0	I3	2.81	O3	2.74
450.0	I4	2.03	O4	3.31
540.0	I5	4.94	O5	1.82
580.0	I6	2.82	O6	2.39

TOTAL NITRATE

Measured Extinction

Time	Sample	*100	Sample	*100
0.0	I1	1.070	O1	1.167
121.0	I2	1.130	O2	1.080
240.0	I3	1.178	O3	1.203
450.0	I4	0.930	O4	1.310
540.0	I5	1.440	O5	0.980
580.0	I6	1.310	O6	1.213

Blank	Standard
0.045	0.901

23.375

Calculated Nitrite

Time	Sample	*100	Sample	*100
0.0	I1	33.57	O1	36.74
121.0	I2	35.53	O2	33.90
240.0	I3	37.11	O3	37.92
450.0	I4	28.98	O4	41.43
540.0	I5	45.69	O5	30.62
580.0	I6	41.43	O6	38.25

REPEATABILITY EXPERIMENT

First Experiment

pH 8.3 Temperarure 23 C

0.14 g NH_4SO_4 added 10 minutes before the first sample was taken.

Measured Extinctions

Time	Sample	NoDil	*2	*5
0.0	0		1.200	0.520
15.0	1		1.050	0.510
30.0	2	0.395	0.252	
45.0	3	0.150	0.110	
60.0	4	0.105		
75.0	5	0.117		
90.0	6	0.100		
105.0	7	0.116		
120.0	8	0.123		

Blank	Standards	F
0.090	0.212	24.590

Calculated Total Ammonia

Time	Sample	NoDil	*2	*5
0.0	0		764.81	740.69
15.0	1		661.46	723.47
30.0	2	105.08	111.62	
45.0	3	20.67	13.78	
60.0	4	5.17		
75.0	5	9.30		
90.0	6	3.45		
105.0	7	8.96		
120.0	8	11.37		

Second Experiment

pH 8.3 Temperarure 23 C

0.173 g $NH_4 SO_4$ added 10 minutes before the first sample was taken.

Measured Extinctions

Time	Sample	NoDil	*2	*5
0.0	0		0.987	0.502
15.0	1		0.793	0.412
30.0	2	1.050	0.586	0.319
45.0	3	0.680	0.405	
60.0	4	0.400	0.261	
75.0	5	0.174		
90.0	6	0.164		
105.0	7	0.156		
120.0	8	0.165		

Blank	Standards	F
0.141	0.267	23.866

Calculated Total Ammonia

Time	Sample	NoDil	*2	*5
0.0	0		565.55	603.03
15.0	1		435.82	452.57
30.0	2	303.84	297.19	297.59
45.0	3	180.12	176.35	
60.0	4	86.50	79.85	
75.0	5	10.93		
90.0	6	7.59		
105.0	7	4.82		
120.0	8	7.82		

TOTAL AMMONIA

pH 6.2 Temperature 23.5 C

0.177 g $(NH_4)_2SO_4$ added 15 minutes before the first sample was taken.

Measured Extinction

Time	Sample	NoDil	*2	*5	*10	*25
0.0	0				0.351	0.240
5.0	1				0.367	0.276
10.00	2				0.368	0.266
15.00	3				0.370	0.233
30.0	4			0.474	0.440	
45.0	5	1.662		0.455		
60.0	6	1.547		0.407		
75.0	7	1.726	0.942	0.515		
90.0	8	1.262		0.377		

Blank	Standards	F
0.155	0.246	33.113

Calculated Total Ammonia

Time	Sample	NoDil	*2	*5	*10	*25
0.0	0				909.26	985.80
5.0	1				983.48	1399.84
10.00	2				988.12	1282.70
15.00	3				995.55	904.62
30.0	4			739.24	1322.14	
45.0	5	699.11		695.86		
60.0	6	645.76		583.83		
75.0	7	728.8	729.91	835.03		
90.0	8	513.55		514.94		

TOTAL AMMONIA

pH 7.2 Temperature 23C

0.177g $(NH_4)_2SO_4$ added 15 minutes before the first sample was taken.

Measured Extinction

Time	Sample	NoDil	*2	*5	*10	*25
0.0	0				0.291	0.187
3.0	1				0.262	0.170
6.0	2				0.258	0.158
9.0	3			0.383	0.241	
12.0	4		0.539	0.289		
15.0	5	0.849	0.468			
20.0	6	0.552	0.324			
25.0	7	0.318	0.235			
30.0	8	0.217	0.171	0.143		

Blank	Standards	F
0.128	0.268	21.429

Calculated Total Ammonia

Time	Sample	NoDil	*2	*5	*10	*25
0.0	0				490.25	445.07
3.0	1				403.19	317.48
6.0	2				390.28	229.66
9.0	3			383.67	341.04	
12.0	4		246.96	242.1		
15.0	5	216.55	204.15			
20.0	6	127.38	117.86			
25.0	7	57.13	64.43			
30.0	8	26.81	26.0	23.0		

TOTAL AMMONIA

pH 8.0 Temperature 23 C

0.17 g $(NH_4)_2SO_4$ added 15 minutes before the first sample was taken.

Measured Extinction

Time	Sample	NoDil	*2	*5	*10
0.0	0			0.478	0.276
3.0	1			0.395	0.245
6.0	2		0.747	0.378	0.240
9.0	3		0.595	0.305	
12.0	4	0.892	0.500		
15.0	5	0.529	0.315		
20.0	6	0.384	0.242		
25.0	7	0.227	0.169		
30.0	8	0.149	0.127		

Blank	Standards	F
0.112	0.248	21.946

Calculated Total Ammonia

Time	Sample	NoDil	*2	*5	*10
0.0	0			562.66	506.08
3.0	1			435.52	409.85
6.0	2		390.48	409.39	393.55
9.0	3		297.19	297.62	
12.0	4	239.91	238.59		
15.0	5	128.4	124.83		
20.0	6	83.81	79.94		
25.0	7	35.36	35.05		
30.0	8	11.56	9.22		

TOTAL AMMONIA

pH 9.0 Temperature 23 C

0.175 g $(NH_4)_2SO_4$ added 15 minutes before the first sample was taken.

Measured Extinction

Time	Sample	NoDil	*2	*5	*10
0.0	0		0.924	0.440	0.269
3.0	1		0.887	0.423	
6.0	2		0.706	0.347	
9.0	3		0.686	0.340	
12.0	4	0.909	0.501		
15.0	5	0.640	0.370		
20.0	6	0.392	0.248		
25.0	7	0.249	0.181		
30.0	8	0.168	0.139		

Blank	Standards	
0.109	0.226	25.641

Calculated Total Ammonia

Time	Sample	NoDil	*2	*5	*10
0.0	0		585.55	594.53	574.77
3.0	1		558.96	564.53	
6.0	2		428.92	427.49	
9.0	3		414.34	414.91	
12.0	4	287.49	281.85		
15.0	5	190.75	187.52		
20.0	6	101.77	99.87		
25.0	7	50.29	51.51		
30.0	8	21.30	21.77		

TOTAL NITRITE

pH 7.5 Temperature 22 C

0.173 g $NaNO_2$ added 5 minutes before the first sample was taken.

Measured Extinction

Time	Sample	NoDil	*2	*5	*10
0.0	0				0.897
3.0	1				0.710
6.0	2			1.083	0.528
9.0	3		2.0	0.713	
12.0	4		1.020	0.418	
15.0	5	0.933			
20.0	6	0.170			
25.0	7	0.039			
30.0	8	0.018			

Blank	Standards	F
0.013	0.444	4.640

Calculated Nitrite

Time	Sample	NoDil	*2	*5	*10
0.0	0				574.70
3.0	1				453.13
6.0	2			347.81	334.81
9.0	3		258.36	227.54	
12.0	4		130.93	131.65	
15.0	5	59.81			
20.0	6	10.21			
25.0	7	1.69			
30.0	8	0.33			

TOTAL NITRITE

pH 8.3 Temperature 24 C

0.169 g $NaNO_2$ added 5 minutes before the first sample was taken.

Measured Extinction

Time	Sample	NoDil	*2	*5	*10	*25
0.0	0				0.713	0.264
3.0	1			0.750	0.523	
6.0	2			0.725	0.363	
9.0	3			0.348		
12.0	4		0.500	0.240		
15.0	5	0.379	0.255			
20.0	6	0.079				
25.0	7	0.036				
30.0	8	0.013				

Blank	Standards	F
0.008	0.364	5.623

Calculated Nitrite

Time	Sample	NoDil	*2	*5	*10	*25
0.0	0				555.12	504.18
3.0	1			292.13	405.45	
6.0	2			282.29	279.41	
9.0	3			133.8		
12.0	4		77.47	91.26		
15.0	5	29.20	38.87			
20.0	6	5.55				
25.0	7	2.15				
30.0	8	0.33				

TOTAL NITRITE

pH 9.0 Temperature 24 C

0.180 g $NaNO_2$ added 5 minutes before the first sample was taken.

Measured Extinction

Time	Sample	NoDil	*2	*5	*10	*25
0.0	0				0.870	0.338
3.0	1				0.675	
6.0	2				1.0	0.473
9.0	3		1.600		0.700	
12.0	4		0.826		0.421	
15.0	5	0.685	0.363			
20.0	6	0.139				
25.0	7	0.029				
30.0	8	0.019				

Blank	Standards	F
0.008	0.364	5.623

Calculated Nitrite

Time	Sample	NoDil	*2	*5	*10	*25
0.0	0				678.8	648.7
3.0	1				525.19	
6.0	2			390.60	366.06	
9.0	3		250.77	272.44		
12.0	4		128.83	162.55		
15.0	5	53.31				
20.0	6	10.3				
25.0	7	1.6				
30.0	8	0.87				

APPENDIX 6.a

European Water Charter

Water knows no frontiers

Water is a human problem

1. There is no life without water. It is a treasure indispensable to all human activity.
2. Fresh water resources are not inexhaustable. It is essential to conserve, control and wherever possible, to increase them.
3. To pollute water is to harm man and other living creatures which are dependant on water.
4. The quality of water must be maintained at levels suitable for further use to be made of it and, in particular, must meet appropriate public health standards.
5. When used water is returned to a common source it must not impair further uses, both public and private, to which the common source will be put.
6. The maintenance of an adequate vegetation cover, preferably forrest land, is imperative for the conservation of water resources.
7. Water resources must be assessed.
8. The wise husbandry of water resources must be planned by the appropriate authorities.
9. Conservation of water calls for intensified scientific research, training of specialists, and public information services.

10. Water is a common heritage, the values of which must be recognized by all. Everyone has the duty to use water carefully and economically.

11. The management of water resources should be based on their natural basins rather than on political and administrative boundaries.

12. Water knows no frontiers; as a common resources it demands international co-operation.

REFERENCES

1. Tiews, K. (Editor) *Proceedings of the World Symposium on Aquaculture in Heated Effluents and Recirculation Systems*. Vol.1 and Vol.11.(1981).

2. Boyd, E. *Water Quality Management for Pond Fish Culture*. Developments in Aquaculture and Fisheries Science, Volume 9.(1982).

3. Poxton, M.G. Water Quality Criteria for Marine Fisheries. *Aquacultural Engineering*, 1,151-191.(1982).

4. Jennings, P.A., Snoeyink, V.L. and Chian, E.S.K. Theoretical Model for a Submerged Biological Filter. *Biotechnology and Bioengineering*, 18,1249-1273.(1976).

5. Poduska, R.A. and Andrews, J.F. Dynamics of Nitrification in the Activated Sludge Process. *J. Wat. Control. Fed.* ,47,2599-2619.(1975).

6. Haug, R.T. and McCarty, P.L. Nitrification with Submerged Filters. *Journal W.P.C.F.* ,44(11),2086-2102.(1972).

7. Brune, D.E and Gunther, D.C. The Design of a New High Rate Nitrification Filter for Aquaculture Water Reuse. *J. World Maricul. Soc.* ,12(1),20-31.(1981).

8. Weatherley, L.R. Rate Models for a Marine Biological Filter. *Aquaculture Engineering* ,3,1-15.(1984).

9. Forster, J.R.M. Studies on Nitrification in Marine Biological Filters. *Aquaculture* ,4,387-397.(1974).

10. Liao, P.B. and Mayo, R.D. Salmonid Hatchery Water Reuse Systems. *Aquaculture* ,1,317-335.(1972).

11. Kaiser, G.E. and Wheaton, F.W. Nitrification Filters

for Aquatic Culture Systems: State of the Art. Scientific Article Number A3350 Contribution Number 6422 of the Maryland Agricultural Experimental Station (Department of Agricultural Engineering).

12. Wheaton, F.W. *Aquacultural Engineering*. John Wiley (1977).

13. Hirayama, K. Water Control by Filtration in Closed Culture Systems. *Aquaculture* ,4,369-385.(1974).

14. Srna, R.F. and Baggaley, A. Kinetic Response of perturbed marine nitrification systems. *J. W.P.C.F.* ,47(3),472-485.(1971).

15. Murray, K.R. Dept. Chemical & Process Engineering. Heriot-Watt University, Edinburgh; private communication.

16. Muir, J.F. and Roberts, R.J. *Recent Advances in Aquaculture*. Croon Helm(1982).

17. Dryden, H. Ammonium Ion Removal from Dilute Solutions and Fish Culture Water by Ion-exchange. PhD. Thesis, Heriot-Watt University(1984).

18. Goldsworthy, G. Dept. Marine Biology, Heriot-Watt University, Edinburgh; Private Communication (1984).

19. Prosser, J. (Editor) *Nitrification*. Soc. J. G. Microbiol. 20.(1986).

20. Sharma, B. and Ahlert, R.C. Nitrification and Nitrogen Removal. *Water Research* ,11,897-925.(1977).

21. Painter, H.A. A Review of Literature on Inorganic Nitrogen Metabolism in Microorganisms. *Water Research* ,4,393-450.(1970).

22. Lai, K.V. and Klontz, G.W. Evaluation of Environmental and Nutritional Factors Influencing the Performance of Biofilters in Fish Rearing Systems. Final report. Contract No.DACW 6877C0118 U.S. Dept. Army, Walla Walla, Washington (1980).

23. Hollocher, T.C., Tate, M.E. and Nicholas, D.J.D. Oxidation of Ammonia by *Nitrosomonas europaea*. *J. Biol. Chem.* ,256,10834-10836.(1981).

24. Anderson, K.K. and Hooper, A.B. O_2 and H_2O are each the source of one O in NO_2^- produced from ammonia by Nitrosomonas. *FEBS Lett.* ,164,236-240.(1983).

25. Poth, M. and Focht, D.D. ^{15}N Kinetic Analysis of N_2O Production by *Nitrosomonas europaea*: An Examination of Nitrifier Denitrification. *Appl. Environ. Microbiol.* ,49,1134-1141.(1985).

26. U.S. Environmental Protection Agency. Process Design Manual for Nitrogen Control. A Design manual prepared for the Office of Technology Transfer of the U.S. E.P.A.(1975).

27. Prosser, J. Experimental and Theoretical Models of Nitrification. In *Nitrification* Edited by J. Prosser. Ch. 4, 63-78.(1987).

28. Cho, C.M. Convective Transport of Ammonium with Nitrification in Soil. *Can. J. Soil Sci.* ,51,339-350.(1971).

29. Newton, A.P.G. Nitrification Kinetics and Mixing in Biological Filters. BSc.(Hons) Research Project. Dept. Chemical & Process Eng., Heriot-Watt University, Edinburgh (1984).

30. Chu, J.C. Mass Transfer in a Fluidised bed. *Chem. Eng. Prog.* ,49,141.(1953).

31. Atkinson, B. *Biochemical Reactors*. Pion (London)(1974).

32. Knowles, G., Downing, A.L. and Barrett, M.J. Determination of Kinetic Constants for Nitrifying Bacteria in Mixed Culture, with the Aid of an Electronic Computer. *J. gen. Microbiol.* ,38,263-278.(1965).

33. Anthonisen, A.C. The Effects of Free Ammonia and Free Nitrous Acid on the Nitrification Process. Ph.D. (Eng) Thesis, Cornell University, Ithaca, New York.(1974).

34. Huang, C.S. Kinetics and Process Factors of Nitrification on a Biological Film Reactor. Ph.D. Thesis, State University of New York at Buffalo.(1973).

35. Metcalf & Eddy Inc. Nitrification and Denitrification Facilities: Waste Water Treatment. Technol. Transfer Seminar Publ. U.S. E.P.A.(1973).

36. Kluyver, A.J. and Donker, H.J. *Chem. Zelle*, 13,134.(1926).

37. Hoffman, T.C. and Lees, H. The Biochemistry of Nitrifying Organisms. *Biochem. J.* ,54,579-583.(1953).

38. Aleem, M.I.H. and Nason, A. Metabolic Pathways of Bacterial Nitrification. *Symposium on Marine Microbiology* Ch. 37 (1963).

39. Wood, P.M. Nitrification as a Bacterial Energy Source. In *Nitrification* Edited by J. Prosser. Ch. 3,

39-62 (1987).

40. Lees, H. Hydroxylamine as an Intermediate in Nitrification. *Nature* ,169,156-157 (1952).

41. Yoshida, T. and Alexander, M. Hydroxylamine Formation by *Nitrosomonas europaea*. *Can. J. Microbiol.* ,10,923-926.(1964).

42. Bock, E., Koops, H-P. and Harms, H. Cell Biology of Nitrifying Bacteria. In *Nitrification*. Edited by J. Prosser.

43. Aleem, M.I.H., Hoch, G.E. and Varner, J.E. Water as the Source of Oxidizing and Reducing Power in Bacterial Chemosynthesis. *Proc. Natl. Acad. Sci. USA*. ,54,869-873 (1965).

44. Lees, H. and Simpson, J.R. The Biochemistry of the Nitrifying Organisms. 5. Nitrite Oxidation by Nitrobacter. *Biochem. J.* ,65,297-305 (1957).

45. Newton, A.P.G. and Weatherley, L.R. Fluid Mixing in Submerged Packed Bed Biofilters for Intensive Aquaculture. *IChemE SYMPOSIUM SERIES* No 111,299-312 (1988).

46. Deans, H.A. *Soc. Petrol Engrs. Jl.* ,3,49 (1963).

47. Levich, V.G., Markin, V.S. and Chismadzhev, Yu.A. On Hydrodynamic Mixing in a Model of a Porous Medium with Stagnant Zones. *Chem. Engng. Sci.* ,22,1357-1367 (1967).

48. Bunday, B.D. *Basic Optimisation Methods* (1984).

49. Box, M.J. A New method of Constrained Optimisation and a Comparison with Other Methods. *The Comp. Journal* ,8,42-52 (1965).

50. Nelder, J.A. and Mead, R. A Simplex Method for Function

Minimisation. *The Comp. Journal* ,7,308-313 (1965).

51. Levenspiel, O. *Chemical Reaction Engineering*. Wiley International.2 nd Edition (1972).

52. Buffham, B.A. and Gibilaro, L.G. The Analytical Solution to the Deans-Levich Model for Dispersion in Porous Media. *Chem. Engng. Sci.* ,23,1399-1401 (1968).

53. Kendall, M.G. *Kendall's Advanced Theory of Statistics* Vol 1. Griffin (1987).

54. Cholette, A. and Cloutier, L. Mixing Efficiency Determinations for Continuous Flow Systems. *Can. Journal of Chemical Eng.* ,37,105-112 (1959).

55. Nauman, E.B. and Buffham, B.A. *Mixing in Continuous Flow Systems*. John Wiley and Sons (1983).

56. Pasquon, I. and Dente, M. *J. Catalysis*. ,1,508 (1962).

57. Pooley, A. Dept. Marine Biology, Heriot-Watt University. Edinburgh, Private Communication (1084).

58. Perry, R.H. and Green, D. *Perry's Chemical Engineers' Handbook*. McGraw-Hill Book company, 6 th Edition (1984).

59. Flanders, H. *Scientific Pascal*. Reston (1984).

60. March, J. *Advanced Organic Chemistry. Reactions, Mechanisms, and Structures*. 3 rd Edition. Wiley Interscience (1985).

61. Perry, R.H. *The Chemical Engineers' Handbook*. 4 th Edition (1963).

62. Van Krevelen, D.W., Hoftijzer, P.J. and Huntjens, F.J. Composition and Vapour Pressures of Aqueous Solutions of Ammonia, Carbon Dioxide and Hydrogen

Sulphide. *RECUEIL* ,68,191-216.(1949).

63. Keenan, C.W. and Wood, J.H. *General College Chemistry.* 5 th Edition. Harper and Row (1976).

64. Edelman, J. and Chapman, J.M. *Basic Biochemistry. A visual approach for college and university students.* Heinemann Educational Books.(1985).

65. Morrison, R.T. and Boyd, R.N. *Organic Chemistry.* 5 th Edition. Allyn and Bacon (1987).

66. Michal, Gerhard. Biochemical Pathways. Boehringer. Mannheim. F.R.G.

67. Anderson, P.M. and Meister, A. Evidence for an Activated Form of Carbon Dioxide in the Reaction Catalyzed by *Escherichia coli. Biochemistry* ,4(12),2803-2808 (1965).

68. Meister, A. (Editor). *Advances in Enzymology,* ,39. John Wiley and Sons (1973).

69. Newton, A.P.G. An Investigation into Biological Filters and their Design, for Use in Aquaculture. MSc (Research). Dept. Chemical & Process Eng., Heriot-Watt University, Edinburgh (1986).

70. Prosser, J.I. Dept. of Microbiology. Aberdeen University, Marischal College. Aberdeen.

71. Skinner, F.A. and Walker, N. Growth of *Nitrosomonas europaea* in Batch and Continuous Culture. *Archs. Mikrobiol.* ,38,339-349 (1961).

72. Ulken, A. Die Herkunft des Nitrits in der Elbe. *Arch. Hydrobiol.* ,59,486-501 (1963).

73. Hooper, A.B. Terry, K.R. Specific Inhibitors of Ammonia Oxidation in Nitrosomonas. *J. Bact.* ,115,480-485 (1975).

74. Olson, R.J. Differential Photoinhibition of Marine Nitrifying Bacteria: A possible Mechanism for the formation of the Primary Nitrite Maximum. *J. Mar. Res.* ,39,227-238 (1981).

75. Bock, E. Vergleichende Untersuchungen ueber die Wirkung sichtbaren Lichtes auf *Nitrosomonas europaea* und *Nitrobacter winogradskyi*. *Arch. Mikrobiol.* ,51,18-41.(1956).

76. Cornish-Bowden, A. *Fundamentals of Enzyme Kinetics.* Butterworths (1979).

77. Golterman, H.L, Clymo, R.S. and Ohnstad, M.A.M. *Methods for Physical & Chemical Analysis of Fresh Waters.* Blackwell Scientific Publications (1978).

78. Strickland, J.D.H. and Parsons, T.R. *A Practical Handbook of Seawater Analysis* (1972).

79. *Flow-Through and Recirculation Systems.* Report of the Working Group on Terminology, Format and Units of Measurement. Food & Agriculture Organization of the United Nations. EIFAC Technical Paper 49 (1986).

80. Emerson, K. et al. Aqueous Ammonia Equilibrium Calculations: Effect of pH and temperature. *J.Fish.Res.Board.Can.* ,32(12),2370-2383 (1975).

81. Tummavuori, J. and Lumme, P. Protolysis of Nitrous Acid in Aqueous Sodium Nitrate and Sodium Nitrite at Different Temperatures. *Acta Chem. Scand.* ,22(6),2003-2011 (1968).

82. Shears, J.H. and Wood, P.M. Spectroscopic Evidence for a Photosensitive Oxygenated Monoxygenase. *Biochem. J.* ,226,499-507 (1985).

83. Suzuki, I., and Kwok, S.-C. *Can. J. Biochem.* 59, 484-488 (1982)

84. Tsang, D.C.Y. and Suzuki, I. Cytochrome c-554 as a Possible Donor in the Hydroxylation of Ammonia and Carbon Monoxide in *Nitrosomonas europea. Can. J. Biochem.* 60,1018-1024 (1982).

85. Andersson, K.K. et al. Tetrahaeme cytochrome c-554 from *Nitosomonas europaea. J. Biol. Chem.* ,261,1126-1138 (1986).

86. Yamanaka, T. and Shina, M. *J. Biochem.* 75,1265-1273 (1974).

87. Feur, H. *The Chemistry of the Nitro and Nitroso groups.* Part 1. Interscience publishers (1969).

88. Hynes, R.K. and Knowles, R. Inhibition by Acetylene of Ammonia Oxidation in *Nitrosomonas europea. F.E.M.S Microbiol. Lett.* 4,319-321 (1978).

89. Pollard, A. *Process Control.* Heinemann Educational Books (1981).

90. Select Commitee on the European Communities. Nitrates in Water. House of Lords Session 1988-89.

91. Miller, D.J. and Nicholas, D.J.L. Further Characterization of the Soluble Cytochrome Oxidase/Nitrite Reductase from *Nitrosomonas europaea. J. Gen. Microbiol.* ,131,2851-2854 (1985).

92. DiSpirito, A.A. et al. A 'Blue' Copper Oxidase from *Nitrosomonas europaea. Biochim. Biophys. Acta.* ,827,320-326 (1985).

93. Goreau, T.J. et al. Production of Nitrite Ions and Nitrous Oxide by Nitrifying Bacteria at Reduced Concentrations of Oxygen. *Appl. Environ. Microbiol.* ,40,526-532 (1980).

94. Jeris, J.S. and Owens, R.W. Pilot-scale, High-rate Biological Denitrification. *Journal W.P.C.F.* ,47(8),2043-2057 (1975).

95. Metzler, D.E. *Biochemistry. The chemical reactions of living cells.* Academic Press (1977).

96. Voysey, P.A. and Wood, P.M. Methanol and Formaldehyde Oxidation by an Autotrophic Nitrifying Bacterium. *Journal of General Microbiol.* ,33,283-290 (1987).

97. Cornish-Bowden, A. *Principles of Enzyme Kinetics.* Butterworths. (1976).

98. Hill, A.V. *J. Physicol.* ,40,iv-vii (1910).

99. Anderson, P.M. and Meister, A. Control of Escherichia Carbamyl Phosphate Synthetase by Purine and Pyrimidine Nucleotides. *Biochemistry.* ,5(10),3164-3169 (1966).

100. Koshland, D.E. *Proc. natn. Acad. Sci. U.S.* 44,98-99 (1958).

101. Levitzki, A., Stallcup, W.B. and Koshland, D.E. *Biochemistry.* 10,3371-3378 (1971).

102. Weatherley, L.R. Chemical Engineering and Aquaculture. *The Chemical Engineer.* 378,99-100 (1982).

103. Hollocher, T.C. Kumar, S. and Nicholas, D.J.D. Respiration Dependent Proton Translocation in *Nitrosomonas europea.* *J. Bacteriol.* 149,1013-1020 (1982).

104. Drozd, J.W. Energy Coupling and Respiration in *Nitrosomonas europea*. *Arch. Microbiol.* 110,257-262 (1976).